PAPER I

Melepat, Balraj, Tao Li, and Michal Vinkler. "Natural selection directing molecular evolution in vertebrate viral sensors." Developmental & Comparative Immunology 154 (2024): 105147**.**

Developmental and Comparative Immunology 154 (2024) 105147

Contents lists available at ScienceDirect

Developmental and Comparative Immunology

journal homepage: www.elsevier.com/locate/devcompimm

Natural selection directing molecular evolution in vertebrate viral sensors

Balraj Melepat, Tao Li, Michal Vinkler *

Charles University, Faculty of Science, Department of Zoology, Viničná 7, 128 43, Prague, EU, Czech Republic

ARTICLE INFO

Keywords:
Evolutionary adaptation
Innate immunity
Molecular evolution
Pattern recognition receptor
Positive selection
Virus detection

ABSTRACT

Diseases caused by pathogens contribute to molecular adaptations in host immunity. Variety of viral pathogens challenging animal immunity can drive positive selection diversifying receptors recognising the infections. However, whether distinct virus sensing systems differ across animals in their evolutionary modes remains unclear. Our review provides a comparative overview of natural selection shaping molecular evolution in vertebrate viral-binding pattern recognition receptors (PRRs). Despite prevailing negative selection arising from the functional constraints, multiple lines of evidence now suggest diversifying selection in the Toll-like receptors (TLRs), NOD-like receptors (NLRs), RIG-I-like receptors (RLRs) and oligoadenylate synthetases (OASs). In several cases, location of the positively selected sites in the ligand-binding regions suggests effects on viral detection although experimental support is lacking. Unfortunately, in most other PRR families including the AIM2-like receptor family, C-type lectin receptors (CLRs), and cyclic GMP-AMP synthetase studies characterising their molecular evolution are rare, preventing comparative insight. We indicate shared characteristics of the viral sensor evolution and highlight priorities for future research.

1. Introduction

Viral infections seriously harm human health, impair agricultural production with significant effects on economics, and threaten wildlife (Jones et al., 2008; Karesh et al., 2012; Socha et al., 2022). Many emerging diseases are caused by zoonotic viruses transmitted from animals to humans (Jones et al., 2008). Often is the origin of the viral pathogens in wild species that are phylogenetically and ecologically distant from humans (Kruse et al., 2004; Nabi et al., 2021). We know still little about infection dynamics and immune variation in these non-model species (Plowright et al., 2016; Vinkler et al., 2022). Recently, global awareness of the importance of relationships between human and wildlife health has led to formulation of the One Health concept (Lebov et al., 2017) and urged for the research of immunogenetic diversity across species. To set effective measures to prevent disease transmission and establish successful therapeutic treatments, we need to better understand the evolution of host immunity responding to evolving pathogens. In this review, we contribute to these efforts by characterising evolutionary patterns diversifying host immunity at the interface with viral pathogens.

Host-pathogen interactions are commonly viewed as arms races, where hosts constantly counter-adapt to pathogen adaptations aimed at overcoming host immunity (Woolhouse et al., 2002). Such co-evolution forms strong diversifying selective pressures on host immunity (Buchmann, 2014; Danilova, 2006). Animal immune genes show impressively rapid evolution, with high levels of variation both within and between species (Bustamante et al., 2005; Fumagalli et al., 2011; Hillier et al., 2004; Lenz et al., 2013; Těšický and Vinkler, 2015; Vinkler et al., 2022). However, host adaptations do not necessarily need to intensify the pathogen-specific immune responses. In certain cases, natural selection can favour diminishing the unnecessary damage in the hosts, optimising the balance between resistance and tolerance to the infection (Henschen et al., 2023; Råberg et al., 2007; Savage and Zamudio, 2016; Weber et al., 2022). This often happens also during viral infections where excessive or dysregulated immune response can cause more harm than the infection itself (Hussell et al., 2001). Such immune adaptations are constrained by interactions with other symbionts (Horrocks et al., 2011) trading-off responses to potential threats and avoidance of immunopathology caused by harmless stimulation (Graham et al., 2005). While recent evolutionary research helped to define some host molecular adaptations to pathogens, evidence indicating distinct evolutionary patterns across immune genes is still rare.

Host immunity is importantly guided and regulated by immune receptors that recognise infection-related signals and trigger immune responses (Palm and Medzhitov, 2009). A large variety of germline-encoded innate immune receptors detecting

* Corresponding author.
E-mail address: michal.vinkler@natur.cuni.cz (M. Vinkler).

https://doi.org/10.1016/j.dci.2024.105147
Received 14 March 2023; Received in revised form 30 December 2023; Accepted 3 February 2024
Available online 6 February 2024

pathogen-derived structures are grouped under the term pattern-recognition receptors (PRRs). Despite their functional linkage in vertebrate immunity, the PRRs belong to several protein families that are heterogenous in their structures, varying in domain composition, cellular location, ligand binding as well as in the mechanism of signal transduction (Li and Wu, 2021; Pålsson-McDermott and O'Neill, 2007; Wu et al., 2022). These include namely the Toll-like receptor (TLR) family, Nucleotide-binding oligomerization domain (NOD)-like receptor (NLR) family, Retinoic-acid inducible gene-I(RIG-I)-like receptor (RLR) family, Absent in melanoma 2 (AIM2)-like receptor (ALRs) family, C-type lectin receptors (CLRs), Oligoadenylate synthetase family (OAS) and Cyclic GMP-AMP synthetase (Bermejo-Jambrina et al., 2018; Ho et al., 2022; H. Jiang et al., 2021; Lee et al., 2019, 2019). Do these sensory systems differ in their pathogen-driven evolutionary modes in vertebrates? Current evolutionary theoretical framework suggests that natural selection modes may differ between different groups of immune receptors based on the ligands they recognise, cellular sites to which they are expressed or even their expression inducibility during infection (Vinkler et al., 2023).Yet, present research data do not provide any conclusive insights so far. In this review, we focus on the molecular evolution of PRRs that specifically sense viral pathogens. We discuss the evidence available for adaptations putatively allowing PRRs of different vertebrate taxa to differentially recognise virus-derived microbe--associated molecular patterns (MAMPs), conserved structures identifying distinct pathogen groups. While for some of the PRR families evidence has recently accumulated to reveal the pattern of their molecular evolution (Fig. 1), we aim to show how limited are still our evolutionary insights into the diversity of the vast majority of these receptors. This review is thus complementary to other recent excellent reviews describing the roles of various PRRs (Liao and Su, 2021; Majzoub et al., 2019; Mojzesz et al., 2020; Neerukonda and Katneni, 2020; Nie et al., 2018) and their diversity or general evolution in distinct taxa (Banerjee et al., 2020; Iwama and Moran, 2023; Magor, 2022), providing a timely overview of host molecular adaptations at the receptor-virus interface.

2. Evolution of Toll-like receptors

Toll-like receptors (TLRs) are PRRs conserved throughout animal evolution (Nie et al., 2018). Typically, 10–12 TLR genes are expressed in vertebrates as transmembrane proteins adapted to recognise the high diversity of extracellular and endosomal MAMPs (Vinkler and Albrecht, 2009). These structures are in TLRs detected through their leucine-rich-repeat (LRR) ectodomains forming a horseshoe-shaped ligand-binding surface. Upon ligand binding, signalling is achieved through dimerization of the receptor proteins, bridging their cytoplasmatic Toll/interleukin-1 (IL-1) receptor (TIR) domains (Akira et al., 2006; Gosu et al., 2019). Although highly conserved in their general architecture, specific structural variation emerged between different TLR ectodomains, determining different TLR subfamilies (Wang et al., 2016). While frequently located in the plasma membrane (e.g. TLR1 subfamily, TLR4 or TLR5 involved mainly in bacterial recognition), the

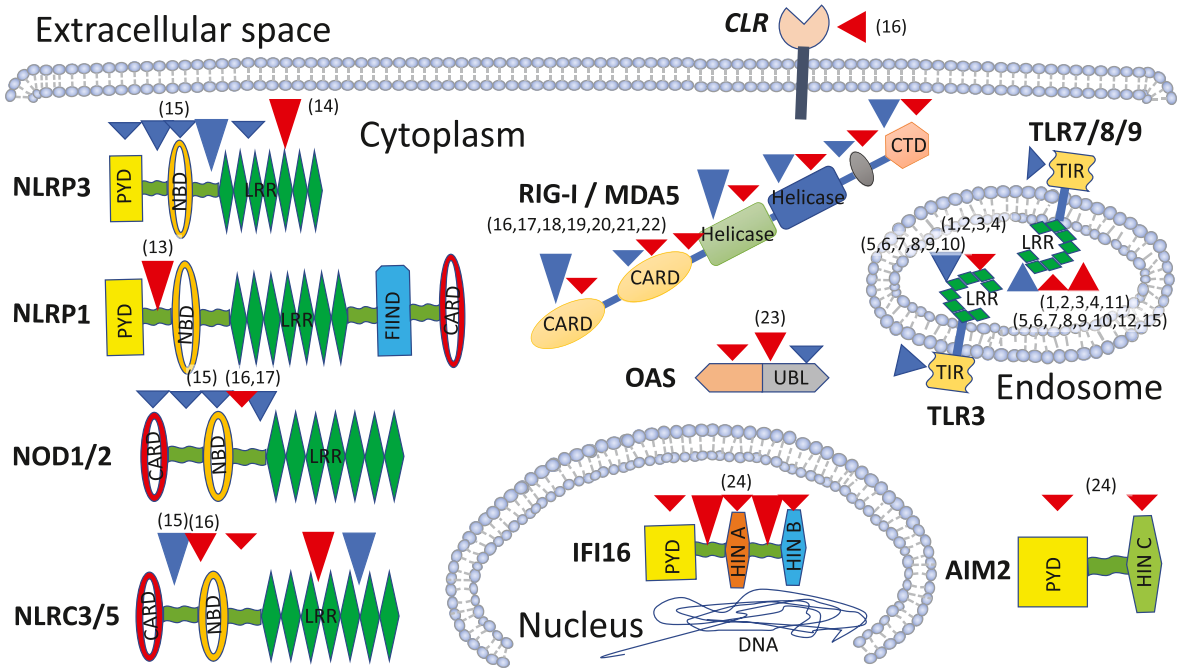

Fig. 1. Positive selection acting in vertebrate viral sensing pattern recognition receptors (PRRs). PRR gene families were selected based on information available to their molecular evolution. Triangles indicate domains and molecular regions (not sites) under positive selection; triangle colour indicates taxon in which positive selection was detected: red = mammals, blue = birds; triangle size indicates the intensity of positive selection in terms of numbers of positively selected sites detected (weak, medium or strong selection; for details see Table 1). TLR = Toll-like receptor, NLRP = nucleotide-binding oligomerization domain-like receptor with pyrin domain (PYD), NLRC = nucleotide-binding oligomerization domain-like receptor with caspase-recruitment domain (CARD) protein, NOD = nucleotide-binding oligomerization domain protein, RIG-I = retinoic acid-inducible gene I, MDA5 = melanoma differentiation-associated protein 5, OAS = oligoadenylate synthetase, AIM2 = Absent in melanoma-2, IFI16 = Interferon-inducible protein 16, CLR = C-type-lectin receptors. To each protein, different domains are shown: TIR = Toll/interleukin-1 (IL-1) receptor (TIR) domain, LRR = leucine-rich repeat, PYD = pyrin domain, CARD = caspase-recruitment domain, NBD = nucleotide-binding domain, FIIND = function to find domain, CTD = C-terminal domain, UBL = C-terminal tandem ubiquitin-like (UBL) domains, HIN = hematopoietic interferon-inducible nuclear antigens. References are indicated by numbers in the brackets: 1 = Wlasiuk and Nachman (2010); 2 = Areal et al. (2011); 3 = Escalera-Zamudio et al. (2015); 4 = Jiang et al. (2017); 5 = Alcaide and Edwards (2011); 6 = Grueber et al. (2014); 7 = Wang et al. (2016); 8 = Velová et al. (2018); 9 = Khan et al. (2019); 10 = Liu et al. (2020); 11 = Fornůsková et al. (2013); 12 = Vinkler et al., (2014); 13 = Chavarría-Smith et al. (2016); 14 = Ahn et al. (2019); 15 = Ma et al. (2021); 16 = Wu et al. (2022); 17 = Tian et al. (2018); 18 = Cagliani et al. (2014b); 19 = Lemos De Matos et al. (2013); 20 = Krchlíková et al. (2021); 21 = Krchlíková et al. (2023); 22 = Zheng and Satta (2018); 23 = Hu et al., (2018); 24 = Cagliani et al. (2014a). (For interpretation of the references to colour in this figure legend, the reader is referred to the Web version of this article.)

Table 1
Strength of positive selection acting in vertebrate viral sensing pattern recognition receptors (PRRs). Intensity of positive selection was categorised based on numbers of positively selected sites (PSS; where available, consensus obtained by more than two predictive methods was taken): weak = 0–2 PSS, medium = 3–5 PSS, strong ≥6 PSS. TLR = Toll-like receptor, NLRP = nucleotide-binding oligomerization domain-like receptor with pyrin domain (PYD), NLRC = nucleotide-binding oligomerization domain-like receptor with caspase-recruitment domain (CARD) protein, NOD = nucleotide-binding oligomerization domain protein, RIG-I = retinoic acid-inducible gene I, MDA5 = melanoma differentiation-associated protein 5, OAS = oligoadenylate synthetase, AIM2 = Absent in melanoma-2, IFI16 = Interferon-inducible protein 16, CLR = C-type-lectin receptors, LRR = leucine-rich repeat, UBL = C-terminal tandem ubiquitin-like (UBL) domains, HIN = hematopoietic interferon-inducible nuclear antigens. References are indicated by numbers in the brackets: 1 = Wlasiuk and Nachman (2010); 2 = Areal et al. (2011); 3 = Escalera-Zamudio et al. (2015); 4 = Jiang et al. (2017); 5 = Alcaide and Edwards (2011); 6 = Grueber et al. (2014); 7 = Wang et al. (2016); 8 = Velová et al. (2018); 9 = Khan et al. (2019); 10 = Liu et al. (2020); 11 = Fornůsková et al. (2013); 12 = Vinkler et al., (2014); 13 = Chavarría-Smith et al. (2016); 14 = Ahn et al. (2019); 15 = Ma et al. (2021); 16 = Wu et al. (2022); 17 = Tian et al. (2018); 18 = Cagliani et al. (2014b); 19 = Lemos De Matos et al. (2013); 20 = Krchlíková et al. (2021); 21 = Krchlíková et al. (2023); 22 = Zheng and Satta (2018); 23 = Hu et al., (2018); 24 = Cagliani et al. (2014a).

Gene	Domain	Taxon	Positive Selection	PSS No.	Reference
TLR3	LRR	Mammals	Weak	**0–2**	1,2,3,4
TLR3	LRR	Birds	Medium	**3–4**	5,6,7,8,9,10
TLR7-9	LRR	Mammals	Weak-Medium	**2–4**	1,2,3,4,11
TLR7-9	LRR	Birds	Weak-Medium	**1–4**	5,6,7,8,9,10,12
NLRP1	linker	Mammals	Strong	**6**	13
NLRP3	LRR	Mammals	Strong	**7**	14
NLRP3	NBD	Birds	Weak	**2**	15
NLRP3	LRR	Birds	Weak	**1**	15
NLRC5	LRR	Mammals	Strong	**9**	16
NLRC5	LRR	Birds	Strong	**12**	15
NOD1/NOD2	LRR	Birds	Weak	**0**	15
NOD1/NOD2	LRR	Mammals	Weak	**0**	17
RIG-I	Helicase	Mammals	Weak-Medium	**2–4**	18,19
RIG-I	Helicase	Birds	Strong	**8–12**	20,22
RIG-I	Linkers	Mammals	Weak	**2**	18
RIG-I	CARD	Mammals	Weak-Medium	**2–4**	18,19
RIG-I	CARD	Birds	Weak	**1–2**	20,22
RIG-I	CTD	Mammals	Weak	**0–2**	18,19
RIG-I	CTD	Birds	Weak-Strong	**1–9**	20,22
MDA5	Helicase	Mammals	Weak	**1–2**	18,19
MDA5	Helicase	Birds	Medium	**4–6**	21,22
MDA5	CARD	Mammals	Weak-Medium	**2–4**	18,19
MDA5	CARD	Birds	Strong	**8–12**	21,22
MDA5	Pincer	Mammals	Weak	**0**	18,19
MDA5	Pincer	Birds	Weak	**3**	21,22
MDA5	CTD	Mammals	Weak	**1–2**	18,19
MDA5	CTD	Birds	Weak	**2**	21,22
OASL1/OASL2	UBL	Mammals	Weak-Medium	**0–4**	23
OASL	UBL	Birds	Weak	**2**	23
AIM2	HIN C	Mammals	Weak	**2**	24
IFI16	Linkler-1	Primates	Strong	**7**	24
IFI16	Linker-2	Primates	Strong	**6**	24
CLR	ECD	Mammals	Medium	**3**	17

key viral-sensing TLRs, such as TLR3 and TLR7 subfamily members are expressed into the endosome where they detect nucleic acids derived from viruses and other intracellular pathogens (Liu et al., 2020). In general, the TLR family genes are mostly under purifying selection constrained by the receptor-conserved function throughout taxa (Darfour-Oduro et al., 2016; Ghosh et al., 2022; Nelson-Flower et al., 2018; Tong et al., 2015; Velová et al., 2018). Interestingly, in most datasets, the dN/dS statistics suggest that in vertebrates the TLRs detecting viruses have been subjected to stronger functional constraints limiting the positive selection than the other TLRs (Liu et al., 2020; Mikami et al., 2012; Velová et al., 2018; Wang et al., 2016; Wlasiuk and Nachman, 2010). Nonetheless, this is contradicted by some amphibian and mammalian research suggesting that viral and non-viral TLRs are under similarly strong positive selection (Areal et al., 2011; Zhang et al., 2022). Despite the general conservatism, positive selection appears to act frequently at various sites of these proteins, especially those located in the ectodomains (Liu et al., 2020; Velová et al., 2018).

In most vertebrate taxa the virus-sensing TLRs show only limited protein-coding interspecific variation and population polymorphism (Astakhova et al., 2009; Heng et al., 2011; Kloch et al., 2018, 2018, 2018; Świderská et al., 2018; Vinkler et al., 2015; Wlasiuk and Nachman, 2010). TLR3 forms a separate TLR subfamily with a single gene conserved throughout all vertebrates (Liu et al., 2020). Unlike some other TLRs including the TLR7 subfamily members (Bainová et al., 2014; Fiddaman et al., 2022; Khan et al., 2019; Philbin et al., 2005; Sharma et al., 2020; Velová et al., 2018) the *TLR3* gene shows no pseudogenization, loss, or duplication in any vertebrate species studied so far, indicating its universal functional importance. The TLR3 protein detects viral double-stranded (ds)RNA through the interaction of its C and N-terminal LRRs with the sugar-phosphate backbone of the RNA, but indifferent to the sequence of the bases (Liu et al., 2008). This probably limits the pathogen-mediated positive selection diversifying the TLR3 virus-recognition capacities. Across mammals, positive selection in TLR3 is only very weak (Jiang et al., 2017; Wlasiuk and Nachman, 2010), although positively selected sites (PSS) have been detected, for instance in the bat lineage (Escalera-Zamudio et al., 2015). Relatively more potentially adaptive non-synonymous variation has been reported in avian TLR3 both on interspecific (Alcaide and Edwards, 2011; Grueber et al., 2014; Khan et al., 2019; Liu et al., 2020; Velová et al., 2018; Wang et al., 2016) and intraspecific (Świderská et al., 2018) levels. Although still generally weaker than in most other TLRs, in birds recent research identified positive selection in TLR3 in the ectodomain and with higher frequency than in other TLRs also in the intracellular TIR domain (Liu et al., 2020; Velová et al., 2018). Compared to other TLRs, in TLR3 there is a relatively lower consistency of PSS identified in different taxa, which suggests (compared to other TLRs; Králová et al., 2018; Těšický et al., 2020) limited convergent evolution in this gene. Yet, even in TLR3 positive selection acts also directly at some functional sites involved in ligand binding, suggesting possible adaptations in viral detection (Jiang et al., 2017). Recent evidence suggests that in birds the putatively functional polymorphism in TLR3 can be explained by past (Davies et al., 2021; Gilroy et al., 2017) or present balancing selection (Lara et al., 2020; Minias and Vinkler, 2022).

In comparison with TLR3, the TLR7 subfamily including TLR7, TLR8 and TLR9 shows in vertebrates stronger evidence for positive selection (Liu et al., 2020). Both TLR7 and TLR8 receptors bind single-stranded (ss)RNA through interaction with the Z-loop, which bridges their ectodomain cleavage site (Zhang et al., 2016). TLR9, which is evolutionarily as well as structurally more derived (Liu et al., 2020) recognizes the unmethylated CpG islands in bacterial and viral DNA. Although otherwise conserved in vertebrates, the TLR7 subfamily has experienced dynamic evolution in modern reptiles and birds where TLR9 was lost entirely, TLR8 was lost in birds but duplicated in crocodilians and turtles (Dolby et al., 2020) and recurrent TLR7 duplication emerged several times independently in birds (Grueber et al., 2012; Liu et al., 2020; Velová et al., 2018) and also in some species of mammalian lagomorphs (Neves et al., 2022). In parallel, TLR8 was also lost in hares (Neves et al., 2022). Furthermore, the functional role of the lost TLR9 has been replaced in birds by TLR21 which is phylogenetically unrelated and missing in mammals (Keestra et al., 2010). This documents the convergent evolution between the vertebrate TLR paralogues. Similar to

TLR3, the positive selection is relatively weak in TLR7 and there is little consistency between the PSS identified in different taxa (Jiang et al., 2017; Liu et al., 2020; Mikami et al., 2012; Velová et al., 2018; Vinkler et al., 2014). This holds also for bats, a group hypothesized to experience strong selection on immunity driven by frequent viral infections (Jiang et al., 2017). Stronger positive selection than in TLR7 has been revealed in mammalian TLR8 (Areal et al., 2011; Jiang et al., 2017), where several lineages, including the bats (Escalera-Zamudio et al., 2015) show increased levels of positive selection. It has been hypothesized that positive selection in bat virus-sensing TLRs provides them unique adaptations to sustain high pathogen loads (Jiang et al., 2017), different from e.g. short-lived rodents, where interspecific (Fornůsková et al., 2013) as well as intraspecific studies (Kloch et al., 2018) show strong negative selection and high levels of homozygosity within populations. In bats the TLR8 PSS are located in or in proximity to predicted ligand-binding and other functional sites in the ectodomain, supporting this hypothesis (Schad and Voigt, 2016). Similar avian TLR7, in mammalian TLR8 positive selection targets namely the region of the intramolecular protein cleavage and the Z-loop, which might indicate the functional significance of the variation. In mammals, the strongest positive selection has been observed in TLR9 (Jiang et al., 2017) where several taxa, including the bats, show increased positive selection. A similar pattern of positive selection has been revealed also in teleost fish (Han et al., 2019). Yet, in TLR9 there is little overlap of the PSS with the ligand-binding sites (Liu et al., 2020). The functionally converging avian TLR21 shows very weak positive selection (Velová et al., 2018). Nevertheless, this pattern might be artificial, resulting from relatively limited sequence and/or functional information available to mammalian TLR9 and especially avian TLR21. This notion is further supported by the fact that a new TLR21-like orthologue has been revealed in non-avian Sauropsids only recently (Dolby et al., 2020) and that amphibian TLR21 is likely under strong positive selection (Zhang et al., 2022). Altogether, current results highlight the present knowledge limitations on TLR evolution in less frequently studied genes and taxa.

Furthermore, other putatively virus-sensing TLRs remain up to now entirely out of the scope of evolutionary studies. These include the mammalian TLR13 (Shi et al., 2011), fish TLR19 (Ji et al., 2018) or TLR22, all of which also recognise viral ligands (Matsuo et al., 2008; Su et al., 2012). Interestingly, initial results show relevant variation in the evolution of some of these TLRs. For example, TLR19 appears to evolve in a similar conserved mode as TLR3 in fish (Wang et al., 2015), but under stronger diversifying selection in amphibians (Zhang et al., 2022). Evidence of relatively increased positive selection was also revealed in the ectodomain of TLR22 in teleost fish (Qi et al., 2017; Sundaram et al., 2012). Finally, even the bacteria-sensing TLR4 that is well characterised for lipopolysaccharide (LPS) binding, has been indicated to recognise viral structures, though closer insights are still missing to reveal the structural mechanism of the interaction and indicate significance of adaptive evolution in modulating the pathogen detection (Akira et al., 2006; Huang et al., 2012; Olejnik et al., 2018; Younan et al., 2017).

3. Evolution of NOD-like receptors

The nucleotide-binding oligomerization domain (NOD)-like receptors (NLRs) are evolutionarily conserved PRRs expressed into the cytoplasm where several of them play essential roles in antiviral innate immune responses throughout the animal kingdom (Wu et al., 2021; Zhu et al., 2022). The general protein structure of these proteins consists of a common C-terminal LRR domain and a central nucleotide-binding domain (NBD, also known as NACHT or NOD; (Wu et al., 2021). In their N-terminal domains the members of the NLR family differ, forming specific NLR subfamilies: i) NLRA containing the acidic transactivating domain (*CIITA*), ii) NLRB containing the inhibitor of apoptosis domain (AIP; e.g.: *NAIP2*, *NAIP5* and *NAIP6*), iii) NLRC containing the caspase-recruitment domain (CARD; e.g.: *NOD1, NOD2, NLRC3, NLRC5, NLRX1*), and iv) NLRP containing the pyrin domain (PYD; e.g.: *NLRP1, NLRP3*) (Liang et al., 2018; Souza et al., 2021; Li et al., 2016; Chu et al., 2018; Zhong et al., 2013). With some exceptions, viral ligands are detected in the cytoplasm by the LRR domain, triggering the NBD domain oligomerization that activates the downstream signalling through the corresponding N-terminal domains (Jacobs and Damania, 2012; Jing et al., 2019). However, not all NLRs directly interact with viral ligands. The NLRA and NLRB subfamilies do not seem to play roles as viral sensors, while several receptors belonging to the NLRC or NLRP subfamilies do (Atyeo and Papp, 2022; Bauernfried et al., 2021; Godkowicz and Druszczyńska, 2022; Gregory et al., 2011; Hong et al., 2012; Ranjan et al., 2015; Wallace and Russell, 2022; Zhang et al., 2014).

In the NLRP gene family, the NLRP1 and NLRP3 can be activated by nucleic acids of both RNA and DNA viruses (Atyeo and Papp, 2022; Bauernfried et al., 2021; Gregory et al., 2011; Wallace and Russell, 2022). The structure of NLRP1 differs from other NLRP proteins because of its extra C-terminal function to find domain (FIIND), which is in the inactive state connected to the linker-1 region connecting the NBD and PYD domains (Atyeo and Papp, 2022; Finger et al., 2012). Even though NLRP1 and NLRP3 have similar ligand detection capabilities, this structural difference diversifies their activation capacities (Atyeo and Papp, 2022; Bauernfried et al., 2021; Gregory et al., 2011). In NLRP1 the linker-1 region contributing to ligand recognition and interacting with FIIND needs to be cleaved by the pathogen proteases to achieve activation. The evolutionary research in primates and rodents has revealed strong positive selection in NLRP1 (Bauernfried and Hornung, 2022; Chavarría-Smith et al., 2016; George et al., 2011) with most PSS being located in the linker-1 region (Chavarría-Smith et al., 2016). Given its diversity among primates and rodents, the linker-1 region putatively evolves to escape cleavage inactivation by specific pathogen-associated proteases (Chavarría-Smith et al., 2016). In contrast, avian NLRP3 shows the majority of the PSS distributed in the NBD, with fewer PSS in the LRR region (Ma et al., 2021). However, this pattern of NLRP3 adaptive diversity may be taxon-specific, since in bats the LRR domain evolves under strong positive selection decreasing the capacity of NLRP3 for activation through oligomerization (Ahn et al., 2019).

In the NLRC family, the first members identified were NOD1 and NOD2 that share similar downstream signalling, which resulted in their joint investigation (Boyle et al., 2013; Li et al., 2015a). While primarily interacting with bacterial peptidoglycans, recent research has indicated that these two receptors can also bind viral ligands. For example, NOD2 is involved in sensing the ssRNA viruses and both NOD1 and NOD2 play roles in the pathogenesis caused by SARS-CoV-2, although the precise interactions are not understood yet (Wang et al., 2021; Yin et al., 2021). NOD1 and NOD2 use the mitochondrial antiviral signalling (MAVS) pathway to evoke antiviral interferon responses (Sabbah et al., 2009; Wu et al., 2020). NOD1 is found in a variety of vertebrate taxa, including mammals, amphibians, reptiles, birds, and fish, while NOD2 is lacking in birds, reptiles, and amphibians (Boyle et al., 2013). In some basal vertebrate species, NOD1 can be duplicated (Li et al., 2015a). Within NODs, purifying selection limits sequence variation at most sites in the LRR, NBD and CARD domains (Boyle et al., 2013; Li et al., 2015a). In the bony fishes, a large number of PSS were revealed in NOD1, while only very few in NOD2, which indicates the difference in the selective pressure experienced by both genes (Li et al., 2015a). Interestingly, no positive selection has been revealed in either NOD1 or NOD2 across tetrapods (Li et al., 2015a), and a low number of PSS were indicated within mammals in general and to lesser extent in birds (Ma et al., 2021; Tian et al., 2018) and in the carnivores in particular (Wu et al., 2022).

The other NLRC family members comprise NLRC3, a negative regulator of inflammation, IFN and T-cell antiviral responses, and NLRC5 involved in either positive or negative regulation of the RIG-I-mediated antiviral signalling (Meissner et al., 2010; Ranjan et al., 2015; Zhang et al., 2014). The NLRC3 gene can directly interact with the double-stranded DNA viruses through positively charged patches of its LRR domain (Li et al., 2019; Lupfer and Kanneganti, 2013; Uchimura et al., 2018; Zhang et al., 2014). For NLRC5 such a direct interaction

with viral particles has not been revealed yet, although this receptor is crucial in some species including humans for inhibiting viral replication (Meissner et al., 2010; Ranjan et al., 2015). The NLRC3 gene is duplicated from the NOD1 gene in a common ancestor of birds and mammals (Hughes, 2006). In birds this gene has fewer PSS compared to other NLR family members, indicating strong purifying selection (Ma et al., 2021). In contrast, in birds and also in carnivores *NLRC5* exhibits the strongest positive selection of all the NLR genes investigated, with the majority of the PSS being located in the LRR domain (Ma et al., 2021; Wu et al., 2022).

Within the NLRC family, NLRX1 is very unusual for its N-terminal domain and mitochondrial location (Hong et al., 2012; Moore et al., 2008). It can alter the NF-κB and interferon-mediated antiviral responses and suppress the inflammasome response mediated by RIG-I (Allen et al., 2011; Jing et al., 2019; Parvatiyar and Cheng, 2011). The NLRX1 LRR domain with large positive amino acid patches can interact with ssRNA and dsRNA (Hong et al., 2012), being used by some RNA viruses (including HIV and SARS-CoV-2) for effective infection (Gordon et al., 2020; Guo et al., 2016). Very weak positive selection is acting in NLRX1 throughout vertebrates, with adaptations in the basal lineages of vertebrates namely in the NBD (Li et al., 2015b). Higher frequencies of PSS were observed in the evolution of carnivores, suggesting accelerated evolution of this gene in specific lineages (Wu et al., 2022).

4. Evolution of RIG-I-like receptors

In the detection of viral infections, the Retinoic acid-inducible gene I (RIG-I)-like receptors (RLRs) play key roles in sensing cytosolic RNAs (Leung and Amarasinghe, 2012). These RNAs can be either viral (derived from both RNA and DNA viruses) or host origin. The RLRs bind RNA through their central DExD/H-box helicase core consisting of two helicase domains attached via a pincer-shaped linker to the zinc-binding C-terminal domain (CTD) (Jiang et al., 2011; Saito et al., 2007; Takahasi et al., 2009). This structure is shared by all three members of the RLR gene family: RIG-I, melanoma differentiation-associated protein 5 (MDA5) and laboratory of genetics and physiology 2 (LGP2) (Fekete et al., 2018, 2020). RIG-I and MDA5 are full-structured receptors containing the N-terminal tandem caspase activation and recruitment domains (CARDs) which oligomerize upon RNA detection and activate antiviral responses through stimulation of type I interferon cytokine signalling (Ramos and Gale, 2011; Yoneyama et al., 2005). In contrast, the LGP2 protein lacks any CARDs. Lacking the signalling activity, LGP2 regulates the activities of RIG-I and MDA5, both positively and negatively (Pippig et al., 2009; Venkataraman et al., 2007). In mammals, LGP2 can inhibit RNA interference and viral RNA cleavage by inhibiting the endoribonuclease Dicer (Van Der Veen et al., 2018). While probably highly redundant in their functions, it has been hypothesized that MDA5 binds longer dsRNA fragments than RIG-I (Li et al., 2009a, 2009b). However, whether distinct viral infections generate specific RNA-binding patterns for RIG- I and MDA5 have yet to be revealed.

Similar to other PRRs sensing viral infections, RLRs have also dominantly evolved under purifying selection in vertebrates (Cagliani et al., 2014b; Krchlíková et al., 2021, Krchlíková et al., 2023; Lemos De Matos et al., 2013; Zheng and Satta, 2018). Relatively few sites or regions show any consistent patterns of positive selection acting across the taxa. In humans, RIG-I is the RLR most constrained in its variation, while in MDA5 and LGP2 stronger signals of positive selection indicate population differentiation (Vasseur et al., 2011). Potentially functional non-synonymous polymorphism that is in human MDA5 and LGP2 likely evolving under positive selection has been identified in the helicase domains and CTD. This partially corresponds with the positive selection revealed across mammals, where MDA5 shows the highest levels of positive selection (Lemos De Matos et al., 2013). However, on the interspecific level, the LGP2 gene is the one with the lowest levels of positive selection (Cagliani et al., 2014b). In contrast to the human population datasets, in mammalian RIG-I the positively selected sites are distributed along all their functional domains, with significant signals of positive selection occurring also in the helicase domains (Cagliani et al., 2014b; Lemos De Matos et al., 2013).This is common also to MDA5 and LGP2 in mammals. Yet, in both RIG-I and MDA5 higher incidences of the positively selected sites can be found in the linkers separating the helicase domains from CARDs that allow the RLR oligomerization and in MDA5 also directly at the CARD interface of contact between the receptor monomers (Cagliani et al., 2014b). Finally, further putative adaptations can be found in MDA5 also in the regions that are specific to this RLR, such as unique parts of the spacer between the CARD and helicase domains and the insertion in the helicase domain (Cagliani et al., 2014b).

In contrast to mammals, in birds it is the MDA5 that appears the most constrained of the three RLRs in its overall variation, which is especially conspicuous in the helicase domain and to a lower level also in the CARDs (Zheng and Satta, 2018). Yet, the same research line also indicates that avian MDA5 has the highest number of sites under positive selection, predictively contributing to functional adaptations. While all three avian RLRs show positive selection in the helicase region (Krchlíková et al., 2021), only MDA5 has increased the number of positively selected sites in the CARDs (Krchlíková et al., 2023; Zheng and Satta, 2018). Furthermore, important variation exists in the RLR evolution between different evolutionary lineages even within birds and mammals. For example, in mammals increased positive selection has been revealed in RIG-I in, e.g., the Xenarthra and the lineages leading to the shrew, dog, rabbit or squirrel, and in MDA5 it occurs in the lineages leading to the Tasmanian devil, shrew, giant panda, guinea pig or alpaca (Cagliani et al., 2014b; Lemos De Matos et al., 2013).

Despite this evidence for diversifying selection in RLRs, parallel evolution (i.e. independent evolution of functionally identical features) at homologous sites has been indicated between the three RLRs (e.g. sites 421 in mammalian RIG-I and 179 in LGP2; Cagliani et al., 2014b; or sites 333 in avian MDA5 and 867 in RIG-I; Zheng and Satta, 2018). Further evidence also suggests parallel evolution acting at the positively selected sites in RLRs across taxa, possibly creating convergent adaptations between various vertebrate lineages (Krchlíková et al., 2021, Krchlíková et al., 2023). Nevertheless, the most conspicuous example of parallel evolution is the repeated RLR gene loss. This happened in RIG-I in the Acanthopterygii fish (Chen et al., 2017), in the Chinese tree shrew RIG-I (Xu et al., 2016), and in various avian lineages, where both cases of RIG-I and MDA5 pseudogenisation were described (Krchlíková et al., 2023). Avian MDA5 has been lost in parallel in cranes (Gruiformes) and storks (Ciconiformes). For avian RIG-I, as many as 16 independent events of functional inactivation were reported, including namely events in some palaeognathae species, most galliforms, various seabirds (Cheradriiformes, Sphenisciformes) and falcons (Falconiformes). This might indicate selective pressures for decreased RLR-based viral recognition. However, since apparently in no lineage both RIG-I and MDA5 have been lost together (Krchlíková et al., 2023), current evidence is consistent with evolution occurring under functional constraints, possibly combined with a stochastic pattern of the individual RLR gene loss events. While adaptations in RIG-I do not appear to compensate the MDA5 function upon its loss (Krchlíková et al., 2021), evidence presently available opens the possibility that MDA5 could have evolved in the galliform birds to partially compensate for the RIG-I loss (Krchlíková et al., 2023). Additional evidence suggests episodic lineage-specific positive selection acting on LGP2 in Galliformes, which could be also related to the loss of RIG-I in this group, although in some other avian lineages, this gene may have experienced relaxation in selection (Zheng and Satta, 2018).

In RLRs the positively selected sites are mostly exposed to the protein surface (Cagliani et al., 2014b), but frequently lie distant from the known RNA binding sites (Krchlíková et al., 2023; Zheng and Satta, 2018). Both in avian RIG-I and MDA5 only a single positively selected site was located in close topological proximity to any of the RNA ligand-binding positions (Krchlíková et al., 2021, Krchlíková et al.,

2023). Other sites under positive selection in these receptors were adjacent to residues involved in the receptor signalling. This is especially obvious in the avian MDA5 where many sit in the regulatory CARD regions. This evidence suggests that in the RLR evolution adaptations could mostly adjust protein-protein interactions during signal transduction.

5. Evolution of oligoadenylate synthetases

The 2′-5′ oligoadenylate synthetases (OAS) are interferon-induced antiviral enzymes detecting viral dsRNA that are capable to initiate the degradation of the viral RNA (Eskildsen, 2003). This gene family is represented in all animals but in differing gene sets in different taxa (Kjaer et al., 2009; Kumar et al., 2000). For example, the full set of mammalian OAS family members consisting of OAS1, OAS2, OAS3, and OASL is present in most mammalian species, except for OAS2 and/or OAS3 absence in Odontoceti and several other species (Liu et al., 2023; Perelygin et al., 2006). Neognathae birds, on the other hand, possess no OAS functional loci and rely only on a single copy of the OASL gene that functions both in an RNase L-dependent and -independent (RIG-I-associated) manner (Hu et al., 2018; Rong et al., 2018). Distinct from OAS proteins, the OASL displays antiviral activity against RNA viruses through its C-terminal tandem ubiquitin-like (UBL) domains. The OAS proteins can also activate the NOD- and RIG-related inflammasome pathways (Oakes et al., 2017). Copy-number variation is known in the OAS genes (e.g. in rodent OAS1; Perelygin et al., 2006). The OAS proteins differ in the number of OAS domains that catalyse the synthesis of 2′-5′ oligoadenylates upon viral dsRNA binding (Neerukonda and Katneni, 2020).

It has been shown that compared to more basal vertebrate lineages, mammals show increased numbers of residues on the OAS/dsRNA interaction interface (Hu et al., 2018). The strongest positive selection is in mammals in OAS1 and the weakest in OAS2 (Liu et al., 2023). Present evidence suggests concerted evolution of the OAS1 paralogous in mammals (Rodentia and Artiodactyla), with multiple inter-locus exchanges achieved through gene conversion distorting the OAS1 divergent evolution (Perelygin et al., 2006). Despite this, strong positive selection has been identified in OAS1, especially in the group Cetartiodactyla (Liu et al., 2023). In primates with a single copy OAS1, positive selection in this gene has been identified specifically targeting the RNA-binding domain (several being directly at the RNA-binding positions) and the region circumscribing the entry to the active site, suggesting adaptations in ligand binding and evasion of viral OAS antagonists (Fish and Boissinot, 2016). Patterns of parallel evolution have been indicated between OAS1, OAS2, and even cGAS in primates and bats (Mozzi et al., 2015). Functional diversification of the OASL genes in tetrapods is suggested by differing gene-wide dN/dS ratios, being higher in the duplicated mammalian OASL1 and OASL2 paralogues than in the single-copy avian OASL (Hu et al., 2018). However, in the numbers of the PSS, the avian OASL and mammalian OASL2 surpass mammalian OASL1. Interestingly, in Sauropsids (reptiles and birds) the OASL genes contain more amino acid substitutions in the second UBL domain assumingly executing anti-viral activity, while in mammalian OASL2 stronger diversification is observed in the first UBL domain. Finally, significant intraspecific polymorphism has been described in some of the OAS genes, with balancing selection and *trans*-species polymorphisms modulating the allele frequencies described in OAS1 in mice and primates (Ferguson et al., 2008, 2012; Fish and Boissinot, 2015).

6. Evolution of the AIM2-like receptor

The Absent in melanoma-2 (AIM2)-like receptor family (ALRs or the PYHIN family) has only recently been discovered in mammals (Cagliani et al., 2014a; Cridland et al., 2012). In humans the ALR family consists of four genes: AIM2, Interferon-inducible protein 16 (IFI16), Interferon-inducible protein X (IFIX), and Myeloid cell nuclear differentiation antigen (MNDA; Brunette et al., 2012; Fan et al., 2022), though in some mammalian species (e.g. mouse) up to 13 ALR genes, while in others (e.g. cow) not a single functional gene can be found (Brunette et al., 2012). Except for *MNDA* all other genes appear to play roles in viral nucleic acid sensing (Crow and Cristea, 2017; Diner et al., 2015; Fan et al., 2022). The general structure of ALRs consists of an N-terminal pyrin (PYD) domain and one or two C-terminal hematopoietic interferon-inducible nuclear antigens with 200 amino acid repeats (HIN) domains (Brunette et al., 2012; Fan et al., 2022). While the HIN domain that is represented in different genes in different numbers and types is critical for the interaction with viral RNA or DNA (Cagliani et al., 2014a; Diner et al., 2015), the PYD domain mediates the downstream signalling (Fairbrother et al., 2001; Jin et al., 2013). The viral-sensing ALRs are located either in the cytoplasm (AIM2) or in the nucleus (IFI16, IFIX (Ding et al., 2004; Fan et al., 2022);). Some ALRs (IFI16) positively regulate RIG-I-mediated inflammation (Z. Jiang et al., 2021).

Evolutionary analysis performed in primates identified in *IFI16* the highest number of PSS in the spacers that connect the PYD domain with HIN or two HIN domains. *IFI16* is also a selection target in human populations, with indication of long-lasting balancing selection (Cagliani et al., 2014a). Less PSS have been identified in primates in the *AIM2* gene, including a few PSS in the HIN domain near the DNA binding site (Cagliani et al., 2014a). With fewer positively selected sites, the *AIM2* gene appears to undergo weaker adaptive evolution in primates than in their ancestors (Cagliani et al., 2014a; Cridland et al., 2012). Interestingly, the IFIX gene, which is only found in primates (Cridland et al., 2012), does not contain any PSS in primates, which suggests its conserved functional roles (Cagliani et al., 2014a). Still, this gene shows positive selection in the human lineage (Bracci et al., 2023).

7. Evolution of C-type-lectin receptors

The C-type-Lectin-receptors (CLRs) belong to a superfamily of C-type lectin-like domains (CTLDs), Ca^{2+}-dependent carbohydrate-binding proteins that are characterised by the presence of a protein domain consisting of double-loop structure stabilized by two highly conserved disulphide bridges (Zelensky and Gready, 2005). CLRs are transmembrane receptors with a cytoplasmatic domain and an ectodomain containing the carbohydrate-recognition domain. The interaction of CLR with the pathogen-associated carbohydrates (in viruses namely mannose, and fucose) that potentially triggers the CLR oligomerization (Bermejo-Jambrina et al., 2018; Brown et al., 2007) leads to pathogen internalization and also the downstream signalling upregulating production of pro-inflammatory cytokines and interferons (Monteiro and Lepenies, 2017).

Compared to other PRRs, the CLRs show in mammals the highest frequencies of PSS, which is due to their relatively small molecular sizes rather than high numbers of PSS (Tian et al., 2018). This applies especially to the Dectin2 protein followed by Dectin1 and MINCLE. The majority of these CLR PSS are found in the extracellular domain interacting with the pathogen-derived ligands (Tian et al., 2018). The results obtained in primates on the CD209 CLR gene subfamily consisting of CD209 (DC-SIGN), CD209L (L-SIGN) and CD209L2 support positive selection acting especially on *CD209L* (Ortiz et al., 2008). In contrast, only limited positive selection has been found in *CD209L* in fish (Shu et al., 2015). It turns out that similar to TLRs the general pattern of CLR evolution is by purifying selection with episodes of strong positive selection acting at specific sites mainly in the ligand-binding regions. However, it needs to be highlighted that many CLRs appear to interact with a broad range of pathogens, including bacteria, viruses, and protozoa (Koppel et al., 2004), suggesting that the positive selection observed is not driven only by viral infections.

8. Evolution of other viral sensing PRRs

Although the abovementioned PRRs play crucial roles in vertebrate antiviral immunity, the list would not be complete without mentioning several other viral sensors. For example, the DExD/H helicase protein family includes several non-RLR members that detect viral RNAs and DNAs, such as e.g. DDX1, DDX3, DDX21, DDX23, DDX24, DDX41, DDX60, DHX9 or DHX36 (Neerukonda and Katneni, 2020). However, virtually nothing is known about molecular evolution in these genes except for their presence or absence in distinct taxa. Highly sporadic evidence available to DDX3 paralogues suggests positive selection acting in specific vertebrate lineages (namely the apes; (Chang and Liu, 2010). In DDX3 adaptations at specific sites have been observed, and while these are located out of the helicase domains, at least in one case positive selection modifies the structure of a region potentially affecting protein ligand-binding specificity. Furthermore, a similar absence of data on molecular evolution concerns also other PRRs, including the RNA-sensing Zinc Finger NFX1-Type Containing 1 (ZNFX1) and DNA-sensing c-GMP-AMP synthase (cGAS) activating the stimulator of IFN genes (STING) (Majzoub et al., 2019; Neerukonda and Katneni, 2020; Wu et al., 2014). Also, the molecular evolution of the protein kinase R (PKR) involved in the dsRNA detection and its fish paralogue PKR-like protein kinase containing Z-DNA binding domain (PKZ) is largely unknown. Initial research has indicated that PKR has rapidly evolved in vertebrates (Rothenburg et al., 2009), with episodes of intense positive selection observed for example in primates (Elde et al., 2009). In primates, signals of positive selection have been revealed in the N-terminal dsRNA-binding domain, the spacer region and namely in the C-terminal kinase domain. Interestingly, adaptations targeting the kinase domain appear to contribute to discrimination of the PKR conserved substrate, the translation initiation factor eIF2α, from viral proteins mimicking this phosphorylation target and thus inhibiting the antiviral responses. The functional roles and significance of other possible virus sensors in vertebrates, such as e.g. the Dicer involved in other animal taxa in RNA interference (Iwama and Moran, 2023) or Adenosine deaminase acting on RNA (ADAR) family members editing RNA (Grice and Degnan, 2015), remain presently unclear and, hence, despite some evidence on positive selection in these genes (e.g. Forni et al., 2015) so is our current idea about importance of their molecular evolution for antiviral responses across vertebrate taxa.

9. Conclusion

Altogether, current evidence suggests that vertebrate virus-sensing receptor systems are relatively heterogeneous. The sensors recognising viral nucleic acids appear more conserved and constrained in their variation than receptor systems detecting more complex ligands (e.g. the carbohydrates bound by the CLRs) or receptors sensing other pathogen groups (e.g. TLRs binding bacterial ligands). This is indicated by generally lower interspecific variation and population polymorphism, and also lower numbers of positively selected sites in the coding regions of many of the receptor genes. Understanding of such differences between PRRs in their variation across taxa could guide future research in wildlife immunology and provide major advantage to our ability to predict the zoonotic potential of different animal hosts (Vinkler et al., 2023). However, data allowing such comparisons between genes or species are still scarce and available only for a few major gene families. The reported results often show variation in the strength of adaptive evolution between vertebrate evolutionary lineages, although variation in dataset sizes, diversity, as well as statistical analysis of the sequence data may to a certain extent bias the results and compromise conclusions based on their comparison. The lack of reported results then prevents any statements in the majority of the virus-sensing receptors. Despite these limitations, present studies have indicated specific sites of potential adaptations distributed in different domains of the viral sensors investigated. Several relevant evolutionary phenomena linked to host adaptations to viral infections have been revealed, including arms races putatively modulating ligand binding (Fish and Boissinot, 2015; Jiang et al., 2017), possible adaptation through gene loss (Krchlíková et al., 2021, Krchlíková et al., 2023), concerted evolution between paralogues (Perelygin et al., 2006), convergent evolution between distantly related paralogous genes (Keestra et al., 2010) or balancing selection maintaining adaptive population polymorphism (Cagliani et al., 2014a; Ferguson et al., 2012; Fish and Boissinot, 2015; Lara et al., 2020; Minias and Vinkler, 2022), intriguingly even across speciation events (Ferguson et al., 2008). Other phenomena still await their investigation, including the possible parallel evolution between vertebrate taxa in their viral receptor molecular phenotypes, analogous to convergence observed in bacterial receptors (Králová et al., 2018; Těšický et al., 2020). The availability of genomic sequences across vertebrate taxa is no longer a limitation. However, the development of a more systematic approach and standardised methodology may be needed in future research to reliably describe the evolutionary phenomena.

CRediT authorship contribution statement

Balraj Melepat: Conceptualization, Writing – original draft, Writing – review & editing, Funding acquisition. **Tao Li:** Writing – original draft, Writing – review & editing. **Michal Vinkler:** Conceptualization, Funding acquisition, Supervision, Visualization, Writing – original draft, Writing – review & editing.

Declaration of competing interest

The authors are not aware of any competing interests.

Data availability

No data was used for the research described in the article.

Acknowledgements

This study was supported by Grant Schemes at Charles University (Grant START/SCI/113 with reg. no. CZ.02.2.69/0.0/0.0/19_073/0016935), Czech Science Foundation (project No. 24-12477S), and Institutional Research Support provided by the Ministry of Education, Youth and Sports of the Czech Republic (No. 260684/2023).

References

Ahn, M., Anderson, D.E., Zhang, Q., Tan, C.W., Lim, B.L., Luko, K., Wen, M., Chia, W.N., Mani, S., Wang, L.C., Ng, J.H.J., Sobota, R.M., Dutertre, C.-A., Ginhoux, F., Shi, Z.-L., Irving, A.T., Wang, L.-F., 2019. Dampened NLRP3-mediated inflammation in bats and implications for a special viral reservoir host. Nat Microbiol 4, 789–799. https://doi.org/10.1038/s41564-019-0371-3.

Akira, S., Uematsu, S., Takeuchi, O., 2006. Pathogen recognition and innate immunity. Cell 124, 783–801. https://doi.org/10.1016/j.cell.2006.02.015.

Alcaide, M., Edwards, S.V., 2011. Molecular evolution of the toll-like receptor multigene family in birds. Mol. Biol. Evol. 28, 1703–1715. https://doi.org/10.1093/molbev/msq351.

Allen, I.C., Moore, C.B., Schneider, M., Lei, Y., Davis, B.K., Scull, M.A., Gris, D., Roney, K. E., Zimmermann, A.G., Bowzard, J.B., Ranjan, P., Monroe, K.M., Pickles, R.J., Sambhara, S., Ting, J.P.Y., 2011. NLRX1 protein attenuates inflammatory responses to infection by interfering with the RIG-I-MAVS and TRAF6-NF-κb signaling pathways. Immunity 34, 854–865. https://doi.org/10.1016/j.immuni.2011.03.026.

Areal, H., Abrantes, J., Esteves, P.J., 2011. Signatures of positive selection in Toll-like receptor (TLR) genes in mammals. BMC Evol. Biol. 11, 368. https://doi.org/10.1186/1471-2148-11-368.

Astakhova, N.M., Perelygin, A.A., Zharkikh, A.A., Lear, T.L., Coleman, S.J., MacLeod, J. N., Brinton, M.A., 2009. Characterization of equine and other vertebrate TLR3, TLR7, and TLR8 genes. Immunogenetics 61, 529–539. https://doi.org/10.1007/s00251-009-0381-z.

Atyeo, N., Papp, B., 2022. The ORF45 protein of kaposi's sarcoma-associated herpesvirus and its critical role in the viral life cycle. Viruses 14 (2010). https://doi.org/10.3390/v14092010.

Bainová, H., Králová, T., Bryjová, A., Albrecht, T., Bryja, J., Vinkler, M., 2014. First evidence of independent pseudogenization of Toll-like receptor 5 in passerine birds. Dev. Comp. Immunol. 45, 151–155. https://doi.org/10.1016/j.dci.2014.02.010.

Banerjee, A., Baker, M.L., Kulcsar, K., Misra, V., Plowright, R., Mossman, K., 2020. Novel insights into immune systems of bats. Front. Immunol. 11, 26. https://doi.org/10.3389/fimmu.2020.00026.

Bauernfried, S., Hornung, V., 2022. Human NLRP1: from the shadows to center stage. J. Exp. Med. 219, e20211405 https://doi.org/10.1084/jem.20211405.

Bauernfried, S., Scherr, M.J., Pichlmair, A., Duderstadt, K.E., Hornung, V., 2021. Human NLRP1 is a sensor for double-stranded RNA. Science 371, eabd0811. https://doi.org/10.1126/science.abd0811.

Bermejo-Jambrina, M., Eder, J., Helgers, L.C., Hertoghs, N., Nijmeijer, B.M., Stunnenberg, M., Geijtenbeek, T.B.H., 2018. C-type lectin receptors in antiviral immunity and viral escape. Front. Immunol. 9, 590. https://doi.org/10.3389/fimmu.2018.00590.

Boyle, J.P., Mayle, S., Parkhouse, R., Monie, T.P., 2013. Comparative genomic and sequence analysis provides insight into the molecular functionality of NOD1 and NOD2. Front. Immunol. 4 https://doi.org/10.3389/fimmu.2013.00317.

Bracci, A.N., Dallmann, A., Ding, Q., Hubisz, M.J., Caballero, M., Koren, A., 2023. The evolution of the human DNA replication timing program. Proc. Natl. Acad. Sci. U.S. A. 120 (10), e2213896120 https://doi.org/10.1073/pnas.2213896120.

Brown, J., O'Callaghan, C.A., Marshall, A.S.J., Gilbert, R.J.C., Siebold, C., Gordon, S., Brown, G.D., Jones, E.Y., 2007. Structure of the fungal β-glucan-binding immune receptor dectin-1: implications for function. Protein Sci. 16, 1042–1052. https://doi.org/10.1110/ps.072791207.

Brunette, R.L., Young, J.M., Whitley, D.G., Brodsky, I.E., Malik, H.S., Stetson, D.B., 2012. Extensive evolutionary and functional diversity among mammalian AIM2-like receptors. J. Exp. Med. 209, 1969–1983. https://doi.org/10.1084/jem.20121960.

Buchmann, K., 2014. Evolution of innate immunity: clues from invertebrates via fish to mammals. Front. Immunol. 5 https://doi.org/10.3389/fimmu.2014.00459.

Bustamante, C.D., Fledel-Alon, A., Williamson, S., Nielsen, R., Todd Hubisz, M., Glanowski, S., Tanenbaum, D.M., White, T.J., Sninsky, J.J., Hernandez, R.D., Civello, D., Adams, M.D., Cargill, M., Clark, A.G., 2005. Natural selection on protein-coding genes in the human genome. Nature 437, 1153–1157. https://doi.org/10.1038/nature04240.

Cagliani, R., Forni, D., Biasin, M., Comabella, M., Guerini, F.R., Riva, S., Pozzoli, U., Agliardi, C., Caputo, D., Malhotra, S., Montalban, X., Bresolin, N., Clerici, M., Sironi, M., 2014a. Ancient and recent selective pressures shaped genetic diversity at AIM2-like nucleic acid sensors. Genome Biology and Evolution 6, 830–845. https://doi.org/10.1093/gbe/evu066.

Cagliani, R., Forni, D., Tresoldi, C., Pozzoli, U., Filippi, G., Rainone, V., De Gioia, L., Clerici, M., Sironi, M., 2014b. RIG-I-like receptors evolved adaptively in mammals, with parallel evolution at LGP2 and RIG-I. J. Mol. Biol. 426, 1351–1365. https://doi.org/10.1016/j.jmb.2013.10.040.

Chang, T.-C., Liu, W.-S., 2010. The molecular evolution of PL10 homologs. BMC Evol. Biol. 10, 127. https://doi.org/10.1186/1471-2148-10-127.

Chavarría-Smith, J., Mitchell, P.S., Ho, A.M., Daugherty, M.D., Vance, R.E., 2016. Functional and evolutionary analyses identify proteolysis as a general mechanism for NLRP1 inflammasome activation. PLoS Pathog. 12, e1006052 https://doi.org/10.1371/journal.ppat.1006052.

Chen, S.N., Zou, P.F., Nie, P., 2017. Retinoic acid-inducible gene I (RIG-I)-like receptors (RLRs) in fish: current knowledge and future perspectives. Immunology 151, 16–25. https://doi.org/10.1111/imm.12714.

Chu, P., He, L., Li, Yangyang, Huang, R., Liao, L., Li, Yongming, Zhu, Z., Wang, Y., 2018. Molecular cloning and functional characterisation of NLRX1 in grass carp (*Ctenopharyngodon idella*). Fish Shellfish Immunol. 81, 276–283. https://doi.org/10.1016/j.fsi.2018.07.031.

Cridland, J.A., Curley, E.Z., Wykes, M.N., Schroder, K., Sweet, M.J., Roberts, T.L., Ragan, M.A., Kassahn, K.S., Stacey, K.J., 2012. The mammalian PYHIN gene family: phylogeny, evolution and expression. BMC Evol. Biol. 12, 140. https://doi.org/10.1186/1471-2148-12-140.

Crow, M.S., Cristea, I.M., 2017. Human antiviral protein IFIX suppresses viral gene expression during herpes simplex virus 1 (HSV-1) infection and is counteracted by virus-induced proteasomal degradation. Mol. Cell. Proteomics 16, S200–S214. https://doi.org/10.1074/mcp.M116.064741.

Danilova, N., 2006. The evolution of immune mechanisms. J. Exp. Zool. 306B, 496–520. https://doi.org/10.1002/jez.b.21102.

Darfour-Oduro, K.A., Megens, H.-J., Roca, A.L., Groenen, M.A.M., Schook, L.B., 2016. Evolutionary patterns of Toll-like receptor signaling pathway genes in the Suidae. BMC Evol. Biol. 16, 33. https://doi.org/10.1186/s12862-016-0602-7.

Davies, C.S., Taylor, M.I., Hammers, M., Burke, T., Komdeur, J., Dugdale, H.L., Richardson, D.S., 2021. Contemporary evolution of the innate immune receptor gene *TLR3* in an isolated vertebrate population. Mol. Ecol. 30, 2528–2542. https://doi.org/10.1111/mec.15914.

Diner, B.A., Lum, K.K., Cristea, I.M., 2015. The emerging role of nuclear viral DNA sensors. J. Biol. Chem. 290, 26412–26421. https://doi.org/10.1074/jbc.R115.652289.

Ding, Y., Wang, L., Su, L.-K., Frey, J.A., Shao, R., Hunt, K.K., Yan, D.-H., 2004. Antitumor activity of IFIX, a novel interferon-inducible HIN-200 gene, in breast cancer. Oncogene 23, 4556–4566. https://doi.org/10.1038/sj.onc.1207592.

Dolby, G.A., Morales, M., Webster, T.H., DeNardo, D.F., Wilson, M.A., Kusumi, K., 2020. Discovery of a new TLR gene and gene expansion event through improved desert tortoise genome assembly with chromosome-scale scaffolds. Genome Biology and Evolution 12, 3917–3925. https://doi.org/10.1093/gbe/evaa016.

Elde, N.C., Child, S.J., Geballe, A.P., Malik, H.S., 2009. Protein kinase R reveals an evolutionary model for defeating viral mimicry. Nature 457, 485–489. https://doi.org/10.1038/nature07529.

Escalera-Zamudio, M., Zepeda-Mendoza, M.L., Loza-Rubio, E., Rojas-Anaya, E., Méndez-Ojeda, M.L., Arias, C.F., Greenwood, A.D., 2015. The evolution of bat nucleic acid-sensing Toll-like receptors. Mol. Ecol. 24, 5899–5909. https://doi.org/10.1111/mec.13431.

Eskildsen, S., 2003. Characterization of the 2'-5'-oligoadenylate synthetase ubiquitin-like family. Nucleic Acids Res. 31, 3166–3173. https://doi.org/10.1093/nar/gkg427.

Fairbrother, W.J., Gordon, N.C., Humke, E.W., O'Rourke, K.M., Starovasnik, M.A., Yin, J.-P., Dixit, V.M., 2001. The PYRIN domain: a member of the death domain-fold superfamily. Protein Sci. 10, 1911–1918. https://doi.org/10.1110/ps.13801.

Fan, X., Jiao, L., Jin, T., 2022. Activation and immune regulation mechanisms of PYHIN family during microbial infection. Front. Microbiol. 12, 809412 https://doi.org/10.3389/fmicb.2021.809412.

Fekete, T., Ágics, B., Bencze, D., Bene, K., Szántó, A., Tarr, T., Veréb, Z., Bácsi, A., Pázmándi, K., 2020. Regulation of RLR-mediated antiviral responses of human dendritic cells by mTOR. Front. Immunol. 11, 572960 https://doi.org/10.3389/fimmu.2020.572960.

Fekete, T., Bencze, D., Szabo, A., Csoma, E., Biro, T., Bacsi, A., Pazmandi, K., 2018. Regulatory NLRs control the RLR-mediated type I interferon and inflammatory responses in human dendritic cells. Front. Immunol. 9, 2314. https://doi.org/10.3389/fimmu.2018.02314.

Ferguson, W., Dvora, S., Fikes, R.W., Stone, A.C., Boissinot, S., 2012. Long-term balancing selection at the antiviral gene OAS1 in central african chimpanzees. Mol. Biol. Evol. 29, 1093–1103. https://doi.org/10.1093/molbev/msr247.

Ferguson, W., Dvora, S., Gallo, J., Orth, A., Boissinot, S., 2008. Long-term balancing selection at the west nile virus resistance gene, Oas1b, maintains transspecific polymorphisms in the house mouse. Mol. Biol. Evol. 25, 1609–1618. https://doi.org/10.1093/molbev/msn106.

Fiddaman, S.R., Vinkler, M., Spiro, S.G., Levy, H., Emerling, C.A., Boyd, A.C., Dimopoulos, E.A., Vianna, J.A., Cole, T.L., Pan, H., Fang, M., Zhang, G., Hart, T., Frantz, L.A.F., Smith, A.L., 2022. Adaptation and cryptic pseudogenization in penguin toll-like receptors. Mol. Biol. Evol. 39, msab354. https://doi.org/10.1093/molbev/msab354.

Finger, J.N., Lich, J.D., Dare, L.C., Cook, M.N., Brown, K.K., Duraiswami, C., Bertin, J.J., Gough, P.J., 2012. Autolytic proteolysis within the function to find domain (FIIND) is required for NLRP1 inflammasome activity. J. Biol. Chem. 287, 25030–25037. https://doi.org/10.1074/jbc.M112.378323.

Fish, I., Boissinot, S., 2016. Functional evolution of the OAS1 viral sensor: insights from old world primates. Infect. Genet. Evol. 44, 341–350. https://doi.org/10.1016/j.meegid.2016.07.005.

Fish, I., Boissinot, S., 2015. Contrasted patterns of variation and evolutionary convergence at the antiviral OAS1 gene in old world primates. Immunogenetics 67, 487–499. https://doi.org/10.1007/s00251-015-0855-0.

Forni, D., Mozzi, A., Pontremoli, C., Vertemara, J., Pozzoli, U., Biasin, M., Bresolin, N., Clerici, M., Cagliani, R., Sironi, M., 2015. Diverse selective regimes shape genetic diversity at *ADAR* genes and at their coding targets. RNA Biol. 12, 149–161. https://doi.org/10.1080/15476286.2015.1017215.

Fornůsková, A., Vinkler, M., Pagès, M., Galan, M., Jousselin, E., Cerqueira, F., Morand, S., Charbonnel, N., Bryja, J., Cosson, J.-F., 2013. Contrasted evolutionary histories of two Toll-like receptors (*Tlr4* and *Tlr7*) in wild rodents (MURINAE). BMC Evol. Biol. 13, 194. https://doi.org/10.1186/1471-2148-13-194.

Fumagalli, M., Sironi, M., Pozzoli, U., Ferrer-Admettla, A., Pattini, L., Nielsen, R., 2011. Signatures of environmental genetic adaptation pinpoint pathogens as the main selective pressure through human evolution. PLoS Genet. 7, e1002355 https://doi.org/10.1371/journal.pgen.1002355.

George, R.D., McVicker, G., Diederich, R., Ng, S.B., MacKenzie, A.P., Swanson, W.J., Shendure, J., Thomas, J.H., 2011. *Trans* genomic capture and sequencing of primate exomes reveals new targets of positive selection. Genome Res. 21, 1686–1694. https://doi.org/10.1101/gr.121327.111.

Ghosh, M., Basak, S., Dutta, S., 2022. Natural selection shaped the evolution of amino acid usage in mammalian toll like receptor genes. Comput. Biol. Chem. 97, 107637 https://doi.org/10.1016/j.compbiolchem.2022.107637.

Gilroy, D.L., Phillips, K.P., Richardson, D.S., van Oosterhout, C., 2017. Toll-like receptor variation in the bottlenecked population of the Seychelles warbler: computer simulations see the 'ghost of selection past' and quantify the 'drift debt. J. Evol. Biol. 30, 1276–1287. https://doi.org/10.1111/jeb.13077.

Godkowicz, M., Druszczyńska, M., 2022. NOD1, NOD2, and NLRC5 receptors in antiviral and antimycobacterial immunity. Vaccines 10, 1487. https://doi.org/10.3390/vaccines10091487.

Gordon, D.E., Jang, G.M., Bouhaddou, M., Xu, J., Obernier, K., White, K.M., O'Meara, M. J., Rezelj, V.V., Guo, J.Z., Swaney, D.L., Tummino, T.A., Hüttenhain, R., Kaake, R. M., Richards, A.L., Tutuncuoglu, B., Foussard, H., Batra, J., Haas, K., Modak, M., Kim, M., Haas, P., Polacco, B.J., Braberg, H., Fabius, J.M., Eckhardt, M., Soucheray, M., Bennett, M.J., Cakir, M., McGregor, M.J., Li, Q., Meyer, B., Roesch, F., Vallet, T., Mac Kain, A., Miorin, L., Moreno, E., Naing, Z.Z.C., Zhou, Y., Peng, S., Shi, Y., Zhang, Z., Shen, W., Kirby, I.T., Melnyk, J.E., Chorba, J.S., Lou, K., Dai, S.A., Barrio-Hernandez, I., Memon, D., Hernandez-Armenta, C., Lyu, J., Mathy, C.J.P., Perica, T., Pilla, K.B., Ganesan, S.J., Saltzberg, D.J., Rakesh, R., Liu, X., Rosenthal, S.B., Calviello, L., Venkataramanan, S., Liboy-Lugo, J., Lin, Y., Huang, X.-P., Liu, Y., Wankowicz, S.A., Bohn, M., Safari, M., Ugur, F.S., Koh, C., Savar, N.S., Tran, Q.D., Shengjuler, D., Fletcher, S.J., O'Neal, M.C., Cai, Y., Chang, J. C.J., Broadhurst, D.J., Klippsten, S., Sharp, P.P., Wenzell, N.A., Kuzuoglu-Ozturk, D., Wang, H.-Y., Trenker, R., Young, J.M., Cavero, D.A., Hiatt, J., Roth, T.L., Rathore, U., Subramanian, A., Noack, J., Hubert, M., Stroud, R.M., Frankel, A.D., Rosenberg, O. S., Verba, K.A., Agard, D.A., Ott, M., Emerman, M., Jura, N., Von Zastrow, M., Verdin, E., Ashworth, A., Schwartz, O., d'Enfert, C., Mukherjee, S., Jacobson, M., Malik, H.S., Fujimori, D.G., Ideker, T., Craik, C.S., Floor, S.N., Fraser, J.S., Gross, J. D., Sali, A., Roth, B.L., Ruggero, D., Taunton, J., Kortemme, T., Beltrao, P.,

Vignuzzi, M., García-Sastre, A., Shokat, K.M., Shoichet, B.K., Krogan, N.J., 2020. A SARS-CoV-2 protein interaction map reveals targets for drug repurposing. Nature 583, 459–468. https://doi.org/10.1038/s41586-020-2286-9.

Gosu, V., Son, S., Shin, D., Song, K.-D., 2019. Insights into the dynamic nature of the dsRNA-bound TLR3 complex. Sci. Rep. 9, 3652. https://doi.org/10.1038/s41598-019-39984-8.

Graham, A.L., Allen, J.E., Read, A.F., 2005. Evolutionary causes and consequences of immunopathology. Annu. Rev. Ecol. Evol. Syst. 36, 373–397. https://doi.org/10.1146/annurev.ecolsys.36.102003.152622.

Gregory, S.M., Davis, B.K., West, J.A., Taxman, D.J., Matsuzawa, S., Reed, J.C., Ting, J.P. Y., Damania, B., 2011. Discovery of a viral NLR homolog that inhibits the inflammasome. Science 331, 330–334. https://doi.org/10.1126/science.1199478.

Grice, L.F., Degnan, B.M., 2015. The origin of the ADAR gene family and animal RNA editing. BMC Evol. Biol. 15, 4. https://doi.org/10.1186/s12862-015-0279-3.

Grueber, C.E., Wallis, G.P., Jamieson, I.G., 2014. Episodic positive selection in the evolution of avian toll-like receptor innate immunity genes. PLoS One 9, e89632. https://doi.org/10.1371/journal.pone.0089632.

Grueber, C.E., Wallis, G.P., King, T.M., Jamieson, I.G., 2012. Variation at innate immunity toll-like receptor genes in a bottlenecked population of a New Zealand robin. PLoS One 7, e45011. https://doi.org/10.1371/journal.pone.0045011.

Guo, H., König, R., Deng, M., Riess, M., Mo, J., Zhang, L., Petrucelli, A., Yoh, S.M., Barefoot, B., Samo, M., Sempowski, G.D., Zhang, A., Colberg-Poley, A.M., Feng, H., Lemon, S.M., Liu, Y., Zhang, Y., Wen, H., Zhang, Z., Damania, B., Tsao, L.-C., Wang, Q., Su, L., Duncan, J.A., Chanda, S.K., Ting, J.P.-Y., 2016. NLRX1 sequesters STING to negatively regulate the interferon response, thereby facilitating the replication of HIV-1 and DNA viruses. Cell Host Microbe 19, 515–528. https://doi.org/10.1016/j.chom.2016.03.001.

Han, C., Li, Q., Liu, J., Hao, Z., Huang, J., Zhang, Y., 2019. Characterization, evolution, and expression analysis of TLR7 gene subfamily members in *Mastacembelus armatus* (Synbranchiformes: mastacembelidae). Dev. Comp. Immunol. 95, 77–88. https://doi.org/10.1016/j.dci.2019.02.002.

Heng, J., Su, J., Huang, T., Dong, J., Chen, L., 2011. The polymorphism and haplotype of TLR3 gene in grass carp (*Ctenopharyngodon idella*) and their associations with susceptibility/resistance to grass carp reovirus. Fish Shellfish Immunol. 30, 45–50. https://doi.org/10.1016/j.fsi.2010.09.004.

Henschen, A.E., Vinkler, M., Langager, M.M., Rowley, A.A., Dalloul, R.A., Hawley, D.M., Adelman, J.S., 2023. Rapid adaptation to a novel pathogen through disease tolerance in a wild songbird. PLoS Pathog. 19, e1011408 https://doi.org/10.1371/journal.ppat.1011408.

Hillier, L.W., Miller, W., Birney, E., Warren, W., Hardison, R.C., Ponting, C.P., 2004. Sequence and comparative analysis of the chicken genome provide unique perspectives on vertebrate evolution. Nature 432, 695–716. https://doi.org/10.1038/nature03154.

Ho, W.-H.J., Law, A.M.K., Masle-Farquhar, E., Castillo, L.E., Mawson, A., O'Bryan, M.K., Goodnow, C.C., Gallego-Ortega, D., Oakes, S.R., Ormandy, C.J., 2022. Activation of the viral sensor oligoadenylate synthetase 2 (Oas2) prevents pregnancy-driven mammary cancer metastases. Breast Cancer Res. 24, 31. https://doi.org/10.1186/s13058-022-01525-z.

Hong, M., Yoon, S., Wilson, I.A., 2012. Structure and functional characterization of the RNA-binding element of the NLRX1 innate immune modulator. Immunity 36, 337–347. https://doi.org/10.1016/j.immuni.2011.12.018.

Horrocks, N.P.C., Matson, K.D., Tieleman, B.I., 2011. Pathogen pressure puts immune defense into perspective. Integr. Comp. Biol. 51, 563–576. https://doi.org/10.1093/icb/icr011.

Hu, J., Wang, X., Xing, Y., Rong, E., Ning, M., Smith, J., Huang, Y., 2018. Origin and development of oligoadenylate synthetase immune system. BMC Evol. Biol. 18, 201. https://doi.org/10.1186/s12862-018-1315-x.

Huang, R., Dong, F., Jang, S., Liao, L., Zhu, Z., Wang, Y., 2012. Isolation and analysis of a novel grass carp toll-like receptor 4 (tlr4) gene cluster involved in the response to grass carp reovirus. Dev. Comp. Immunol. 38, 383–388. https://doi.org/10.1016/j.dci.2012.06.002.

Hughes, A.L., 2006. Evolutionary relationships of vertebrate NACHT domain-containing proteins. Immunogenetics 58, 785–791. https://doi.org/10.1007/s00251-006-0148-8.

Hussell, T., Pennycook, A., Openshaw, P.J.M., 2001. Inhibition of tumor necrosis factor reduces the severity of virus-specific lung immunopathology. Eur. J. Immunol. 31, 2566–2573. https://doi.org/10.1002/1521-4141(200109)31:9<2566::AID-IMMU2566>3.0.CO;2-L.

Iwama, R.E., Moran, Y., 2023. Origins and diversification of animal innate immune responses against viral infections. Nat Ecol Evol. https://doi.org/10.1038/s41559-022-01951-4.

Jacobs, S.R., Damania, B., 2012. NLRs, inflammasomes, and viral infection. J. Leukoc. Biol. 92, 469–477. https://doi.org/10.1189/jlb.0312132.

Ji, J., Rao, Y., Wan, Q., Liao, Z., Su, J., 2018. Teleost-specific TLR19 localizes to endosome, recognizes dsRNA, recruits TRIF, triggers both IFN and NF-κB pathways, and protects cells from grass carp reovirus infection. J. Immunol. 200, 573–585. https://doi.org/10.4049/jimmunol.1701149.

Jiang, F., Ramanathan, A., Miller, M.T., Tang, G.Q., Gale, M., Patel, S.S., Marcotrigiano, J., 2011. Structural basis of RNA recognition and activation by innate immune receptor RIG-I. Nature 423–427. https://doi.org/10.1038/nature10537, 2011 479:7373 479.

Jiang, H., Li, J., Li, L., Zhang, X., Yuan, L., Chen, J., 2017. Selective evolution of Toll-like receptors 3, 7, 8, and 9 in bats. Immunogenetics 69, 271–285. https://doi.org/10.1007/s00251-016-0966-2.

Jiang, H., Swacha, P., Gekara, N.O., 2021. Nuclear AIM2-like receptors drive genotoxic tissue injury by inhibiting DNA repair. Adv. Sci. 8, 2102534 https://doi.org/10.1002/advs.202102534.

Jiang, Z., Wei, F., Zhang, Y., Wang, T., Gao, W., Yu, S., Sun, H., Pu, J., Sun, Y., Wang, M., Tong, Q., Gao, C., Chang, K.-C., Liu, J., 2021. IFI16 directly senses viral RNA and enhances RIG-I transcription and activation to restrict influenza virus infection. Nat Microbiol 6, 932–945. https://doi.org/10.1038/s41564-021-00907-x.

Jin, T., Perry, A., Smith, P., Jiang, J., Xiao, T.S., 2013. Structure of the absent in melanoma 2 (AIM2) pyrin domain provides insights into the mechanisms of AIM2 autoinhibition and inflammasome assembly. J. Biol. Chem. 288, 13225–13235. https://doi.org/10.1074/jbc.M113.468033.

Jing, H., Song, T., Cao, S., Sun, Y., Wang, J., Dong, W., Zhang, Y., Ding, Z., Wang, T., Xing, Z., Bao, W., 2019. Nucleotide-binding oligomerization domain-like receptor X1 restricts porcine reproductive and respiratory syndrome virus-2 replication by interacting with viral Nsp9. Virus Res. 268, 18–26. https://doi.org/10.1016/j.virusres.2019.05.011.

Jones, K.E., Patel, N.G., Levy, M.A., Storeygard, A., Balk, D., Gittleman, J.L., Daszak, P., 2008. Global trends in emerging infectious diseases. Nature 451, 990–993. https://doi.org/10.1038/nature06536.

Karesh, W.B., Dobson, A., Lloyd-Smith, J.O., Lubroth, J., Dixon, M.A., Bennett, M., Aldrich, S., Harrington, T., Formenty, P., Loh, E.H., Machalaba, C.C., Thomas, M.J., Heymann, D.L., 2012. Ecology of zoonoses: natural and unnatural histories. Lancet 380, 1936–1945. https://doi.org/10.1016/S0140-6736(12)61678-X.

Keestra, A.M., de Zoete, M.R., Bouwman, L.I., van Putten, J.P.M., 2010. Chicken TLR21 is an innate CpG DNA receptor distinct from mammalian TLR9. J. Immunol. 185, 460–467. https://doi.org/10.4049/jimmunol.0901921.

Khan, I., Maldonado, E., Silva, L., Almeida, D., Johnson, W.E., O'Brien, S.J., Zhang, G., Jarvis, E.D., Gilbert, M.T.P., Antunes, A., 2019. The vertebrate TLR supergene family evolved dynamically by gene gain/loss and positive selection revealing a host–pathogen arms race in birds. Diversity 11, 131. https://doi.org/10.3390/d11080131.

Kjaer, K.H., Poulsen, J.B., Reintamm, T., Saby, E., Martensen, P.M., Kelve, M., Justesen, J., 2009. Evolution of the 2′-5′-oligoadenylate synthetase family in eukaryotes and bacteria. J. Mol. Evol. 69, 612–624. https://doi.org/10.1007/s00239-009-9299-1.

Kloch, A., Wenzel, M.A., Laetsch, D.R., Michalski, O., Bajer, A., Behnke, J.M., Welc-Falęciak, R., Piertney, S.B., 2018. Signatures of balancing selection in toll-like receptor (TLRs) genes – novel insights from a free-living rodent. Sci. Rep. 8, 8361. https://doi.org/10.1038/s41598-018-26672-2.

Koppel, E.A., Van Gisbergen, K.P.J.M., Geijtenbeek, T.B.H., Van Kooyk, Y., 2004. Distinct functions of DC-SIGN and its homologues L-SIGN (DC-SIGNR) and mSIGNR1 in pathogen recognition and immune regulation: functions of DC-SIGN and its homologues. Cell Microbiol. 7, 157–165. https://doi.org/10.1111/j.1462-5822.2004.00480.x.

Králová, T., Albrecht, T., Bryja, J., Hořák, D., Johnsen, A., Lifjeld, J.T., Novotný, M., Sedláček, O., Velová, H., Vinkler, M., 2018. Signatures of diversifying selection and convergence acting on passerine Toll-like receptor 4 in an evolutionary context. Mol. Ecol. 27, 2871–2883. https://doi.org/10.1111/mec.14724.

Krchlíková, V., Hron, T., Těšický, M., Li, T., Hejnar, J., Vinkler, M., Elleder, D., 2021. Repeated MDA5 gene loss in birds: an evolutionary perspective. Viruses 13, 2131. https://doi.org/10.3390/v13112131.

Krchlíková, V., Hron, T., Těšický, M., Li, T., Ungrová, L., Hejnar, J., Vinkler, M., Elleder, D., 2023. Dynamic evolution of avian RNA virus sensors: repeated loss of RIG-I and RIPLET. Viruses 15, 3. https://doi.org/10.3390/v15010003.

Kruse, H., Kirkemo, A.-M., Handeland, K., 2004. Wildlife as source of zoonotic infections. Emerg. Infect. Dis. 10, 2067–2072. https://doi.org/10.3201/eid1012.040707.

Kumar, S., Mitnik, C., Valente, G., Floyd-Smith, G., 2000. Expansion and molecular evolution of the interferon-induced 2′–5′ oligoadenylate synthetase gene family. Mol. Biol. Evol. 17, 738–750. https://doi.org/10.1093/oxfordjournals.molbev.a026352.

Lara, C.E., Grueber, C.E., Holtmann, B., Santos, E.S.A., Johnson, S.L., Robertson, B.C., Castaño-Villa, G.J., Lagisz, M., Nakagawa, S., 2020. Assessment of the dunnocks' introduction to New Zealand using innate immune-gene diversity. Evol. Ecol. 34, 803–820. https://doi.org/10.1007/s10682-020-10070-0.

Lebov, J., Grieger, K., Womack, D., Zaccaro, D., Whitehead, N., Kowalcyk, B., MacDonald, P.D.M., 2017. A framework for One Health research. One Health 3, 44–50. https://doi.org/10.1016/j.onehlt.2017.03.004.

Lee, H.-C., Chathuranga, K., Lee, J.-S., 2019. Intracellular sensing of viral genomes and viral evasion. Exp. Mol. Med. 51, 1–13. https://doi.org/10.1038/s12276-019-0299-y.

Lemos De Matos, A., McFadden, G., Esteves, P.J., 2013. Positive evolutionary selection on the RIG-I-like receptor genes in mammals. PLoS One 8, e81864. https://doi.org/10.1371/JOURNAL.PONE.0081864.

Lenz, T.L., Eizaguirre, C., Kalbe, M., Milinski, M., 2013. Evaluating patterns of convergent evolution and trans-species polymorphism at MHC immunogenes in two sympatric stickleback species: MHC evolution in two sympatric stickleback species. Evolution 67, 2400–2412. https://doi.org/10.1111/evo.12124.

Leung, D.W., Amarasinghe, G.K., 2012. Structural insights into RNA recognition and activation of RIG-I-like receptors. Curr. Opin. Struct. Biol. 22, 297–303. https://doi.org/10.1016/j.sbi.2012.03.011.

Li, D., Wu, M., 2021. Pattern recognition receptors in health and diseases. Sig Transduct Target Ther 6, 291. https://doi.org/10.1038/s41392-021-00687-0.

Li, J., Gao, Y., Xu, T., 2015a. Comparative genomic and evolution of vertebrate NOD1 and NOD2 genes and their immune response in miiuy croaker. Fish Shellfish Immunol. 46, 387–397. https://doi.org/10.1016/j.fsi.2015.06.026.

Li, J., Kong, L., Gao, Y., Wu, C., Xu, T., 2015b. Characterization of NLR-A subfamily members in miiuy croaker and comparative genomics revealed NLRX1 underwent

duplication and lose in actinopterygii. Fish Shellfish Immunol. 47, 397–406. https://doi.org/10.1016/j.fsi.2015.09.024.
Li, L., Yu, H., Jiang, Y., Deng, B., Bai, L., Kijlstra, A., Yang, P., 2016. Genetic variations of NLR family genes in behcet's disease. Sci. Rep. 6, 20098 https://doi.org/10.1038/srep20098.
Li, X., Deng, M., Petrucelli, A.S., Zhu, C., Mo, J., Zhang, L., Tam, J.W., Ariel, P., Zhao, B., Zhang, S., Ke, H., Li, P., Dokholyan, N.V., Duncan, J.A., Ting, J.P.-Y., 2019. Viral DNA binding to NLRC3, an inhibitory nucleic acid sensor, unleashes STING, a cyclic dinucleotide receptor that activates type I interferon. Immunity 50, 591–599.e6. https://doi.org/10.1016/j.immuni.2019.02.009.
Li, X., Lu, C., Stewart, M., Xu, H., Strong, R.K., Igumenova, T., Li, P., 2009a. Structural basis of double-stranded RNA recognition by the RIG-I like receptor MDA5. Arch. Biochem. Biophys. 488, 23–33. https://doi.org/10.1016/j.abb.2009.06.008.
Li, X., Ranjith-Kumar, C.T., Brooks, M.T., Dharmaiah, S., Herr, A.B., Kao, C., Li, P., 2009b. The RIG-I-like receptor LGP2 recognizes the termini of double-stranded RNA. J. Biol. Chem. 284, 13881–13891. https://doi.org/10.1074/jbc.M900818200.
Liang, N., Yang, Y.-P., Li, W., Wu, Y.-Y., Zhang, Z.-W., Luo, Y., Fan, Y.-M., 2018. Overexpression of NLRP3, NLRC4 and AIM2 inflammasomes and their priming-associated molecules (TLR2, TLR4, Dectin-1, Dectin-2 and NFκB) in *Malassezia folliculitis*. Mycoses 61, 111–118. https://doi.org/10.1111/myc.12711.
Liao, Z., Su, J., 2021. Progresses on three pattern recognition receptor families (TLRs, RLRs and NLRs) in teleost. Dev. Comp. Immunol. 122, 104131 https://doi.org/10.1016/j.dci.2021.104131.
Liu, G., Wu, X., Shang, Y., Wang, X., Zhou, S., Zhang, H., 2023. Adaptive evolution of the OAS gene family provides new insights into the antiviral ability of laurasiatherian mammals. Animals 13, 209. https://doi.org/10.3390/ani13020209.
Liu, G., Zhang, Huanxin, Zhao, C., Zhang, Honghai, 2020. Evolutionary history of the toll-like receptor gene family across vertebrates. Genome Biology and Evolution 12, 3615–3634. https://doi.org/10.1093/gbe/evz266.
Liu, L., Botos, I., Wang, Y., Leonard, J.N., Shiloach, J., Segal, D.M., Davies, D.R., 2008. Structural basis of toll-like receptor 3 signaling with double-stranded RNA. Science 320, 379–381. https://doi.org/10.1126/science.1155406.
Lupfer, C., Kanneganti, T.-D., 2013. Unsolved mysteries in NLR biology. Front. Immunol. 4 https://doi.org/10.3389/fimmu.2013.00285.
Ma, X., Liu, B., Gong, Z., Yu, X., Cai, J., 2021. Structural and evolutionary adaptation of NOD-like receptors in birds. BioMed Res. Int. 2021, 1–11. https://doi.org/10.1155/2021/5546170.
Magor, K.E., 2022. Evolution of RNA sensing receptors in birds. Immunogenetics 74, 149–165. https://doi.org/10.1007/s00251-021-01238-1.
Majzoub, K., Wrensch, F., Baumert, T.F., 2019. The innate antiviral response in animals: an evolutionary perspective from flagellates to humans. Viruses 11, 758. https://doi.org/10.3390/v11080758.
Matsuo, A., Oshiumi, H., Tsujita, T., Mitani, H., Kasai, H., Yoshimizu, M., Matsumoto, M., Seya, T., 2008. Teleost TLR22 recognizes RNA duplex to induce IFN and protect cells from birnaviruses. J. Immunol. 181, 3474–3485. https://doi.org/10.4049/jimmunol.181.5.3474.
Meissner, T.B., Li, A., Biswas, A., Lee, K.-H., Liu, Y.-J., Bayir, E., Iliopoulos, D., van den Elsen, P.J., Kobayashi, K.S., 2010. NLR family member NLRC5 is a transcriptional regulator of MHC class I genes. Proc. Natl. Acad. Sci. U.S.A. 107, 13794–13799. https://doi.org/10.1073/pnas.1008684107.
Mikami, T., Miyashita, H., Takatsuka, S., Kuroki, Y., Matsushima, N., 2012. Molecular evolution of vertebrate Toll-like receptors: evolutionary rate difference between their leucine-rich repeats and their TIR domains. Gene 503, 235–243. https://doi.org/10.1016/j.gene.2012.04.007.
Minias, P., Vinkler, M., 2022. Selection balancing at innate immune genes: adaptive polymorphism maintenance in toll-like receptors. Mol. Biol. Evol. 39, msac102. https://doi.org/10.1093/molbev/msac102.
Mojzesz, M., Rakus, K., Chadzinska, M., Nakagami, K., Biswas, G., Sakai, M., Hikima, J., 2020. Cytosolic sensors for pathogenic viral and bacterial nucleic acids in fish. IJMS 21, 7289. https://doi.org/10.3390/ijms21197289.
Monteiro, J., Lepenies, B., 2017. Myeloid C-type lectin receptors in viral recognition and antiviral immunity. Viruses 9, 59. https://doi.org/10.3390/v9030059.
Moore, C.B., Bergstralh, D.T., Duncan, J.A., Lei, Y., Morrison, T.E., Zimmermann, A.G., Accavitti-Loper, M.A., Madden, V.J., Sun, L., Ye, Z., Lich, J.D., Heise, M.T., Chen, Z., Ting, J.P.-Y., 2008. NLRX1 is a regulator of mitochondrial antiviral immunity. Nature 451, 573–577. https://doi.org/10.1038/nature06501.
Mozzi, A., Pontremoli, C., Forni, D., Clerici, M., Pozzoli, U., Bresolin, N., Cagliani, R., Sironi, M., 2015. OASes and STING: adaptive evolution in concert. Genome Biology and Evolution 7, 1016–1032. https://doi.org/10.1093/gbe/evv046.
Nabi, G., Wang, Y., Lü, L., Jiang, C., Ahmad, S., Wu, Y., Li, D., 2021. Bats and birds as viral reservoirs: a physiological and ecological perspective. Sci. Total Environ. 754, 142372 https://doi.org/10.1016/j.scitotenv.2020.142372.
Neerukonda, S.N., Katneni, U., 2020. Avian pattern recognition receptor sensing and signaling. Veterinary Sciences 7, 14. https://doi.org/10.3390/vetsci7010014.
Nelson-Flower, M.J., Germain, R.R., MacDougall-Shackleton, E.A., Taylor, S.S., Arcese, P., 2018. Purifying selection in the toll-like receptors of song sparrows melospiza melodia. J. Hered. 109, 501–509. https://doi.org/10.1093/jhered/esy027.
Neves, F., Marques, J.P., Areal, H., Pinto-Pinho, P., Colaço, B., Melo-Ferreira, J., Fardilha, M., Abrantes, J., Esteves, P.J., 2022. TLR7 and TLR8 evolution in lagomorphs: different patterns in the different lineages. Immunogenetics 74, 475–485. https://doi.org/10.1007/s00251-022-01262-9.
Nie, L., Cai, S.-Y., Shao, J.-Z., Chen, J., 2018. Toll-like receptors, associated biological roles, and signaling networks in non-mammals. Front. Immunol. 9, 1523. https://doi.org/10.3389/fimmu.2018.01523.
Oakes, S.R., Gallego-Ortega, D., Stanford, P.M., Junankar, S., Au, W.W.Y., Kikhtyak, Z., von Korff, A., Sergio, C.M., Law, A.M.K., Castillo, L.E., Allerdice, S.L., Young, A.I.J., Piggin, C., Whittle, B., Bertram, E., Naylor, M.J., Roden, D.L., Donovan, J., Korennykh, A., Goodnow, C.C., O'Bryan, M.K., Ormandy, C.J., 2017. A mutation in the viral sensor 2'-5'-oligoadenylate synthetase 2 causes failure of lactation. PLoS Genet. 13, e1007072 https://doi.org/10.1371/journal.pgen.1007072.
Olejnik, J., Hume, A.J., Mühlberger, E., 2018. Toll-like receptor 4 in acute viral infection: too much of a good thing. PLoS Pathog. 14, e1007390 https://doi.org/10.1371/journal.ppat.1007390.
Ortiz, M., Kaessmann, H., Zhang, K., Bashirova, A., Carrington, M., Quintana-Murci, L., Telenti, A., 2008. The evolutionary history of the CD209 (DC-SIGN) family in humans and non-human primates. Genes Immun 9, 483–492. https://doi.org/10.1038/gene.2008.40.
Palm, N.W., Medzhitov, R., 2009. Pattern recognition receptors and control of adaptive immunity. Immunol. Rev. 227, 221–233. https://doi.org/10.1111/j.1600-065X.2008.00731.x.
Pålsson-McDermott, E.M., O'Neill, L.A.J., 2007. Building an immune system from nine domains. Biochem. Soc. Trans. 35, 1437–1444. https://doi.org/10.1042/BST0351437.
Parvatiyar, K., Cheng, G., 2011. NOD so fast: NLRX1 puts the brake on inflammation. Immunity 34, 821–822. https://doi.org/10.1016/j.immuni.2011.06.006.
Perelygin, A.A., Zharkikh, A.A., Scherbik, S.V., Brinton, M.A., 2006. The mammalian 2′-5′ oligoadenylate synthetase gene family: evidence for concerted evolution of paralogous Oas1 genes in rodentia and Artiodactyla. J. Mol. Evol. 63, 562–576. https://doi.org/10.1007/s00239-006-0073-3.
Philbin, V.J., Iqbal, M., Boyd, Y., Goodchild, M.J., Beal, R.K., Bumstead, N., Young, J., Smith, A.L., 2005. Identification and characterization of a functional, alternatively spliced Toll-like receptor 7 (TLR7) and genomic disruption of TLR8 in chickens. Immunology 114, 507–521. https://doi.org/10.1111/j.1365-2567.2005.02125.x.
Pippig, D.A., Hellmuth, J.C., Cui, S., Kirchhofer, A., Lammens, K., Lammens, A., Schmidt, A., Rothenfusser, S., Hopfner, K.P., 2009. The regulatory domain of the RIG-I family ATPase LGP2 senses double-stranded RNA. Nucleic Acids Res. 37, 2014. https://doi.org/10.1093/NAR/GKP059.
Plowright, R.K., Peel, A.J., Streicker, D.G., Gilbert, A.T., McCallum, H., Wood, J., Baker, M.L., Restif, O., 2016. Transmission or within-host dynamics driving pulses of zoonotic viruses in reservoir–host populations. PLoS Negl Trop Dis 10, e0004796. https://doi.org/10.1371/journal.pntd.0004796.
Qi, D., Xia, M., Chao, Y., Zhao, Y., Wu, R., 2017. Identification, molecular evolution of toll-like receptors in a Tibetan schizothoracine fish (*Gymnocypris eckloni*) and their expression profiles in response to acute hypoxia. Fish Shellfish Immunol. 68, 102–113. https://doi.org/10.1016/j.fsi.2017.07.014.
Råberg, L., Sim, D., Read, A.F., 2007. Disentangling genetic variation for resistance and tolerance to infectious diseases in animals. Science 318, 812–814. https://doi.org/10.1126/science.1148526.
Ramos, H.J., Gale, M., 2011. RIG-I like receptors and their signaling crosstalk in the regulation of antiviral immunity. Current Opinion in Virology 1, 167–176. https://doi.org/10.1016/J.COVIRO.2011.04.004.
Ranjan, P., Singh, N., Kumar, A., Neerincx, A., Kremmer, E., Cao, W., Davis, W.G., Katz, J.M., Gangappa, S., Lin, R., Kufer, T.A., Sambhara, S., 2015. NLRC5 interacts with RIG-I to induce a robust antiviral response against influenza virus infection: immunity to infection. Eur. J. Immunol. 45, 758–772. https://doi.org/10.1002/eji.201344412.
Rong, E., Wang, X., Chen, H., Yang, C., Hu, J., Liu, W., Wang, Z., Chen, X., Zheng, H., Pu, J., Sun, H., Smith, J., Burt, D.W., Liu, J., Li, N., Huang, Y., 2018. Molecular mechanisms for the adaptive switching between the OAS/RNase L and OASL/RIG-I pathways in birds and mammals. Front. Immunol. 9, 1398. https://doi.org/10.3389/fimmu.2018.01398.
Rothenburg, S., Seo, E.J., Gibbs, J.S., Dever, T.E., Dittmar, K., 2009. Rapid evolution of protein kinase PKR alters sensitivity to viral inhibitors. Nat. Struct. Mol. Biol. 16, 63–70. https://doi.org/10.1038/nsmb.1529.
Sabbah, A., Chang, T.H., Harnack, R., Frohlich, V., Tominaga, K., Dube, P.H., Xiang, Y., Bose, S., 2009. Activation of innate immune antiviral responses by Nod2. Nat. Immunol. 10, 1073–1080. https://doi.org/10.1038/ni.1782.
Saito, T., Hirai, R., Loo, Y.M., Owen, D., Johnson, C.L., Sinha, S.C., Akira, S., Fujita, T., Gale, M., 2007. Regulation of innate antiviral defenses through a shared repressor domain in RIG-1 and LGP2. In: Proceedings of the National Academy of Sciences of the United States of America, vol. 104, pp. 582–587. https://doi.org/10.1073/PNAS.0606699104/SUPPL_FILE/06699FIG8.PDF.
Savage, A.E., Zamudio, K.R., 2016. Adaptive tolerance to a pathogenic fungus drives major histocompatibility complex evolution in natural amphibian populations. Proc. R. Soc. A B. 283, 20153115 https://doi.org/10.1098/rspb.2015.3115.
Schad, J., Voigt, C.C., 2016. Adaptive evolution of virus-sensing toll-like receptor 8 in bats. Immunogenetics 68, 783–795. https://doi.org/10.1007/s00251-016-0940-z.
Sharma, V., Hecker, N., Walther, F., Stuckas, H., Hiller, M., 2020. Convergent losses of TLR5 suggest altered extracellular flagellin detection in four mammalian lineages. Mol. Biol. Evol. 37, 1847–1854. https://doi.org/10.1093/molbev/msaa058.
Shi, Z., Cai, Z., Sanchez, A., Zhang, T., Wen, S., Wang, J., Yang, J., Fu, S., Zhang, D., 2011. A novel toll-like receptor that recognizes vesicular stomatitis virus. J. Biol. Chem. 286, 4517–4524. https://doi.org/10.1074/jbc.M110.159590.
Shu, C., Wang, S., Xu, T., 2015. Characterization of the duplicate L-SIGN and DC-SIGN genes in miiuy croaker and evolutionary analysis of L-SIGN in fishes. Dev. Comp. Immunol. 50, 19–25. https://doi.org/10.1016/j.dci.2015.01.004.
Socha, W., Kwasnik, M., Larska, M., Rola, J., Rozek, W., 2022. Vector-borne viral diseases as a current threat for human and animal health—one health perspective. JCM 11, 3026. https://doi.org/10.3390/jcm11113026.

Souza, J.G., Starobinas, N., Ibañez, O.C.M., 2021. Unknown/enigmatic functions of extracellular ASC. Immunology 163, 377–388. https://doi.org/10.1111/imm.13375.

Su, J., Heng, J., Huang, T., Peng, L., Yang, C., Li, Q., 2012. Identification, mRNA expression and genomic structure of TLR22 and its association with GCRV susceptibility/resistance in grass carp (*Ctenopharyngodon idella*). Dev. Comp. Immunol. 36, 450–462. https://doi.org/10.1016/j.dci.2011.08.015.

Sundaram, A.Y.M., Consuegra, S., Kiron, V., Fernandes, J.M.O., 2012. Positive selection pressure within teleost toll-like receptors tlr21 and tlr22 subfamilies and their response to temperature stress and microbial components in zebrafish. Mol. Biol. Rep. 39, 8965–8975. https://doi.org/10.1007/s11033-012-1765-y.

Świderská, Z., Šmídová, A., Buchtová, L., Bryjová, A., Fabiánová, A., Munclinger, P., Vinkler, M., 2018. Avian Toll-like receptor allelic diversity far exceeds human polymorphism: an insight from domestic chicken breeds. Sci. Rep. 8, 17878 https://doi.org/10.1038/s41598-018-36226-1.

Takahasi, K., Kumeta, H., Tsuduki, N., Narita, R., Shigemoto, T., Hirai, R., Yoneyama, M., Horiuchi, M., Ogura, K., Fujita, T., Inagaki, F., 2009. Solution structures of cytosolic RNA sensor MDA5 and LGP2 C-terminal domains: identification of the RNA recognition loop in rig-I-like receptors. J. Biol. Chem. 284, 17465–17474. https://doi.org/10.1074/JBC.M109.007179.

Těšický, M., Velová, H., Novotný, M., Kreisinger, J., Beneš, V., Vinkler, M., 2020. Positive selection and convergent evolution shape molecular phenotypic traits of innate immunity receptors in tits (Paridae). Mol. Ecol. 29, 3056–3070. https://doi.org/10.1111/mec.15547.

Těšický, M., Vinkler, M., 2015. Trans-species polymorphism in immune genes: general pattern or MHC-restricted phenomenon? Journal of Immunology Research 2015, 1–10. https://doi.org/10.1155/2015/838035.

Tian, R., Chen, M., Chai, S., Rong, X., Chen, B., Ren, W., Xu, S., Yang, G., 2018. Divergent selection of pattern recognition receptors in mammals with different ecological characteristics. J. Mol. Evol. 86, 138–149. https://doi.org/10.1007/s00239-018-9832-1.

Tong, C., Lin, Y., Zhang, C., Shi, J., Qi, H., Zhao, K., 2015. Transcriptome-wide identification, molecular evolution and expression analysis of Toll-like receptor family in a Tibet fish, *Gymnocypris przewalskii*. Fish Shellfish Immunol. 46, 334–345. https://doi.org/10.1016/j.fsi.2015.06.023.

Uchimura, T., Oyama, Y., Deng, M., Guo, H., Wilson, J.E., Rampanelli, E., Cook, K.D., Misumi, I., Tan, X., Chen, L., Johnson, B., Tam, J., Chou, W.-C., Brickey, W.J., Petrucelli, A., Whitmire, J.K., Ting, J.P.Y., 2018. The innate immune sensor NLRC3 acts as a rheostat that fine-tunes T cell responses in infection and autoimmunity. Immunity 49, 1049–1061.e6. https://doi.org/10.1016/j.immuni.2018.10.008.

Van Der Veen, A.G., Maillard, P.V., Schmidt, J.M., Lee, S.A., Deddouche-Grass, S., Borg, A., Kjær, S., Snijders, A.P., Reis E Sousa, C., 2018. The RIG-I-like receptor LGP2 inhibits Dicer-dependent processing of long double-stranded RNA and blocks RNA interference in mammalian cells. EMBO J. 37, e97479 https://doi.org/10.15252/embj.201797479.

Vasseur, E., Patin, E., Laval, G., Pajon, S., Fornarino, S., Crouau-Roy, B., Quintana-Murci, L., 2011. The selective footprints of viral pressures at the human RIG-I-like receptor family. Hum. Mol. Genet. 20, 4462–4474. https://doi.org/10.1093/hmg/ddr377.

Velová, H., Gutowska-Ding, M.W., Burt, D.W., Vinkler, M., 2018. Toll-like receptor evolution in birds: gene duplication, pseudogenization, and diversifying selection. Mol. Biol. Evol. 35, 2170–2184. https://doi.org/10.1093/molbev/msy119.

Venkataraman, T., Valdes, M., Elsby, R., Kakuta, S., Caceres, G., Saijo, S., Iwakura, Y., Barber, G.N., 2007. Loss of DExD/H box RNA helicase LGP2 manifests disparate antiviral responses. J. Immunol. 178, 6444–6455. https://doi.org/10.4049/JIMMUNOL.178.10.6444.

Vinkler, M., Adelman, J.S., Ardia, D.R., 2022. Evolutionary and ecological immunology. In: Avian Immunology. Elsevier, pp. 519–557. https://doi.org/10.1016/B978-0-12-818708-1.00008-7.

Vinkler, M., Albrecht, T., 2009. The question waiting to be asked: innate immunity receptors in the perspective of zoological research. Folia Zoologica -Praha- 58, 15–28.

Vinkler, M., Bainová, H., Bryja, J., 2014. Protein evolution of Toll-like receptors 4, 5 and 7 within Galloanserae birds. Genet. Sel. Evol. 46, 72. https://doi.org/10.1186/s12711-014-0072-6.

Vinkler, M., Bainová, H., Bryjová, A., Tomášek, O., Albrecht, T., Bryja, J., 2015. Characterisation of Toll-like receptors 4, 5 and 7 and their genetic variation in the grey partridge. Genetica 143, 101–112. https://doi.org/10.1007/s10709-015-9819-4.

Vinkler, M., Fiddaman, S.R., Těšický, M., O'Connor, E.A., Savage, A.E., Lenz, T.L., Smith, A.L., Kaufman, J., Bolnick, D.I., Davies, C.S., Dedić, N., Flies, A.S., Samblás, M.M.G., Henschen, A.E., Novák, K., Palomar, G., Raven, N., Samaké, K., Slade, J., Veetil, N.K., Voukali, E., Höglund, J., Richardson, D.S., Westerdahl, H., 2023. Understanding the evolution of immune genes in jawed vertebrates. J of Evolutionary Biology 36, 847–873. https://doi.org/10.1111/jeb.14181.

Wallace, H.L., Russell, R.S., 2022. Promiscuous inflammasomes: the false dichotomy of RNA/DNA virus-induced inflammasome activation and pyroptosis. Viruses 14, 2113. https://doi.org/10.3390/v14102113.

Wang, F., Liu, R., Yang, J., Chen, B., 2021. New insights into genetic characteristics between multiple myeloma and COVID-19: an integrative bioinformatics analysis of gene expression omnibus microarray and the cancer genome atlas data. Int J Lab Hematology 43, 1325–1333. https://doi.org/10.1111/ijlh.13717.

Wang, J., Zhang, Z., Fu, H., Zhang, S., Liu, J., Chang, F., Li, F., Zhao, J., Yin, D., 2015. Structural and evolutionary characteristics of fish-specific TLR19. Fish Shellfish Immunol. 47, 271–279. https://doi.org/10.1016/j.fsi.2015.09.005.

Wang, J., Zhang, Z., Liu, J., Zhao, J., Yin, D., 2016. Ectodomain architecture affects sequence and functional evolution of vertebrate toll-like receptors. Sci. Rep. 6, 26705 https://doi.org/10.1038/srep26705.

Weber, J.N., Steinel, N.C., Peng, F., Shim, K.C., Lohman, B.K., Fuess, L.E., Subramanian, S., Lisle, S.P.D., Bolnick, D.I., 2022. Evolutionary gain and loss of a pathological immune response to parasitism. Science 377, 1206–1211. https://doi.org/10.1126/science.abo3411.

Wlasiuk, G., Nachman, M.W., 2010. Adaptation and constraint at toll-like receptors in primates. Mol. Biol. Evol. 27, 2172–2186. https://doi.org/10.1093/molbev/msq104.

Woolhouse, M.E.J., Webster, J.P., Domingo, E., Charlesworth, B., Levin, B.R., 2002. Biological and biomedical implications of the co-evolution of pathogens and their hosts. Nat. Genet. 32, 569–577. https://doi.org/10.1038/ng1202-569.

Wu, J.-Y., Xue, J.-Y., Van de Peer, Y., 2021. Evolution of NLR resistance genes in magnoliids: dramatic expansions of CNLs and multiple losses of TNLs. Front. Plant Sci. 12, 777157 https://doi.org/10.3389/fpls.2021.777157.

Wu, X., Chen, J., Wang, X., Shang, Y., Wei, Q., Zhang, H., 2022. Evolutionary impacts of pattern recognition receptor genes on carnivora complex habitat stress adaptation. Animals 12, 3331. https://doi.org/10.3390/ani12233331.

Wu, X., Wu, F.-H., Wang, X., Wang, L., Siedow, J.N., Zhang, W., Pei, Z.-M., 2014. Molecular evolutionary and structural analysis of the cytosolic DNA sensor cGAS and STING. Nucleic Acids Res. 42, 8243–8257. https://doi.org/10.1093/nar/gku569.

Wu, X.M., Zhang, J., Li, P.W., Hu, Y.W., Cao, L., Ouyang, S., Bi, Y.H., Nie, P., Chang, M. X., 2020. NOD1 promotes antiviral signaling by binding viral RNA and regulating the interaction of MDA5 and MAVS. J. Immunol. 204, 2216–2231. https://doi.org/10.4049/jimmunol.1900667.

Xu, L., Yu, D., Fan, Y., Peng, L., Wu, Y., Yao, Y.-G., 2016. Loss of RIG-I leads to a functional replacement with MDA5 in the Chinese tree shrew. Proc. Natl. Acad. Sci. U.S.A. 113, 10950–10955. https://doi.org/10.1073/pnas.1604939113.

Yin, X., Riva, L., Pu, Y., Martin-Sancho, L., Kanamune, J., Yamamoto, Y., Sakai, K., Gotoh, S., Miorin, L., De Jesus, P.D., Yang, C.-C., Herbert, K.M., Yoh, S., Hultquist, J. F., García-Sastre, A., Chanda, S.K., 2021. MDA5 governs the innate immune response to SARS-CoV-2 in lung epithelial cells. Cell Rep. 34, 108628 https://doi.org/10.1016/j.celrep.2020.108628.

Yoneyama, M., Kikuchi, M., Matsumoto, K., Imaizumi, T., Miyagishi, M., Taira, K., Foy, E., Loo, Y.-M., Gale, M., Akira, S., Yonehara, S., Kato, A., Fujita, T., 2005. Shared and unique functions of the DExD/H-box helicases RIG-I, MDA5, and LGP2 in antiviral innate immunity. J. Immunol. 175, 2851–2858. https://doi.org/10.4049/JIMMUNOL.175.5.2851.

Younan, P., Ramanathan, P., Graber, J., Gusovsky, F., Bukreyev, A., 2017. The toll-like receptor 4 antagonist eritoran protects mice from lethal filovirus challenge. mBio 8, e00226. https://doi.org/10.1128/mBio.00226-17, 17.

Zelensky, A.N., Gready, J.E., 2005. The C-type lectin-like domain superfamily. FEBS J. 272, 6179–6217. https://doi.org/10.1111/j.1742-4658.2005.05031.x.

Zhang, L., Liu, G., Xia, T., Yang, X., Sun, G., Zhao, C., Xu, C., Zhang, H., 2022. Evolution of toll-like receptor gene family in amphibians. Int. J. Biol. Macromol. 208, 463–474. https://doi.org/10.1016/j.ijbiomac.2022.03.112.

Zhang, L., Mo, J., Swanson, K.V., Wen, H., Petrucelli, A., Gregory, S.M., Zhang, Z., Schneider, M., Jiang, Y., Fitzgerald, K.A., Ouyang, S., Liu, Z.-J., Damania, B., Shu, H.-B., Duncan, J.A., Ting, J.P.-Y., 2014. NLRC3, a member of the NLR family of proteins, is a negative regulator of innate immune signaling induced by the DNA sensor STING. Immunity 40, 329–341. https://doi.org/10.1016/j.immuni.2014.01.010.

Zhang, Z., Ohto, U., Shibata, T., Krayukhina, E., Taoka, M., Yamauchi, Y., Tanji, H., Isobe, T., Uchiyama, S., Miyake, K., Shimizu, T., 2016. Structural analysis reveals that toll-like receptor 7 is a dual receptor for guanosine and single-stranded RNA. Immunity 45, 737–748. https://doi.org/10.1016/j.immuni.2016.09.011.

Zheng, W., Satta, Y., 2018. Functional evolution of avian rig-i-like receptors. Genes 9, 1–15. https://doi.org/10.3390/genes9090456.

Zhong, Y., Kinio, A., Saleh, M., 2013. Functions of NOD-like receptors in human diseases. Front. Immunol. 4 https://doi.org/10.3389/fimmu.2013.00333.

Zhu, X., Mu, K., Wan, Y., Zhang, L., 2022. Evolutionary history of the NLR gene families across lophotrochozoans. Gene 843, 146807. https://doi.org/10.1016/j.gene.2022.146807.

PAPER II

Balraj Melepat, Daniel Divín, Kateřina Marková, Tao Li, Nithya Kuttiyarthu Veetil, Eleni Voukali, Lucie Schmiedová, Martin Těšický and Michal Vinkler "The neuro-immune crosstalk between CNS and periphery during acute immune response to virus-mimicking RNA in parrots" (Submitted in Veterinary Research).

Veterinary Research

The neuro-immune crosstalk between CNS and periphery during acute immune response to virus-mimicking RNA in parrots

--Manuscript Draft--

Manuscript Number:	
Full Title:	The neuro-immune crosstalk between CNS and periphery during acute immune response to virus-mimicking RNA in parrots
Article Type:	Research article
Funding Information:	Univerzita Karlova v Praze (PRIMUS/17/SCI/12) — Dr. Michal Vinkler Univerzita Karlova v Praze (START/SCI/113 (reg. no. CZ.02.2.69/0.0/0.0/19_073/0016935)) — Mr. Balraj Melepat Grantová Agentura České Republiky (19-20152Y) — Dr. Michal Vinkler Grantová Agentura České Republiky (24-12477S) — Dr. Michal Vinkler Ministerstvo Školství, Mládeže a Tělovýchovy (260684/2023) — Not applicable
Abstract:	Parrots are important companion animals with concerning conservation status that can serve as reservoirs for transmission of human zoonotic diseases. In many infectious diseases, including those caused by viruses, systemic inflammation has a crucial impact on host health. There is presently little understanding of the regulation of systemic inflammatory responses in parrots. In this study, we assessed the parrot expression of key inflammation markers in the context of viral-mimicking stimulation. In budgerigar (Melopsittacus undulatus), a novel avian model for the investigation of neuroinflammation, we induced sterile inflammation with synthetic poly(I:C) RNA and followed the dose-, time- and tissue-dependent patterns of gene expression changes in selected pattern recognition receptor genes (TLR3 and NLRP3), signal mediator CASP1 and pro-inflammatory cytokines (IL1B and IL6) during acute response. Our results show significant correlations between the expression of the inflammation-related genes (namely IL1B) in intestine (site of the local stimulation) and brain (site of systemic response). In response to poly(I:C), peripheral IL6 mRNA expression was up-regulated at 3 and 6 hours after stimulation with both high and low poly(I:C) doses. In parrot brain, we found stronger patterns of activation in multiple inflammation-related genes (TLR3, IL1B and IL6) at the beginning of the immune response (3-6 hours after stimulation). Our results demonstrate that parrots are likely susceptible to severe neuroinflammation induced by peripheral viral infections. These findings set a basis essential for future comparative research of the avian neuro-immune crosstalk and neuroinflammation-linked behavioural disorders in parrots.
Corresponding Author:	Michal Vinkler, Ph.D. Charles University Faculty of Science: Univerzita Karlova Prirodovedecka fakulta CZECHIA
Corresponding Author E-Mail:	michal.vinkler@natur.cuni.cz
Corresponding Author Secondary Information:	
Corresponding Author's Institution:	Charles University Faculty of Science: Univerzita Karlova Prirodovedecka fakulta
Corresponding Author's Secondary Institution:	
First Author:	Balraj Melepat
First Author Secondary Information:	
Order of Authors:	Balraj Melepat Daniel Divín

	Kateřina Marková
	Tao Li
	Nithya Kuttiyarthu Veetil
	Eleni Voukali
	Lucie Schmiedová
	Martin Těšický
	Michal Vinkler, Ph.D.
Order of Authors Secondary Information:	
Suggested Reviewers:	Lonneke Vervelde Royal GD l.vervelde@gddiergezondheid.nl Expert in avian immune regulation to viruses
	Kate Sutton The University of Edinburgh The Roslin Institute Kate.Sutton@roslin.ed.ac.uk Expert in avian cytokine regulation
	Dieter Liebhart University of Veterinary Medicine Vienna: Veterinarmedizinische Universitat Wien Dieter.Liebhart@vetmeduni.ac.at Expert in avian immunology
Additional Information:	
Question	**Response**
Is this study a clinical trial?<hr>A clinical trial is defined by the World Health Organisation as 'any research study that prospectively assigns human participants or groups of humans to one or more health-related interventions to evaluate the effects on health outcomes'.	No
Are you submitting to a Thematic Series?	No

The neuro-immune crosstalk between CNS and periphery during acute immune response to virus-mimicking RNA in parrots

Authors: Balraj Melepat[1], Daniel Divín[1], Kateřina Marková[1], Tao Li[1], Nithya Kuttiyarthu Veetil[1], Eleni Voukali[1], Lucie Schmiedová[1], Martin Těšický[1] and Michal Vinkler[1]*

Addresses:

1) Charles University, Faculty of Science, Department of Zoology, Viničná 7, 128 43 Prague, Czech Republic, EU

* Author for correspondence: Michal Vinkler, e-mail: michal.vinkler@natur.cuni.cz, tel.: +420221951845

Correspondence address: Michal Vinkler, Charles University, Department of Zoology, Viničná 7, 128 43 Prague, Czech Republic, EU

Abstract

Parrots are important companion animals with concerning conservation status that can serve as reservoirs for transmission of human zoonotic diseases. In many infectious diseases, including those caused by viruses, systemic inflammation has a crucial impact on host health. There is presently little understanding of the regulation of systemic inflammatory responses in parrots. In this study, we assessed the parrot expression of key inflammation markers in the context of viral-mimicking stimulation. In budgerigar (*Melopsittacus undulatus*), a novel avian model for the investigation of neuroinflammation, we induced sterile inflammation with synthetic poly(I:C) RNA and followed the dose-, time- and tissue-dependent patterns of gene expression changes in selected pattern recognition receptor genes (*TLR3* and *NLRP3*), signal mediator *CASP1* and pro-inflammatory cytokines (*IL1B* and *IL6*) during acute response. Our results show significant correlations between the expression of the inflammation-related genes (namely *IL1B*) in intestine (site of the local stimulation) and brain (site of systemic response). In response to poly(I:C), peripheral *IL6* mRNA expression was up-regulated at 3 and 6 hours after stimulation with both high and low poly(I:C) doses. In parrot brain, we found stronger patterns of activation in multiple inflammation-related genes (*TLR3*, *IL1B* and *IL6*) at the beginning of the immune response (3-6 hours after stimulation). Our results demonstrate that parrots are likely susceptible to severe neuroinflammation induced by peripheral viral infections. These findings set a basis essential for future comparative research of the avian neuro-immune crosstalk and neuroinflammation-linked behavioural disorders in parrots.

Keywords:

avian immunology, cytokine signalling, gastrointestinal tract, neuro-immune regulation, neuroimmunology, neural inflammation

Introduction

Despite extensive medical and veterinary efforts, infections continue to represent one of the key threats to human and animal health [1, 2]. It has been estimated that 60% of human infectious diseases and 75% of all emerging infectious diseases represent zoonoses originating from animals [3, 4]. Birds are involved in 18.4% of emerging diseases [3], and being distinct from mammalian reservoirs, they require special attention. Avian hosts act as prominent wild and domestic reservoirs for several bacterial and viral pathogens of key economic and public health importance, including, salmonella, listeria, avian influenza, and New Castle disease virus [5–10]. Compared to mammals, relatively little is known about interspecific variation in avian immune function [11]. Domestic chicken provides the key and mostly universal reference for the description of biological distinctions between birds and mammals [12–14]. Yet, birds are highly diversified (equally to mammals) and, hence, heterogeneity has been observed across avian species in immunogenetics [15] as well as immune responsiveness to stimulation [16–18]. Most infectious diseases are interspecifically transmitted through close contacts between the different hosts [19]. Since many birds share their environment with humans, also avian species phylogenetically distantly related to chickens, but kept as pets and companion animals, such as parrots are relevant [9].

Parrots (Psittaciformes) are a group of birds in which many species became highly endangered in nature (https://www.iucnredlist.org/). Almost 60% of all parrot species are experiencing global population declines [20], urging conservation efforts based on the captive populations. High diversity of parrot species is now bred throughout the world in captivity, some even serving as the most popular avian pets [21]. Current estimates suggest that about half of the global parrot population is presently domestic and thus living in close contact with humans [22]. Captive parrots frequently suffer from various health issues that may be linked to their altered living environment, including digestive and behavioural disorders [23, 24]. Recent research suggests that some of these disorders may be immune-mediated [25]. Parrots were also reported to transmit pathogens such as Psittacosis and influenza to humans and other domestic animals [26–28]. Several viral diseases that are common in parrots, such as the Newcastle Disease and Borna viruses, cause birds' severe neurological disorders [6, 7]. Our prior research has indicated that parrots may be particularly susceptible to these disorders linked to neuroinflammation given their genomic loss of the *CNR2* gene regulating neuro-immune interplay [25].

Inflammation is a complex biological phenomenon during which the pathogen is cleared while at the same time, a potential damage arises also to the host tissue [29]. The equilibrium between pathogen clearance and self-damage becomes particularly crucial when inflammation affects the central nervous system (CNS), where neurons generally lack regenerative capacities [30]. Like in all other animals, also in birds inflammation requires a precise regulation, which is mediated by cytokines [31–33]. Assessing the expression levels of the pro-inflammatory and anti-inflammatory cytokines offers valuable insight into the dynamics of inflammation regulation in both peripheral and central nervous tissues [31, 32]. Similar to bacterial infections, also viral pathogens typically trigger tissue-specific responses in the periphery through their microbe-associated molecular patterns (MAMPs) [34, 35]. These are in birds detected by diversified pathogen-sensing pattern recognition receptors (PRRs), including Toll-like receptors (TLRs) or NOD-like receptors (NLRs) that activate the signalling cascades up-regulating the expression of a range of pro-inflammatory cytokines and other immunomodulating molecules [36, 37].

Among TLRs and NLRs, especially Toll-like receptor 3 (TLR3) and the NLR family pyrin domain containing 3 (NLRP3*)* canonically activate inflammation during viral infections [38–40]. Previous research has suggested that both viral and synthetic double-stranded RNA and Polyinosinic:polycytidylic acid [poly(I:C)] are recognised by TLR3, which induces up-regulation of pro-inflammatory cytokines such as interleukin 1β (IL1B*)*, interleukin 6 (IL6) and interferons type I -α (IFNA) and -β (IFNB) both in vivo and in vitro in birds [36, 39]. However, there are also studies indicating that interferons are not activated in birds

by poly(I:C) stimulation [41]. Meanwhile, the NLRP3 which activates caspase-1 (CASP1), also regulates the expression of the *IL1B* gene [42]. During normal physiological conditions, an interaction between the peripheral immune system and CNS has several positive effects on the brain, including helping in normal memory development and learning [43–45]. However, a substantial increase in the pro-inflammatory cytokines in the periphery leads to the disruption of the blood-brain barrier, infiltration of peripheral immune cells, and activation of the brain glial cells and results in pathological neuroinflammation [44, 46, 47].

In this study, we assessed the differential gene expression of key molecular markers of viral-induced inflammation in parrots, a novel avian model for the investigation of neuroinflammation involved in the neuro-immune crosstalk between periphery and CNS [25]. We triggered sterile inflammation by stimulating the immune system with synthetic poly(I:C) RNA, a TLR3 ligand mimicking the viral dsRNA. Poly(I:C) has been previously applied in the periphery to induce neuroinflammation in both mammals and birds [36, 39, 48, 49]. We followed the dose- and time-dependent patterns of this stimulation on gene expression changes in the PRR genes *TLR3* and *NLRP3*, the signal mediator *CASP1* and the cytokines *IL1B* and *IL6* during acute inflammatory response in the area of the gastrointestinal tract (small intestine in the region of ileum that is located at the site adjacent to the abdominal site of the peripheral stimulation) and brain (hyperpallial region in CNS affected through a systemic immune response) in the budgerigar (*Melopsittacus undulatus*). This research aimed to set a basis that is essential for further comparative research on the neuro-immune crosstalk in birds.

Materials and Methods

Experimental design

The experimental procedures mostly followed our previous experimental strategy applied for investigation of passerine [46] and parrot [25, 50, 51] immune responses to bacterial lipopolysaccharide (LPS), taking also into consideration the previously published research on immune response to poly(I:C) in birds and rodents [52–54]. Briefly, twenty-seven budgerigars (18 females, 9 males) purchased from Vyškov Zoo and from local hobby breeders (January 2022) (for details see Table S1 in Electronic supplementary material 1, ESM1) were transported into the animal facility of the Faculty of Science, Charles University, Czech Republic, EU. For each bird, the body weight and tarsus length were measured. The birds were then marked with coloured aluminium rings with identification numbers and housed in pairs in standard 100×50×40 cm cages with regular light conditions (L12:D12 with 1-hour gradual shading, 22°C) and access to food and water ad libitum. We allowed the birds four weeks of acclimatisation before any experimental procedures. For the experiment, the 27 birds were divided into three-time groups (immune response measured after 3, 6, and 24 hours), each group contained nine individuals of which 3 were administrated with low dose poly(I:C), 3 with high dose poly(I:C) and 3 served as controls. The maximum stimulation period to measure the immune response was set to 24 hours, which is the time for which the previous research in mice revealed the return of the immune activity back to its baseline [53].

The poly(I:C) solution used for immune stimulation in this experiment was prepared following the procedures reported in previous studies [53, 54]. In short, 1 mg poly(I:C) (product. no. P1530, Sigma-Aldrich, Massachusetts USA) was diluted in 100 µl of 0.9% sterile NaCl saline solution (cat. no. 200608, Unolab manufacturing, S.L, Madrid, Spain) and was heated for 10 minutes to 50°C, after which it was cooled down to the room temperature to achieve re-annealing. During the experimental treatment, all the individuals administrated with low-dose poly(I:C) received an intra-abdominal injection of 0.5 mg of poly(I:C) dissolved in 200 µl of sterile saline solution (approximately 12.5 mg/kg). All individuals administrated with high-dose poly(I:C) received 2 mg of poly(I:C) dissolved in 200 µl of sterile saline solution (approximately 50 mg/kg) and the control birds were injected with 200µl of the 0.9% saline

solution. The dosages adopted in this experiment were selected based on the previously reported in-vivo experiments with poly(I:C) in birds [52, 54]. The experiment was conducted in two consecutive days. Based on their time groups, the birds were euthanized by decapitation, at the time intervals of 3, 6 and 24 hours. After the post-mortem blood collection from carotids, blood smears were made, and different selected tissues were immediately collected (including the brain and ileum used in this study) and placed into the RNA-later solution where they were stored at +4°C overnight and then frozen at -80°C until analysis (Details on the materials provided in ESM1 Table S2). The blood smears were used to analyse the different haematological parameters. The research was approved by the Ethical Committee of Charles University, Faculty of Science (permits13882/2011-30) and was carried out by the current laws of the Czech Republic and the European Union.

RNA extraction and RT-qPCR

The brain and ileum samples from all experimental individuals were homogenized in MagNa Lyser (Roche, Basel, Switzerland) using PCR clean beaded tubes (OMNI International, Kennesaw GA USA - cat. no.: 2150600). Subsequently, total RNA was extracted from these homogenized samples using the High Pure RNA Tissue Kit (Roche) and the quality and quantity of RNA was measured using a Nanodrop instrument (NanoDrop ND-1000) (ESM1 Table S2).

The RT-qPCR was done consistently with our previous research [25]. While the RT-qPCR primers, probes, and synthetic cDNA standards for *IL1B* and *IL6* were available from our previous experiments [50] those for *TLR3, NLRP3* and *CASP1* genes were specifically designed for this research. The new primers, probes and synthetic cDNA standards were designed utilizing the Geneious software (version 11.1.5, Biomatters), with a focus on regions conserved in the avian interspecific alignments (created based on publicly available gene-specific sequences from the Ensembl database; Table S3). For coding regions covering the RT-qPCR targets within the *TLR3*, *NLRP3* and *CASP1* genes we first designed PCR primers allowing specific amplification of a broader DNA fragment. These fragments PCR-amplified from cDNA were Sanger-sequenced and checked for any polymorphism that could impair the RT-qPCR. The sequences were submitted to NCBI Gen Bank under the accession numbers OR825009-OR825034, and OR940510-OR940516. The final RT-qPCR primers, probes, and synthetic cDNA standards (gBlocks; IDT, Coralville, IA, USA) for our target genes were designed based on this input to specifically match the invariant sites of the genes (Table S4, Table S5 in ESM1).

For RT-qPCR we used RNA diluted in molecular grade water supplemented with carrier tRNA (Qiagen, cat. no. 1068337) at a ratio of 1:5 for the target genes and 1:500 for the *28S rRNA* gene which served as the reference gene. The efficiency of each primer pair was determined from calibration curves obtained using the synthetic cDNA standards across dilution series ranging from 10^8 to 10^2 copies / µl [55]. The RNA samples were amplified using the Luna Universal Probe One-Step RT-PCR Kit (New England Biolabs, MA, USA- cat. no. E3006X) (Table S2, Table S6 in ESM1) using Light Cycler 480 Instrument (Roche Diagnostics, Rotkreuz, Switzerland) under the conditions reported in Table S7 in ESM1. All runs included template-free negative controls and freshly prepared synthetic cDNA (standard) positive controls. The crossing point (Cp) values were determined by the second derivative maximum, together with the efficiency E values calculated using the inbuild LightCycler480 software v.1.5.1 The gene expression quantification was calculated as standard gene expression quantity (Qst) [55] allowing the comparisons of gene expression between the treatments and controls (Table S8 in ESM1).

Statistical analysis

Statistical analysis was conducted using R version 4.1.0 and R-studio software version (v.2021.09.0) [56, 57]. Data normality was assessed using the Shapiro-Wilk test. Given the non-Gaussian distribution of the

Qst values, normalization was performed using a common logarithm (logQst). The effects of experimental treatment on gene expression were evaluated through testing linear models (LMs) within the 'lme4' package, using gene expression (continuous) as the response variable. The full models included treatment, time, sex, and mass, and the interaction between treatment and time as explanatory variables. The minimum adequate models, defined as models with all terms significant at $p \leq 0.05$, were obtained by backward elimination of non-significant terms from the full models. Backward elimination of individual variables followed the Akaike information criterion and was confirmed by changes in deviance and degrees of freedom using analysis of variance (ANOVA) with F statistics. Gene expression changes in different tissues, considering combinations of treatment and time were plotted as boxplots using the ggplot2 package. The post-hoc test for the gene expression pattern and haematological parameters was performed as the TukeyHSD test. The correlation between the gene expression in the ileum and brain was checked using Pearson's product-moment correlation tests. The correlation matrix was visualised using the corrplot package.

Results

Haematological assessment of health

First, we analysed the health state of the experimental individuals using selected haematological markers (H/L ratio and the relative basophil count). Our analysis revealed significant differences between the low treatment group and other treatments already before the poly(I:C) stimulation (P = 0.030, Table S9, ESM1;). This was driven by the high initial H/L ratio in two visually healthy individuals assigned to the low poly(I:C) treatment group (Table S9, ESM1, Figure S1 in ESM2). Given the relatively small sample size, we did not exclude the birds from the analysis but adjusted the interpretation of our results accordingly.

Associations in the expression of inflammation-related genes in different tissues

We found significant correlations between the expression of different inflammation-related genes in different tissues (ileum = peripheral site induced by local stimulation, brain = CNS site induced through systemic effects; Figure 1 and Table S10). In both the intestine and CNS, *IL1B* was positively correlated with *IL6* and *CASP1* expression. However, the systemic effect indicated by the association of the gene expression in the periphery and brain was observed only for *IL1B*, the expression of which in the intestine was linked to brain levels of *IL1B* and *IL6*. While intestinal *TLR3* levels were correlated only with intestinal *IL6*, the expression of *TLR3* in the brain was related to peripheral (intestinal) *IL6* (non-significantly also to *IL1B*) as well as brain expression of *IL1B*, *IL6* and *CASP1*. Although in the periphery we were able to find no associations between *NLRP3* expression and expression of any other gene, brain *NLRP3* was correlated with the brain levels of *IL1B*, *IL6*, *CASP1* and also *TLR3*.

Inflammation-related gene expression in the small intestine (ileum)

At the site of the local inflammation, in the ileum, *TLR3* gene expression did not show any significant changes during the course of the response (Full model 1 in Table S11, ESM1 and Figure S2 in ESM2) Similarly, we observed no significant up-regulation in the expression of *NLRP3* or *CASP1*in birds treated with poly(I: C) (Full models 2 and 3 in Table S11, ESM1; Figure S3 and S4 in ESM2).

For the *IL1B* gene, analysis of the full model indicated significant up-regulation in the gene expression only at 3 hours after stimulation with the high poly(I:C) dose (P = 0.043; Full model 4 in Table S11, ESM1, Figure 2A). However, the analysis of MAM did not support the significance of this change. Yet, we found a highly significant up-regulation of *IL6* expression at 3 and 6 hours after stimulation for both high-dose

poly(I:C) (P = 0.008, P = 0.001) and low-dose poly(I:C) (P = 0.013, P = 0.003) treated birds compared to the controls (MAM5, interaction Treatment: Time P << 0.001, Table 1; Full model 5 in Table S11, ESM1; TukeyHSD in Table S12; Figure 2B). Later, 24 hours after stimulation, the difference between the treatment groups and controls became insignificant).

Table 1. Statistically significant Minimum adequate models (MAMs) to inflammation-related genes expressed during response to poly(I:C) in budgerigar ileum and brain. DF = degrees of freedom. For all genes, the expression has been expressed as log (Qst) values.

	Tissue	MAM/variables	DF	F	P
MAM5	Ileum	IL6 ~ Treatment + Time + Treatment:Time	8/18	13.032	<<0.001
		Treatment	6/18	13.349	<<0.001
		Time	6/18	11.923	<<0.001
		Treatment: Time	4/18	11.844	<<0.001
MAM6	Brain	TLR3 ~ Treatment	2/24	3.366	0.051
MAM9	Brain	IL1B ~ Treatment + Time + Treatment:Time	8/18	4.742	0.003
		Treatment	6/18	5.962	0.001
		Time	6/18	2.589	0.055
		Treatment: Time	4/18	3.344	0.033
MAM10	Brain	IL6 ~ Treatment	2/24	10.46	<<0.001

Inflammation-related gene expression in the brain

In contrast to the ileum, for *TLR3* gene expression in the brain, our analysis revealed a significant peak at 6 hours after stimulation for the high (P = 0.002) as well as the low (P = 0.019) poly(I:C) dose groups compared to the controls (TukeyHSD in Table S12, ESM1). Despite the whole MAM is marginally non-significant (MAM6, Treatment, p = 0.051, Table 1, Full model 6 in Table S11, ESM1, Figure 3A), this suggests systemic PRR response to the poly(I:C) stimulation. Yet, even in the brain, we did not detect any significant changes in the expression of the *NLRP3* or *CASP1* genes (Full models 7 and 8 in Table S11, ESM1, Figure S5 and S6 in ESM2).

In contrast, for both the pro-inflammatory cytokines, our study identified highly significant time patterns in the brain. The *IL1B* gene expression exhibited a significant up-regulation in the birds treated with the high poly(I:C) dose (MAM9, interaction Treatment: Time, P = 0.033, Table 1, Full model 9 in Table S11, ESM1, Figure 3B). The *IL1B* response to the high poly(I:C) dose started at 3 hours (P = 0.029) and subsequently increased at 6 hours (P = 0.006) and later decreased to a non-significant difference (P = 0.818) between the high-dose poly(I:C) treatments and controls at the 24th hour (TukeyHSD in Table S12, ESM1). We observed a very similar pattern of up-regulation also in *IL6* where the high poly(I:C) dose and low poly(I:C) triggered a significant gene expression up-regulation (MAM10, Treatment, P << 0.001, Table 1, Full model 10 in Table S11, ESM1, Figure 3C). For the high poly(I:C) treatment the *IL6* gene expression started to significantly up-regulate (P = 0.022) at 3 hours after stimulation, which increased to a maximum at 6 hours (P << 0.001), returning to the original levels (p = 0.902) later at 24 hours (no significant difference between the treatments and the controls (TukeyHSD in Table S12, ESM1)). A similar pattern was observed for the low poly(I:C) dose group, only weaker. At 3 hours after stimulation, we found no significant difference in

239 the *IL6* gene expression compared to controls, but later at 6 hours after stimulation, there was a significant
240 peak in the response (P = 0.003). Finally, at 24 hours after stimulation the difference in *IL6* expression
241 between the low poly(I:C) treatment group and the control group became insignificant (TukeyHSD in Table
242 S12, ESM1).

243 Discussion

244 Although diversified immune strategies can be expected among birds [58], little is presently known about
245 regulation of immune responses in other avian models than the poultry. To provide fundamental basis for
246 exploration of avian variation in immune responses, in this study we focused on parrots that are lacking
247 important neuro-immune modulator CNR2, which may alter their regulation of neuroinflammation [25]. In
248 birds stimulated with poly(I:C), we found significant correlations between the expression of different
249 inflammation-related genes across the tissues. This pattern is marked namely for the pro-inflammatory
250 cytokines. Surprisingly, we did not find any change in the receptor recognising poly(I:C), *TLR3*, in the
251 periphery where the response was stimulated. In ileum, we detected significant up-regulation of mRNA
252 expression only in *IL6*, peaking between 3 to 6 hours after stimulation. More complex was the immune
253 response in brain, where 3 to 6 hours after the peripheral poly(I:C) stimulation the pattern recognition
254 receptor *TLR3*, and both the pro-inflammatory cytokines *IL1B* and *IL6* increased their expression. This
255 indicates that the local activation of the immune response in the periphery induces in parrots systemic
256 response, during which neuroinflammation can be triggered.

257 The poly(I:C) treatment has been widely applied to mimic immune responses to viral infection [52–54, 59,
258 60]. In mammals, namely rodents, is the immune response linked with neural regulation inducing
259 physiological responses including fever, sickness behaviour and anorexia [61–63]. Few studies targeted this
260 response in birds [41, 52, 54, 64]. Application of poly(I:C) early in life causes developmental changes in
261 avian brain both in chicks [64] and in zebra finch nestlings [54]. However, the molecular mechanism causing
262 these developmental effects remain elusive. Certain insight into the diversity of this regulation provides
263 recent research exploring chicken responses to intraabdominal poly(I:C) injections [41]. Chickens treated
264 with poly(I:C) displayed reduction in food intake as soon as 3 hours after the injection, which was
265 comparable to the previous reports in rodents [61, 65]. However, unlike in rodents the poly (I:C)-induced
266 anorexia in chickens was not related to the cytokine responses investigated, namely interferon α (*IFNA*),
267 interferon γ (*IFNG*) or tumor necrosis factor (TNF)-like cytokine 1A (*TL1A*) gene expression levels in
268 either brain or spleen [41]. This implies an IFN and TNF-independent inflammation response in birds during
269 poly (I:C) treatment.

270 In our research, we focused both on genes involved in poly(I:C) recognition (TLR3 and possibly also
271 NLRP3 as a part of the inflammasome detecting cell damage) and the assumed alternative signalling
272 pathways running through non-specific inflammation mediated by IL1B and IL6, assumingly modulated by
273 the enzyme CASP1. Our results show positive correlations between the intestinal and brain expression of
274 *IL1B*, *IL6* and *CASP1* expression. This is similar to the findings of other avian studies, showing consistency
275 in expression patterns of different pro-inflammatory cytokines [55]. In the budgerigar, *IL1B* showed even
276 correlations between the periphery and CNS, which is consistent with its anticipated role in modulation of
277 neuroinflammation from the periphery [66]. Interestingly, in brain the *IL1B, IL6* and *CASP1* levels were
278 positively corelated with the expression of *TLR3* and also *NLRP3*, indicating complex activation of
279 neuroinflammation.

280 We have analysed the effects of peripheral inflammation across three time points: 3, 6 and 24 hours. This
281 timescale is consistent with previous studies of acute inflammation in mice treated with poly(I:C) by
282 Cunningham et al. [53], that have shown that pro-inflammatory cytokines IL1B and IL6 peak in expression

during the response to poly(I:C) at 3 hours and then decline to the baseline level after 24 hours. However, in contrast to our research, Cunningham et al. [53] measured the protein levels of the cytokines in blood plasma to assess the peripheral inflammation, so the link to the peripheral mRNA levels is not clear. Our previous study analysing parrot responses to subcutaneous injections of LPS also showed a systemic inflammatory response, with cytokine expression peak at 6 hours after stimulation [51], which is consistent with the peak of the *IL6* expression in response to the poly(I:C) treatment. Both poly(I:C) doses showed similar patterns of the pro-inflammatory cytokine activation, with the decline back to the baseline levels at 24 hours after stimulation, which is consistent with Cunningham et al. [53].

The poly(I:C) is detected by the TLR3 receptor and the downstream signalling is fully dependent on the TRIF (TIR domain-containing adaptor protein inducing interferon beta) related pathway [67, 68]. In mice models it is found that the poly(I:C) can breakdown the blood-brain barrier [69, 70], and the brain cells such as the astrocytes and microglia in humans and mice express the TLR3 receptor capable of recognising poly(I:C) [71–74]. In our study, we found significant up-regulation of *TLR3* gene expression in brain, which is comparable to previous reports in mice, where intraperitoneal poly(I:C) treatment also induced up-regulation of *TLR3* gene expression in the brain, mainly in the hypothalamus and hippocampus regions, 6 hours after application [69]. An in-vitro analyses of astrocytes treated with poly(I:C) also showed up-regulation of the TLR3 protein both in humans [71] and rodents [73].

In the budgerigars, *IL6* was found to be up-regulated both in the ileum and brain between the 3 and 6 hours after stimulation with the high poly(I:C) dose, suggesting that either the poly(I:C) or the cytokines passed the blood-brain barrier, similar to the cases previously reported in mice [69, 70]. In contrast to the mouse in-vitro and in-vivo models [68, 75], in parrots the poly (I:C) treatment does not lead to any decrease in the IL6 expression, which serves in mammals as the mechanism of neuronal protection. Moreover, in our study, the poly(I:C) treatment increased also the *IL1B* expression in brain. This is also consistent with our previous research of the parrot immune response to LPS [50]. These results support the hypothesis that parrots may be highly susceptible to neuroinflammation, probably due to the absence of the CNR2 modulator of the neuro-immune interplay [25].

Previous in-vitro research in poly(I:C)-treated mice showed that the IL1B up-regulation is dependent on the NLRP3-mediated inflammatory pathway that leads to the activation of CASP1, independent of the TLR3 pathway [76, 77]. In a recent study conducted in chickens by Ogaili et al. [78], he examined the presence of the *NLRP3* gene in different chicken tissues and found that the LPS alone can stimulate the *NLRP3* gene expression in the chicken intestinal tissues. This suggests an activation mechanism slightly different from mammals, where LPS or poly(I:C) activate the *NLRP3* gene expression only in combination with extracellular ATP, typically indicating cell damage [77, 79, 80]. In chickens, the peak of *NLRP3* expression was detected between 12 to 24 hours post-injection which is comparable with the rodent studies [76, 77]. Nevertheless, to our knowledge there is presently no study examining such effects of the poly(I:C) injection on the *NLRP3* gene activation in birds. In our study, we checked the expression of the *NLRP3* in both ileum and brain, but in contrast to the LPS-treated chickens [78], in parrots we did not find any change in the *NLRP3* expression even 24 hours after stimulation with the poly(I:C).

Conclusion

Taken altogether, this study is to our knowledge the first one to explore the in vivo immune response to poly(I:C) in the parrots and also the first one in birds to check the expression patterns of *NLRP3* and *CASP1* genes during poly(I:C) treatment in both ileum and brain. The time dynamics and expression patterns of the pro-inflammatory cytokines revealed in our study illuminate the immune crosstalk between periphery and CNS during the poly(I:C) stimulation. Our results demonstrate that parrots are likely susceptible to severe

neuroinflammation induced by peripheral viral infections. Future research should broaden the characterisation of immune-related gene expression, adopting transcriptomic approaches and analysing also the long-term effects of the poly(I:C) stimulation in parrots.

Declarations

Ethics approval and consent to participate

The research was approved by the Ethical Committee of Charles University, Faculty of Science (permits13882/2011-30) and was carried out by the current laws of the Czech Republic and the European Union.

Consent for publication

"Not applicable"

Availability of data and material

The datasets generated during and/or analysed during the current study are available as the Supplementary file 1 attached to this manuscript.

The sequences generated in this study were submitted to NCBI Gen Bank under the accession numbers OR825009-OR825034, and OR940510-OR940516.

Competing interests

The authors declare no competing interests.

Funding

Charles University supported this study through the internal support Nos. PRIMUS/17/SCI/12 and START/SCI/113 (reg. no. CZ.02.2.69/0.0/0.0/19_073/0016935), and the Czech Science Foundation through the grants No. 19-20152Y and 24-12477S. The Czech Ministry of Education, Youth and Sports supported this research through the institutional support No. 260684/2023.

Acknowledgement

"Not applicable"

Authors' contributions

The authors confirm contribution to the paper as follows: (1) conceptualization and methodology: BM, MV (2) investigation: BM, MV, DD, KM, TL, NKV, EV, LS, MT; (3) data curation and formal analysis: BM, MV; (4) Writing-original draft; review and editing: BM, MV; (5) Funding acquisition: MV, BM. All authors contributed to final approval of the version to be submitted.

Reference

1. Ellwanger JH, Veiga ABGD, Kaminski VDL, Valverde-Villegas JM, Freitas AWQD, Chies JAB. Control and prevention of infectious diseases from a One Health perspective. Genet Mol Biol. 2021;44 1 suppl 1:e20200256.

2. Thal DA, Mettenleiter TC. One Health—Key to Adequate Intervention Measures against Zoonotic Risks. Pathogens. 2023;12:415.

3. Cleaveland S, Laurenson MK, Taylor LH. Diseases of humans and their domestic mammals: pathogen characteristics, host range and the risk of emergence. Phil Trans R Soc Lond B. 2001;356:991–9.

4. Taylor LH, Latham SM, Woolhouse MEJ. Risk factors for human disease emergence. Phil Trans R Soc Lond B. 2001;356:983–9.

5. Crespo R, Garner MM, Hopkins SG, Shah DH. Outbreak of Listeria monocytogenes in an urban poultry flock. BMC Vet Res. 2013;9:204.

6. Rahman A-, Habib M, Shabbir MZ. Adaptation of Newcastle Disease Virus (NDV) in Feral Birds and their Potential Role in Interspecies Transmission. TOVJ. 2018;12:52–68.

7. Rubbenstroth D. Avian Bornavirus Research—A Comprehensive Review. Viruses. 2022;14:1513.

8. Tizard I. Salmonellosis in wild birds. Seminars in Avian and Exotic Pet Medicine. 2004;13:50–66.

9. Boseret G, Losson B, Mainil JG, Thiry E, Saegerman C. Zoonoses in pet birds: review and perspectives. Vet Res. 2013;44:36.

10. Abdelwhab EM, Veits J, Mettenleiter TC. Prevalence and control of H7 avian influenza viruses in birds and humans. Epidemiol Infect. 2014;142:896–920.

11. Kaspers B, Schat KA, Göbel TW, Vervelde L, editors. Avian Immunology. Third edition. London: Elsevier Academic Press; 2022.

12. Flores-Santin J, Burggren WW. Beyond the Chicken: Alternative Avian Models for Developmental Physiological Research. Front Physiol. 2021;12:712633.

13. Kaufman J, Milne S, Göbel TWF, Walker BA, Jacob JP, Auffray C, et al. The chicken B locus is a minimal essential major histocompatibility complex. Nature. 1999;401:923–5.

14. Sharma JM. Overview of the avian immune system. Veterinary Immunology and Immunopathology. 1991;30:13–7.

392 15. Minias P, Pikus E, Whittingham LA, Dunn PO. Evolution of Copy Number at the MHC Varies across
393 the Avian Tree of Life. Genome Biology and Evolution. 2019;11:17–28.

394 16. Blount JD, Houston DC, Møller AP, Wright J. Do individual branches of immune defence correlate? A
395 comparative case study of scavenging and non-scavenging birds. Oikos. 2003;102:340–50.

396 17. Hasselquist D. Comparative immunoecology in birds: hypotheses and tests. J Ornithol. 2007;148:571–
397 82.

398 18. Tella JL, Scheuerlein A, Ricklefs RE. Is cell–mediated immunity related to the evolution of life-history
399 strategies in birds? Proc R Soc Lond B. 2002;269:1059–66.

400 19. Kruse H, Kirkemo A-M, Handeland K. Wildlife as Source of Zoonotic Infections. Emerg Infect Dis.
401 2004;10:2067–72.

402 20. Tella JL, Blanco G, Carrete M. Recent Advances in Parrot Research and Conservation. Diversity.
403 2022;14:419.

404 21. Forshaw JM, Knight F. Parrots of the World. Princeton University Press; 2010.

405 22. Mellor EL, McDonald Kinkaid HK, Mendl MT, Cuthill IC, Van Zeeland YRA, Mason GJ. Nature
406 calls: intelligence and natural foraging style predict poor welfare in captive parrots. Proc R Soc B.
407 2021;288:20211952.

408 23. Gaskins LA, Bergman L. Surveys of Avian Practitioners and Pet Owners Regarding Common
409 Behavior Problems in Psittacine Birds. Journal of Avian Medicine and Surgery. 2011;25:111–8.

410 24. Girling S. Diseases of the digestive tract of psittacine birds. In Practice. 2004;26:146–53.

411 25. Divín D, Goméz Samblas M, Kuttiyarthu Veetil N, Voukali E, Świderská Z, Krajzingrová T, et al.
412 Cannabinoid receptor 2 evolutionary gene loss makes parrots more susceptible to neuroinflammation. Proc
413 R Soc B. 2022;289:20221941.

414 26. Greenacre CB. Viral diseases of companion birds. Veterinary Clinics of North America: Exotic Animal
415 Practice. 2005;8:85–105.

416 27. Jones JC, Sonnberg S, Koçer ZA, Shanmuganatham K, Seiler P, Shu Y, et al. Possible Role of
417 Songbirds and Parakeets in Transmission of Influenza A(H7N9) Virus to Humans. Emerg Infect Dis.
418 2014;20.

419 28. Smith KA, Campbell CT, Murphy J, Stobierski MG, Tengelsen LA. Compendium of Measures to
420 Control Chlamydophila psittaci Infection Among Humans (Psittacosis) and Pet Birds (Avian
421 Chlamydiosis), 2010 National Association of State Public Health Veterinarians (NASPHV). Journal of
422 Exotic Pet Medicine. 2011;20:32–45.

423 29. Ashley NT, Weil ZM, Nelson RJ. Inflammation: Mechanisms, Costs, and Natural Variation. Annu Rev
424 Ecol Evol Syst. 2012;43:385–406.

425 30. Illis LS. Central nervous system regeneration does not occur. Spinal Cord. 2012;50:259–63.

426 31. Kany S, Vollrath JT, Relja B. Cytokines in Inflammatory Disease. IJMS. 2019;20:6008.

427 32. Kogut MH. Cytokines and prevention of infectious diseases in poultry: A review. Avian Pathology.
428 2000;29:395–404.

429 33. Konsman J. Cytokines in the Brain and Neuroinflammation: We Didn't Starve the Fire!
430 Pharmaceuticals. 2022;15:140.

431 34. Magor KE. Evolution of RNA sensing receptors in birds. Immunogenetics. 2022;74:149–65.

432 35. Mogensen TH. Pathogen Recognition and Inflammatory Signaling in Innate Immune Defenses. Clin
433 Microbiol Rev. 2009;22:240–73.

434 36. Abo-Samaha MI, Sharaf MM, El Nahas AF, Odemuyiwa SO. Innate immune response to double-
435 stranded RNA in American heritage chicken breeds. Poultry Science. 2024;103:103318.

436 37. Jacobs SR, Damania B. NLRs, inflammasomes, and viral infection. Journal of Leukocyte Biology.
437 2012;92:469–77.

438 38. Kalaiyarasu S, Kumar M, Senthil Kumar D, Bhatia S, Dash SK, Bhat S, et al. Highly pathogenic avian
439 influenza H5N1 virus induces cytokine dysregulation with suppressed maturation of chicken monocyte-
440 derived dendritic cells. Microbiology and Immunology. 2016;60:687–93.

441 39. Kc M, Ngunjiri JM, Lee J, Ahn J, Elaish M, Ghorbani A, et al. Avian Toll-like receptor 3 isoforms and
442 evaluation of Toll-like receptor 3–mediated immune responses using knockout quail fibroblast cells.
443 Poultry Science. 2020;99:6513–24.

444 40. Yu M, Levine SJ. Toll-like receptor 3, RIG-I-like receptors and the NLRP3 inflammasome: Key
445 modulators of innate immune responses to double-stranded RNA viruses. Cytokine & Growth Factor
446 Reviews. 2011;22:63–72.

447 41. Tachibana T, Ishimaru Y, Makino R, Khan SI, Cline MA. Effect of central injection of tumor-necrosis
448 factor-like cytokine 1A and interferons on food intake in chicks. Physiology & Behavior. 2018;194:199–
449 204.

450 42. Blevins HM, Xu Y, Biby S, Zhang S. The NLRP3 Inflammasome Pathway: A Review of Mechanisms
451 and Inhibitors for the Treatment of Inflammatory Diseases. Front Aging Neurosci. 2022;14:879021.

452 43. Derecki NC, Cardani AN, Yang CH, Quinnies KM, Crihfield A, Lynch KR, et al. Regulation of
453 learning and memory by meningeal immunity: a key role for IL-4. Journal of Experimental Medicine.
454 2010;207:1067–80.

455 44. DiSabato DJ, Quan N, Godbout JP. Neuroinflammation: the devil is in the details. Journal of
456 Neurochemistry. 2016;139:136–53.

457 45. Ziv Y, Ron N, Butovsky O, Landa G, Sudai E, Greenberg N, et al. Immune cells contribute to the
458 maintenance of neurogenesis and spatial learning abilities in adulthood. Nat Neurosci. 2006;9:268–75.

459 46. Kuttiyarthu Veetil N, Cedraz De Oliveira H, Gomez-Samblas M, Divín D, Melepat B, Voukali E, et al.
460 Peripheral inflammation-induced changes in songbird brain gene expression: 3' mRNA transcriptomic
461 approach. Developmental & Comparative Immunology. 2024;151:105106.

462 47. Salinas S, Schiavo G, Kremer EJ. A hitchhiker's guide to the nervous system: the complex journey of
463 viruses and toxins. Nat Rev Microbiol. 2010;8:645–55.

464 48. Jax E, Müller I, Börno S, Borlinghaus H, Eriksson G, Fricke E, et al. Health monitoring in birds using
465 bio-loggers and whole blood transcriptomics. Sci Rep. 2021;11:10815.

466 49. Tamura Y, Yamato M, Kataoka Y. Animal Models for Neuroinflammation and Potential Treatment
467 Methods. Front Neurol. 2022;13:890217.

468 50. Gómez Samblás M, Melepat B, Divín D, Li T, Voukali E, Marková K, et al. Dynamics of cytokine
469 expression profile changes during inflammation induced by bacterial lipopolysaccharide in a model parrot.
470 in prep.

471 51. Voukali E, Divín D, Samblas MG, Veetil NK, Krajzingrová T, Těšický M, et al. Subclinical peripheral
472 inflammation has systemic effects impacting central nervous system proteome in budgerigars.
473 Developmental & Comparative Immunology. 2024;159:105213.

474 52. Coon CAC, Warne RW, Martin LB. Acute-phase responses vary with pathogen identity in house
475 sparrows (Passer domesticus). American Journal of Physiology-Regulatory, Integrative and Comparative
476 Physiology. 2011;300:R1418–25.

477 53. Cunningham C, Campion S, Teeling J, Felton L, Perry VH. The sickness behaviour and CNS
478 inflammatory mediator profile induced by systemic challenge of mice with synthetic double-stranded
479 RNA (poly I:C). Brain, Behavior, and Immunity. 2007;21:490–502.

480 54. Uysal AK, Martin LB, Burkett-Cadena ND, Barron DG, Shimizu T. Simulated viral infection in early-
481 life alters brain morphology, activity and behavior in zebra finches (Taeniopygia guttata). Physiology &
482 Behavior. 2018;196:36–46.

483 55. Vinkler M, Leon AE, Kirkpatrick L, Dalloul RA, Hawley DM. Differing House Finch Cytokine
484 Expression Responses to Original and Evolved Isolates of Mycoplasma gallisepticum. Front Immunol.
485 2018;9:13.

486 56. R Core Team. R: A Language and Environment for Statistical Computing. 2021.

487 57. RStudio Team. RStudio: Integrated Development Environment for R. 2021.

488 58. Vinkler M, Fiddaman SR, Těšický M, O'Connor EA, Savage AE, Lenz TL, et al. Understanding the
489 evolution of immune genes in jawed vertebrates. Journal of Evolutionary Biology. 2023;36:847–73.

490 59. Wang J, Wang Y, Wang H, Hao X, Wu Y, Guo J. Selection of Reference Genes for Gene Expression
491 Studies in Porcine Whole Blood and Peripheral Blood Mononuclear Cells under
492 Polyinosinic:Polycytidylic Acid Stimulation. Asian Australas J Anim Sci. 2014;27:471–8.

493 60. Zhang J, Shi H, Zhang L, Feng T, Chen J, Zhang X, et al. Swine acute diarrhea syndrome coronavirus
494 nucleocapsid protein antagonizes the IFN response through inhibiting TRIM25 oligomerization and
495 functional activation of RIG-I/TRIM25. Vet Res. 2024;55:44.

496 61. Fortier M-E, Kent S, Ashdown H, Poole S, Boksa P, Luheshi GN. The viral mimic,
497 polyinosinic:polycytidylic acid, induces fever in rats via an interleukin-1-dependent mechanism. American
498 Journal of Physiology-Regulatory, Integrative and Comparative Physiology. 2004;287:R759–66.

499 62. McGarry N, Murray CL, Garvey S, Wilkinson A, Tortorelli L, Ryan L, et al. Double stranded RNA
500 drives anti-viral innate immune responses, sickness behavior and cognitive dysfunction dependent on
501 dsRNA length, IFNAR1 expression and age. Brain, Behavior, and Immunity. 2021;95:413–28.

502 63. Rymut HE, Bolt CR, Corbett MP, Rund LA, Johnson RW, Rodriguez-Zas SL. PSV-18 Program Chair
503 Poster Pick: Poly(I:C) dose response and its effects on piglet sickness behaviors. Journal of Animal
504 Science. 2020;98 Supplement_4:218–218.

505 64. Yu MC, Young PA, Yu WH. Ultrastructural changes in chick cerebellum induced by polyinosinic
506 polycytidylic acid. Am J Pathol. 1971;64:305–20.

507 65. Hopwood N, Maswanganyi T, Harden LM. Comparison of anorexia, lethargy, and fever induced by
508 bacterial and viral mimetics in rats. Can J Physiol Pharmacol. 2009;87:211–20.

509 66. Yirmiya R, Goshen I. Immune modulation of learning, memory, neural plasticity and neurogenesis.
510 Brain, Behavior, and Immunity. 2011;25:181–213.

511 67. Bao M, Hofsink N, Plösch T. LPS versus Poly I:C model: comparison of long-term effects of bacterial
512 and viral maternal immune activation on the offspring. American Journal of Physiology-Regulatory,
513 Integrative and Comparative Physiology. 2022;322:R99–111.

514 68. Pan L, Zhu W, Li C, Xu X, Guo L, Lu Q. Toll-like receptor 3 agonist Poly I:C protects against
515 simulated cerebral ischemia in vitro and in vivo. Acta Pharmacol Sin. 2012;33:1246–53.

516 69. Field R, Campion S, Warren C, Murray C, Cunningham C. Systemic challenge with the TLR3 agonist
517 poly I:C induces amplified IFNα/β and IL-1β responses in the diseased brain and exacerbates chronic
518 neurodegeneration. Brain, Behavior, and Immunity. 2010;24:996–1007.

519 70. Wang T, Town T, Alexopoulou L, Anderson JF, Fikrig E, Flavell RA. Toll-like receptor 3 mediates
520 West Nile virus entry into the brain causing lethal encephalitis. Nat Med. 2004;10:1366–73.

521 71. Bsibsi M, Persoon-Deen C, Verwer RWH, Meeuwsen S, Ravid R, Van Noort JM. Toll-like receptor 3
522 on adult human astrocytes triggers production of neuroprotective mediators. Glia. 2006;53:688–95.

523 72. Farina C, Krumbholz M, Giese T, Hartmann G, Aloisi F, Meinl E. Preferential expression and function
524 of Toll-like receptor 3 in human astrocytes. Journal of Neuroimmunology. 2005;159:12–9.

525 73. Scumpia PO, Kelly KM, Reeves WH, Stevens BR. Double-stranded RNA signals antiviral and
526 inflammatory programs and dysfunctional glutamate transport in TLR3-expressing astrocytes. Glia.
527 2005;52:153–62.

528 74. Town T, Jeng D, Alexopoulou L, Tan J, Flavell RA. Microglia Recognize Double-Stranded RNA via
529 TLR3. The Journal of Immunology. 2006;176:3804–12.

530 75. St. Paul M, Mallick AI, Read LR, Villanueva AI, Parvizi P, Abdul-Careem MF, et al. Prophylactic
531 treatment with Toll-like receptor ligands enhances host immunity to avian influenza virus in chickens.
532 Vaccine. 2012;30:4524–31.

533 76. Kanneganti T-D, Body-Malapel M, Amer A, Park J-H, Whitfield J, Franchi L, et al. Critical Role for
534 Cryopyrin/Nalp3 in Activation of Caspase-1 in Response to Viral Infection and Double-stranded RNA.
535 Journal of Biological Chemistry. 2006;281:36560–8.

536 77. Rajan JV, Warren SE, Miao EA, Aderem A. Activation of the NLRP3 inflammasome by intracellular
537 poly I:C. FEBS Letters. 2010;584:4627–32.

78. Ogaili A, Hameed S, Noori N. LPS-induced NLRP3 gene-expression in chicken. Open Vet J. 2022;12:197.

79. Gurung P, Li B, Subbarao Malireddi RK, Lamkanfi M, Geiger TL, Kanneganti T-D. Chronic TLR Stimulation Controls NLRP3 Inflammasome Activation through IL-10 Mediated Regulation of NLRP3 Expression and Caspase-8 Activation. Sci Rep. 2015;5:14488.

80. Koller BH, Nguyen M, Snouwaert JN, Gabel CA, Ting JP-Y. Species-specific NLRP3 regulation and its role in CNS autoinflammatory diseases. Cell Reports. 2024;43:113852.

Figures

Figure 1. Correlation matrix comparing the relative gene expression in budgerigar ileum and brain during response to poly (I:C). The gene-pairs with positive correlation are depicted with positive slopes and blue colour and genes with negative correlation are depicted with negative slopes and red colour. Intensity of the colour and cloud shape indicate size of the correlation coefficient.

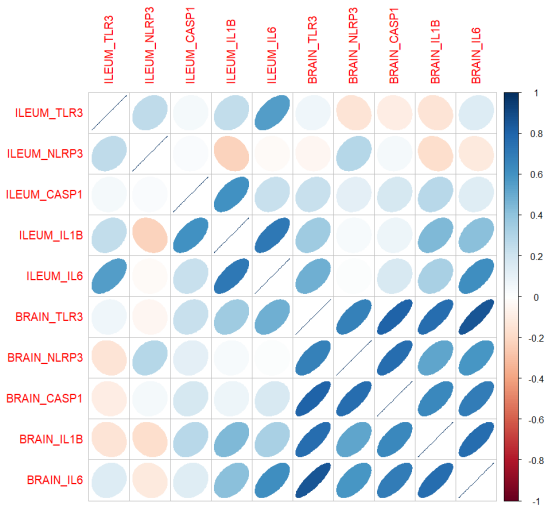

Figure 2. Changes in relative *IL1B* (A) and *IL6* (B) gene expression in budgerigar ileum at different time points during response to poly(I:C). The cytokine gene expression is shown as logQst values on the y axis, time across three sampling time points (3, 6 and 24 hours) is plotted on the x axis. C = controls (blue),

L = low dose of poly(I:C) (orange), H = high dose of Poly(I:C) (red). The asterisks indicate the significant differences revealed by the TukeyHSD test: * for 0.010<P<0.050, ** for 0.001<P<0.010, *** for P << 0.001 (for details see Table S12 in ESM1).

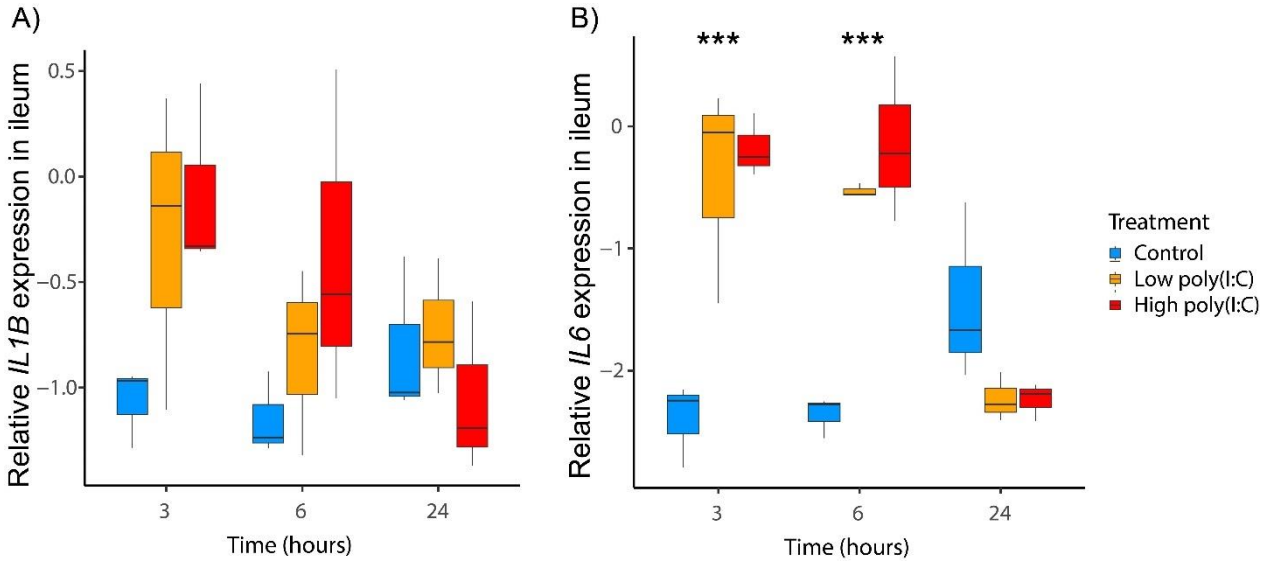

Figure 3. Changes in relative *TLR3* (A) *IL1B* (B) *IL6* (C) gene expression in budgerigar brain at different time points during response to poly(I:C). The *TLR3* gene expression is shown as logQst values on the y axis, time across three sampling time points (3, 6 and 24 hours) is plotted on the x axis. C = controls (green), L = low dose of poly(I:C) (orange), H = high dose of Poly(I:C) (red). The asterisks indicate the significant differences revealed by the TukeyHSD test: * for 0.010<P<0.050, ** for 0.001<P<0.010, *** for P << 0.001 (for details see Table S12 in ESM1).

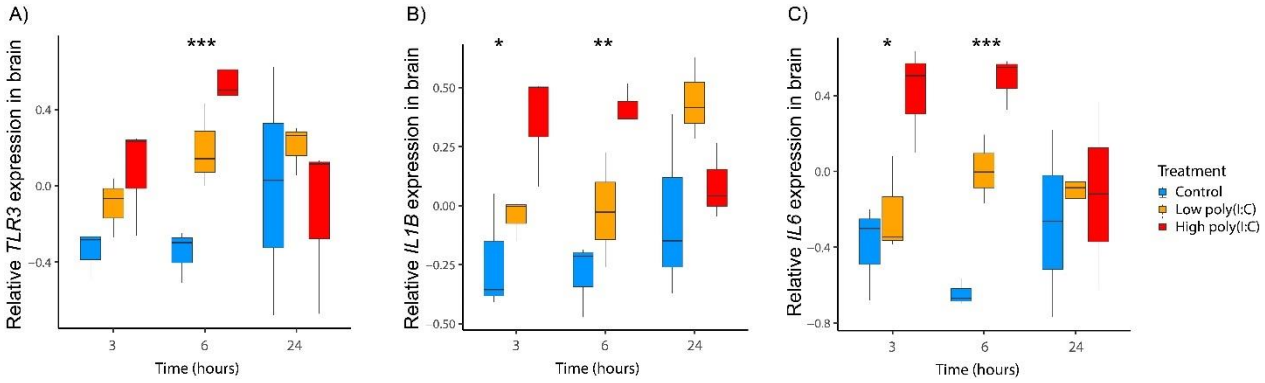

PAPER III

Voukali, Eleni, Daniel Divín, Mercedes Goméz Samblas, Nithya Kuttiyarthu Veetil, Tereza Krajzingrová, Martin Těšický, Tao Li, **Balraj Melepat**, Pavel Talacko, and Michal Vinkler. "Subclinical peripheral inflammation has systemic effects impacting central nervous system proteome in budgerigars." Developmental & Comparative Immunology 159 (2024): 105213.

Developmental and Comparative Immunology 159 (2024) 105213

Contents lists available at ScienceDirect

Developmental and Comparative Immunology

journal homepage: www.elsevier.com/locate/devcompimm

Subclinical peripheral inflammation has systemic effects impacting central nervous system proteome in budgerigars

Eleni Voukali [a,*], Daniel Divín [a], Mercedes Goméz Samblas [a], Nithya Kuttiyarthu Veetil [a], Tereza Krajzingrová [a], Martin Těšický [a], Tao Li [a], Balraj Melepat [a], Pavel Talacko [b], Michal Vinkler [a,**]

[a] Charles University, Faculty of Science, Department of Zoology, Viničná 7, 128 43, Prague, Czech Republic
[b] Biotechnology and Biomedicine Centre of Academy of Sciences and Charles University, Laboratory of OMICS Proteomics and Metabolomics, Průmyslová 595, 252 50, Vestec, Czech Republic

ARTICLE INFO

Keywords:
Cerebrospinal fluid
Dextran sulphate sodium
Endotoxin
Parrot
Plasma
Proteomics

ABSTRACT

Regulation of neuroimmune interactions varies across avian species. Little is presently known about the interplay between periphery and central nervous system (CNS) in parrots, birds sensitive to neuroinflammation. Here we investigated the systemic and CNS responses to dextran sulphate sodium (DSS)- and lipopolysaccharide (LPS)-induced subclinical acute peripheral inflammation in budgerigar (*Melopsittacus undulatus*). Three experimental treatment groups differing in DSS and LPS stimulation were compared to controls. Individuals treated with DSS showed significant histological intestinal damage. Through quantitative proteomics we described changes in plasma (PL) and cerebrospinal fluid (CSF) composition. In total, we identified 180 proteins in PL and 978 proteins in CSF, with moderate co-structure between the proteomes. Between treatments we detected differences in immune, coagulation and metabolic pathways. Proteomic variation was associated with the levels of pro-inflammatory cytokine mRNA expression in intestine and brain. Our findings shed light on systemic impacts of peripheral low-grade inflammation in birds.

1. Introduction

Even mild immune responses in the periphery frequently initiate systemic responses, modulating immunity in remote tissues, including the central nervous system (CNS). Proinflammatory pathways may trigger signals activating glial cells in brain, namely the astrocytes and microglia. Response in these brain cells facilitates shaping of the subsequent neural feedback to the peripheral stimulation that is often linked with attenuation of the inflammatory pathways and onset of sickness behaviour (Dantzer et al., 2008). Among sources of the peripheral inflammation, gastrointestinal tract (GIT) and skin can be of special importance because they directly interact with high microbial loads. At both sites, injuries combined with microbial infections can alter homeostasis (microbiota dysbiosis), causing deviations from the immune tolerogenic regulatory balance (Belkaid and Hand, 2014).

In non-model species, the neuroimmune interplay forms an unfamiliar landscape in which even the well-known actors, such as the cytokines, neuropeptides and other immunomodulatory molecules may show shifted physiological roles. Our recent research has indicated that parrots represent an interesting animal model for investigation of the interaction between peripheral immune stimulation and CNS responses. Due to genomic rearrangement, the parrots entirely lack functional

Abbreviations: **ANK1**, Ankyrin-1; **APOA4**, Apolipoprotein A-IV; **BP**, Biological processes; **BR**, Hyperpallial Region of Brain; **CNS**, Central Nervous System; **CO**, Colon; **COMP**, Cartilage Oligomeric Matrix Protein; **CRK**, Adapter Molecule CRK; **CSF**, Cerebrospinal Fluid; **DSS**, Dextran Sulphate Sodium; **EPB41**, Protein 4.1; **FC**, Fold Change; **FDR**, False Discovery Rate; **FGA**, Fibrinogen A; **FGB**, Fibrinogen B; **FGG**, Fibrinogen G; **FHL2**, Four and a half LIM domains protein 2; **GIT**, Gastrointestinal Tract; **GO**, Gene Ontology; **GSEA**, Gene Set Enrichment Analysis; **IL**, Ileum; **IL1B**, Interleukin 1B; **IL6**, Interleukin 6; **IL18**, Interleukin 18; **KEGG**, Kyoto Encyclopaedia of Genes and Genomes; **LC-MS/MS**, liquid chromatography-tandem mass spectrometry; **LMNB1**, Lamin-B1; **LPS**, Lipopolysaccharide; **PC1**, First Component of PCA; **PCA**, Principal Component Analysis; **PL**, Plasma; **PLCB1**, 1-Phosphatidylinositol 4,5-Bisphosphate Phosphodiesterase Beta-1; **PHA**, Phytohemagglutinin; **RT-qPCR**, Reverse Transcriptase Quantitative Real Time Polymerase Chain Reaction; **SAA**, Serum amyloid A protein; **VTN**, Vitronectin.

* Corresponding author. Charles University, Faculty of Science, Department of Zoology, Viničná 7, 128 43, Prague, Czech Republic.
** Corresponding author. Charles University, Faculty of Science, Department of Zoology, Viničná 7, 128 43, Prague, Czech Republic.
E-mail addresses: voukalie@natur.cuni.cz (E. Voukali), michal.vinkler@natur.cuni.cz (M. Vinkler).

https://doi.org/10.1016/j.dci.2024.105213
Received 31 January 2024; Received in revised form 13 June 2024; Accepted 13 June 2024
Available online 14 June 2024

cannabinoid receptor 2 (*CNR2*) gene. This loss apparently makes them susceptible to neuroinflammation, a condition of up-regulation of inflammatory pathways in the nervous tissue which can alter the brain function, including mood and cognitive effects (Divín et al., 2022). Among birds, parrots are known for their exceptional cognitive abilities and have been studied for complex social interactions mediated by learned vocalization (Ali et al., 1993). These cognitive abilities have been attributed to their relatively large brains (Iwaniuk et al., 2005) with high neuronal densities especially in telencephalon (Olkowicz et al., 2016). Thus, parrots may serve as valuable models to study immunity effects on brain physiology, adult neurogenesis, social interactions, and intricate behavioural traits under the condition of acute or chronic neuroinflammation.

Animal models of induced dysbiosis are often based on induction of colitis by oral administration of dextran sulphate sodium (DSS) (Okayasu et al., 1990; Wirtz et al., 2017). DSS dissolved in drinking water causes damage to gut epithelial cells of the basal crypts and affects the integrity of the mucosal barrier (Chassaing et al., 2014; Okayasu et al., 1990; Wirtz et al., 2017). This tissue damage triggers mucosal intestinal inflammation, serving as a model of the innate immune response during the colonic diseases (Chassaing et al., 2014). The DSS treatment is also known to alter the intestinal microbiota composition (Okayasu et al., 1990). DSS-induced colitis has advantages over other models because DSS administration is reproducible and stress free, when compared to colorectal instillation required by other methods (e.g., using dinitrobenzene sulfonic acid and 2,4,6-trinitrobenzenesulfonic acid (Elson et al., 1995). Recently, the DSS-induced colitis has become a frequent intestinal inflammatory model also in poultry. DSS treatment in poultry activates expression of a range of pro-inflammatory cytokines and other markers (Dal Pont et al., 2021; Liu et al., 2022; Zou et al., 2018) and affects egg production due to liver inflammation (Nii et al., 2020). Nevertheless, only very few studies have so far focused on the neuro-immune interactions in birds. In an experimental model designed to explore gut-brain interactions in chicken, heat stress and intestinal infection of *Clostridium perfringens* altered behavioural patterns, corticosterone serum levels, and CNS activity in hypothalamus, amygdala, preoptic area and globus pallidus (Calefi et al., 2016). Yet, limited information is still available to systemic regulatory effects of the DSS-induced inflammation even in the chicken and no immune response data exist to any non-poultry avian species.

In non-poultry birds, systemic inflammation is more commonly experimentally induced in the periphery by immune stimulation of skin by plant (e.g. phytohemagglutinin, PHA) (Smits et al., 1999; Vinkler et al., 2010, 2014) or bacterial (e.g. lipopolysaccharide, LPS) toxins (Sköld-Chiriac et al., 2015). This mode of activation serves as a model of skin injury-induced inflammation. Both PHA and LPS trigger infiltration of leukocytes into the skin that is linked with up-regulation of expression of various pro-inflammatory cytokines, namely interleukin 1β (*IL1B*) and interleukin 6 (*IL6*) (Divín et al., 2022). The known systemic effects of such stimulation include changes in body temperature (Sköld-Chiriac et al., 2015), transcriptomic changes in blood (Meitern et al., 2014) and also up-regulated inflammatory cytokine expression in the brain of some species (Divín et al., 2022). It is particularly the interaction between the peripheral stimulation and the immune response in brain that awakes the interest when further exploration of the immunomodulation in parrots is concerned.

Proteomics represents a suitable approach to study the inflammatory responses in various tissues (Mohanty et al., 2023). Plasma (PL) protein composition offers an insight into the systemic effects of the immune response. On the other hand, the proteome of the cerebrospinal fluid (CSF) provides a perspective of the brain response to stimulation. Thus, investigation of both these fluids is important to elucidate the relevance of peripheral regulation of neuroinflammation. Unfortunately, there is currently little evidence available for any comparative approach in vertebrates (Voukali et al., 2021; Voukali and Vinkler, 2022). Only recently, proteomics of colitis induced by the DSS treatment has been studied in mouse colon (Dou et al., 2020; Du et al., 2022; Wang et al., 2022), and PL (Huang et al., 2022). No evidence is available for the effects of such treatment on the CSF proteome. However, in mammals as well as in the chicken, proteomic evidence reveals significant systemic changes in protein expression triggered in PL (Burnap et al., 2021; Harberts et al., 2020; Horvatić et al., 2019; Kuleš et al., 2020; Mohanty et al., 2023; Packialakshmi et al., 2016; Puris et al., 2022) and brain (Imamura et al., 2023; Wang et al., 2016) by the intraperitoneal application of LPS. Nevertheless, proteomic evidence is presently lacking to the systemic effects of the skin LPS treatment in any vertebrate species.

In the present project, we focused on the proteomics of inflammation-associated neuro-immune interaction between periphery and CNS in a model species of a parrot, the budgerigar (*Melopsittacus undulatus*), analysing composition of the soluble proteins represented in PL and CSF. The objectives of this study were (1) to describe the effects of DSS on the budgerigar GIT histology, (2) to characterize the budgerigar PL and CSF proteomic profiles, and (3) to compare the acute low-grade peripheral inflammation effects of DSS and LPS in parrots.

2. Methods

2.1. Animals and experimental stimulation of low-grade peripheral inflammation

Thirty-five regular adult budgerigars of apparently clinically healthy status were purchased from hobby breeders in Prague, Czech Republic. The birds were introduced to the animal facility of the Charles University, Faculty of Science, where they were housed in pairs under standard conditions (12 L:12D) in cages 50 × 50 × 100 cm with free access to food and tap water. Budgerigars belong to parrots, i.e. avian group showing advanced cognitive abilities. Research in this model needs to follow high ethical standards, including reduction of the numbers of experimental individuals used. The research was approved by the Ethical Committee of Charles University, Faculty of Science and in accordance with ARRIVE guidelines, the current laws of the Czech Republic (permit MSMT-18874/2020–3) and the EU Directive 2010/63/EU for animal experiments.

After two weeks of acclimation, the birds were divided into the following experimental groups: 1) DSS treatment (DSS-C low dose, n = 3; high dose, n = 3; very high dose, n = 3); 2) lipopolysaccharide (LPS) treatment (LPS-C, n = 9); 3) combined DSS and LPS treatment (DSS-LPS, low DSS and LPS, n = 7; high DSS and LPS, n = 7); and 4) controls (C-C, n = 3). Based on our previous results obtained in the zebra finch (*Taeniopygia guttata*), we expected high inter-individual variation in the immune responses to LPS stimulation in skin (Kuttiyarthu Veetil et al., 2024). To avoid inconsistent findings, we assigned higher numbers of individuals to the LPS treatment groups. An overview of the experimental groups and workflow is shown on Fig. 1. Based on the previous research conducted in chicken (Menconi et al., 2015), the animals treated with DSS were administered 25 mg/day (low dose), 50 mg/day (high dose) or 75 mg/day (very high dose; MP Biomedicals, cat. no. 216011025). The DSS treatment was administrated to the animals in doses provided two-times a day (morning and afternoon) for 7 days by oral gavage (Kuttappan et al., 2015). For each dose, the DSS was diluted in a regular fresh tap water in the total volume of 0.5 ml. The control animals were respectively receiving the tap water. The doses used here for the budgerigar are comparable to those previously used in chicken, only adjusted to ½-¼ of the water volume naturally drunk by this desert parrot (ca. 2–4 ml/day). The individuals subjected to the LPS treatment were injected with 0.2 mg LPS (*E. coli* O55:B5, Sigma-Aldrich, cat. no. L2880) freshly suspended in 20 μl sterile saline, subcutaneously into the centre of the left wing patagium on the day following the DSS or control treatment termination.

Throughout the experiment, birds were monitored for any clinical signs of colitis and overall morbidity. Since we observed symptoms of pronounced sickness (cloacal bleeding) in the individuals

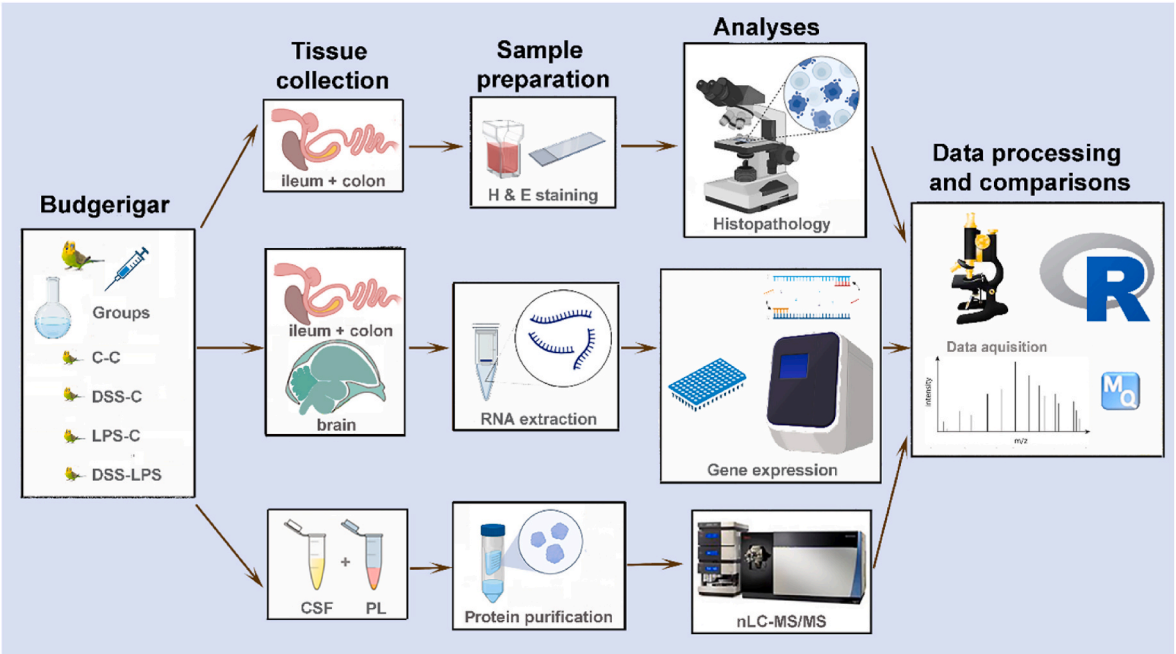

Fig. 1. A schematic overview of the experimental treatment groups and analysis workflows. The initial histopathology screening of the intestine (ileum and colon segments) after administration of low and high dosages of dextran sulphate sodium (DSS) was done only in the DSS-C and C-C groups. Mass spectrometry and gene expression analyses were done in all experimental groups, but the DSS treatments were represented only by the low DSS dose group. C-C, controls; DSS-C, DSS treatment only; LPS-C, lipopolysaccharide (LPS) treatment only; DSS-LPS, combined treatment with both DSS and LPS; PL, plasma; CSF, cerebrospinal fluid; H & E, haematoxylin and eosin. Created using Biorender.com.

experimentally treated with the very high dose of the DSS and high dose of DSS combined with LPS, in these treatment groups we terminated the experiment before completion, i.e., without sample collection (data from these individuals are not included in the present study). Therefore, the data available originate from 22 birds showing no apparent clinical syndromes of the inflammation. Body weight was measured twice, before the DSS/vehicle treatment and prior to tissue collection.

2.2. Tissue collection and processing

Six hours after the LPS treatment, time frequently used in avian studies to measure skin immune responses (Martin et al., 2006; Vinkler et al., 2012, 2014), a blood plasma (PL) sample was taken from all individuals and all the experimental animals were sacrificed by CO_2 to collect CSF. Harvesting and preparation of the CSF and PL samples was conducted as previously reported (Voukali et al., 2021). After CSF collection, tissue samples of the hyperpallial region of brain (BR) and intestine (5 mm-long segments of ileum, IL; and colon, CO; collected ca. 30 mm and 5 mm upwards from cloaca, respectively) were collected from all the experimental animals. Immediately after their collection, the subparts of the samples were immersed in RNAlater (Qiagen, cat. no. 76106), stored at +4 °C for 24 h and then frozen at −80 °C until the subsequent reverse transcriptase quantitative real time polymerase chain reaction (RT-qPCR) analysis.

2.3. Histology and image processing

Subsamples of the CO and IL were fixed in 4% paraformaldehyde, embedded in paraffin as previously described (Moolenbeek and Ruitenberg, 1981), cut into 7 μm microtome sections, stained separately with haematoxylin-eosin and examined by light microscopy at 20 × magnification. Photomicrographs of three randomly selected fields per individual were captured using a Zeiss AxioImager upright microscope equipped with high-resolution digital colour camera (Zeiss, Gottingen, Germany). Image J (v1.52a) was used for morphometric analysis of total mucosal area, villi length and total number of crypts as previously reported (Zou et al., 2018).

2.4. PL and CSF protein purification

The protein purification steps were performed on ice to prevent any sample degradation. All samples were diluted with 0.2-μm-filtered Nanopure water (Thermo, Waltham, MA, USA) at a ratio of 1 g–2 ml of H2O and purified via gel filtration using PD MidiTrap G-25 columns (Cat. No. 28–9180-08, GE Healthcare Life Sciences). Then, the samples were concentrated using lyophilization, and the protein content was determined using Bradford reagent (Sigma-Aldrich) in a microplate, with bovine serum albumin used as a calibration standard. The protein content determined was also used for the calculation of the total proteins. The samples were then processed (Erban et al., 2021) and their trypsin digests were subjected to analysis using nano liquid chromatography tandem mass spectrometry (nLC-MS/MS).

2.5. nLC−MS/MS analysis

Nano reversed-phase columns were used to elute peptide cations. The eluting peptide cations were converted to gas-phase ions by electrospray ionization and analysed on a Thermo Orbitrap Fusion mass spectrometer (Q-OT-qIT, Thermo). Survey scans of peptide precursors from 350 to 1400 m/z were performed at 120 K resolution (at 200 m/z) with a 5×10^5 ion count target. Tandem MS/MS was performed by isolation at 1.5 Th with the quadrupole, high-energy collision dissociation fragmentation with a normalised collision energy of 30 and rapid scan MS analysis in the ion trap. The MS/MS ion count target was set to 10^4 and the max injection time was 35 ms. Only those precursors with a charge state of 2–6 were sampled for MS/MS. The dynamic exclusion duration was set to 45 s with a 10-ppm tolerance around the selected pre-cursor and its isotopes. Monoisotopic precursor selection was turned on and the instrument was run at top speed with 2 s cycles.

2.6. Protein identification

All data were collected and quantified using MaxQuant software version 1.6.10.43 (Cox et al., 2014). False discovery rate (FDR) was set to 1 % for identification of all peptides and proteins. We set a minimum peptide length of seven amino acids. The Andromeda search engine was used for the MS/MS spectra search against the budgerigar *Melopsittacus undulatus* Uniprot reference proteome (downloaded in February 2020, containing 23,704 entries), with all duplicates removed. Enzyme specificity was set as C-terminal to Arg and Lys, also allowing cleavage at proline bonds and a maximum of two missed cleavages. Dithiomethylation of cysteine was selected as a fixed modification and N-terminal protein acetylation and methionine oxidation as variable modifications. Quantifications were performed with the label-free quantification algorithms using a combination of unique and razor peptides (Cox et al., 2014). The mass spectrometry proteomics data have been deposited to the ProteomeXchange Consortium via the PRIDE partner repository with the dataset identifier PXD047322.

We excluded all the unlabelled peptides, peptides only identified by site or reverse, all contaminants, proteins identified by < 2 peptides and, thereafter, we kept only proteins identified in all replicates of at least one group. For the purpose of the pathway enrichment annotations, the corresponding human ortholog gene names and IDs were assigned to all identified proteins using the databases OrthoDB (v10.1) (Kriventseva et al., 2019) and http://birdgenenames.org. When the protein code was not possible to retrieve, the Uniprot protein ID was used.

2.7. RT-qPCR analysis of the cytokine gene expression

In IL, CO and BR, selected cytokine (*IL1B*, *IL6* and *IL18*) mRNA expression levels were quantified by RT-qPCR according to Vinkler et al. (2018). Total RNA was first extracted from the tissue samples using the High Pure RNA Tissue Kit (Cat. No. 12033674001; Roche, Rotkreuz, Switzerland) and its concentration and quality was measured on a NanoDrop 1000 Spectrophotometer (Thermo Fisher Scientific). The RNA was then diluted with transfer RNA carrier (Qiagen, Cat. No. 1068337). To calculate the efficiency of each assay (specific primer pair and a probe), a calibration curve was constructed with a synthetic DNA standard (gBlocks; IDT, Coralville, Iowa, USA; Fig. S1 in Electronic Supplementary Material 1, ESM1). The RNA samples and standards were amplified using the Luna® Universal Probe One-Step RT-PCR Kit (E3006, BioLabs®Inc, Ipswich, Massachusetts, USA) (Table S1 in Electronic supplementary material 2, ESM2). The RT-qPCR was conducted using a LightCycler 480 PCR platform (Roche) set with the following cycling conditions: (1) 50 °C for 10 min, (2) 95 °C for 1 min and (3) (95 °C for 10 s, 60 °C for 30 s) × 45. All assays were performed with template-free negative controls and synthetic DNA standards as positive controls in a freshly prepared dilution series. To test for the gene expression changes for each sample we calculated the standardised relative quantities (Qst).

2.8. Statistical and bioinformatic analyses

The statistical and bioinformatics analysis was conducted in the R software (R Core Team, 2024) (version 4.4.0). We conducted unpaired t-tests, following normality assessment with Shapiro test and nested ANOVA for the quantification of DSS effect on the budgerigar intestinal histological structure. In order to supress the minor technical variation between samples, the abundances of the identified proteins were previously normalised using the Variance stabilization normalization method. Missing data for the protein abundances were imputed using a mixed imputation method provided by DEP 1.22.0 R package after evaluating the random and non-random missing values. Significantly differentially expressed proteins were identified by multifactorial analysis with limma corrected by the Permutation Based FDR (FDR-adjusted p value < 0.05). The Retrieval of Interacting Genes (STRING 12.0; http://string-db.org) web-tool (von Mering et al., 2003) was used to analyse and construct the protein-protein interaction (PPI) network of the over-represented proteins in the treatment groups compared to the unstimulated controls. Significant PPIs were considered those with a combined score >0.4 and annotations from human (*Homo sapiens*). Gene Set Enrichment Analysis (GSEA) was performed using the R package ClusterProfiler (Yu et al., 2012), using as a reference *Homo sapiens* and the annotation data sets of the Gene Ontology (GO) (Ashburner et al., 2000) and biological pathways (Kyoto Encyclopaedia of Genes and Genomes, KEGG; REACTOME) (Kanehisa et al., 2012; Fabregat et al., 2018). The Benjamini-Hochberg FDR threshold was set to 0.05 of all enriched pathways in PL and CSF. The lists of GO for Biological processes (BP) from PL and CSF were analysed by REVIGO (revigo.irb.hr, accessed on October 20, 2023), to remove redundancy (Supek et al., 2011). Computation of coinertia was performed to explore the co-structuring between the PL and CSF proteomes using the package made 4 (Culhane et al., 2003). Also, we performed two-way ANOVA with Tukey multiple corrections to detect the differences in the mRNA expression of proinflammatory cytokines. We constructed a Pearson correlation matrix to explore the expression relationships between different cytokines across tissues and performed the principal component analyses (PCA) in proteome and cytokine mRNA expression datasets. For graphical visualisation, the R package ggplot2 (Wickham, 2009) was used.

3. Results

3.1. Clinical symptoms and histopathology of the GI tract following the DSS treatment

Our results suggest that daily DSS doses higher than 50 mg can be vitally dangerous for the budgerigars, due to extensive gastrointestinal bleeding. At lower doses we did not observe bleeding or find any significant decrease in body weight ($p > 0.05$) in the DSS-treated animals. Therefore, we consider these doses as subclinical. However, our histological examination of the small and large intestine showed that the DSS treatment affected the integrity of the intestinal wall when administrated at both low and high doses, with notable structural difference in the villi emerging from the muscularis mucosa. Specifically, villi lost their characteristic elongated structure, erosion of the epithelial layer has been noted, crypts showed irregular with abnormal architecture and the overall mucosal layer shortened (Fig. 2a). While there was no significant difference between the low-dose and high-dose groups in measurements of the mucosal area, length of the villi and number of the crypts (Welch Two Sample *t*-test, $p > 0.05$), the combined data for both the DSS doses revealed significant reduction in the mucosal area (ANOVA nested with the slide replicates per bird; $t = -4.549$, $df = 6.996$, $p < 0.01$) as well as the length of the villi in ileum and colon (ANOVA nested with the slide replicates per bird; $t = 6.779$, $df = 6.860$, $p < 0.001$, Fig. 2b and c) in the DSS-treated animals compared to controls. Also, the number of crypts non-significantly tented to be lower in the DSS-treated gut (ANOVA nested with the slide replicates per bird; $p > 0.098$, Fig. 2d). Therefore, we selected the low-dose group for further evaluation of low-grade inflammation reflecting poor subclinical intestinal health.

3.2. Proteomics of PL and CSF

We identified 180 individual protein hits in PL and 978 in CSF (Tables S2 and S3, ESM2). PL had an overlap with CSF in 155 proteins (Fig. S2a in ESM1). Our multifactorial analysis revealed that sex had no significant effect on either the PL or CSF proteome comparison, so this variable has not been further considered.

In PL, PCA showed that the first two components explained 50.28% of the variance in protein composition (Fig. S2b in ESM1). Differential expression analysis identified 10 proteins with significantly different

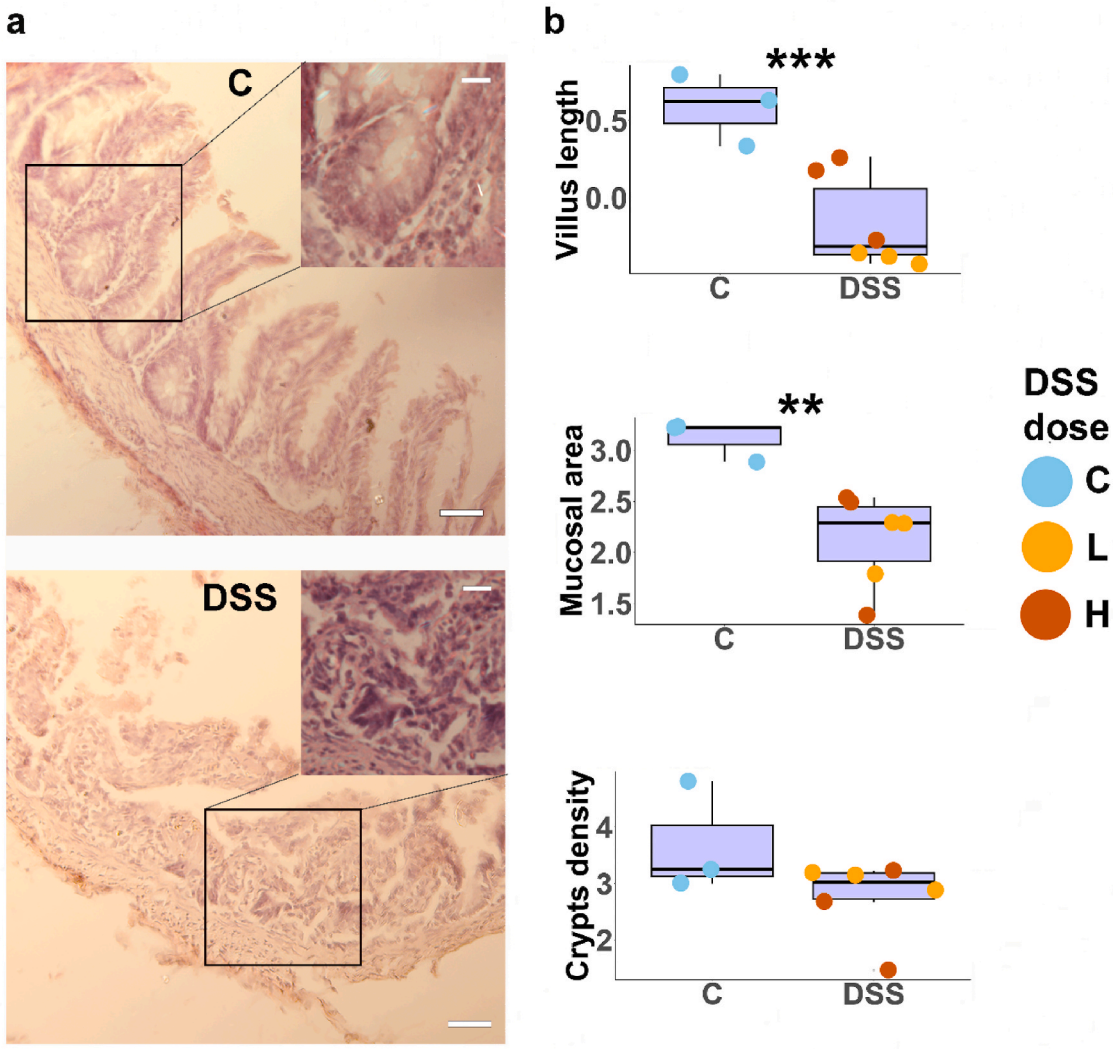

Fig. 2. Dextran sulphate sodium (DSS) induced significant structural alterations in the budgerigar intestine. **(a)** Haematoxylin & eosin microscopic images of the ileum of control (C) and DSS low-dose-treated birds with induced colitis (20x; 40x; scale bars represent 50 μm and 20 μm respectively). **(b)** Boxplots showing the quantitative differences in the DSS-induced histological changes measured as disruption of the mucosal area, shortening of intestinal villi and reduction in crypt density (non-significant trend). Asterisks indicate statistical significance of $p < 0.01$ (**) and $p < 0.001$ (***); C, n = 3; DSS low dose (L), n = 3; DSS high dose (H), n = 3.

abundances between our treatment groups (FDR <0.05, log2 fold change, log2FC ≥ 1.5, Fig. 3a, Table S4 in ESM2). The significantly up-regulated and down-regulated proteins for each group are shown in Fig. 3b and c. Serum amyloid A protein (SAA or *SAA1*, ortholog for *Homo sapiens*) was commonly up-regulated in all treatment-stimulated individuals (C-C vs DSS-C/LPS-C/DSS-LPS; Fig. 3b and c). For DSS-treated birds, vitronectin (VTN) was significantly down-regulated in PL compared to controls, although less than the threshold of log2FC ≥ 1.5 (log2FC = 1.15). The parrots stimulated with LPS alone or combined with DSS additionally had up-regulated three fibrinogen proteins, fibrinogen A (FGA), fibrinogen B (FGB) and fibrinogen G (FGG), while down-regulated Four and a half LIM domains protein 2 (FHL2). The comparison of DSS vs. LPS showed significantly decreased abundances of FGA, FGB and FGG in DSS samples (or increased for LPS) and increased (or decreased for LPS) mitochondrial aconitate hydratase (ACO2), adenylate kinase isoenzyme 1 (two isoforms, AK1), FHL2, glyceraldehyde-3-phosphate dehydrogenase (GAPDH) and phosphoglucomutase-1 (PGM1). For the comparisons LPS-C vs DSS-LPS and DSS-C vs DSS-LPS, none of the proteins exceeded the threshold of statistical significance. The heatmap of significantly different protein abundance values illustrates that the control individuals were more similar to the DSS group, while the LPS- were similar to the DSS-LPS treated birds (Fig. 3a). The PPI analysis of the significantly differentially expressed proteins revealed two associative networks with pathways related to immune processes (coagulation and complement cascades, and platelet activation) and metabolism (glycolysis and ATP metabolic processes; Fig. 3d–Table S5 in ESM2). In line with these results, GSEA analysis using KEGG, REACTOME and GO revealed up-regulation of coagulation and complement cascades, fibrin clot formation and extracellular matrix reorganisation for DSS-C, LPS-C or LPS-DSS samples. LPS, both combined with DSS or not, stimulated wound healing and proteolysis and down-regulated carbohydrate metabolic processes. Enriched terms for GO Cellular Components included platelet granules and secretory vesicles for all treatments ($p < 0.05$, FDR <0.05, Fig. 4a, b, Table S6, ESM2). The enriched pathways mostly overlapped for comparisons of LPS-C and DSS-LPS with the control individuals (Fig. 4a–Table S6 in ESM2).

In CSF, the first two components of PCA explained 50.28% of the variation in protein composition (Fig. S2b in ESM1). We identified 73 significantly differentially abundant proteins between our treatment

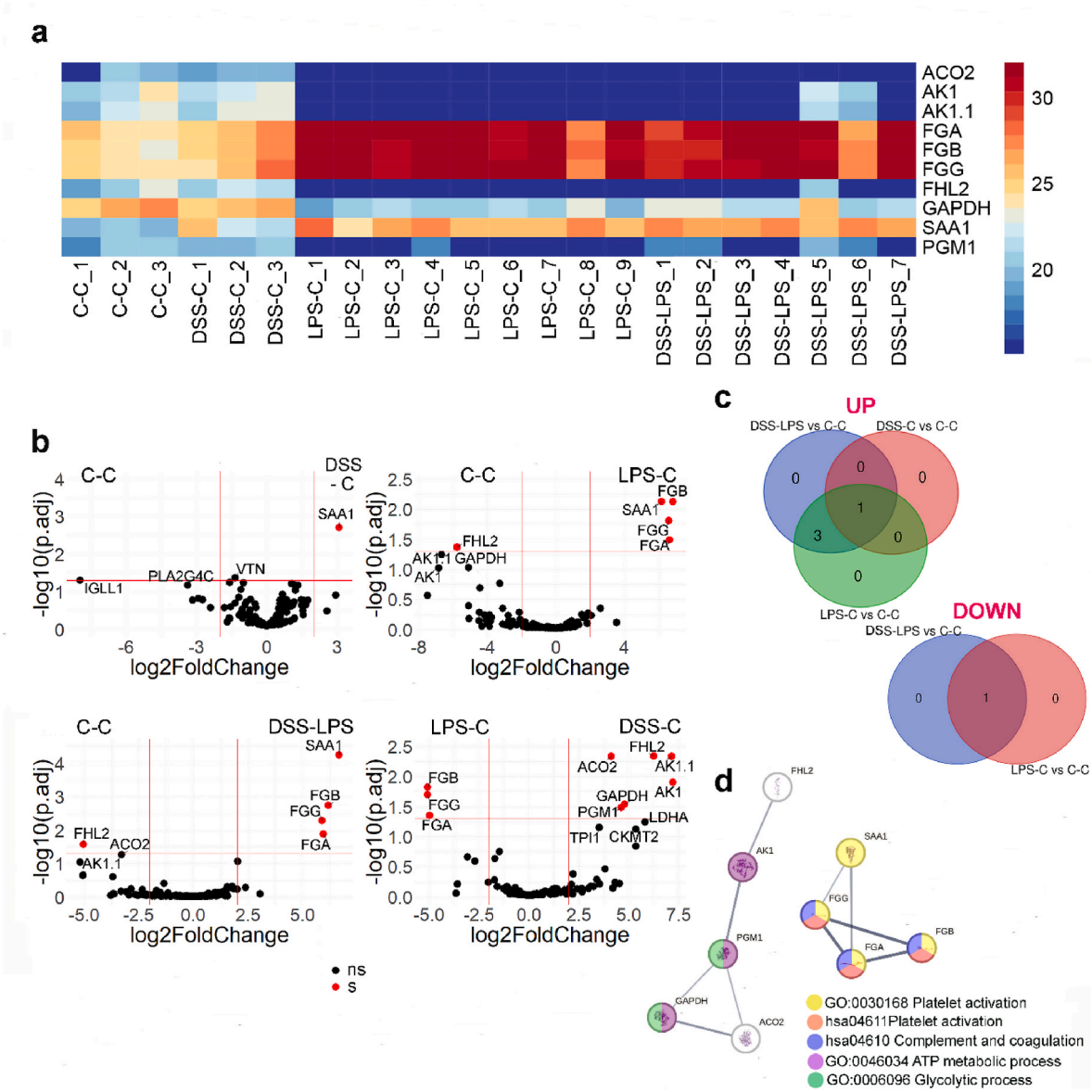

Fig. 3. Differential protein expression analysis of the budgerigar plasma proteomes after dextran sulphate sodium (DSS), lipopolysaccharide (LPS) treatment or their combination. (a) A heatmap depicting variation in all significantly differentially abundant proteins (rows) across all the samples analysed (columns). (b) Volcano plots showing the protein expression fold changes and their significance across the comparisons of the treatment groups tested. The p-adjusted values are expressed as negative decadic logarithm of the Permutation Based false-discovery rate (FDR). The fold change differences of the plasma proteins (x-axis) dependent on their FDRs (y-axis) are shown in dots, colour coded as red = significant (s) and black = non-significant (ns), based on a significance threshold set to p. adj <0.05 and fold change cut-off ≥1.5. Significant and marginally non-significant proteins are labelled with their corresponding human orthologs. (c) Overlaps of the significantly up-regulated (UP) and down-regulated (DOWN) proteins compared to controls across treatments. (d) Protein-protein interactions of the 10 significantly dysregulated proteins shown in (a) compared to the unstimulated controls. Connections indicate functional associations between the proteins. Line thickness indicates the strength of the data support. Indicative enriched terms (False discovery rate <0.05) from Gene Ontology Biological Processes and Kyoto Encyclopaedia of Genes and Genomes are shown as colour-codes in circles indicating the individual proteins. Controls (C-C, n = 3), birds treated with DSS (DSS-C, n = 3), LPS (LPS-C, n = 9), or both DSS and LPS (DSS-LPS, n = 7). (For interpretation of the references to colour in this figure legend, the reader is referred to the Web version of this article.)

groups (FDR <0.05, log2FC ≥ 1.5, Fig. 5a, b, Table S7 in ESM2). The significantly up-regulated and down-regulated proteins for each group are depicted in Fig. 5b and c. Comparisons of all the treatments (C-C vs DSS-C/LPS-C/DSS-LPS) against controls showed common decrease in the abundances of ten proteins: erythrocyte membrane protein band 4.1 (EPB41), histones (H1-1, H2AFX, H1-0), ribosomal proteins (RPS17, RPS13), ankyrin-1 (ANK1), lamin-B1 (LMNB1), and high mobility group proteins (HMGB3, HMGB1). We found a significant increase in the relative abundances of 10 proteins exclusively in the DSS group and decrease in 19 proteins, 7 of which exclusively in DSS samples (Fig. 5b and c). Apolipoprotein A-IV (APOA4) and cartilage oligomeric matrix protein (COMP) were commonly up-regulated in the CSF of birds stimulated with LPS with or without DSS (Fig. 5b). There was a big overlap of down-regulated gene products across the two LPS-treated groups (with or without DSS) (Fig. 5c), involving mostly mitochondrial proteins. For LPS-C vs. DSS-LPS, none of the proteins exceeded the threshold of statistical significance. The significantly differentially expressed proteins from all comparisons formed a densely interacting network consisting of two parts connected by the protein alpha synuclein. The network was especially enriched with pathways associated to oxidative phosphorylation, response to stress and transport (Fig. 6, Table S8 in ESM2). The GSEA analysis of KEGG, GO and REACTOME showed a depletion of

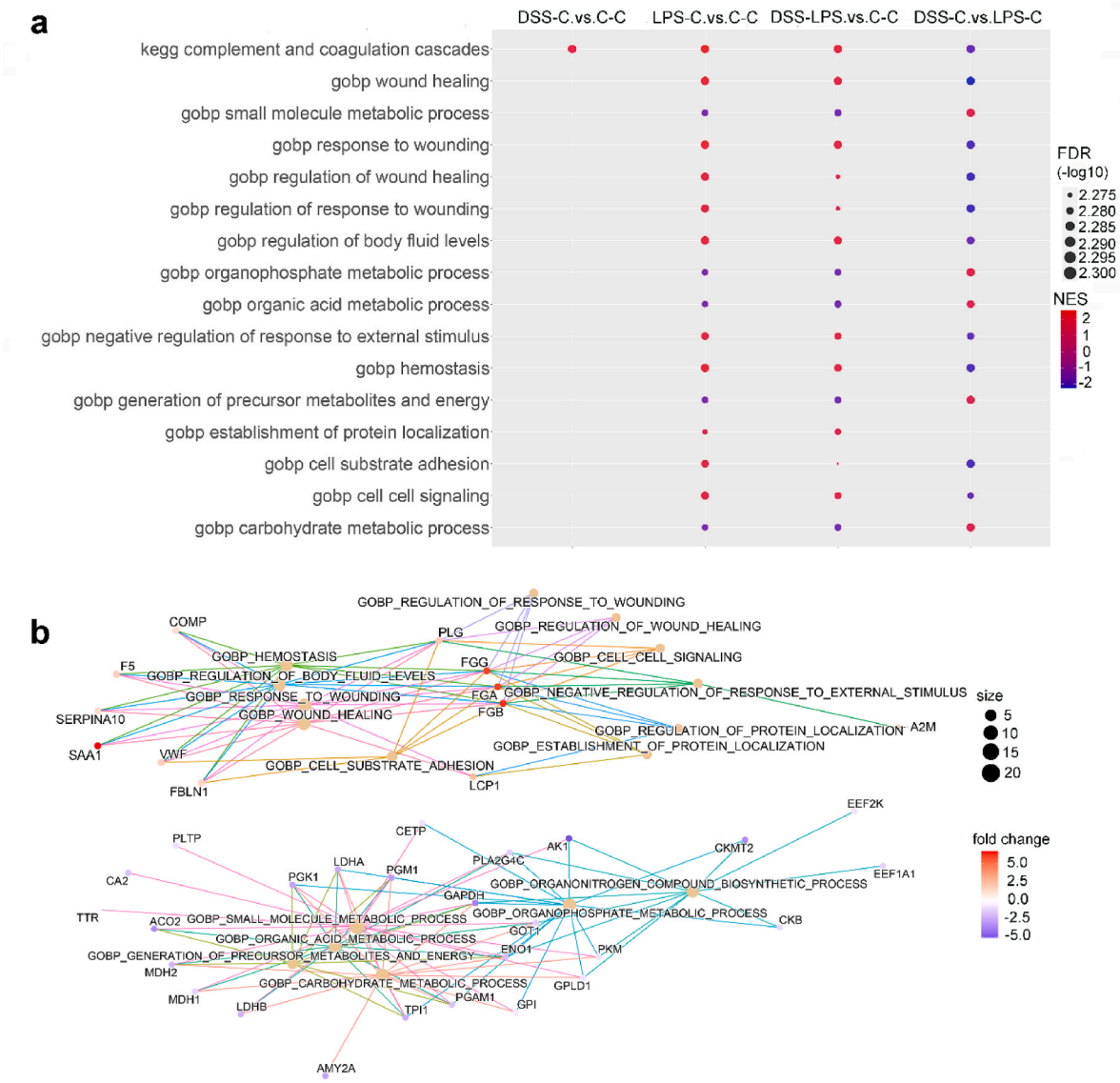

Fig. 4. Plasma (PL) proteomics: Gene Set Enrichment Analysis (GSEA) based on the Kyoto Encyclopaedia of Genes and Genomes (KEGG) pathways and Gene Ontology (GO) for Biological Processes (BP). (a) Non-redundant enriched pathways in PL are plotted for each comparison. The dots represent term enrichment with colour coding according to the normalised enrichment score (NES). The sizes of the dots represent the negative logarithmic value of false discovery rate (FDR) with increasing value indicating higher significance. Controls (C-C, n = 3), birds treated with DSS (DSS-C, n = 3), LPS (LPS-C, n = 9), or both DSS and LPS (DSS-LPS, n = 7). (b) Network plot showing the linkages of the GO BP enriched terms and the gene products in the PL samples from birds treated with DSS-LPS compared to unstimulated controls. The sizes of the dots corresponding to each term represent their numbers of proteins covered and the dot colours show the degree of the log fold change of the proteins in DSS-LPS samples after comparison with controls. The enriched pathways shown were statistically significant at $p < 0.05$, FDR <0.05 (shown as -log). (For interpretation of the references to colour in this figure legend, the reader is referred to the Web version of this article.)

metabolic pathways mainly involving cell respiration in the LPS-treated groups. Common to all treatments, including DSS-C, were pathways associated with chromatin organisation. Like in PL, the pathway enrichment result was almost overlapping between LPS and DSS-LPS vs. controls. Enriched cellular parts were mostly annotated as mitochondrial components and histones ($p < 0.05$, FDR <0.05, Fig. 7a and b, Table S9 in ESM2).

3.3. Association between the PL and CSF proteomes

Using the subset of 155 proteins common between PL and CSF, we explored the per-individual co-structuring of the two proteomes. The global similarity of PL and CSF datasets was moderate (Coinertia analysis, RV coefficient = 0.54, Fig. 8a). The unstimulated animals clustered with the DSS-treated group, and the ones challenged with LPS alone or in combination to DSS made up another major cluster in both the PL and CSF samples.

3.4. Associations of PL and CSF proteomic changes to intensity of the inflammation measured through cytokine mRNA expression in brain and intestine

Since our proteomic analysis indicated several systemic effects of the DSS and LPS treatments on immune function in parrot brain and periphery, next we tested for the associations of the proteomic changes to intensity of the tissue-specific inflammatory responses. Inflammation was measured as levels of the *IL1B*, *IL6* and *IL18* mRNA expression. As predicted, we found a significant increase in the relative *IL1B* expression in the intestine (two-way ANOVA with Tukey multiple comparisons of means, df = 6, F = 4.774) following the LPS treatment alone (n = 9, p <

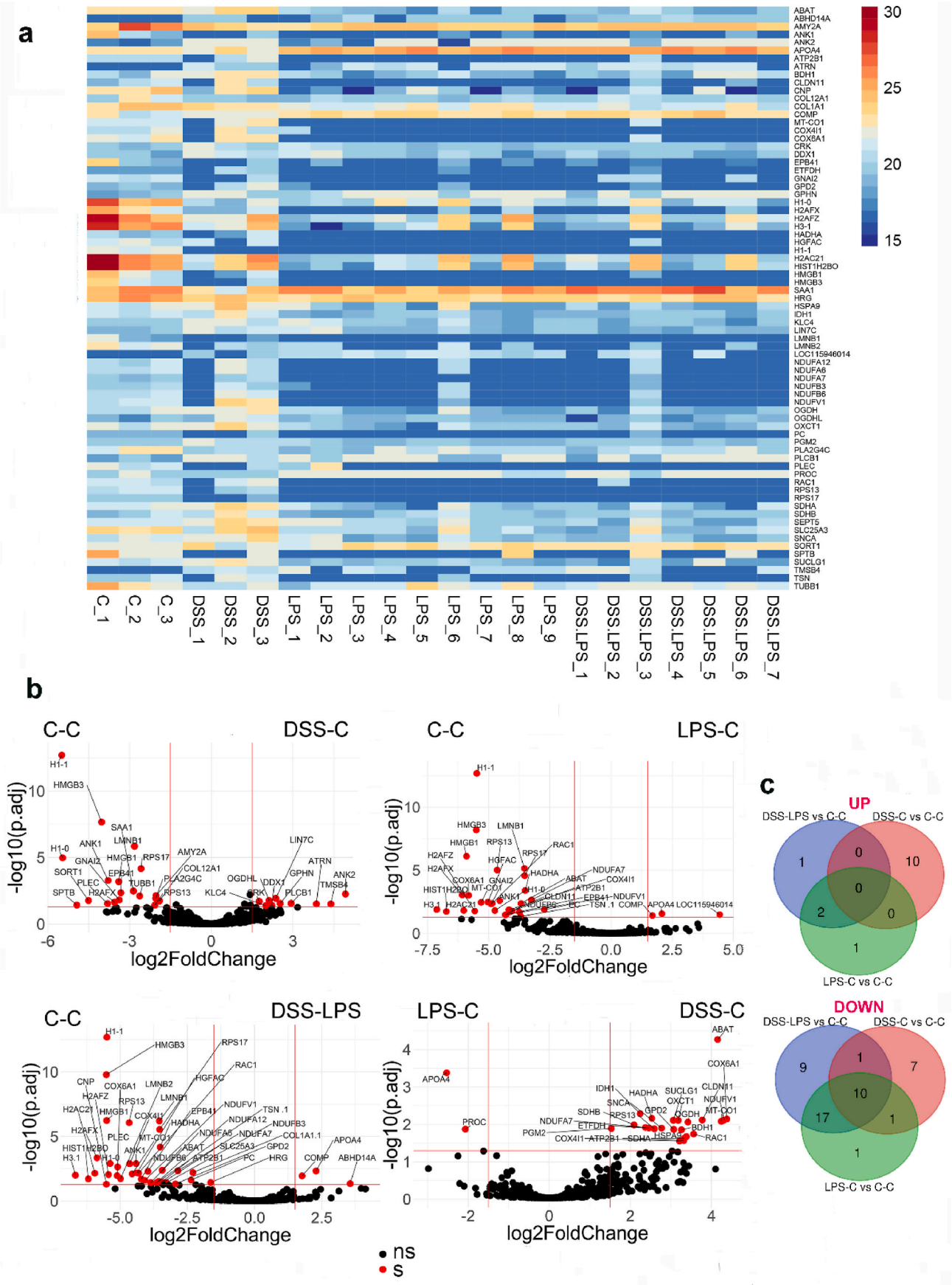

(caption on next page)

Fig. 5. Differential protein expression analysis of the budgerigar cerebrospinal fluid (CSF) proteomes after dextran sulphate sodium (DSS) and lipopolysaccharide (LPS) treatment. (a) A heatmap depicting variation in all significantly differentially abundant proteins (rows) across all the samples analysed (columns). (b) Volcano plots showing the protein expression fold changes and their significance across the comparisons of the treatment groups tested. The p-adjusted values are expressed as negative decadic logarithm of the Permutation Based false-discovery rate (FDR). The fold change differences of the CSF proteins (x-axis) dependent on their FDRs (y-axis) are shown in dots, colour coded as red = significant (s) and black = non-significant (ns) based on a significance threshold set to p. adj <0.05 and fold change cut-off ≥1.5. Significant proteins are labelled with their codes (human orthologs). (c) Overlaps of the significantly up-regulated (UP) and down-regulated (DOWN) proteins compared to controls across treatments. Controls (C-C, n = 3), birds treated with DSS (DSS-C, n = 3), LPS (LPS-C, n = 9), or both DSS and LPS (DSS-LPS, n = 7). (For interpretation of the references to colour in this figure legend, the reader is referred to the Web version of this article.)

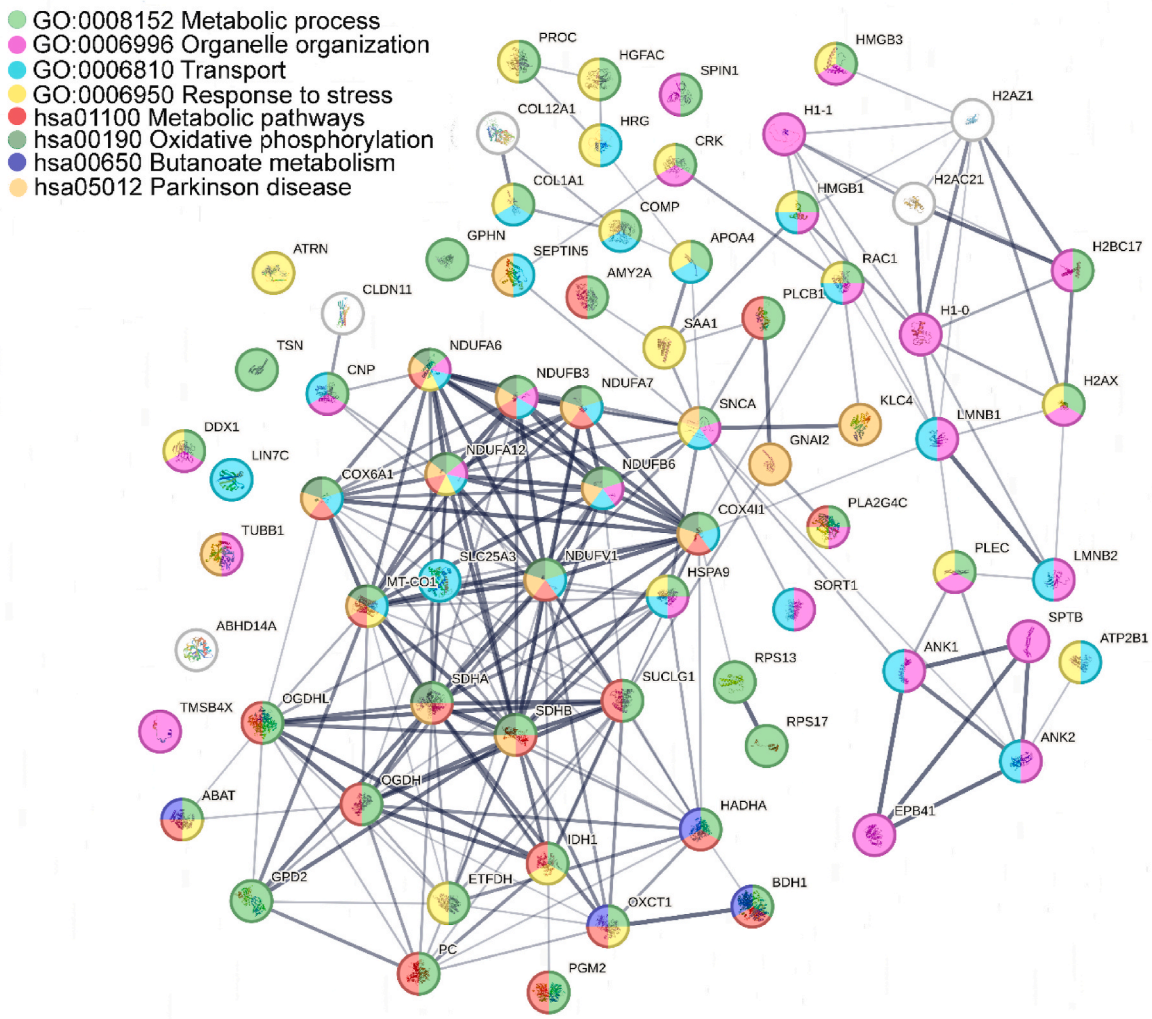

Fig. 6. Protein interaction network of differentially expressed proteins in the budgerigar cerebrospinal fluid. Protein-protein interactions of 72 proteins significantly dysregulated in the treatment groups (DSS-C, n = 3; LPS-C, n = 9; or DSS-LPS, n = 7) compared to the unstimulated controls (n = 3). Connections indicate functional associations between the proteins. Line thickness indicates the strength of the data support. Indicative enriched terms (False discovery rate <0.05) from Gene Ontology Biological Processes and Kyoto Encyclopaedia of Genes and Genomes are shown as colour-codes in circles indicating the individual proteins. (For interpretation of the references to colour in this figure legend, the reader is referred to the Web version of this article.)

0.001 for both CO and IL) or LPS-treatment combined with DSS (n = 7, p < 0.001 for both CO and IL) vs. controls (n = 3, Fig. S3a in ESM1). Interestingly, DSS caused no significant changes in the *IL1B* expression in the GIT (n = 3, p > 0.05). In the brain, the trend for the *IL1B* expression increase was not significant for any treatment. The pattern of relative gene expression variation between the treatment groups was similar for *IL6*, but here the increase was statistically significant only in the CO following LPS with or without DSS (two-way ANOVA with Tukey multiple comparisons of means, df = 6, F = 0.961, p < 0.01 and < 0.05 for LPS-C and DSS-LPS groups compared to controls, respectively; Fig. S3a in ESM1). *IL6* expression in the brain was similar to the controls following any treatment. We found no significant effect of our experimental treatment on the *IL18* expression in any of the tissues (p > 0.05; Fig. S3a in ESM1).

Because there were strong and significant correlations between the cytokine mRNA expression levels across genes and tissues (Fig. S3b in ESM1), to obtain per sample quantification to the general pro-inflammatory cytokine profile, we performed a PCA analysis of the *IL1B*, *IL6* and *IL18* gene expression levels for each tissue (Fig. 8b–Table S10 in ESM2) and extracted the first component (PC1) values, explaining 70.95% of variation in the data. Despite the PC1 trend for distinction in intensity of the systemic pro-inflammatory response between no response in the controls and the strongest response in LPS-injected individuals, the cytokine expression profiles were not

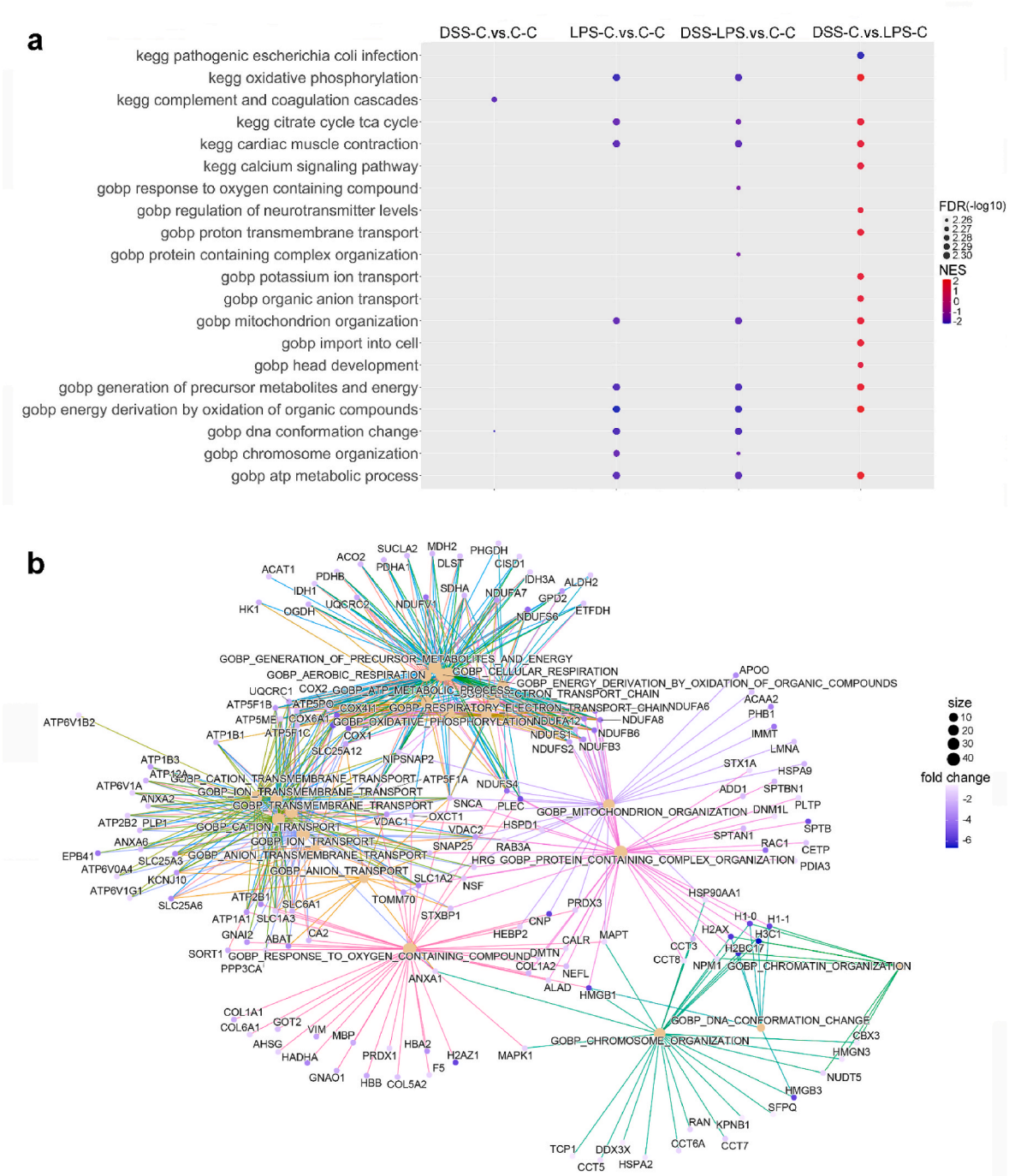

Fig. 7. Cerebrospinal fluid (CSF) proteomics: Gene Set Enrichment Analysis (GSEA) based on the Kyoto Encyclopaedia of Genes and Genomes (KEGG) pathways and Gene Ontology (GO) for Biological Processes (BP). (a) Non-redundant enriched pathways in CSF are plotted for each comparison. The dots represent term enrichment with colour coding according to the normalised enrichment score (NES). The sizes of the dots represent the negative logarithmic value of false discovery rate (FDR) with increasing value indicating higher significance. Controls (C-C, n = 3), birds treated with DSS (DSS-C, n = 3), LPS (LPS-C, n = 9), or both DSS and LPS (DSS-LPS, n = 7). (b) Network plot showing the linkages of the GO BP enriched terms and the gene products for the CSF samples from birds treated with DSS-LPS compared to unstimulated controls. The sizes of the dots corresponding to each term represent their numbers of proteins covered and the dot colours show the degree of the log fold change of the gene products in DSS-LPS samples after comparison with controls. The proteins are labelled with their codes (human orthologs). The enriched pathways shown were statistically significant at $p < 0.05$, FDR <0.05 (shown as -log). (For interpretation of the references to colour in this figure legend, the reader is referred to the Web version of this article.)

significantly different ($p > 0.05$ for all comparisons, Fig. S3c in ESM1). Yet, we found weak but significant relationships of the cytokine mRNA PC1 and the PC1 of PL and CSF proteomes (Fig. 8c). The protein abundance of SAA in PL was also significantly correlated with the pro-inflammatory cytokine profile (Fig. 8c).

4. Discussion

In this study, we report the establishment and initial characterization of the acute immune response model in a new animal species, the budgerigar, set for investigation of subclinical peripheral inflammation through standardised challenges mimicking the immunological effects

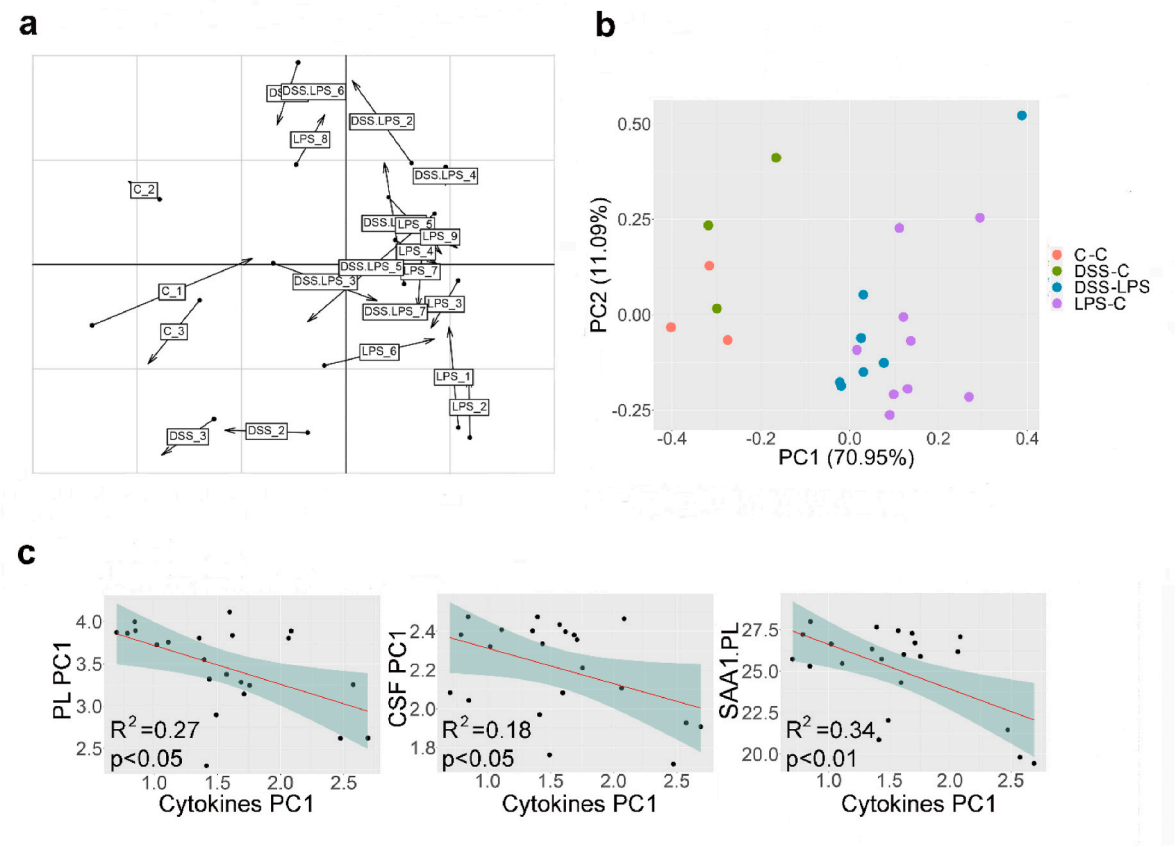

Fig. 8. Integrated protein profiles in plasma (PL) and cerebrospinal fluid (CSF) in association with the pro-inflammatory cytokine profile in low-grade inflammation following stimulation with dextran sulphate sodium (DSS), liposaccharide (LPS) or combination. (a) Results of the Co-inertia analysis of associations between the PL and CSF proteomes. For each individual (marked with the group code and number) the arrows interconnect the PL proteome to CSF proteome along the first two axes of the multidimensional space. (b) PCA of the mRNA expression of the pro-inflammatory cytokines *IL1B, IL6* and *IL18* in DSS (DSS-C, n = 3), LPS (LPS-C, n = 9) or combined (DSS-LPS, n = 7)-treated and unstimulated control (C-C, n = 3) birds. First two axes (PC1 and PC2) shown with the percentage of gene expression variation explained. (c) Correlation of the integrated PL (left-hand panel) and CSF (middle panel) protein profiles with the mRNA expression profiles of *IL1B, IL6* and *IL18* in brain, colon and ileum based on their first dimension (PC1) values following PCA. On the right-hand panel, the acute phase protein, serum amyloid 1 (SAA1, human ortholog of serum amyloid alpha), abundances in PL are correlated with the PC1 of pro-inflammatory cytokines.

of dysbiosis. Our findings demonstrate that even a small dosage of subcutaneous LPS can cause a systemic inflammatory response over a 6-h period, whereas a 7-day oral DSS administration had no such impact on immunity. Nevertheless, DSS or LPS induced proteomic changes, evidenced by enrichment of coagulation- and complement-related proteins in PL, alterations in the CSF proteome reflecting depression of metabolism and changes in the pro-inflammatory cytokine profiles. We detected clear associations between the variation in PL and CSF proteomes and identified their links to the systemic cytokine expression levels. This was exemplified by the correlation between the systemic pro-inflammatory cytokine levels and plasma levels of the acute phase protein SAA.

The aim of our study was to describe the effects of DSS in inducing low-grade intestinal inflammation in budgerigars and compare it with the immunostimulating effects of LPS. Except for mice, DSS has been so far used to induce intestinal inflammation in a range of other species. Our dosage scheme was similar to that previously reported for chickens (Menconi et al., 2015). Like chicken, budgerigars tolerated only lower doses of DSS, which contrasts the effects observed in rodents that seem to develop acute colitis at higher DSS doses (Solomon et al., 2010; Wirtz et al., 2017). We found that the parrots responded with clinical resilience to DSS in the dose of 25 mg/day. Yet, our histological evaluation showed epithelial loss and villi shortening indicating mild subclinical colitis. Despite these histologically relevant changes, like in the chicken treated with a dose of 0.75% previously reported (Zou et al., 2018), we found that at 25 mg/day, proinflammatory cytokine expression, weight loss or clinical signs were at the same levels as the controls. However, in this study we did not follow the time dynamics of the response to DSS, and it is possible that prolonging the interval of DSS administration would pronounce the inflammatory effects.

Despite the plethora of studies describing the colonic proteome mainly in mice (Dou et al., 2020; Du et al., 2022; Wang et al., 2022), proteomic studies reporting systemic colitis effects in PL are scarce. In mice, DSS-induced colitis resulted in profound down-regulation of proteins mostly related to carbohydrate metabolism and only few up-regulated proteins were detected (Huang et al., 2022). In terms of the functional annotation of the differentially expressed proteins, our results were similar to those reported previously in mice. In a study analysing equine serum, 11 proteins were reported as up-regulated in colitis-affected horses (Minamijima et al., 2022), including SAA also identified in our results. VTN has been slightly but significantly down-regulated in PL of the DSS-affected birds. VTN is a multifunctional glycoprotein, enriched in plasma, extracellular matrix and platelets that belongs to the family of adhesive proteins exerting inhibitory action in complement membrane attack complex (Preissner, 1989), so decrease in its expression could promote strength of the immune response. Consistent with our finding, VTN was decreased in the PL of patients with ulcerative colitis, and its decrease in PL is thought to be related to VTN binding at sites of intestinal tissue injury and the severity of the colitis (Tsuchiya, 1994).

The effects of colitis on the protein composition of CSF have not yet been reported in any species and our study is, thus, the first report on the

DSS-induced alterations in CSF proteome across all vertebrates. Nevertheless, experimental colitis induced by DSS have demonstrated impaired adult neurogenesis in hippocampus (Gampierakis et al., 2021) that is probably linked to malfunctioning of the gut-brain axis during dysbiosis, leading to the emergence of neuropsychiatric and neurodegenerative disorders. Following mild colitis induced in the parrots by DSS, we found alterations in CSF proteome involving the up-regulation of protein attractin, ATP-dependent RNA helicase DDX1 and Adapter Molecule CRK which are immune regulators (Bonaventure and Goujon, 2022; Duke-Cohan et al., 1998; Lin et al., 2021; Liu, 2014) and 1-Phosphatidylinositol 4,5-Bisphosphate Phosphodiesterase Beta-1 (PLCB1), implicated in phospholipase signalling. Elevation of PLCB1 might indicate neurotoxicity (Park et al., 2022). Interestingly, in budgerigars, the DSS-induced changes were not associated with altered pro-inflammatory cytokine transcription in brain or intestine, possibly due to the mild effects of the selected DSS dose and/or the temporal frame of our sampling. Given the extensive evidence of behavioural and biochemical effects of ulcerative colitis on brain function in human patients, experimental animals (Bisgaard et al., 2022; Talley et al., 2021) and novel findings suggesting potential of the parrot neuroimmunological research (Divín et al., 2022), our results urge for further exploration of the CSF proteomic changes linked to dysbiosis in parrots.

Another goal of this study was to compare the DSS effects to skin inflammation induced by bacterial LPS endotoxin. In budgerigars, peripheral endotoxin exposure resulted in systemic elevation of pro-inflammatory cytokine expression levels and proteomic up-regulation of several inflammatory cascades in PL. We detected LPS-induced up-regulation of expression of coagulation and complement components and of the acute phase protein SAA1, consistent with the effects previously reported in chickens (Horvatić et al., 2019), mice (Harberts et al., 2020) and humans (Qian et al., 2005). In addition, GAPDH, AK1 and FHL2 were decreased in PL of LPS-treated birds. Since FHL2 is involved in development, control of cell survival, transcription, and signal transduction (Johannessen et al., 2006), our data indicate link of the response to down-regulation of metabolic pathways. This is consistent with the overall quantitative proteomic pattern of the response to LPS in PL evidencing opposing trends in regulation of immune and metabolic processes.

The depletion of energy-related proteins was even more dramatic in the CSF proteome of LPS samples with or without DSS. We found 17 mitochondrial proteins with significantly decreased abundances implying loss of mitochondrial homeostasis and bioenergetic disturbances. Compared to mammals, birds—including budgerigars—have more effective defences against oxidative stress and hyperglycaemia, prolonged lifespans with respect to their body size, because of their mitochondrial characteristics (West, 2010). Yet, this observation suggests that peripheral immune responses can alter the brain metabolism in parrots. APOA4 and COMP, on the other hand, were commonly up-regulated in LPS-treated CSF (with or without DSS). COMP is a non-collagenous extracellular matrix protein that is used as a serum biomarker of tissue fibrosis (Cui and Zhang, 2022). APOA4 levels are controlled by leptin in the hypothalamus to allow inhibition of food intake, regulation of body weight, cholesterol transport and energy homeostasis (Shen et al., 2007) and this protein marker could be correlated to the weight loss related to the sickness response. Consistent with our findings, studies of mouse brain proteomes after LPS stimulation have also revealed metabolic abnormalities (Imamura et al., 2023; Puris et al., 2022; Wang et al., 2016). Importantly, these studies have suggested using the paradigm of LPS-induced peripheral inflammation to model depression and neurodegeneration. Several proteins, parts of intracellular non-membrane bound organelles were reduced in the CSF in response to DSS and LPS stimulations. It is possible that their higher abundance in controls results from waste removal and clearance of CSF that was disrupted by the inflammation-inducing treatments.

Overall, similar to the findings of Talley et al. in mice (Talley et al., 2021), in budgerigar, the LPS-induced neuroinflammation was more pronounced than that caused by DSS, and when we administered the two substances together, the effects of LPS overshadowed those of DSS. This was demonstrated also by the variance in the PL and CSF proteomes and systemic cytokine expression levels that correlated significantly. In addition, our results suggest that protein levels of SAA in PL can be used as a possible biomarker to monitor low-grade inflammation in parrots. In PL, increase in both SAA and fibrinogen may indicate acute bacterial infection in budgerigars. Fibrinogen plays a role in tissue repair as well as homeostasis by acting as a matrix for the migration of inflammatory-related cells and promoting degranulation, phagocytosis and adaptive immune response (Murata et al., 2004). *SAA1* (human ortholog) encodes an apolipoprotein which interacts with high density lipoproteins to export cholesterol from the site of inflammation. The SAA protein is also serving as a chemoattractant for monocytes and polymorphonuclear leukocytes (Badolato et al., 1994) that promotes secretion of IL8 (He et al., 2003) and directly acts as an opsonin for Gram-negative bacteria (Shah et al., 2006). In veterinary studies, SAA is commonly used as a marker of inflammation (Hooijberg and Cray, 2023). In both mammals and birds, chronically high serum SAA levels in combination with an inflammatory or viral condition may lead to the misfolded amyloid protein A (AA) and AA amyloidosis, a condition brought on by the buildup of this SAA derivative into organs and tissues (Röcken and Shakespeare, 2002). In humans, amyloidosis is a pathological condition related to emergence of Alzheimer's disease (Ma et al., 2022).

Comparative immunology employing proteomics may enable a fascinating novel understanding of how the host response to pathogens has evolved by comparing differences and similarities between proteomes across species in health and disease. We identified general and stimulus-dependent inflammatory markers in budgerigar PL and CSF following challenges mimicking low-grade peripheral inflammation resulting from tissue injury and bacterial infection linked to dysbiosis. Our research contributes to establishment of budgerigar as a novel, previously unexplored model organism in avian immunology. Since parrots appear to be prone to neuroinflammation (Divín et al., 2022), this is especially important for increasing the experimental potential of parrots to promote the future research in neuroimmunology. For both the DSS and LPS treatments, we observed systemic effects with impacts on brain physiology. We also revealed that for a low-grade inflammation in the budgerigar model, LPS rapidly dysregulates the proteome composition in biological fluids, which is linked to the pro-inflammatory cytokine transcription profiles, while the DSS has much milder effects. This is consistent with previous studies in mice (Talley et al., 2021). Due to its economic impact in industry, chicken is a frequently used avian model in immunology. With the release of the budgerigar genome, this small sized and easy to handle parrot may also provide valuable insights in comparative immunology and neuroscience.

Although parrots such as the budgerigar may serve as a novel and relevant immunological model for answering certain biological questions appealing, for example, with respect to human mental health, extrapolating the results to human disorders has certain limits. First, parrots have different anatomy of GIT than humans, but also distinct from poultry (Caviedes-Vidal et al., 2007). Budgerigars have cloaca, shorter colon and lack caeca, which can affect microbiota interacting with the host immune system (Hird et al., 2014; Schmiedová et al., 2024). While the links between microbiota and neuroimmune interactions underlying the neuropsychiatric diseases are increasingly explored (Hashimoto, 2023), the effects of interspecific microbial variation still remain unknown. Thus, this variation can affect the proteome composition as well as other aspects of the physiological regulation of immunity. From a technical aspect, given the lacking specifically parrot and, more generally, avian gene functional annotations, we had to use annotations of the orthologs in human, a species that is phylogenetically relatively distant. Furthermore, there is presently severe lack of related proteomic studies describing inflammation-induced variation in CSF proteomes, not only in birds, but across vertebrates. Lacking specific

molecular tools for budgerigars, it was not possible to validate our results through an antibody-based approach. Despite these shortcomings, our findings can be used as a reference for future manipulative experiments in neuroinflammation offering further insights into the comparative regulation of the gut-brain axis.

Competing interests statement

The authors declare no competing interests.

CRediT authorship contribution statement

Eleni Voukali: Writing – review & editing, Writing – original draft, Methodology, Investigation, Formal analysis, Data curation, Conceptualization. **Daniel Divín:** Investigation. **Mercedes Goméz Samblas:** Investigation. **Nithya Kuttiyarthu Veetil:** Investigation. **Tereza Krajzingrová:** Investigation. **Martin Těšický:** Investigation. **Tao Li:** Investigation. **Balraj Melepat:** Investigation. **Pavel Talacko:** Investigation. **Michal Vinkler:** Writing – review & editing, Writing – original draft, Methodology, Investigation, Funding acquisition, Formal analysis, Data curation, Conceptualization.

Data availability

Proteomic data are available though PRIDE database

Acknowledgements

We are grateful the Mass Spectromentry and Proteomics Service Laboratory, Faculty of Science, Charles University for performing the LC-MS/MS run and Robert Černý, Ph. D for his guidance in histology experiments. Charles University supported this study through the grant No. PRIMUS/17/SCI/12, and the Czech Science Foundation through the grants No. 19-20152Y and 24-12477 S. The Czech Ministry of Education, Youth and Sports supported this research through the Inter-ACTION project LUAUS24184 and institutional support No. 260684/2023. Computational resources were supplied by the project "e-Infrastruktura CZ" (e-INFRA CZ LM2018140) supported by the Ministry of Education, Youth and Sports of the Czech Republic.

Appendix A. Supplementary data

Supplementary data to this article can be found online at https://doi.org/10.1016/j.dci.2024.105213.

References

Ali, N.J., Farabaugh, S., Dooling, R., 1993. Recognition of contact calls by the budgerigar *Melopsittacus undulatus*. Bull. Psychonomic Soc. 31, 468–470. https://doi.org/10.3758/BF03334965.

Ashburner, M., Ball, C.A., Blake, J.A., Botstein, D., Butler, H., Cherry, J.M., Davis, A.P., Dolinski, K., Dwight, S.S., Eppig, J.T., Harris, M.A., Hill, D.P., Issel-Tarver, L., Kasarskis, A., Lewis, S., Matese, J.C., Richardson, J.E., Ringwald, M., Rubin, G.M., Sherlock, G., 2000. Gene Ontology: tool for the unification of biology. Nat. Genet. 25, 25–29. https://doi.org/10.1038/75556.

Badolato, R., Wang, J.M., Murphy, W.J., Lloyd, A.R., Michiel, D.F., Bausserman, L.L., Kelvin, D.J., Oppenheim, J.J., 1994. Serum amyloid A is a chemoattractant: induction of migration, adhesion, and tissue infiltration of monocytes and polymorphonuclear leukocytes. J. Exp. Med. 180, 203–209. https://doi.org/10.1084/jem.180.1.203.

Belkaid, Y., Hand, T., 2014. Role of the microbiota in immunity and inflammation. Cell 157, 121–141. https://doi.org/10.1016/j.cell.2014.03.011.

Bisgaard, T.H., Allin, K.H., Keefer, L., Ananthakrishnan, A.N., Jess, T., 2022. Depression and anxiety in inflammatory bowel disease: epidemiology, mechanisms and treatment. Nat. Rev. Gastroenterol. Hepatol. 19, 717–726. https://doi.org/10.1038/s41575-022-00634-6.

Bonaventure, B., Goujon, C., 2022. DExH/D-box helicases at the frontline of intrinsic and innate immunity against viral infections. J. Gen. Virol. 103 https://doi.org/10.1099/jgv.0.001766.

Burnap, S.A., Mayr, U., Shankar-Hari, M., Cuello, F., Thomas, M.R., Shah, A.M., Sabroe, I., Storey, R.F., Mayr, M., 2021. A proteomics-based assessment of inflammation signatures in endotoxemia. Mol. Cell. Proteomics MCP 20, 100021. https://doi.org/10.1074/mcp.RA120.002305.

Calefi, A.S., Fonseca, da S., Garcia, J., Cohn, D.W.H., Honda, B.T.B., Costola-de-Souza, C., Tsugiyama, L.E., Quinteiro-Filho, W.M., Ferreira, P., J, A., Palermo-Neto, J., 2016. The gut-brain axis interactions during heat stress and avian necrotic enteritis. Poultry Sci. 95, 1005–1014. https://doi.org/10.3382/ps/pew021.

Caviedes-Vidal, E., McWhorter, T.J., Lavin, S.R., Chediack, J.G., Tracy, C.R., Karasov, W. H., 2007. The digestive adaptation of flying vertebrates: high intestinal paracellular absorption compensates for smaller guts. Proc. Natl. Acad. Sci. U.S.A. 104, 19132–19137. https://doi.org/10.1073/pnas.0703159104.

Chassaing, B., Aitken, J.D., Malleshappa, M., Vijay-Kumar, M., 2014. Dextran sulfate sodium (DSS)-Induced colitis in mice. Curr. Protoc. Im. https://doi.org/10.1002/0471142735.im1525s104. John E Coligan Al 104, Unit-15.25.

Cox, J., Hein, M.Y., Luber, C.A., Paron, I., Nagaraj, N., Mann, M., 2014. Accurate proteome-wide label-free quantification by delayed normalization and maximal peptide ratio extraction, termed MaxLFQ. Mol. Cell. Proteomics MCP 13, 2513–2526. https://doi.org/10.1074/mcp.M113.031591.

Cui, J., Zhang, J., 2022. Cartilage oligomeric matrix protein, diseases, and therapeutic opportunities. Int. J. Mol. Sci. 23, 9253. https://doi.org/10.3390/ijms23169253.

Culhane, A.C., Perrière, G., Higgins, D.G., 2003. Cross-platform comparison and visualisation of gene expression data using co-inertia analysis. BMC Bioinf. 4, 59. https://doi.org/10.1186/1471-2105-4-59.

Dal Pont, G.C., Belote, B.L., Lee, A., Bortoluzzi, C., Eyng, C., Sevastiyanova, M., Khadem, A., Santin, E., Farnell, Y.Z., Gougoulias, C., Kogut, M.H., 2021. Novel models for chronic intestinal inflammation in chickens: intestinal inflammation pattern and biomarkers. Front. Immunol. 12, 676628 https://doi.org/10.3389/fimmu.2021.676628.

Dantzer, R., O'Connor, J.C., Freund, G.G., Johnson, R.W., Kelley, K.W., 2008. From inflammation to sickness and depression: when the immune system subjugates the brain. Nat. Rev. Neurosci. 9, 46–56. https://doi.org/10.1038/nrn2297.

Divín, D., Goméz Samblas, M., Kuttiyarthu Veetil, N., Voukali, E., Świderská, Z., Krajzingrová, T., Těšický, M., Beneš, V., Elleder, D., Bartoš, O., Vinkler, M., 2022. Cannabinoid receptor 2 evolutionary gene loss makes parrots more susceptible to neuroinflammation. Proc. R. Soc. B Biol. Sci. 289, 20221941 https://doi.org/10.1098/rspb.2022.1941.

Dou, B., Hu, W., Song, M., Lee, R.J., Zhang, X., Wang, D., 2020. Anti-inflammation of Erianin in dextran sulphate sodium-induced ulcerative colitis mice model via collaborative regulation of TLR4 and STAT3. Chem. Biol. Interact. 324, 109089 https://doi.org/10.1016/j.cbi.2020.109089.

Du, C., Zhao, Y., Wang, K., Nan, X., Chen, R., Xiong, B., 2022. Effects of milk-derived extracellular vesicles on the colonic transcriptome and proteome in murine model. Nutrients 14, 3057. https://doi.org/10.3390/nu14153057.

Duke-Cohan, J.S., Gu, J., McLaughlin, D.F., Xu, Y., Freeman, G.J., Schlossman, S.F., 1998. Attractin (DPPT-L), a member of the CUB family of cell adhesion and guidance proteins, is secreted by activated human T lymphocytes and modulates immune cell interactions. Proc. Natl. Acad. Sci. U.S.A. 95, 11336–11341. https://doi.org/10.1073/pnas.95.19.11336.

Elson, C.O., Sartor, R.B., Tennyson, G.S., Riddell, R.H., 1995. Experimental models of inflammatory bowel disease. Gastroenterology 109, 1344–1367. https://doi.org/10.1016/0016-5085(95)90599-5.

Erban, T., Shcherbachenko, E., Talacko, P., Harant, K., 2021. A single honey proteome dataset for identifying adulteration by foreign amylases and mining various protein markers natural to honey. J. Proteonomics 239, 104157. https://doi.org/10.1016/j.jprot.2021.104157.

Fabregat, A., Jupe, S., Matthews, L., Sidiropoulos, K., Gillespie, M., Garapati, P., Haw, R., Jassal, B., Korninger, F., May, B., Milacic, M., Roca, C.D., Rothfels, K., Sevilla, C., Shamovsky, V., Shorser, S., Varusai, T., Viteri, G., Weiser, J., Wu, G., Stein, L., Hermjakob, H., D'Eustachio, P., 2018. The reactome pathway knowledgebase. Nucleic Acids Res. 46, D649–D655. https://doi.org/10.1093/nar/gkx1132.

Gampierakis, I.-A., Koutmani, Y., Semitekolou, M., Morianos, I., Polissidis, A., Katsouda, A., Charalampopoulos, I., Xanthou, G., Gravanis, A., Karalis, K.P., 2021. Hippocampal neural stem cells and microglia response to experimental inflammatory bowel disease (IBD). Mol. Psychiatr. 26, 1248–1263. https://doi.org/10.1038/s41380-020-0651-6.

Harberts, E., Liang, T., Yoon, S.H., Opene, B.N., McFarland, M.A., Goodlett, D.R., Ernst, R.K., 2020. TLR4-Independent effects of LPS identified using longitudinal serum proteomics. J. Proteome Res. 19, 1258–1266. https://doi.org/10.1021/acs.jproteome.9b00765.

Hashimoto, K., 2023. Emerging role of the host microbiome in neuropsychiatric disorders: overview and future directions. Mol. Psychiatr. 28, 3625–3637. https://doi.org/10.1038/s41380-023-02287-6.

He, R., Sang, H., Ye, R.D., 2003. Serum amyloid A induces IL-8 secretion through a G protein-coupled receptor, FPRL1/LXA4R. Blood 101, 1572–1581. https://doi.org/10.1182/blood-2002-05-1431.

Hird, S.M., Carstens, B.C., Cardiff, S.W., Dittmann, D.L., Brumfield, R.T., 2014. Sampling locality is more detectable than taxonomy or ecology in the gut microbiota of the brood-parasitic Brown-headed Cowbird (Molothrus ater). PeerJ 2, e321. https://doi.org/10.7717/peerj.321.

Hooijberg, E.H., Cray, C., 2023. Acute phase reactants in nondomesticated mammals-A veterinary clinical pathology perspective. Vet. Clin. Pathol. 52 (Suppl. 1), 19–36. https://doi.org/10.1111/vcp.13189.

Horvatić, A., Guillemin, N., Kaab, H., McKeegan, D., O'Reilly, E., Bain, M., Kuleš, J., Eckersall, P.D., 2019. Quantitative proteomics using tandem mass tags in relation to the acute phase protein response in chicken challenged with Escherichia coli lipopolysaccharide endotoxin. J. Proteonomics 192, 64–77. https://doi.org/10.1016/j.jprot.2018.08.009.

Huang, C., Wang, Y., Lin, X., Chan, T.F., Lai, K.P., Li, R., 2022. Uncovering the functions of plasma proteins in ulcerative colitis and identifying biomarkers for BPA-induced severe ulcerative colitis: a plasma proteome analysis. Ecotoxicol. Environ. Saf. 242, 113897 https://doi.org/10.1016/j.ecoenv.2022.113897.

Imamura, Y., Matsumoto, H., Imamura, J., Matsumoto, N., Yamakawa, K., Yoshikawa, N., Murakami, Y., Mitani, S., Nakagawa, J., Yamada, T., Ogura, H., Oda, J., Shimazu, T., 2023. Ultrasound stimulation of the vagal nerve improves acute septic encephalopathy in mice. Front. Neurosci. 17.

Iwaniuk, A.N., Dean, K.M., Nelson, J.E., 2005. Interspecific allometry of the brain and brain regions in parrots (psittaciformes): comparisons with other birds and primates. Brain Behav. Evol. 65, 40–59. https://doi.org/10.1159/000081110.

Johannessen, M., Møller, S., Hansen, T., Moens, U., Ghelue, M.V., 2006. The multifunctional roles of the four-and-a-half-LIM only protein FHL2. Cell. Mol. Life Sci. CMLS 63, 268–284. https://doi.org/10.1007/s00018-005-5438-z.

Kanehisa, M., Goto, S., Sato, Y., Furumichi, M., Tanabe, M., 2012. KEGG for integration and interpretation of large-scale molecular data sets. Nucleic Acids Res. 40, D109–D114. https://doi.org/10.1093/nar/gkr988.

Kriventseva, E.V., Kuznetsov, D., Tegenfeldt, F., Manni, M., Dias, R., Simão, F.A., Zdobnov, E.M., 2019. OrthoDB v10: sampling the diversity of animal, plant, fungal, protist, bacterial and viral genomes for evolutionary and functional annotations of orthologs. Nucleic Acids Res. 47, D807–D811. https://doi.org/10.1093/nar/gky1053.

Kuleš, J., Horvatić, A., Guillemin, N., Ferreira, R.F., Mischke, R., Mrljak, V., Chadwick, C. C., Eckersall, P.D., 2020. The plasma proteome and the acute phase protein response in canine pyometra. J. Proteonomics 223, 103817. https://doi.org/10.1016/j.jprot.2020.103817.

Kuttappan, V.A., Berghman, L.R., Vicuna, E.A., Latorre, J.D., Menconi, A., Wolchok, J.D., Wolfenden, A.D., Faulkner, O.B., Tellez, G.I., Hargis, B.M., Bielke, L.R., 2015. Poultry enteric inflammation model with dextran sodium sulfate mediated chemical induction and feed restriction in broilers. Poultry Sci. 94, 1220–1226. https://doi.org/10.3382/ps/pev114.

Kuttiyarthu Veetil, N., Cedraz de Oliveira, H., Gomez-Samblas, M., Divín, D., Melepat, B., Voukali, E., Świderská, Z., Krajzingrová, T., Těšický, M., Jung, F., Beneš, V., Madsen, O., Vinkler, M., 2024. Peripheral inflammation-induced changes in songbird brain gene expression: 3' mRNA transcriptomic approach. Dev. Comp. Immunol. 151, 105106 https://doi.org/10.1016/j.dci.2023.105106.

Lin, Z., Wang, J., Zhu, W., Yu, X., Wang, Z., Ma, J., Wang, H., Yan, Y., Sun, J., Cheng, Y., 2021. Chicken DDX1 acts as an RNA sensor to mediate IFN-β signaling pathway activation in antiviral innate immunity. Front. Immunol. 12, 742074 https://doi.org/10.3389/fimmu.2021.742074.

Liu, D., 2014. The adaptor protein Crk in immune response. Immunol. Cell Biol. 92, 80–89. https://doi.org/10.1038/icb.2013.64.

Liu, Lixuan, Sui, W., Yang, Y., Liu, Lily, Li, Q., Guo, A., 2022. Establishment of an enteric inflammation model in broiler chickens by oral administration with dextran sulfate sodium. Animals 12, 3552. https://doi.org/10.3390/ani12243552.

Ma, C., Hong, F., Yang, S., 2022. Amyloidosis in Alzheimer's disease: pathogeny, etiology, and related therapeutic directions. Molecules 27, 1210. https://doi.org/10.3390/molecules27041210.

Martin, L.B., Han, P., Lewittes, J., Kuhlman, J.R., Klasing, K.C., Wikelski, M., 2006. Phytohemagglutinin-induced skin swelling in birds: histological support for a classic immunoecological technique. Funct. Ecol. 20, 290–299. https://doi.org/10.1111/j.1365-2435.2006.01094.x.

Meitern, R., Andreson, R., Hõrak, P., 2014. Profile of whole blood gene expression following immune stimulation in a wild passerine. BMC Genom. 15, 1–10. https://doi.org/10.1186/1471-2164-15-533.

Menconi, A., Hernandez-Velasco, X., Vicuna, E.A., Kuttappan, V.A., Faulkner, O.B., Tellez, G., Hargis, B.M., Bielke, L.R., 2015. Histopathological and morphometric changes induced by a dextran sodium sulfate (DSS) model in broilers. Poultry Sci. 94, 906–911. https://doi.org/10.3382/ps/pev054.

Minamijima, Y., Tozaki, T., Kuroda, T., Urayama, S., Nomura, M., Yamamoto, K., 2022. A comprehensive and comparative proteomic analysis of horse serum proteins in colitis. Equine Vet. J. 54, 1039–1046. https://doi.org/10.1111/evj.13554.

Mohanty, T., Karlsson, C.A.Q., Chao, Y., Malmström, E., Bratanis, E., Grentzmann, A., Mørch, M., Nizet, V., Malmström, L., Linder, A., Shannon, O., Malmström, J., 2023. A pharmacoproteomic landscape of organotypic intervention responses in Gram-negative sepsis. Nat. Commun. 14 https://doi.org/10.1038/s41467-023-39269-9.

Moolenbeek, C., Ruitenberg, E.J., 1981. The "Swiss roll": a simple technique for histological studies of the rodent intestine. Lab. Anim. 15, 57–59.

Murata, H., Shimada, N., Yoshioka, M., 2004. Current research on acute phase proteins in veterinary diagnosis: an overview. Vet. J. 168, 28–40. https://doi.org/10.1016/S1090-0233(03)00119-9.

Nii, T., Bungo, T., Isobe, N., Yoshimura, Y., 2020. Intestinal inflammation induced by dextran sodium sulphate causes liver inflammation and lipid metabolism disfunction in laying hens. Poultry Sci. 99, 1663–1677. https://doi.org/10.1016/j.psj.2019.11.028.

Okayasu, I., Hatakeyama, S., Yamada, M., Ohkusa, T., Inagaki, Y., Nakaya, R., 1990. A novel method in the induction of reliable experimental acute and chronic ulcerative colitis in mice. Gastroenterology 98, 694–702. https://doi.org/10.1016/0016-5085(90)90290-H.

Olkowicz, S., Kocourek, M., Lučan, R.K., Porteš, M., Fitch, W.T., Herculano-Houzel, S., Němec, P., 2016. Birds have primate-like numbers of neurons in the forebrain. Proc. Natl. Acad. Sci. USA 113, 7255–7260. https://doi.org/10.1073/pnas.1517131113.

Packialakshmi, B., Liyanage, R., Jackson, O., Lay, J., Makkar, S.K., Rath, N.C., 2016. Proteomic changes in chicken plasma induced by Salmonella typhimurium lipopolysaccharides. Proteomics Insights 7, 1. https://doi.org/10.4137/PRI.S31609.

Park, J., Kim, S.H., Kim, Y.-J., Kim, H., Oh, Y., Choi, K.Y., Kim, B.C., Lee, K.H., Song, W. K., 2022. Elevation of phospholipase C-β1 expression by amyloid-β facilitates calcium overload in neuronal cells. Brain Res. 1788, 147924 https://doi.org/10.1016/j.brainres.2022.147924.

Preissner, K.T., 1989. The role of vitronectin as multifunctional regulator in the hemostatic and immune systems. Blut 59, 419–431. https://doi.org/10.1007/BF00349063.

Puris, E., Kouřil, Š., Najdekr, L., Auriola, S., Loppi, S., Korhonen, P., Gómez-Budia, M., Fricker, G., Kanninen, K.M., Malm, T., Friedecký, D., Gynther, M., 2022. Metabolomic, lipidomic and proteomic characterisation of lipopolysaccharide-induced inflammation mouse model. Neuroscience 496, 165–178. https://doi.org/10.1016/j.neuroscience.2022.05.030.

Qian, W.-J., Jacobs, J.M., Camp, D.G., Monroe, M.E., Moore, R.J., Gritsenko, M.A., Calvano, S.E., Lowry, S.F., Xiao, W., Moldawer, L.L., Davis, R.W., Tompkins, R.G., Smith, R.D., 2005. Comparative proteome analyses of human plasma following in vivo lipopolysaccharide administration using multidimensional separations coupled with tandem mass spectrometry. Proteomics 5, 572–584. https://doi.org/10.1002/pmic.200400942.

R Core Team, 2024. R: A Language and Environment for Statistical Computing. R Foundation for Statistical Computing, Vienna, Austria. https://www.R-project.org/.

Röcken, C., Shakespeare, A., 2002. Pathology, diagnosis and pathogenesis of AA amyloidosis. Virchows Arch. 440, 111–122. https://doi.org/10.1007/s00428-001-0582-9.

Schmiedová, L., Černá, K., Li, T., Těšický, M., Kreisinger, J., Vinkler, M., 2024. Bacterial communities along parrot digestive and respiratory tracts: the effects of sample type, species and time. Int. Microbiol. 27, 127–142. https://doi.org/10.1007/s10123-023-00372-y.

Shah, C., Hari-Dass, R., Raynes, J.G., 2006. Serum amyloid A is an innate immune opsonin for Gram-negative bacteria. Blood 108, 1751–1757. https://doi.org/10.1182/blood-2005-11-011932.

Shen, L., Tso, P., Woods, S.C., Sakai, R.R., Davidson, W.S., Liu, M., 2007. Hypothalamic apolipoprotein A-IV is regulated by leptin. Endocrinology 148, 2681–2689. https://doi.org/10.1210/en.2006-1596.

Sköld-Chiriac, S., Nord, A., Tobler, M., Nilsson, J.-Å., Hasselquist, D., 2015. Body temperature changes during simulated bacterial infection in a songbird: fever at night and hypothermia during the day. J. Exp. Biol. 218, 2961–2969. https://doi.org/10.1242/jeb.122150.

Smits, J.E., Bortolotti, G.R., Tella, J.L., 1999. Simplifying the phytohaemagglutinin skin-testing technique in studies of avian immunocompetence. Funct. Ecol. 13, 567–572. https://doi.org/10.1046/j.1365-2435.1999.00338.x.

Solomon, L., Mansor, S., Mallon, P., Donnelly, E., Hoper, M., Loughrey, M., Kirk, S., Gardiner, K., 2010. The dextran sulphate sodium (DSS) model of colitis: an overview. Comp. Clin. Pathol. 19, 235–239. https://doi.org/10.1007/s00580-010-0979-4.

Supek, F., Bošnjak, M., Škunca, N., Šmuc, T., 2011. REVIGO summarizes and visualizes long lists of gene Ontology terms. PLoS One 6, e21800. https://doi.org/10.1371/journal.pone.0021800.

Talley, S., Valiauga, R., Anderson, L., Cannon, A.R., Choudhry, M.A., Campbell, E.M., 2021. DSS-induced inflammation in the colon drives a proinflammatory signature in the brain that is ameliorated by prophylactic treatment with the S100A9 inhibitor paquinimod. J. Neuroinflammation 18, 263. https://doi.org/10.1186/s12974-021-02317-6.

Tsuchiya, K., 1994. [Vitronectin in plasma and colonic mucosa of patients with ulcerative colitis]. Nihon Shokakibyo Gakkai Zasshi Jpn. J. Gastro-Enterol. 91, 1190–1196.

Vinkler, M., Bainova, H., Albrecht, T., 2010. Functional analysis of the skin-swelling response to phytohaemagglutinin. Funct. Ecol. 24, 1081–1086. https://doi.org/10.1111/j.1365-2435.2010.01711.x.

Vinkler, M., Leon, A.E., Kirkpatrick, L., Dalloul, R.A., Hawley, D.M., 2018. Differing house finch cytokine expression responses to original and evolved isolates of Mycoplasma gallisepticum. Front. Immunol. 9, 314926. https://doi.org/10.3389/fimmu.2018.00013.

Vinkler, M., Schnitzer, J., Munclinger, P., Albrecht, T., 2012. Phytohaemagglutinin skin-swelling test in scarlet rosefinch males: low-quality birds respond more strongly. Anim. Behav. 83, 17–23. https://doi.org/10.1016/j.anbehav.2011.10.001.

Vinkler, M., Svobodova, J., Gabrielova, B., Bainova, H., Bryjova, A., 2014. Cytokine expression in phytohaemagglutinin-induced skin inflammation in a galliform bird. J. Avian Biol. 45, 43–50. https://doi.org/10.1111/j.1600-048X.2011.05860.x.

von Mering, C., Huynen, M., Jaeggi, D., Schmidt, S., Bork, P., Snel, B., 2003. STRING: a database of predicted functional associations between proteins. Nucleic Acids Res. 31, 258–261. https://doi.org/10.1093/nar/gkg034.

Voukali, E., Veetil, N.K., Němec, P., Stopka, P., Vinkler, M., 2021. Comparison of plasma and cerebrospinal fluid proteomes identifies gene products guiding adult neurogenesis and neural differentiation in birds. Sci. Rep. 11 https://doi.org/10.1038/s41598-021-84274-x.

Voukali, E., Vinkler, M., 2022. Proteomic-based evidence for adult neurogenesis in birds and mammals as indicated from cerebrospinal fluid. Neural Regen. Res. 17, 2576–2581. https://doi.org/10.4103/1673-5374.329002.

Wang, H., Liu, Z., Yu, T., Zhang, Y., Jiao, Y., Wang, X., Du, H., Jiang, R., Liu, D., Xu, Y., Guan, Q., Lu, M., 2022. The effect of tuina on ulcerative colitis model mice analyzed by gut microbiota and proteomics. Front. Microbiol. 13, 976239 https://doi.org/10.3389/fmicb.2022.976239.

Wang, Z., Li, W., Chen, J., Shi, H., Zhao, M., You, H., Rao, C., Zhan, Y., Yang, Y., Xie, P., 2016. Proteomic analysis reveals energy metabolic dysfunction and neurogenesis in the prefrontal cortex of a lipopolysaccharide-induced mouse model of depression. Mol. Med. Rep. 13, 1813–1820. https://doi.org/10.3892/mmr.2015.4741.

West, J.B., 2010. Did differences in mitochondrial properties influence the evolution of avian and mammalian lungs? Am. J. Physiol. Lung Cell. Molecul. Physiol. 299 (5), L595–L596. https://doi.org/10.1152/ajplung.00219.2010.

Wickham, H., 2009. ggplot2: Elegant Graphics for Data Analysis, Use R. Springer-Verlag, New York. https://doi.org/10.1007/978-0-387-98141-3.

Wirtz, S., Popp, V., Kindermann, M., Gerlach, K., Weigmann, B., Fichtner-Feigl, S., Neurath, M.F., 2017. Chemically induced mouse models of acute and chronic intestinal inflammation. Nat. Protoc. 12, 1295–1309. https://doi.org/10.1038/nprot.2017.044.

Yu, G., Wang, L.-G., Han, Y., He, Q.-Y., 2012. clusterProfiler: an R Package for comparing biological themes among gene clusters. OMICS A J. Integr. Biol. 16, 284–287. https://doi.org/10.1089/omi.2011.0118.

Zou, X., Ji, J., Wang, J., Qu, H., Shu, D.M., Guo, F.Y., Luo, C.L., 2018. Dextran sulphate sodium (DSS) causes intestinal histopathology and inflammatory changes consistent with increased gut leakiness in chickens. Br. Poultry Sci. 59, 166–172. https://doi.org/10.1080/00071668.2017.1418498.

PAPER IV

Veetil, Nithya Kuttiyarthu, Haniel Cedraz de Oliveira, Mercedes Gomez-Samblas, Daniel Divín, **Balraj Melepat,** Eleni Voukali, Zuzana Świderská et al. "Peripheral inflammation-induced changes in songbird brain gene expression: 3'mRNA transcriptomic approach." Developmental & Comparative Immunology 151 (2024): 105106.

Developmental and Comparative Immunology 151 (2024) 105106

Contents lists available at ScienceDirect

Developmental and Comparative Immunology

journal homepage: www.elsevier.com/locate/devcompimm

Peripheral inflammation-induced changes in songbird brain gene expression: 3' mRNA transcriptomic approach

Nithya Kuttiyarthu Veetil [a], Haniel Cedraz de Oliveira [b,c], Mercedes Gomez-Samblas [a,d], Daniel Divín [a], Balraj Melepat [a], Eleni Voukali [a], Zuzana Świderská [a], Tereza Krajzingrová [a], Martin Těšický [a], Ferris Jung [e], Vladimír Beneš [e], Ole Madsen [b], Michal Vinkler [a,*]

[a] Charles University, Faculty of Science, Department of Zoology, Viničná 7, 128 43, Prague, Czech Republic
[b] Wageningen University and Research, Department of Animal Sciences, Animal Breeding and Genomics, Droevendaalsesteeg 1, 6708PB, Wageningen, the Netherlands
[c] Federal University of Viçosa, Viçosa, MG, 36570-900, Brazil
[d] Granada University, Science faculty, Department of Parasitology, CP:18071, Granada, Granada, Spain
[e] EMBL, Genomics Core Facility, Meyerhofstraße 1, 69117, Heidelberg, Germany

ARTICLE INFO

Keywords:
Neuroimmune interaction
Avian cytokine
Differential gene expression
Neurogenic inflammation
Peripheral immunity
Transcriptome

ABSTRACT

Species-specific neural inflammation can be induced by profound immune signalling from periphery to brain. Recent advances in transcriptomics offer cost-effective approaches to study this regulation. In a population of captive zebra finch (*Taeniopygia guttata*), we compare the differential gene expression patterns in lipopolysaccharide (LPS)-triggered peripheral inflammation revealed by RNA-seq and QuantSeq. The RNA-seq approach identified more differentially expressed genes but failed to detect any inflammatory markers. In contrast, QuantSeq results identified specific expression changes in the genes regulating inflammation. Next, we adopted QuantSeq to relate peripheral and brain transcriptomes. We identified subtle changes in the brain gene expression during the peripheral inflammation (e.g. up-regulation in *AVD-like* and *ACOD1* expression) and detected co-structure between the peripheral and brain inflammation. Our results suggest benefits of the 3′end transcriptomics for association studies between peripheral and neural inflammation in genetically heterogeneous models and identify potential targets for the future brain research in birds.

1. Introduction

Inflammation in brain is often linked with serious behavioural changes and health disorders (Kempuraj et al., 2017). In humans, the outcomes of mild neuroinflammation affect behaviour and psychiatric state, including development of clinical depression (Brites and Fernandes, 2015; DiSabato et al., 2016; Yoshino et al., 2021). In rodents, anxiety and depression-like behaviour can be triggered by stimulation of inflammation in the periphery (Bluthé et al., 1994; Mayerhofer et al., 2017; Painsipp et al., 2010; Sulakhiya et al., 2016). During inflammation, profound immune signalling from periphery to the central nervous system (CNS) can induce neuroinflammation (Danielski et al., 2018; Hernández-Romero et al., 2012). Important roles in this regulation are played by soluble signalling molecules, pro-inflammatory cytokines (e.g. interleukin 1 β, *IL1B* (Lopez-Castejon and Brough, 2011); produced by stimulated peripheral leukocytes that cross the blood brain barrier, stimulate microglia and astrocytes and induce neuroinflammation (Becher et al., 2017; Erickson et al., 2012). While recent evidence suggests interspecific differences in this regulation (Divín et al., 2022), presently we are not sure how common this phenomenon is across vertebrates. Except for humans and rodents in which research of neuroinflammation is widespread, only few studies describe this phenomenon in chickens (Asfor et al., 2021; Du et al., 2020; Song et al., 2020; Zeng et al., 2019) and data from other taxa are sparse (Scalf et al., 2019).

Across vertebrates, variability is observed in peripheral immune responses, contributing to variation in susceptibility to infections (Seal et al., 2021; Vinkler et al., 2023; Zheng et al., 2020). Much of this variation is adaptive, diversified and shaped by natural selection acting across species and populations (Eskew et al., 2021; Minias and Vinkler,

* Corresponding author.
E-mail addresses: kuttiyan@natur.cuni.cz (N. Kuttiyarthu Veetil), hanielcedraz@gmail.com (H. Cedraz de Oliveira), gomezsama@natur.cuni.cz (M. Gomez-Samblas), daniel.divin@natur.cuni.cz (D. Divín), melepatb@natur.cuni.cz (B. Melepat), voukalie@natur.cuni.cz (E. Voukali), zana.bain@gmail.com (Z. Świderská), t.krajzingrova@gmail.com (T. Krajzingrová), martin.tesicky@natur.cuni.cz (M. Těšický), fjung@embl.de (F. Jung), benes@embl.de (V. Beneš), ole.madsen@wur.nl (O. Madsen), michal.vinkler@natur.cuni.cz (M. Vinkler).

https://doi.org/10.1016/j.dci.2023.105106
Received 4 August 2023; Received in revised form 3 November 2023; Accepted 21 November 2023
Available online 25 November 2023

Abbreviations

BAQCOM – Bioinformatics Analysis for Quality Control and Mapping
CIA – Co-Inertia multivariate Analysis
DEG – Differentially Expressed Genes
DGE – Differential Gene Expression
GATK – Genome Analysis Toolkit
LPS – Lipopolysaccharide
RS – RNA-seq dataset
PCA – Principal Component Analysis
QS – QuantSeq dataset
RIN – RNA Integrity Number
RT-qPCR – Reverse transcription quantitative real-time PCR

2022; Peralta-Sánchez et al., 2012; Těšický et al., 2020). Model organisms often provide genetic uniformity that meets the research needs in controlled laboratory experiments but they lack the inter-individual variation observed in nature (Russell et al., 2017). While much is presently known about regulation of local and systemic inflammation in humans and laboratory rodents, little information is available to other species and especially birds, which represent an evolutionary parallel to mammals (Vinkler et al., 2022). Studies in new model species can provide novel insights into general mechanisms underlying immunity regulation and its interaction with other biological systems (Russell et al., 2017).

Avian-oriented research could become highly informative for the current understanding of neuroimmunology (Bramley et al., 2016). Birds show high neuronal densities and developed cognitive skills, comparable to mammals of much larger body mass (Olkowicz et al., 2016). However, majority of the research in avian neuroimmunology has so far been focused at the domestic chicken (*Gallus domesticus*) as a key model (Flores-Santin and Burggren, 2021; International Chicken Genome Sequencing Consortium, 2004). In chickens, the neuronal structures and cognitive skills are less developed than in other evolutionarily derived birds (Kverková et al., 2022), such as the passerines representing the majority of the extant avian species (Arnaiz-Villena et al., 2010; Hellgren and Ekblom, 2010; Romanov et al., 2014). Passerines share a number of cognitive and physiological adaptations convergent to primates. They mastered the vocal learning, which is linked to changes in brain structures analogous to humans (Aamodt et al., 2020). These birds also display memory-dependent behaviour associated with visual identification of food items, and often live in social groups like the primates, but are easier to handle and breed faster (Balakrishnan et al., 2010; Mello, 2014). Zebra finch (*Taeniopygia guttata*) is a recently emerged songbird model for immunological (Batra et al., 2020; Lopes et al., 2012; Mishra et al., 2019; Pedersen et al., 2017; Poole and Kitchen, 2022; Vinkler et al., 2022) and neurobehavioral research (Spierings and ten Cate, 2016), to which much information on the regulation of neuroimmune pathways is still missing (David et al., 2011). Furthermore, it has a fully sequenced high-quality genome and gene annotation (Warren et al., 2010), making it a suitable model for transcriptomic investigation.

Transcriptomics is a powerful approach for identification of key pathway-activation markers in non-model species. Several advancements in RNA sequencing have recently made transcript detection more precise (Hong et al., 2020; Ozsolak and Milos, 2011; Satam et al., 2023). Full-length RNA transcriptomics (RNA-seq) helps to precisely quantify the gene expression levels, assemble the sequences of new transcripts and understand alternative RNA processing (Ramsköld et al., 2012; Finotello and Di Camillo, 2015). Previously, the RNA-seq approach has provided relevant insights on gene expression changes during neuroinflammation and associated diseases in mice and humans (Canchi et al., 2020; Pulido-Salgado et al., 2018). However, RNA-seq approach requires deep sequencing and accurate standardisation of the library preparation procedures since otherwise bias can emerge from fragmentation and library construction steps, altering transcript representation and resulting in more enriched differentially expressed genes (DEGs) for longer transcripts than for the shorter ones (Wang et al., 2009). Furthermore, in cases of less common model species with substantially high inter-individual variation in immune responsiveness, RNA-seq requires investigation of high number of experimental subjects even for relatively simple experimental designs. Hence, despite the falling costs of sequencing, the sample size still can represent a limitation, urging for innovations in library processing, sequencing strategy and data analysis (Moll et al., 2014). To describe the general expression patterns of genes in the transcriptome, full-length sequence RNA-seq can represent an unnecessary investment. New 3' RNA-seq methods, such as QuantSeq, were designed to reduce the costs of general gene expression analysis (Jarvis et al., 2020; Moll et al., 2014), allowing comparing expression patterns across larger sets of samples. The QuantSeq, uses a protocol without any prior poly(A) enrichment or rRNA depletion, in which total RNA is not fragmented before reverse transcription and only single read per transcript is obtained (Ma et al., 2019), sequencing the RNA string close to its 3′ end (generally from the last exon and/or the 3′ untranslated region). Thus, in QuantSeq the number of reads mapped to a given transcript sequence is fully proportional to its expression (Corley et al., 2019).

The main objective of our study was to explore neural inflammation patterns of gene expression in zebra finch after stimulation of mild peripheral sterile inflammation triggered with bacterial lipopolysaccharide (LPS). Despite previous rich transcriptomic research conducted in the zebra finch brain, earlier research focused mostly on variation in gene expression of specific genes (e.g. MHC; Ekblom et al., 2010), transcriptomics of parental care (Kumari et al., 2022) and especially sex- (Friedrich et al., 2022; He et al., 2022) and species-specific (Pfenning et al., 2014) differences in gene expression related to vocal learning. Limited research has been so far conducted in passerine brain immunotranscriptomics (but see e.g. Scalf et al., 2019). First, we investigated the peripheral and systemic effects of our immune manipulation. Since previous studies in avian ecophysiology considered skin as a tissue of interest (Santiago-Quesada et al., 2015; Vinkler et al., 2010, 2012) that is also suitable for the investigation of the regulatory interconnection between the peripheral and systemic immune responses (Arck et al., 2006; Chen and Lyga, 2014; Paus et al., 2006; Peters et al., 2005), we started with analysis of the inflammation effects in skin. We adopted the classical Illumina RNA-seq method from the number of individuals equivalent to similar studies performed in lab mice (Crowell et al., 2020; Liu et al., 2021). Obtaining compromised results (likely due to inter-individual variation in immune responsiveness), we then adopted the QuantSeq approach that is applicable to an enlarged data set. Decreasing the per sample sequencing cost, we doubled the size of our transcriptomic data set. Here we report comparison of results from the two approaches, RNA-seq and QuantSeq. Next, we used the QuantSeq method for brain tissue transcriptomics to reveal the effects of our LPS treatment on gene expression changes in avian brain. Finally, we verified our key results through reverse transcription quantitative polymerase chain reaction (RT-qPCR) analysis.

2. Materials and methods

2.1. Experimental design

Twenty-four adult zebra finch males healthy in appearance were purchased from local hobby breeders (November 2018) and were immediately transported into the animal facility of the Faculty of Science, Charles University, Czech Republic, EU. For each individual, the body weight and tarsus length were measured. For this research, we selected only males, because of the known transcriptomic differences

between the sexes (Friedrich et al., 2022) and the need to limit the overall biological heterogeneity of our experimental sample. The birds were marked with coloured aluminium rings with ID codes and housed in two large aviaries where they were fed with millet and received tap drinking water *ad libitum*. The birds were kept for 3 days in quarantine under regular conditions (D12:N12, 22 °C). Before any manipulation, the magnitude of the tissue of the left wing-web (patagium) was measured in each bird three times with accuracy to 0.01 mm (Vinkler et al., 2010, 2012), using a thickness gage (Mitutoyo, Sakado, Japan, Cat. No. 547-312S). For the experiment, the 24 individuals were divided into two equally sized groups: 12 individuals represented unstimulated controls and 12 immune-stimulated treatments (for dataset details see Table S1 in Electronic Supplementary Material 1, ESM1). All treatment individuals received intraabdominal injection of 0.1 mg *Escherichia coli* LPS O55:B5 (product No. L2880, Sigma-Aldrich, St. Louis, Missouri, USA) dissolved in 100 μl Dulbecco's phosphate-buffered saline (product No. D5652, Sigma-Aldrich). Furthermore, the treatment birds also received an injection of 0.1 mg LPS O55:B5 (Abou Elazab et al., 2022; Casebere et al., 2015) dissolved in 20 μl sterile DPBS administrated subcutaneously into the left wing web (patagium) for testing the local inflammatory response (Wegmann et al., 2015). The experimental manipulations were performed in two consecutive days (two batches of 14 and 10 birds, both containing equal proportions of treatments and controls i.e. in the first batch 7 LPS-treated and 7 control birds, in the second batch 5 LPS-treated and 5 control birds). The LPS-treated birds and no-treatment controls were manipulated in the same way to experience similar levels of the handling stress. For each bird the stimulation period was individually set to 24 h (± 1 h), a period of assumed peripheral inflammation peak (Adelman et al., 2013) after which a second metrical tissue-magnitude measurement was taken from both the left and right patagium (again three times) and then each bird was euthanized by decapitation (Scalf et al., 2019; Vinkler et al., 2018). The research was approved by the Ethical Committee of Charles University, Faculty of Science (permits 13882/2011-30) and was carried out in accordance with the current laws of the Czech Republic and the European Union.

After the post-mortem blood collection from carotids (immediately after decapitation, using sodium heparin to prevent blood coagulation), blood smears were made by spreading a drop of blood over a glass slide. Selected tissues were immediately collected into RNAlater (Cat. No. R0901, Sigma-Aldrich), including brain hyperpallium (ca. 24 mm^3) and skin tissue necropsies from the patagium (wing web, area of ca. 6 mm^2, containing a layer of the skin tissue and associated leukocyte infiltrate). The total dissection time for each bird was <20 min. The collected tissues were immediately placed into the RNAlater, stored at +4 °C overnight and then frozen at −80 °C until analysis. The wing swelling score was later calculated as the average tissue thickness of the left wing after stimulation minus the average thickness of the right wing.

2.2. RNA isolation and sequencing

The brain and skin tissues were homogenized in 2 ml hard tissue homogenizing tubes containing beads (Cat. No: 19-628D, OMNI International, Kennesaw, GA, USA) using MagnaLyser (Cat. No. 41984075, Roche, Basel, Switzerland) and the total RNA was extracted by High Pure RNA Tissue Kit with the DNase-treatment step included (Cat. No. 12033674001, Roche). The RNA yield and purity were estimated using Nanodrop (Cat. No. 9380, ND-1000 UV/Vis, Nanodrop Spectrophotometer, USA) and Agilent 2100 Bioanalyzer (Cat. No. DE00001234, Agilent Technologies, CA, USA). For the skin necropsies (given their small size, ~3 × 2 mm patch), the RNA concentrations ranged between 1 and 10 ng/μl with RNA Integrity Number (RIN) > 6.0, A260/280 values between 1.6 and 2.11 and A260/230 values between 1.52 and 2.48 while for the brain samples (~8 mm^3) the RNA concentrations ranged between 8 and 160 ng/μl with RIN >9.5, A260/280 values between 2.01 and 2.24 and A260/230 values between 2.16 and 2.37.

The library preparation and sequencing were performed at the European Molecular Biology Laboratory (EMBL), Heidelberg, Germany. All the samples were first barcoded with Illumina TruSeq adapters. The NGS libraries were prepared using two different approaches, namely the RNA-seq and QuantSeq. The RNA-seq libraries were generated from the whole RNA and QuantSeq sequences were generated from the RNA 3′ends. The RNA-seq libraries were prepared using NEBNext Ultra II Directional RNA Library Prep Kit for Illumina, and the QuantSeq libraries were prepared using Lexogen QuantSeq 3′ polyadenylated RNA Library Prep Kit FWD for Illumina. For both applications, the sequencing was carried out using the Illumina NextSeq 500 platform, with the RNA-seq reads being 80 base pair (bp) paired-end (PE), and the QuantSeq reads being 80 bp single-end (SE).

For the RNA-seq we sequenced skin samples (left wing patagium) from six randomly selected treatment individuals, representing their LPS-stimulated wing-web skin (hereafter referred to as 'treatment-treatment', tt), the control skin samples (right wing patagium) from the same six LPS-stimulated individuals (hereafter referred to as 'control-treatment', ct) and unmanipulated skin samples (left wing patagium) from six randomly chosen control individuals (hereafter referred to as 'control-control', cc). The general immune response was estimated by comparing cc samples to tt samples. The comparison of ct samples to tt samples served us for description of the relative effects of the local immune response, while the comparison of cc samples to ct samples served us to disentangle the effects of the systemic immune responses in the periphery. To reach comparable sequencing costs for both approaches focusing on the tt and cc comparison, for QuantSeq we compared 12 treatment skin samples from the treatment individuals (tt) to 12 control skin samples from the control individuals (cc). Using the advantage of the cost-efficient QuantSeq approach, we were able to cover larger population sample and hence overcome the issue of inter-individual variability in transcriptomic patterns biasing the results. Finally, to meet our main objective, using QuantSeq we sequenced brain samples from the same 12 treatment individuals and 12 control individuals. The raw sequences were uploaded in the Sequence Read Archive (SRA) of NCBI (accession number: PRJNA751848).

2.3. Transcriptome bioinformatics

The transcriptome bioinformatic analysis was carried out in Wageningen University and Research (WUR), the Netherlands. The BAQCOM pipeline v. 0.3.2 (https://github.com/hanielcedraz/BAQCOM; Adapter trimming: Trimmomatic v. 0.39; Alignment STAR v. 2.7.2b; Readcounts: featurecounts v. 2.0.3) with the zebra finch reference genome (Taeniopygia_guttata.bTaeGut1_v1.p.dna.toplevel.fa) and annotation file (Taeniopygia_guttata.bTaeGut1_v1.p.108.gtf) downloaded from Ensembl (Howe et al., 2021) was adopted for the data analysis. This was based on initial testing of the BAQCOM and the bluebee pipeline (https://www.bluebee.com/lexogen/; Adapter trimming: bbduk v. 35.92; Alignment STAR v. 2.5.2a; Readcounts: HTSeq-count v. 0.6.0).

On average, the RNA-seq generated in the skin samples ~130 million reads per individual (range from 85,612,614 to 167,895,520 reads; Table S3, ESM1) with the alignment percentage ranging between 55.50% and 95.98% (Table S4, ESM1). For QuantSeq, the sequence data obtained were on average ~9.5 million reads per individual (range from 1,586,888 to 21,400,263 reads) for the skin samples and ~13.4 million reads per individual (range between 11,309,173 and 16,028,933 reads; Table S3, ESM1) for the brain samples. For the skin samples, the alignment percentage ranged between 65.56% and 95.86% and for the brain samples, the alignment percentage ranged between 68.99% and 91.38% (Table S4, ESM1).

As outlined above, for DEG analysis in RNA-seq data we used the in-depth capacity of the platform to gain insight into the additive effects of local and systemic immune response: i) the general response was estimated by comparing the groups cc vs. tt (as for the QuantSeq), ii) the local effects were estimated by comparing treatment and control wings

from the same treatment individuals (ct vs. tt), and finally iii) the systemic effects were estimated by comparing unmanipulated controls to untreated skin in the intraabdominally LPS-injected individuals (cc vs. ct). The DESeq2 program was used with default settings to calculate the fold change gene expression values that were then transformed to their $\log_2$ values. Genes with padj value ≤ 0.05 and a $\log_2$ fold change value ≥ 1 were considered as significantly differentially expressed. Gene functional annotations (gene ontology, GO) were attributed using the Ensembl BioMart (Smedley et al., 2015) with a zebra finch reference, manually supplemented with Uniprot (The UniProt Consortium et al., 2021) annotations. The GO terms for unannotated genes were assigned by finding orthologous genes in the chicken or human reference using gprofiler (Raudvere et al., 2019).

To reveal similarities and differences in the results obtained through the RNA-seq and QuantSeq platforms, we used the Co-Inertia multivariate Analysis (CIA) (Dolédec and Chessel, 1994; Dray et al., 2003) combined with the Monte Carlo permutation test (see Bílková et al., 2018). CIA identifies co-relationships between the samples from the same individuals represented in multiple datasets. Furthermore, the correlations between the QuantSeq and RNA-seq data were analysed using corrplot package (Version 0.84) and Spearman's correlation in R software (version 4.1.1; (Team, 2013). Since the total number of experimental animals differed between our RNA-seq and QuantSeq datasets, we applied these two approaches on identically subsampled datasets, using only the QuantSeq data from samples simultaneously sequenced also through the RNA-seq. We also ran the GATK (Genome Analysis Toolkit) pipeline (Poplin et al., 2017) to check for the relatedness-independent assortment of the individuals between the treatment groups; we used SNPRelate package (default settings) (Zheng et al., 2012) in R software for generating the dendrogram of individual relatedness. The result showed us that the birds were distributed between the treatment groups randomly with respect to their relatedness (Supplementary Fig. S1, ESM2). We generated Venn diagrams to indicate the DEGs common between the all the full length RNA-seq comparisons (RS) as well as between all RS vs. QuantSeq (QS) comparisons using Venny (version 2.1.0) (Oliveros, 2007). We used online tool ShinyGO v. 0.77 (http://bioinformatics.sdstate.edu/go/) to generate the gene interaction network for the differentially expressed genes from the QS data of both skin and brain tissues (Ge et al., 2020).

2.4. RT-qPCR validation of the gene expression changes in brain and skin

For the selected top DEGs (based on the fold change values from the QuantSeq analysis) expressed in both brain and skin we verified the expression patterns using RT-qPCR. The target genes included *IL1B*, avidin (*AVD-like*), antimicrobial protein avian β defensin 10 (*AvBD10*), two chemokine genes *CXCLi1, CXCLi2* (orthologous genes for the chemokine *CXCL8* ~ *IL8* in mammals; Poh et al., 2008) and anti-inflammatory gene aconitate decarboxylase 1 (*ACOD1*). The *28S rRNA* was used as a reference gene. The RT-qPCR was performed in triplicates, together with plate negative (no-template triplicate) and positive (standard dilution series 10^2-10^8 copies) controls, using Luna Universal Probe One-Step RT-PCR Kit (E3006, BioLabs Inc.) with 0.6 mM primer and 0.2 mM probe concentrations in a Light Cycler LC480 Instrument (Roche Diagnostics, Rotkreuz, Switzerland) set to cycling conditions: (1) 50 °C 10 min, (2) 95 °C 1 min, (3) (95 °C 10 s, 60 °C 30 s) × 45. The RNA for the RT-qPCR analysis was diluted in molecular water enriched with carrier-tRNA (Qiagen, Cat. No. 1068337): 1:5 for the target gene quantification and 1:500 for the reference gene (28S rRNA) quantification. Details to the RT-qPCR assays are provided in Table S5, ESM1. As positive controls we used the synthetic DNA standards (g-Blocks; Table S6, ESM1). Our assay efficiency was on average 1.911 (ranging between 1.72 and 2.00, Table S6, ESM1; standard curves for the RT-qPCR assays are provided in Fig. S2, ESM2). Prior the RT-qPCR analysis, we checked the sequence population variability in the primers and probes used for our RT-qPCR assays to identify any possible mismatches (extraction of genomic DNA from blood of 10 zebra finches using DNeasy Blood & Tissue Kit, Qiagen, cat. number 69581; amplification with Qiagen Multiplex PCR Plus kit in a reaction with 0.2 μM final concentration of primers; Sanger sequencing of the targets with BigDye Terminator v. 3.1 Cycle Sequencing Kit and 3500xL Genetic Analyzer Applied Biosystem platform). In the final assays that we designed for this study we did not find any sequence variation that could differentially affect the assay efficiencies between individuals (GenBank IDs are provided in Table S7, ESM1).

The gene expression quantification was calculated either as standard gene expression quantity (Qst; Vinkler et al., 2018) that allows comparison of the gene expression between treatments and controls or as the relative gene expression ratio (R) which provides the measure of gene expression fold change in the treatments against the controls (Pfaffl, 2001). In the *ACOD1* gene, non-specificities were repeatedly revealed when amplifying different regions of the gene with different combinations of primer pairs, probably resulting from repetitive GCs, indels variable in the population or multiple isoforms. Also, the efficiency of our *ACOD1* qPCR was very low in this gene (1.72). Therefore, *ACOD1* was excluded from the final DGE analysis. The analysis was limited only to the top target genes and a single reference gene because of the low amounts of RNA that was remining after the transcriptomics and was available for the RT-qPCR analysis.

The statistical analysis of the RT-qPCR results was conducted using the R software (Team, 2013). We assessed data normality distribution through the Shapiro-Wilk test. Due to the non-normal distribution of the Qst values, we opted to employ the non-parametric Wilcox test for further analysis. The differences in gene expression between treatment groups were visualised as boxplots using the *ggplot2* package (v. 3.4.2). Correlation tests and Principal Component Analyses (PCA) were performed for the selected genes studied via RT-qPCR in both skin and brain tissues, respectively. The relative expression data were normalized using a common logarithm.

3. Results

3.1. Skin swelling response to LPS stimulation

Before transcriptomic analysis, we checked whether the inflammatory immune response to the LPS stimulation occurred in skin of the treatment birds in the time of tissue collection. This was revealed by the significant swelling of the tissue in treatments compared to controls (Wilcoxon signed rank test: $n = 24$, $V = 1.00$, $p = 0.003$; Fig. 1).

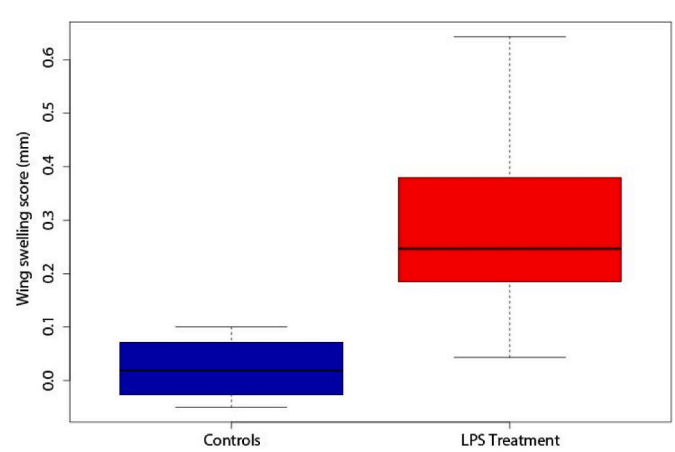

Fig. 1. Difference in the wing patagium swelling response between the LPS-treatment birds and controls. The wing swelling score was used as an inflammatory response measure, calculated as the difference in skin thickness between the left (treatment) wing patagium and the right (control) wing patagium (mm). Mean and variation in SD is shown.

3.2. Skin transcriptomics analysed by the RNA-seq approach

Based on the zebra finch RNA-seq data from skin peripheral inflammation, our experimental design allows us to elucidate the relative effects of systemic and local responses from the general transcriptomic changes. First, the DGE analysis of the general response (tt vs. cc; dataset RS1) revealed in total 370 DEGs with 117 of them having annotation of the gene function. Out of these 62 were up-regulated and 57 down-regulated (gene list with GO annotations provided in Table S8, ESM1). Interestingly, the most significant up-regulated genes belonged to the GO terms muscle fibre development pathway, positive regulation of Rho protein signal transduction pathway and post-translational protein modification pathway. Only six upregulated genes were involved in immune function, including innate immune response (*SUSD4*), leukocyte migration involved in inflammatory response (*TRIM55*) and negative regulation of interferon-gamma-mediated signalling pathway (*PPARG*). Neither most of the significantly down-regulated genes were involved in immune function; those that were (5 genes) belonged to the pathways including negative regulation of inflammatory response (*CCN3*) and positive regulation of interleukin-1 production (*PANX2*). Second, analysis of the local effects of the LPS treatment (ct vs. tt; dataset RS2) identified 103 DEGs out of which only 43 DEGs had gene function annotations, with as few as 14 up-regulated ones and the remaining 29 genes being down-regulated (Table S9, ESM1). The most significant up-regulated genes belonged to the regulation of apoptotic process and activation of JUN kinase activity pathways. Minority of the up-regulated DEGs were associated with immunity: inflammatory response (*KLRG1*), response to bacterium (*CLPS*) and cytokine-mediated signalling pathway (*IL17RD*). Key down-regulated genes belonged to the following pathways: intracellular signal transduction, lipid metabolic process, and calcium ion transport. Among the few down-regulated immune genes belonged those linked with negative regulation of NIK/NF-kappaB signalling (*CCN3*), positive regulation of interleukin-1 production (*PANX2*) and innate immune response (*POLR3E*). Third, analysis of the systemic effects of the peripheral LPS stimulation (cc vs. ct; dataset RS3) identified 76 DEGs in total, but only 37 genes annotated. Among these, 33 were up-regulated and 4 down-regulated (Table S10, ESM1). The main pathways identified were partially consistent with the results of our general (cc-tt; RS1) analysis, although we could only find a single gene which was directly involved in immune function (*ANKRD1*).

We found limited overlaps between the gene sets revealed by the three separate DGE analyses, with no genes common among all of them (Fig. S3; Table S11, ESM1). There were 32 genes common between RS1 and RS2, indicating their involvement in the local response, although only a single one (*BIRC7*) showed a direct immune function). There were 25 genes common between RS1 and RS3, suggesting their role in systemic response, but none had any specific role in immunity. Thus, surprisingly, our RNA-seq analysis did not reveal any important involvement of immune genes in the immune response. Therefore, we conclude that within the existing budget constraints, our RNA-seq was not very successful in detecting the immunological effect of an avian systemic inflammation. These pilot results indicated that simple increase in the sample size and sequencing depth would not be a cost-effective and budget-feasible solution to reach our objective. Therefore, an alternative strategy was adopted, applying the QuantSeq approach to identify the immunological effect of the LPS stimulations.

3.3. Skin transcriptomics analysed by the QuantSeq approach

In an enlarged dataset of 24 individuals potentially better representing the inter-individual variation, we analysed the general skin inflammatory response (cc vs. tt) using the QuantSeq approach (dataset QS; equivalent RS1). We identified the differential expression in 265 genes. Out of the 168 significant DEGs with functional annotation available, 113 genes were up-regulated, and 55 genes were down-regulated (Table S12, ESM1; the gene interaction networks for the up-regulated and down-regulated genes are shown in Fig. S4 and Fig. S5, respectively). In contrast to the RS1 dataset, several of the up-regulated DEGs represented key regulators of immune response and known inflammation markers. As expected, the major immune pathways detected were immune response (*SCAP*), innate immune response (*CXCL8*), and cellular response to lipopolysaccharide (*IL1B, TNIP3*). Our analysis also identified changes in expression of other genes functionally related with altered physiology during inflammation, including, e.g., cell-cell junction assembly (*CDH12*), maintenance of epithelial cell apical/basal polarity (*LHX2*) and anatomical structure morphogenesis (*SOX3*).

We found little overlap between the most significant up-regulated pathways revealed by the four skin sample comparisons we performed (Fig. 2). Searching for possible overlaps (Fig. 3), we found only 6 DEGs with defined GO annotation common between the RNA-seq and QuantSeq results (cc-tt) in skin: *MB*, *MYOZ1*, *CKMT2*, *MYL1*, *TNNT3* and *PLCXD3* with most of them having their roles in skeletal muscle development and muscle contraction, but no associations to immunity. Yet, CIA showed significant co-structure between the RNA-seq and QuantSeq datasets (RV = 0.445, Monte Carlo test p = 0.001), indicating that both approaches captured at least part of the same biologically relevant differences between the samples (Table S13, ESM1).

3.4. Identification of differentially expressed genes in brain during peripheral inflammation

We used the QuantSeq approach to identify also suitable neuroinflammatory markers in the zebra finch. Our analysis of DGE in the hyperpallial region of brain in the full dataset of 24 individuals identified seven consistently represented DEGs, out of which 6 genes were up regulated (Table S14, the gene interaction network is shown in Fig. S6). The up-regulated genes refer to pathways involved in antibacterial humoral response (*AVD-like*), cellular response to interleukin-1 (*ACOD1*), inflammatory response (*EX-FABP-like*), clustering of voltage-gated sodium channels (*GLDN*), iron ion transport (*FTH1*) and positive regulation of Notch signalling pathway (*BMP2K*; Fig. 4). The single down-regulated gene is *MIR29B2*, which is a miRNA with unknown function in birds. *AVD-like* and *ACOD1* were then selected as our putative neuroinflammatory markers. CIA showed significant co-structure between the brain and skin QuantSeq datasets (RV = 0.33, Monte Carlo test p = 0.001; Table S15).

3.5. Validation of the QuantSeq-identified DEGs in skin and brain using RT-qPCR

To verify the accuracy of the QuantSeq estimates of gene expression changes during inflammation in the zebra finch, 5 selected DEGs (*IL1B*, *AvBD10*, *AVD-like*, *CXCLi1* and *CXCLi2*) identified in either skin or brain were targeted by the RT-qPCR (details on the RT-qPCR results are provided in Table S16). Unfortunately, we were unable to develop a functional RT-qPCR for *ACOD1* where we experienced non-specificities in amplified products (Table S5 and Table S6 in ESM1). In skin, we found that expression of all the 5 remaining genes was significantly up-regulated, consistently with our QuantSeq results (Table S12). Interestingly, this trend was not captured by the RNA-seq, which showed no significant difference in the expression of these genes in skin (Fig. 5). The expression of several of these selected genes in skin, as revealed by the RT-qPCR, was intercorrelated, but did not correlate with the metrical measurement of the skin swelling (Table S17). Also the PCA analysis of the RT-qPCR gene expression data in skin showed that all the tested genes consistently followed the same trend of activation (PC1 explained 61.8% of the variation, PC2 explained 20.9% of the variation; Fig. S7). In the brain, the PCA showed two gene clusters, one formed by *AvBD10* and *CXCLi1* and the other one by *IL1B*, *AVD-LIKE* and *CXCLi2* (PC1 explained 66.9% variability, PC2 explained 18.5% of the variation; Fig. S7). The correlation matrices for *IL1B*, *AVD-LIKE*, *AvBD10*, *CXCLi1*

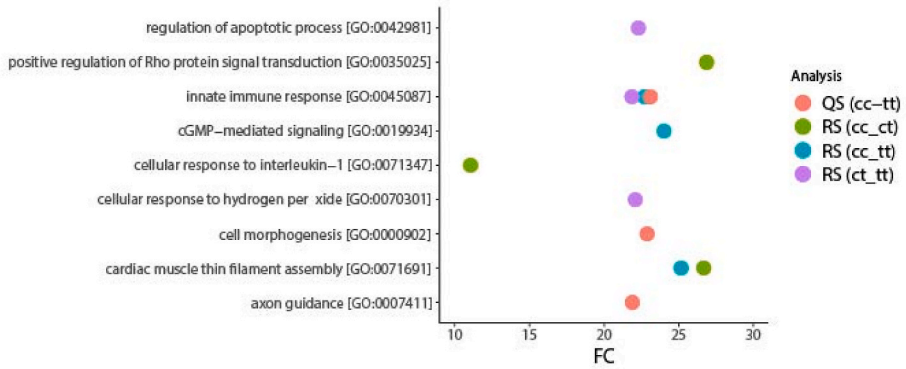

Fig. 2. The most significant up-regulated pathways revealed in the four transcriptomic analyses of the skin peripheral response to bacterial lipopolysaccharide (LPS) in the zebra finch. Two approaches (RS = RNA-seq and QS = QuantSeq) were adopted to reveal the differential gene expression between skin samples obtained from control patagium tissue in control individuals (cc), control patagium tissue in treatment individuals (ct) and treatment patagium tissue in treatment individuals (tt), x-axis shows $\log_2$ fold change (FC), y-axis shows the most significant pathways.

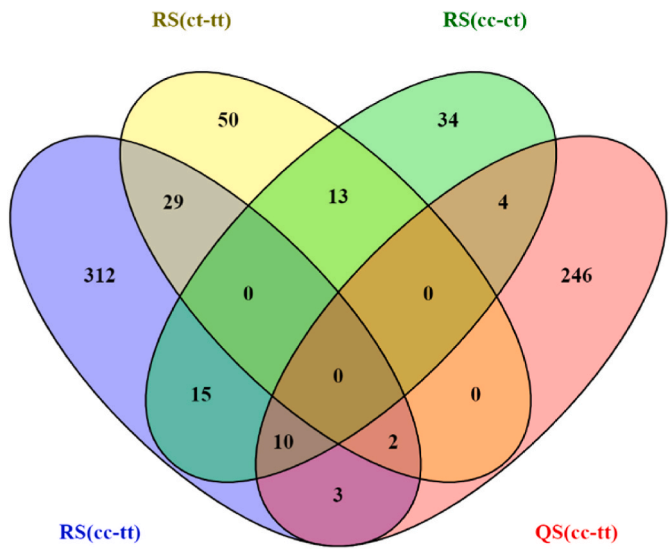

Fig. 3. Venn diagram showing the number of common differentially expressed genes between the four transcriptomic analyses of the skin peripheral response to bacterial lipopolysaccharide (LPS) in zebra finch. Two approaches (RS = RNA-seq and QS = QuantSeq) were adopted to reveal the differential gene expression between skin samples obtained from control patagium tissue in control individuals (cc), control patagium tissue in treatment individuals (ct) and treatment patagium tissue in treatment individuals (tt).

and *CXCLi2* showing the RT-qPCR-detected gene expression trends for brain and skin are provided in the supplementary files (Table S18 and Table S19 in ESM1, and Fig. S8 and Fig. S9 in ESM2). None of the cytokine genes serving as peripheral inflammatory markers (*IL1B*, *CXCLi1* and *CXCLi2*) was in the brain differentially expressed between the treatments and the controls (in all cases $p > 0.100$). This result was again consistent with the QuantSeq results. In contrast, *AVD-like* gene expression up-regulation was detected by RT-qPCR in the brain, validating the QuantSeq results (Fig. 5; rest of the figures are provided in Fig. S10 and Fig. S11 in ESM2). Furthermore, we found increased expression of *AvBD10* gene in the brain of the LPS-stimulated individuals, which was not captured by the QuantSeq transcriptomics. For all the selected genes in skin (*AVD-like*: $r = 0.751$, $p \ll 0.001$; *AvBD10*: $r = 0.758$, $p \ll 0.001$; *CXCLi1*: $r = 0.797$, $p \ll 0.001$; *CXCLi2*: $r = 0.621$, $p = 0.001$; *IL1B*: $r = 0.489$, $p = 0.015$) and for *AVD-like* in brain ($r = 0.581$, $p < 0.003$) we found strong correlations between the QuantSeq and RT-qPCR data (for *AVD-like* shown in Fig. 5, for the other four genes expressed in skin and brain see Figs. S12 and S13 in ESM2). Our results indicate that within comparable expense limits, the QuantSeq method showed improved sensitivity over to the traditional RNA-seq to the changes in expression of the immune genes.

4. Discussion

Diverse transcriptomic methods are now available to analyse variation in gene expression, but not all are equally suitable for all types of datasets. Our initial attempts to describe the gene expression patterns during local and systemic immune response to LPS using RNA-seq in 12

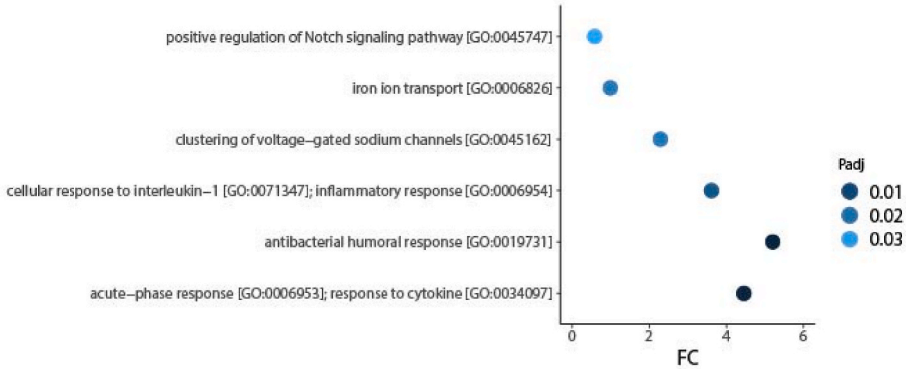

Fig. 4. The most significant up-regulated pathways revealed in the transcriptomic analysis of the brain response to peripheral stimulation with bacterial lipopolysaccharide (LPS) in zebra finch. QuantSeq (QS) approach was adopted to reveal differential gene expression, x-axis shows $\log_2$ fold change (FC), y-axis shows the most significant pathways.

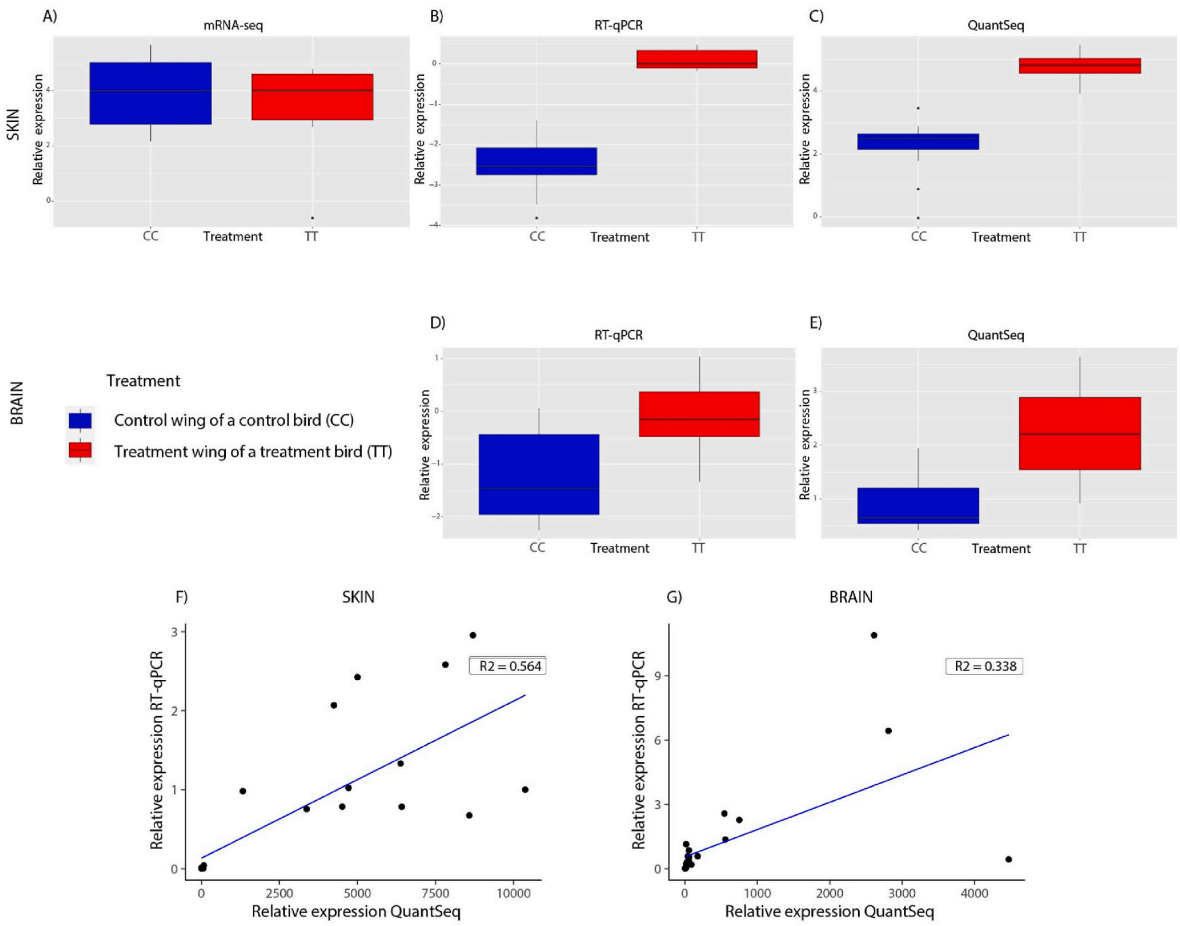

Fig. 5. Expression changes in the *AVD-like* gene estimated through (A) RNA-seq (RS1), (B) RT-qPCR, (C) QuantSeq approaches in the skin samples of controls (CC) and treatment individuals (TT) with peripheral response stimulated with bacterial lipopolysaccharide (LPS) in zebra finch. (D) RT-qPCR and (E) QuantSeq show *AVD-like* gene expression in brain during this peripheral response. Correlation between the RT-qPCR and QuantSeq data on the *AVD-like* gene expression in skin, $r = 0.751$, $p << 0.001$ (F) and in brain, $r = 0.581$, $p = 0.003$ (G).

zebra finch individuals (6 control and 6 treatment birds) revealed much inconsistency to Scalf et al. (2019) regarding the immune gene expression. Assuming that high inter-individual variation in our experimental zebra finch dataset could have contributed to this result, we opted another library preparation technique, the QuantSeq. Using the single 3′end sequencing, the cost efficiency of this approach (per sample 1/5th of the RNA-seq price) allowed us to increase the sequenced transcriptomic dataset, consisting of skin and brain samples, to 24 individuals (12 control and 12 treatment birds). Based on this approach we were able to identify candidate genes expressed in brain during peripheral inflammation. Our RT-qPCR analysis in selected genes validated the application of the QuantSeq method for identification of immune gene expression changes in the genetically heterogeneous domestic zebra finch model.

Given the dynamics of the immune response, timing of the response measurement is an important parameter in characterisation of inflammation. In our study we selected the 24-h response period, because this timing is often adopted in studies aimed at investigation of the skin immune responsiveness in passerine birds, corresponding to the peak of the tissue swelling response (Vinkler et al., 2010). Our result evidence significant tissue swelling at 24 h after stimulation, which is assumed to reflect tissue infiltration with various leukocyte types (Martin et al., 2006). Based on the understood molecular mechanism of the immune stimulation with LPS in the zebra finch (Vinkler et al., 2009), our experiment characterises gene expression changes during non-specific sterile inflammation activated in the skin through TLR4-mediated signalling.

Consistent with results of other studies (Jarvis et al., 2020; Vo et al., 2021), we show important differences between the DGE analysis results obtained through the RNA-seq and the QuantSeq approaches. While in the skin response the RNA-seq method identified more DEGs in total (371 genes compared to 265 genes identified by the QuantSeq method), this difference did not hold for the subset of the genes with available databased annotations, where QuantSeq provided more results (168 genes compared to only 120 genes detected by the RNA-seq approach). The two approaches differ in the depth of sequencing, with the QuantSeq having higher coverage, but only in a much shorter part of the full-length transcript than RNA-seq. We assume that most of the unannotated genes could be sequences of non-coding RNAs in which the function is typically not known in less frequently studied species. Thus, for the zebra finch population datasets, the QuantSeq approach appears as a more cost-effective approach to identify the gene expression changes associated with inflammatory response. Similar to our findings, previous research reported that RNA-seq identifies in general more DEGs, but QuantSeq can detect more transcripts with specific features, e.g. shorter genes (Ma et al., 2019) that often act in immunity as effector and signalling molecules (Vo et al., 2021). It is important to note that although we sequenced lower number of samples using the RNA-seq method than using QuantSeq, the number of samples analysed by RNA-seq was still comparable to many other transcriptomic experiments in model organisms, e.g. in laboratory rodents (Liu et al., 2021; Söllner et al., 2017). However, the domestic zebra finch population is genetically more heterogenous than the common laboratory models (Forstmeier et al., 2007; Gasch et al., 2016), which can affect the levels of

inter-individual variation in immune responsiveness and decrease power of the DGE analysis. Yet, the results of our CIA indicate that despite this issue, both the RNA-seq and QuantSeq approaches captured in the zebra finch biologically relevant variation between the samples analysed, documenting the relevance of those results that we were able to obtained. Comparisons of the local (ct vs. tt) and systemic response (cc vs. ct) using the RNA-seq generally showed pathways unrelated to immunity. Interestingly, in skin there were just 15 DEGs in common between the RNA-seq and QuantSeq results, out of which six genes only had defined gene names and functions. All the six shared genes were down-regulated in both RS1(cc-tt) and QS(cc-tt) and were mainly involved in movement physiology, suggesting changes in the physiology of subcutaneous muscles towards movement restrictions during the sickness phase, commonly observed during later stages of the acute response (Adelman et al., 2013; Deak et al., 2005; Sköld-Chiriac et al., 2014). Similar results were described earlier in fish and mammals (Brant et al., 2019; Liu et al., 2022; Sousa et al., 2022).

Importantly, the QuantSeq approach identified 56 genes involved in immune function whereas the RNA-seq only identified 12 immune genes as DEGs. Using the QuantSeq approach, we revealed in the skin up-regulation of key inflammation markers such as *IL1B* (Bent et al., 2018; Kaneko et al., 2019) and *CXCL8(IL8)* (Bent et al., 2018; Bernhard et al., 2021; Lopez-Castejon and Brough, 2011; Shahzad et al., 2010), showing the ongoing acute inflammation in the periphery (Lopez-Castejon and Brough, 2011). Our RT-qPCR results obtained from skin samples validate the QuantSeq results, but contradict the negative results obtained from RNA-seq (all the five genes tested).

Studies in rodents have shown that IL1B expressed in the periphery can activate both astrocytes and microglia in the brain, triggering neuroinflammation (Shaftel et al., 2008). *IL8* has a role in neutrophil activation and chemotaxis within the CNS during inflammation. In human microglia *IL8* levels increase in response to LPS (Ehrlich et al., 1998). *IL1B* also promotes the expression of avian β-defensins, which are important antimicrobial peptides (Hancock and Diamond, 2000; McDermott, 2004; Scott and Hancock, 2000). Especially *AvBD*10 has been reported in the brain tissues of many avian species (Li et al., 2015). Our RT-qPCR captured similar *AvBD10* gene expression change in the brain that remained unidentified through the transcriptomics.

Unlike previous research of zebra finch neuroinflammation performed during the early phase of activation (2 h; Scalf et al., 2019), our study focused at the response observed 24 h after the LPS injection, identifying the delayed changes in gene expression. This could be responsible for the difference in the DGE pattern observed. In brain, our QuantSeq analysis identified only seven DEGs, i.e. less DEGs than identified during the early response (Scalf et al., 2019). Such a time-dependent change in the gene expression pattern is known also from mammalian studies (Rankine et al., 2006; Terenina et al., 2017). Yet, among the up-regulated DEGs detected in the brain, all six, *AVD--LIKE, EX-FABP-like, ACOD1, GLDN, FTH1, BMP2K*, are involved in immune response modulation, suggesting that expression of these genes could contribute to the regulation of neuroinflammation and related sickness physiology. Up-regulation of Avidin (*AVD*)-related genes is observed during inflammation and infections in chickens (Korpela et al., 1982; Kunnas et al., 1993). *AVD* up-regulation can induce expression of a stress protein family of Fatty acid-binding proteins (*FABPs*) (Zerega et al., 2001), lipid chaperones having a roles also in neurodegenerative diseases (Guo et al., 2022) and regulation of neuroinflammation (So et al., 2022, p. 4). Similar to our results, in chickens *EX-FABP* expression increases after stimulation with LPS and *IL6* (Cermelli et al., 2000), supporting the role of this gene in immunomodulation. Aconitate decarboxylase 1 (*ACOD1*, also known as immune responsive gene 1, *IRG1*) is a key regulator of immunometabolism during infection with important anti-inflammatory effects (Wu et al., 2022). In mice, both viral (Mills et al., 2018) and bacterial (Ganta et al., 2017; Shi et al., 2005) pathogens importantly enhance the expression of *ACOD1,* especially in microglia (Kanthasamy and Rangaraju, 2020). *FTH1* is known to be involved in macrophage activation, as evidenced by stimulation with LPS (Mesquita et al., 2020). Transcriptomics in mice microglial cells showed up-regulation of *FTH1* expression in late neurodegenerative diseases (Hunter et al., 2021). The associations of the remaining two DGEs with immunity are less direct, but previous studies showed elevated expression of bone morphogenetic protein 2 inducible kinase (*BMP2K*) during prolonged inflammation (Vance, 2014) and gliomedin (*GLDN*) is associated with profound macrophage infiltration into wounds and may be involved in the healing process (Etich et al., 2019).

To conclude, our results provide evidence for transcriptomic changes induced in the periphery (skin) by a local and systemic stimulation of inflammation, affecting gene expression regulation in the brain. These results on the late response complete the previously published evidence on early phases of the neuroimmune response to peripheral inflammation in the songbird model (Scalf et al., 2019). Twenty-four hours after stimulation the pro-inflammatory regulation is detectable in the periphery but has only very modest effects on the gene expression in zebra finch brain. Here the signalling is mostly anti-inflammatory, including up-regulated expression of genes involved in resolving the acute neuroinflammation. Further studies are required to bring understanding to the precise timing of the shift between neuroinflammatory and anti-inflammatory regulation and specific roles of individual genes and related pathways in this process, similar to the time scale experiments in rodent (Borniger et al., 2017; Lesur et al., 2010; Seok et al., 2013). Comparative research is key to reveal the basic principles of the neuro-immune interplay regulation. Our study including also the RT-qPCR validation indicates that specific cost-effective alternatives to the classical RNA-seq, such as the QuantSeq, can promote this demanding investigation in non-model, genetically heterogenous species, facilitating identification of key markers of peripheral inflammation and neuroinflammation applicable across species.

Statements and Declarations

The authors declare no potential conflicts of interest.

Author contributions

Conceptualization Ideas: Michal Vinkler, Nithya Kuttiyarthu Veetil.

Data curation: Nithya Kuttiyarthu Veetil.

Formal analysis: Nithya Kuttiyarthu Veetil, Mercedes Gomez-Samblas, Daniel Divín, Balraj Melepat.

Funding acquisition: Michal Vinkler, Nithya Kuttiyarthu Veetil, Balraj Melepat.

Investigation: Michal Vinkler, Nithya Kuttiyarthu Veetil, Daniel Divín, Eleni Voukali, Zuzana Świderska, Tereza Krajzingrová, Martin Těšický, Ferris Jung.

Methodology: Vladimír Beneš, Ole Madsen, Haniel Cedraz de Oliveira, Michal Vinkler, Nithya Kuttiyarthu Veetil.

Project administration: Michal Vinkler.

Software: Ole Madsen, Haniel Cedraz de Oliveira, Nithya Kuttiyarthu Veetil, Mercedes Gomez-Samblas.

Supervision: Michal Vinkler, Vladimír Beneš, Ole Madsen, Haniel Cedraz de Oliveira.

Visualization: Michal Vinkler, Nithya Kuttiyarthu Veetil, Mercedes Gomez-Samblas.

Writing – original draft: Nithya Kuttiyarthu Veetil, Michal Vinkler.

Writing – review & editing Preparation: Nithya Kuttiyarthu Veetil, Michal Vinkler, Mercedes Gomez-Samblas, Balraj Melepat, Ole Madsen, Haniel Cedraz de Oliveira, Vladimír Beneš, Ferris Jung, Daniel Divín, Eleni Voukali, Zuzana Świderska, Tereza Krajzingrová, Martin Těšický.

Data availability

Data will be made available on request.

Acknowledgements

This study was supported by Grant Schemes at Charles University (grant nos. GAUK 646119, PRIMUS/17/SCI/12, and START/SCI/113 with reg. no. CZ.02.2.69/0.0/0.0/19_073/0016935) and the Czech Science Foundation Grant No. P502/19-20152Y. The research visit of NKV to Wageningen University was supported by the Short-Term Scientific Mission programme of the European Cooperation in Science and Technology (COST) Action CA15112 (FAANG-Europe) and INTER-COST grant No. LTC18060 provided by the Ministry of Education, Youth and Sports of the Czech Republic. Computational resources were provided by the Wageningen University and data storage facility by the Czech Education and Scientific NETwork CESNET; project e-INFRA CZ LM2018140 supported by the Ministry of Education, Youth and Sports of the Czech Republic). We are also grateful to Martin Kocourek and Pavel Němec for the guidance in bird brain dissection. The study was further supported by the Institutional Research Support No. 260684/2023.

Appendix A. Supplementary data

Supplementary data to this article can be found online at https://doi.org/10.1016/j.dci.2023.105106.

References

Aamodt, C.M., Farias-Virgens, M., White, S.A., 2020. Birdsong as a window into language origins and evolutionary neuroscience. Philos. Trans. R. Soc. B. 375, 20190060. http://doi.org/10.1098/rstb.2019.0060.

Abou Elazab, M.F., Nasr, N.E., Ahmed, M.S., Alrashdi, B.M., Dahran, N., Alblihed, M.A., Elmahallawy, E.K., 2022. The effects of bacterial lipopolysaccharide (LPS) on Turkey poults: assessment of biochemical parameters and histopathological changes. Vet. Sci. 9, 240.

Adelman, J.S., Kirkpatrick, L., Grodio, J.L., Hawley, D.M., 2013. House finch populations differ in early inflammatory signaling and pathogen tolerance at the peak of *Mycoplasma gallisepticum* infection. Am. Nat. 181, 674–689. https://doi.org/10.1086/670024.

Arck, P.C., Slominski, A., Theoharides, T.C., Peters, E.M., Paus, R., 2006. Neuroimmunology of stress: skin takes center stage. J. Invest. Dermatol. 126, 1697–1704.

Arnaiz-Villena, A., Ruiz-del-Valle, V., Reche, P., Gomez-Prieto, P., Lowry, E., Zamora, J., Areces, C., Rey, D., Parga, C., Serrano-Vela, J.I., 2010. Songbirds conserved sites and intron size of MHC class I molecules reveal a unique evolution in vertebrates. Open Ornithol. J. 3, 156–165. https://doi.org/10.2174/1874453201003010156.

Asfor, A.S., Nazki, S., Reddy, V.R.A.P., Campbell, E., Dulwich, K.L., Giotis, E.S., Skinner, M.A., Broadbent, A.J., 2021. Transcriptomic analysis of inbred chicken lines reveals infectious bursal disease severity is associated with greater bursal inflammation in vivo and more rapid induction of pro-inflammatory responses in primary bursal cells stimulated ex vivo. Viruses 13, 933. https://doi.org/10.3390/v13050933.

Balakrishnan, C.N., Edwards, S.V., Clayton, D.F., 2010. The Zebra Finch genome and avian genomics in the wild. Emu - Austral Ornithol. 110, 233–241. https://doi.org/10.1071/MU09087.

Batra, T., Malik, I., Prabhat, A., Bhardwaj, S.K., Kumar, V., 2020. Sleep in unnatural times: illuminated night negatively affects sleep and associated hypothalamic gene expressions in diurnal zebra finches. Proc. R. Soc. A B 287, 20192952.

Becher, B., Spath, S., Goverman, J., 2017. Cytokine networks in neuroinflammation. Nat. Rev. Immunol. 17, 49–59. https://doi.org/10.1038/nri.2016.123.

Bent, R., Moll, L., Grabbe, S., Bros, M., 2018. Interleukin-1 beta—a friend or foe in malignancies? Int. J. Mol. Sci. 19, 2155.

Bernhard, S., Hug, S., Stratmann, A.E.P., Erber, M., Vidoni, L., Knapp, C.L., Thomaß, B.D., Fauler, M., Nilsson, B., Ekdahl, K.N., 2021. Interleukin 8 elicits rapid physiological changes in neutrophils that are altered by inflammatory conditions. J. Innate Immun. 13, 225–241.

Bílková, B., Świderská, Z., Zita, L., Laloë, D., Charles, M., Beneš, V., Stopka, P., Vinkler, M., 2018. Domestic fowl breed variation in egg white protein expression: application of proteomics and transcriptomics. J. Agric. Food Chem. 66, 11854–11863. https://doi.org/10.1021/acs.jafc.8b03099.

Bluthé, R., Bret-Dibat, J., Layé, S., Walter, V., Parnet, P., Lestage, J., Verrier, D., Poole, S., Stenning, B., Kelley, K., 1994. Cytokines induce sickness behaviour by a vagal mediated mechanism. J. Neuroimmunol. 54, 160.

Borniger, J.C., Walker II, W.H., Gaudier-Diaz, M.M., Stegman, C.J., Zhang, N., Hollyfield, J.L., Nelson, R.J., DeVries, A.C., 2017. Time-of-day dictates transcriptional inflammatory responses to cytotoxic chemotherapy. Sci. Rep. 7, 1–11.

Bramley, J.C., Collins, S.V.A., Clark, K.B., Buchser, W.J., 2016. Avian axons undergo Wallerian degeneration after injury and stress. J. Comp. Physiol. 202, 813–822. https://doi.org/10.1007/s00359-016-1123-y.

Brant, J.O., Boatwright, J.L., Davenport, R., Sandoval, A.G.W., Maden, M., Barbazuk, W. B., 2019. Comparative transcriptomic analysis of dermal wound healing reveals de novo skeletal muscle regeneration in Acomys cahirinus. PLoS One 14, e0216228.

Brites, D., Fernandes, A., 2015. Neuroinflammation and depression: microglia activation, extracellular microvesicles and microRNA dysregulation. Front. Cell. Neurosci. 9 https://doi.org/10.3389/fncel.2015.00476.

Canchi, S., Swinton, M.K., Rissman, R.A., Fields, J.A., 2020. Transcriptomic analysis of brain tissues identifies a role for CCAAT enhancer binding protein β in HIV-associated neurocognitive disorder. J. Neuroinflammation 17, 112. https://doi.org/10.1186/s12974-020-01781-w.

Casebere, K.R., Kaiser, M.G., Lamont, S.J., 2015. Bacterial component induced inflammatory response in roosters from diverse genetic lines. Iowa State Univ. Anim. Ind. Rep. 12.

Cermelli, S., Zerega, B., Carlevaro, M., Gentili, C., Thorp, B., Farquharson, C., Cancedda, R., Descalzi Cancedda, F., 2000. Extracellular fatty acid binding protein (Ex-FABP) modulation by inflammatory agents: "physiological" acute phase response in endochondral bone formation. Eur. J. Cell Biol. 79, 155–164. https://doi.org/10.1078/S0171-9335(04)70018-7.

Chen, Y., Lyga, J., 2014. Brain-skin connection: stress, inflammation and skin aging. Inflamm. Allergy-Drug Targets Former. Curr. Drug Targets-Inflamm. AllergyDiscontinued 13, 177–190.

Corley, S.M., Troy, N.M., Bosco, A., Wilkins, M.R., 2019. QuantSeq. 3′ Sequencing combined with Salmon provides a fast, reliable approach for high throughput RNA expression analysis. Sci. Rep. 9, 18895 https://doi.org/10.1038/s41598-019-55434-x.

Crowell, H.L., Soneson, C., Germain, P.-L., Calini, D., Collin, L., Raposo, C., Malhotra, D., Robinson, M.D., 2020. Muscat detects subpopulation-specific state transitions from multi-sample multi-condition single-cell transcriptomics data. Nat. Commun. 11, 6077. https://doi.org/10.1038/s41467-020-19894-4.

Danielski, L.G., Giustina, A.D., Badawy, M., Barichello, T., Quevedo, J., Dal-Pizzol, F., Petronilho, F., 2018. Brain barrier breakdown as a cause and consequence of neuroinflammation in sepsis. Mol. Neurobiol. 55, 1045–1053. https://doi.org/10.1007/s12035-016-0356-7.

David, M., Cézilly, F., Giraldeau, L.-A., 2011. Personality affects zebra finch feeding success in a producer–scrounger game. Anim. Behav. 82, 61–67. https://doi.org/10.1016/j.anbehav.2011.03.025.

Deak, T., Bellamy, C., Bordner, K.A., 2005. Protracted Increases in Core Body Temperature and Interleukin-1 Following Acute Administration of Lipopolysaccharide: Implications for the Stress Response 12.

DiSabato, D.J., Quan, N., Godbout, J.P., 2016. Neuroinflammation: the devil is in the details. J. Neurochem. 139, 136–153. https://doi.org/10.1111/jnc.13607.

Divín, D., Goméz Samblas, M., Kuttiyarthu Veetil, N., Voukali, E., Świderská, Z., Krajzingrová, T., Těšický, M., Beneš, V., Elleder, D., Bartoš, O., Vinkler, M., 2022. Cannabinoid receptor 2 evolutionary gene loss makes parrots more susceptible to neuroinflammation. Proc. R. Soc. B Biol. Sci. 289, 20221941 https://doi.org/10.1098/rspb.2022.1941.

Dolédec, S., Chessel, D., 1994. Co-inertia analysis: an alternative method for studying species–environment relationships. Freshw. Biol. 31, 277–294.

Dray, S., Chessel, D., Thioulouse, J., 2003. CO-INERTIA analysis and the linking of ECOlogical data tables. Ecology 84, 3078–3089. https://doi.org/10.1890/03-0178.

Du, Y., Li, X.-S., Chen, L., Chen, G.-Y., Cheng, Y., 2020. A network analysis of epigenetic and transcriptional regulation in a neurodevelopmental rat model of schizophrenia with implications for translational research. Schizophr. Bull. 46, 612–622. https://doi.org/10.1093/schbul/sbz114.

Ehrlich, L.C., Hu, S., Sheng, W.S., Sutton, R.L., Rockswold, G.L., Peterson, P.K., Chao, C. C., 1998. Cytokine regulation of human microglial cell IL-8 production. J. Immunol. 160, 1944–1948.

Ekblom, R., Balakrishnan, C.N., Burke, T., Slate, J., 2010. Digital gene expression analysis of the zebra finch genome. BMC Genom. 11, 1–13.

Erickson, M.A., Dohi, K., Banks, W.A., 2012. Neuroinflammation: a common pathway in CNS diseases as mediated at the blood-brain barrier. Neuroimmunomodulation 19, 121–130. https://doi.org/10.1159/000330247.

Eskew, E.A., Fraser, D., Vonhof, M.J., Pinsky, M.L., Maslo, B., 2021. Host gene expression in wildlife disease: making sense of species-level responses. Mol. Ecol. 30, 6517–6530. https://doi.org/10.1111/mec.16172.

Etich, J., Koch, M., Wagener, R., Zaucke, F., Fabri, M., Brachvogel, B., 2019. Gene expression profiling of the extracellular matrix signature in macrophages of different activation status: relevance for skin wound healing. Int. J. Mol. Sci. 20, 5086. https://doi.org/10.3390/ijms20205086.

Finotello, F., Di Camillo, B., 2015. Measuring differential gene expression with RNA-seq: challenges and strategies for data analysis. Brief. Funct. Genomics 14, 130–142. https://doi.org/10.1093/bfgp/elu035.

Flores-Santin, J., Burggren, W.W., 2021. Beyond the chicken: alternative avian models for developmental physiological research. Front. Physiol. 12, 712633 https://doi.org/10.3389/fphys.2021.712633.

Forstmeier, W., Segelbacher, G., Mueller, J.C., Kempenaers, B., 2007. Genetic variation and differentiation in captive and wild zebra finches (*Taeniopygia guttata*): zebra FINCH population genetics. Mol. Ecol. 16, 4039–4050. https://doi.org/10.1111/j.1365-294X.2007.03444.x.

Friedrich, S.R., Nevue, A.A., Andrade, A.L., Velho, T.A., Mello, C.V., 2022. Emergence of sex-specific transcriptomes in a sexually dimorphic brain nucleus. Cell Rep. 40.

Ganta, V.C., Choi, M.H., Kutateladze, A., Fox, T.E., Farber, C.R., Annex, B.H., 2017. A MicroRNA93–interferon regulatory factor-9–immunoresponsive gene-1–itaconic acid pathway modulates M2-like macrophage polarization to revascularize ischemic muscle. Circulation 135, 2403–2425. https://doi.org/10.1161/CIRCULATIONAHA.116.025490.

Gasch, A.P., Payseur, B.A., Pool, J.E., 2016. The power of natural variation for model organism Biology. Trends Genet. 32, 147–154. https://doi.org/10.1016/j.tig.2015.12.003.
Ge, S.X., Jung, D., Yao, R., 2020. ShinyGO: a graphical gene-set enrichment tool for animals and plants. Bioinformatics 36, 2628–2629.
Guo, Q., Kawahata, I., Cheng, A., Jia, W., Wang, H., Fukunaga, K., 2022. Fatty acid-binding proteins: their roles in ischemic stroke and potential as drug targets. Int. J. Mol. Sci. 23, 9648. https://doi.org/10.3390/ijms23179648.
Hancock, R.E.W., Diamond, G., 2000. The role of cationic antimicrobial peptides in innate host defences. Trends Microbiol. 8, 402–410. https://doi.org/10.1016/S0966-842X(00)01823-0.
He, J., Fu, T., Zhang, L., Gao, L.W., Rensel, M., Remage-Healey, L., White, S.A., Gedman, G., Whitelegge, J., Xiao, X., 2022. Improved zebra finch brain transcriptome identifies novel proteins with sex differences. Gene 843, 146803.
Hellgren, O., Ekblom, R., 2010. Evolution of a cluster of innate immune genes (β-defensins) along the ancestral lines of chicken and zebra finch. Immunome Res. 6, 3. https://doi.org/10.1186/1745-7580-6-3.
Hernández-Romero, M.C., Delgado-Cortés, M.J., Sarmiento, M., de Pablos, R.M., Espinosa-Oliva, A.M., Argüelles, S., Bández, M.J., Villarán, R.F., Mauriño, R., Santiago, M., Venero, J.L., Herrera, A.J., Cano, J., Machado, A., 2012. Peripheral inflammation increases the deleterious effect of CNS inflammation on the nigrostriatal dopaminergic system. Neurotoxicology 33, 347–360. https://doi.org/10.1016/j.neuro.2012.01.018.
Hong, M., Tao, S., Zhang, L., Diao, L.-T., Huang, X., Huang, S., Xie, S.-J., Xiao, Z.-D., Zhang, H., 2020. RNA sequencing: new technologies and applications in cancer research. J. Hematol. Oncol.J Hematol Oncol 13, 1–16.
Howe, K.L., Achuthan, P., Allen, James, Allen, Jamie, Alvarez-Jarreta, J., Amode, M.R., Armean, I.M., Azov, A.G., Bennett, R., Bhai, J., Billis, K., Boddu, S., Charkhchi, M., Cummins, C., Da Rin Fioretto, L., Davidson, C., Dodiya, K., El Houdaigui, B., Fatima, R., Gall, A., Garcia Giron, C., Grego, T., Guijarro-Clarke, C., Haggerty, L., Hemrom, A., Hourlier, T., Izuogu, O.G., Juettemann, T., Kaikala, V., Kay, M., Lavidas, I., Le, T., Lemos, D., Gonzalez Martinez, J., Marugán, J.C., Maurel, T., McMahon, A.C., Mohanan, S., Moore, B., Muffato, M., Oheh, D.N., Paraschas, D., Parker, A., Parton, A., Prosovetskaia, I., Sakthivel, M.P., Salam, A.I.A., Schmitt, B.M., Schuilenburg, H., Sheppard, D., Steed, E., Szpak, M., Szuba, M., Taylor, K., Thormann, A., Threadgold, G., Walts, B., Winterbottom, A., Chakiachvili, M., Chaubal, A., De Silva, N., Flint, B., Frankish, A., Hunt, S.E., Iisley, G.R., Langridge, N., Loveland, J.E., Martin, F.J., Mudge, J.M., Morales, J., Perry, E., Ruffier, M., Tate, J., Thybert, D., Trevanion, S.J., Cunningham, F., Yates, A.D., Zerbino, D.R., Flicek, P., 2021. Ensembl 2021. Nucleic Acids Res. 49, D884–D891. https://doi.org/10.1093/nar/gkaa942.
Hunter, M., Spiller, K.J., Dominique, M.A., Xu, H., Hunter, F.W., Fang, T.C., Canter, R.G., Roberts, C.J., Ransohoff, R.M., Trojanowski, J.Q., Lee, V.M.-Y., 2021. Microglial transcriptome analysis in the rNLS8 mouse model of TDP-43 proteinopathy reveals discrete expression profiles associated with neurodegenerative progression and recovery. Acta Neuropathol. Commun. 9, 140. https://doi.org/10.1186/s40478-021-01239-x.
International Chicken Genome Sequencing Consortium, 2004. Sequence and comparative analysis of the chicken genome provide unique perspectives on vertebrate evolution. Nature 432, 695–716. https://doi.org/10.1038/nature03154.
Jarvis, S., Birsa, N., Secrier, M., Fratta, P., Plagnol, V., 2020. A comparison of low read depth QuantSeq 3′ sequencing to total RNA-seq in FUS mutant mice. Front. Genet. 11, 1412. https://doi.org/10.3389/fgene.2020.562445.
Kaneko, N., Kurata, M., Yamamoto, T., Morikawa, S., Masumoto, J., 2019. The role of interleukin-1 in general pathology. Inflamm. Regen. 39, 12. https://doi.org/10.1186/s41232-019-0101-5.
Kanthasamy, A.G., Rangaraju, S., 2020. Molecular signatures of neuroinflammation induced by αSynuclein aggregates in microglial cells. Front. Immunol. 11, 16.
Kempuraj, D., Thangavel, R., Selvakumar, G.P., Zaheer, S., Ahmed, M.E., Raikwar, S.P., Zahoor, H., Saeed, D., Natteru, P.A., Iyer, S., Zaheer, A., 2017. Brain and peripheral atypical inflammatory mediators potentiate neuroinflammation and neurodegeneration. Front. Cell. Neurosci. 11, 216. https://doi.org/10.3389/fncel.2017.00216.
Korpela, J., Kulomaa, M., Tuohimaa, P., Vaheri, A., 1982. Induction of avidin in chickens infected with the acute leukemia virus OK 10. Int. J. Cancer 30, 461–464.
Kumari, R., Fazekas, E.A., Morvai, B., Udvari, E.B., Dóra, F., Zachar, G., Székely, T., Pogány, Á., Dobolyi, Á., 2022. Transcriptomics of parental care in the hypothalamic–septal region of female zebra finch brain. Int. J. Mol. Sci. 23, 2518.
Kunnas, T.A., Wallén, M.J., Kulomaa, M.S., 1993. Induction of chicken avidin and related mRNAs after bacterial infection. Biochim. Biophys. Acta BBA - Gene Struct. Expr. 1216, 441–445. https://doi.org/10.1016/0167-4781(93)90012-3.
Kverková, K., Marhounová, L., Polonyiová, A., Kocourek, M., Zhang, Y., Olkowicz, S., Straková, B., Pavelková, Z., Vodička, R., Frynta, D., Němec, P., 2022. The evolution of brain neuron numbers in amniotes. Proc. Natl. Acad. Sci. USA 119, e2121624119. https://doi.org/10.1073/pnas.2121624119.
Lesur, I., Textoris, J., Loriod, B., Courbon, C., Garcia, S., Leone, M., Nguyen, C., 2010. Gene expression profiles characterize inflammation stages in the acute lung injury in mice. PLoS One 5, e11485.
Li, Y., Xu, Q., Zhang, T., Gao, M., Wang, Q., Han, Z., Shao, Y., Ma, D., Liu, S., 2015. Host avian beta-defensin and toll-like receptor responses of pigeons following infection with pigeon paramyxovirus type 1. Appl. Environ. Microbiol. 81, 6415–6424. https://doi.org/10.1128/AEM.01413-15.
Liu, S., Zhang, S., Sun, Y., Zhou, W., 2021. Transcriptomics changes in the peritoneum of mice with lipopolysaccharide-induced peritonitis. Int. J. Mol. Sci. 22, 13008 https://doi.org/10.3390/ijms222313008.
Liu, Z., Li, W., Geng, L., Sun, L., Wang, Q., Yu, Y., Yan, P., Liang, C., Ren, J., Song, M., 2022. Cross-species metabolomic analysis identifies uridine as a potent regeneration promoting factor. Cell Discov 8, 6.
Lopes, P., Wingfield, J., Bentley, G., 2012. Lipopolysaccharide injection induces rapid decrease of hypothalamic GnRH mRNA and peptide, but does not affect GnIH in zebra finches. Horm. Behav. 62, 173–179.
Lopez-Castejon, G., Brough, D., 2011. Understanding the mechanism of IL-1β secretion. Cytokine Growth Factor Rev. 22, 189–195.
Ma, F., Fuqua, B.K., Hasin, Y., Yukhtman, C., Vulpe, C.D., Lusis, A.J., Pellegrini, M., 2019. A comparison between whole transcript and 3' RNA sequencing methods using Kapa and Lexogen library preparation methods. BMC Genom. 20, 9. https://doi.org/10.1186/s12864-018-5393-3.
Martin, L.B., Han, P., Lewittes, J., Kuhlman, J.R., Klasing, K.C., Wikelski, M., 2006. Phytohemagglutinin-induced skin swelling in birds: histological support for a classic immunoecological technique. Funct. Ecol. 20, 290–299. https://doi.org/10.1111/j.1365-2435.2006.01094.x.
Mayerhofer, R., Fröhlich, E.E., Reichmann, F., Farzi, A., Kogelnik, N., Fröhlich, E., Sattler, W., Holzer, P., 2017. Diverse action of lipoteichoic acid and lipopolysaccharide on neuroinflammation, blood-brain barrier disruption, and anxiety in mice. Brain Behav. Immun. 60, 174–187. https://doi.org/10.1016/j.bbi.2016.10.011.
McDermott, A.M., 2004. Defensins and other antimicrobial peptides at the ocular surface. Ocul. Surf. 2, 229–247. https://doi.org/10.1016/S1542-0124(12)70111-8.
Mello, C.V., 2014. The zebra finch, *Taeniopygia guttata* : an avian model for investigating the neurobiological basis of vocal learning. Cold Spring Harb. Protoc. 2014, emo084574 https://doi.org/10.1101/pdb.emo084574 pdb.
Mesquita, G., Silva, T., Gomes, A.C., Oliveira, P.F., Alves, M.G., Fernandes, R., Almeida, A.A., Moreira, A.C., Gomes, M.S., 2020. H-Ferritin is essential for macrophages' capacity to store or detoxify exogenously added iron. Sci. Rep. 10, 3061. https://doi.org/10.1038/s41598-020-59898-0.
Mills, E.L., Ryan, D.G., Prag, H.A., Dikovskaya, D., Menon, D., Zaslona, Z., Jedrychowski, M.P., Costa, A.S.H., Higgins, M., Hams, E., Szpyt, J., Runtsch, M.C., King, M.S., McGouran, J.F., Fischer, R., Kessler, B.M., McGettrick, A.F., Hughes, M. M., Carroll, R.G., Booty, L.M., Knatko, E.V., Meakin, P.J., Ashford, M.L.J., Modis, L. K., Brunori, G., Sévin, D.C., Fallon, P.G., Caldwell, S.T., Kunji, E.R.S., Chouchani, E. T., Frezza, C., Dinkova-Kostova, A.T., Hartley, R.C., Murphy, M.P., O'Neill, L.A., 2018. Itaconate is an anti-inflammatory metabolite that activates Nrf2 via alkylation of KEAP1. Nature 556, 113–117. https://doi.org/10.1038/nature25986.
Minias, P., Vinkler, M., 2022. Selection balancing at innate immune genes: adaptive polymorphism maintenance in toll-like receptors. Mol. Biol. Evol. 39, msac102 https://doi.org/10.1093/molbev/msac102.
Mishra, I., Knerr, R.M., Stewart, A.A., Payette, W.I., Richter, M.M., Ashley, N.T., 2019. Light at night disrupts diel patterns of cytokine gene expression and endocrine profiles in zebra finch (Taeniopygia guttata). Sci. Rep. 9, 15833.
Moll, P., Ante, M., Seitz, A., Reda, T., 2014. QuantSeq 3′ mRNA sequencing for RNA quantification. Nat. Methods 11, i–iii. https://doi.org/10.1038/nmeth.f.376.
Oliveros, J.C., 2007. VENNY. An Interactive Tool for Comparing Lists with Venn Diagrams. https://bioinfogp.cnb.csic.es/tools/venny/index.html.
Olkowicz, S., Kocourek, M., Lučan, R.K., Porteš, M., Fitch, W.T., Herculano-Houzel, S., Němec, P., 2016. Birds have primate-like numbers of neurons in the forebrain. Proc. Natl. Acad. Sci. USA 113, 7255–7260. https://doi.org/10.1073/pnas.1517131113.
Ozsolak, F., Milos, P.M., 2011. RNA sequencing: advances, challenges and opportunities. Nat. Rev. Genet. 12, 87–98. https://doi.org/10.1038/nrg2934.
Painsipp, E., Herzog, H., Holzer, P., 2010. Evidence from knockout mice that neuropeptide-Y Y2 and Y4 receptor signalling prevents long-term depression-like behaviour caused by immune challenge. J. Psychopharmacol. 24, 1551–1560.
Paus, R., Theoharides, T.C., Arck, P.C., 2006. Neuroimmunoendocrine circuitry of the 'brain-skin connection. Trends Immunol. 27, 32–39.
Pedersen, A.L., Gould, C.J., Saldanha, C.J., 2017. Activation of the peripheral immune system regulates neuronal aromatase in the adult zebra finch brain. Sci. Rep. 7, 10191.
Peralta-Sánchez, J.M., Martín-Vivaldi, M., Martín-Platero, A.M., Martínez-Bueno, M., Oñate, M., Ruiz-Rodríguez, M., Soler, J.J., 2012. Avian life history traits influence eggshell bacterial loads: a comparative analysis. Ibis 154, 725–737. https://doi.org/10.1111/j.1474-919X.2012.01256.x.
Peters, E.M.J., Kuhlmei, A., Tobin, D.J., Müller-Röver, S., Klapp, B.F., Arck, P.C., 2005. Stress exposure modulates peptidergic innervation and degranulates mast cells in murine skin. Brain Behav. Immun. 19, 252–262.
Pfaffl, M.W., 2001. A new mathematical model for relative quantification in real-time RT–PCR. Nucleic Acids Res. 29 e45–e45.
Pfenning, A.R., Hara, E., Whitney, O., Rivas, M.V., Wang, R., Roulhac, P.L., Howard, J.T., Wirthlin, M., Lovell, P.V., Ganapathy, G., 2014. Convergent transcriptional specializations in the brains of humans and song-learning birds. Science 346, 1256846.
Poh, T.Y., Pease, J., Young, J.R., Bumstead, N., Kaiser, P., 2008. Re-evaluation of chicken CXCR1 determines the true gene structure: CXCLi1 (K60) and CXCLi2 (CAF/interleukin-8) are ligands for this receptor. J. Biol. Chem. 283, 16408–16415.
Poole, J., Kitchen, G.B., 2022. Circadian Regulation of Innate Immunity in Animals and Humans and Implications for Human Disease. Presented at the Seminars in Immunopathology. Springer, pp. 183–192.
Poplin, R., Ruano-Rubio, V., DePristo, M.A., Fennell, T.J., Carneiro, M.O., Van der Auwera, G.A., Kling, D.E., Gauthier, L.D., Levy-Moonshine, A., Roazen, D., Shakir, K., Thibault, J., Chandran, S., Whelan, C., Lek, M., Gabriel, S., Daly, M.J., Neale, B., MacArthur, D.G., Banks, E., 2017. Scaling accurate genetic variant discovery to tens of thousands of samples (preprint). Genomics. https://doi.org/10.1101/201178.

Pulido-Salgado, M., Vidal-Taboada, J.M., Barriga, G.G.-D., Solà, C., Saura, J., 2018. RNA-Seq transcriptomic profiling of primary murine microglia treated with LPS or LPS + IFNγ. Sci. Rep. 8, 16096 https://doi.org/10.1038/s41598-018-34412-9.

Ramsköld, D., Luo, S., Wang, Y.-C., Li, R., Deng, Q., Faridani, O.R., Daniels, G.A., Khrebtukova, I., Loring, J.F., Laurent, L.C., Schroth, G.P., Sandberg, R., 2012. Full-length mRNA-Seq from single-cell levels of RNA and individual circulating tumor cells. Nat. Biotechnol. 30, 777–782. https://doi.org/10.1038/nbt.2282.

Rankine, E.L., Hughes, P.M., Botham, M.S., Perry, V.H., Felton, L.M., 2006. Brain cytokine synthesis induced by an intraparenchymal injection of LPS is reduced in MCP-1-deficient mice prior to leucocyte recruitment. Eur. J. Neurosci. 24, 77–86. https://doi.org/10.1111/j.1460-9568.2006.04891.x.

Raudvere, U., Kolberg, L., Kuzmin, I., Arak, T., Adler, P., Peterson, H., Vilo, J., 2019. g: Profiler: a web server for functional enrichment analysis and conversions of gene lists (2019 update). Nucleic Acids Res. 47, W191–W198. https://doi.org/10.1093/nar/gkz369.

Romanov, M.N., Farré, M., Lithgow, P.E., Fowler, K.E., Skinner, B.M., O'Connor, R., Fonseka, G., Backström, N., Matsuda, Y., Nishida, C., Houde, P., Jarvis, E.D., Ellegren, H., Burt, D.W., Larkin, D.M., Griffin, D.K., 2014. Reconstruction of gross avian genome structure, organization and evolution suggests that the chicken lineage most closely resembles the dinosaur avian ancestor. BMC Genom. 15, 1060. https://doi.org/10.1186/1471-2164-15-1060.

Russell, J.J., Theriot, J.A., Sood, P., Marshall, W.F., Landweber, L.F., Fritz-Laylin, L., Polka, J.K., Oliferenko, S., Gerbich, T., Gladfelter, A., Umen, J., Bezanilla, M., Lancaster, M.A., He, S., Gibson, M.C., Goldstein, B., Tanaka, E.M., Hu, C.-K., Brunet, A., 2017. Non-model model organisms. BMC Biol. 15 (55) https://doi.org/10.1186/s12915-017-0391-5 s12915-017-0391–5.

Santiago-Quesada, F., Albano, N., Castillo-Guerrero, J.A., Fernández, G., González-Medina, E., Sánchez-Guzmán, J.M., 2015. Secondary phytohaemagglutinin (PHA) swelling response is a good indicator of T-cell-mediated immunity in free-living birds. Ibis 157, 767–773.

Satam, H., Joshi, K., Mangrolia, U., Waghoo, S., Zaidi, G., Rawool, S., Thakare, R.P., Banday, S., Mishra, A.K., Das, G., 2023. Next-generation sequencing technology: current trends and advancements. Biology 12, 997.

Scalf, C.S., Chariker, J.H., Rouchka, E.C., Ashley, N.T., 2019. Transcriptomic analysis of immune response to bacterial lipopolysaccharide in zebra finch (*Taeniopygia guttata*). BMC Genom. 20, 647. https://doi.org/10.1186/s12864-019-6016-3.

Scott, M.G., Hancock, R.E., 2000. Cationic antimicrobial peptides and their multifunctional role in the immune system. Crit. Rev. Immunol. 20, 407–31.

Seal, S., Dharmarajan, G., Khan, I., 2021. Evolution of pathogen tolerance and emerging infections: a missing experimental paradigm. Elife 10, e68874. https://doi.org/10.7554/eLife.68874.

Seok, J., Warren, H.S., Cuenca, A.G., Mindrinos, M.N., Baker, H.V., Xu, W., Richards, D. R., McDonald-Smith, G.P., Gao, H., Hennessy, L., 2013. Genomic responses in mouse models poorly mimic human inflammatory diseases. Proc. Natl. Acad. Sci. USA 110, 3507–3512.

Shaftel, S.S., Griffin, W.S.T., O'Banion, M.K., 2008. The role of interleukin-1 in neuroinflammation and Alzheimer disease: an evolving perspective. J. Neuroinflammation 5, 7. https://doi.org/10.1186/1742-2094-5-7.

Shahzad, A., Knapp, M., Lang, I., Köhler, G., 2010. Interleukin 8 (IL-8)-a universal biomarker? Int. Arch. Med. 3, 1–4.

Shi, S., Blumenthal, A., Hickey, C.M., Gandotra, S., Levy, D., Ehrt, S., 2005. Expression of many immunologically important genes in Mycobacterium tuberculosis-infected macrophages is independent of both TLR2 and TLR4 but dependent on IFN-αβ receptor and STAT11. J. Immunol. 175, 3318–3328. https://doi.org/10.4049/jimmunol.175.5.3318.

Sköld-Chiriac, S., Nord, A., Nilsson, J.-Å., Hasselquist, D., 2014. Physiological and behavioral responses to an acute-phase response in zebra finches: immediate and short-term effects. Physiol. Biochem. Zool. 87, 288–298.

Smedley, D., Haider, S., Durinck, S., Pandini, L., Provero, P., Allen, J., Arnaiz, O., Awedh, M.H., Baldock, R., Barbiera, G., Bardou, P., Beck, T., Blake, A., Bonierbale, M., Brookes, A.J., Bucci, G., Buetti, I., Burge, S., Cabau, C., Carlson, J.W., Chelala, C., Chrysostomou, C., Cittaro, D., Collin, O., Cordova, R., Cutts, R.J., Dassi, E., Genova, A.D., Djari, A., Esposito, A., Estrella, H., Eyras, E., Fernandez-Banet, J., Forbes, S., Free, R.C., Fujisawa, T., Gadaleta, E., Garcia-Manteiga, J.M., Goodstein, D., Gray, K., Guerra-Assunção, J.A., Haggarty, B., Han, D.-J., Han, B.W., Harris, T., Harshbarger, J., Hastings, R.K., Hayes, R.D., Hoede, C., Hu, S., Hu, Z.-L., Hutchins, L., Kan, Z., Kawaji, H., Keliet, A., Kerhornou, A., Kim, S., Kinsella, R., Klopp, C., Kong, L., Lawson, D., Lazarevic, D., Lee, J.-H., Letellier, T., Li, C.-Y., Lio, P., Liu, C.-J., Luo, J., Maass, A., Mariette, J., Maurel, T., Merella, S., Mohamed, A.M., Moreews, F., Nabihoudine, I., Ndegwa, N., Noirot, C., Perez-Llamas, C., Primig, M., Quattrone, A., Quesneville, H., Rambaldi, D., Reecy, J., Riba, M., Rosanoff, S., Saddiq, A.A., Salas, E., Sallou, O., Shepherd, R., Simon, R., Sperling, L., Spooner, W., Staines, D.M., Steinbach, D., Stone, K., Stupka, E., Teague, J.W., Dayem Ullah, A.Z., Wang, J., Ware, D., Wong-Erasmus, M., Youens-Clark, K., Zadissa, A., Zhang, S.-J., Kasprzyk, A., 2015. The BioMart community portal: an innovative alternative to large, centralized data repositories. Nucleic Acids Res. 43, W589–W598. https://doi.org/10.1093/nar/gkv350.

So, S.W., Fleming, K.M., Duffy, C.M., Nixon, J.P., Bernlohr, D.A., Butterick, T.A., 2022. Microglial FABP4-UCP2 Axis modulates neuroinflammation and cognitive decline in obese mice. Int. J. Mol. Sci. 23, 4354. https://doi.org/10.3390/ijms23084354.

Söllner, J.F., Leparc, G., Hildebrandt, T., Klein, H., Thomas, L., Stupka, E., Simon, E., 2017. An RNA-Seq atlas of gene expression in mouse and rat normal tissues. Sci. Data 4, 170185. https://doi.org/10.1038/sdata.2017.185.

Song, X., Li, M., Wu, W., Dang, W., Gao, Y., Bian, R., Bao, R., Hu, Y., Hong, D., Gu, J., Liu, Y., 2020. Regulation of BMP2K in AP2M1-mediated EGFR internalization during the development of gallbladder cancer. Signal Transduct. Targeted Ther. 5, 154. https://doi.org/10.1038/s41392-020-00250-3.

Sousa, C.S., Power, D.M., Guerreiro, P.M., Louro, B., Chen, L., Canário, A.V., 2022. Transcriptomic down-regulation of immune system components in barrier and hematopoietic tissues after lipopolysaccharide injection in antarctic notothenia coriiceps. Fishes 7, 171.

Spierings, M.J., ten Cate, C., 2016. Zebra finches as a model species to understand the roots of rhythm. Front. Neurosci. 10 https://doi.org/10.3389/fnins.2016.00345.

Sulakhiya, K., Keshavlal, G.P., Bezbaruah, B.B., Dwivedi, S., Gurjar, S.S., Munde, N., Jangra, A., Lahkar, M., Gogoi, R., 2016. Lipopolysaccharide induced anxiety- and depressive-like behaviour in mice are prevented by chronic pre-treatment of esculetin. Neurosci. Lett. 611, 106–111. https://doi.org/10.1016/j.neulet.2015.11.031.

Team, R.C., 2013. R: A Language and Environment for Statistical Computing.

Terenina, E., Sautron, V., Ydier, C., Bazovkina, D., Sevin-Pujol, A., Gress, L., Lippi, Y., Naylies, C., Billon, Y., Liaubet, L., Mormede, P., Villa-Vialaneix, N., 2017. Time course study of the response to LPS targeting the pig immune gene networks. BMC Genom. 18, 988. https://doi.org/10.1186/s12864-017-4363-5.

Těšický, M., Velová, H., Novotný, M., Kreisinger, J., Beneš, V., Vinkler, M., 2020. Positive selection and convergent evolution shape molecular phenotypic traits of innate immunity receptors in tits (Paridae). Mol. Ecol. 29, 3056–3070.

The UniProt Consortium, Bateman, A., Martin, M.-J., Orchard, S., Magrane, M., Agivetova, R., Ahmad, S., Alpi, E., Bowler-Barnett, E.H., Britto, R., Bursteinas, B., Bye-A-Jee, H., Coetzee, R., Cukura, A., Da Silva, A., Denny, P., Dogan, T., Ebenezer, T., Fan, J., Castro, L.G., Garmiri, P., Georghiou, G., Gonzales, L., Hatton-Ellis, E., Hussein, A., Ignatchenko, A., Insana, G., Ishtiaq, R., Jokinen, P., Joshi, V., Jyothi, D., Lock, A., Lopez, R., Luciani, A., Luo, J., Lussi, Y., MacDougall, A., Madeira, F., Mahmoudy, M., Menchi, M., Mishra, A., Moulang, K., Nightingale, A., Oliveira, C.S., Pundir, S., Qi, G., Raj, S., Rice, D., Lopez, M.R., Saidi, R., Sampson, J., Sawford, T., Speretta, E., Turner, E., Tyagi, N., Vasudev, P., Volynkin, V., Warner, K., Watkins, X., Zaru, R., Zellner, H., Bridge, A., Poux, S., Redaschi, N., Aimo, L., Argoud-Puy, G., Auchincloss, A., Axelsen, K., Bansal, P., Baratin, D., Blatter, M.-C., Bolleman, J., Boutet, E., Breuza, L., Casals-Casas, C., de Castro, E., Echioukh, K.C., Coudert, E., Cuche, B., Doche, M., Dornevil, D., Estreicher, A., Famiglietti, M.L., Feuermann, M., Gasteiger, E., Gehant, S., Gerritsen, V., Gos, A., Gruaz-Gumowski, N., Hinz, U., Hulo, C., Hyka-Nouspikel, N., Jungo, F., Keller, G., Kerhornou, A., Lara, V., Le Mercier, P., Lieberherr, D., Lombardot, T., Martin, X., Masson, P., Morgat, A., Neto, T.B., Paesano, S., Pedruzzi, I., Pilbout, S., Pourcel, L., Pozzato, M., Pruess, M., Rivoire, C., Sigrist, C., Sonesson, K., Stutz, A., Sundaram, S., Tognolli, M., Verbregue, L., Wu, C.H., Arighi, C.N., Arminski, L., Chen, C., Chen, Y., Garavelli, J.S., Huang, H., Laiho, K., McGarvey, P., Natale, D.A., Ross, K., Vinayaka, C.R., Wang, Q., Wang, Y., Yeh, L.-S., Zhang, J., Ruch, P., Teodoro, D., 2021. UniProt: the universal protein knowledgebase in 2021. Nucleic Acids Res 49, D480–D489. https://doi.org/10.1093/nar/gkaa1100.

Vance, D.D., 2014. Dynamic gene expression profile changes in synovial fluid following meniscal injury; osteoarthritis (OA) markers found. J. Exerc. Sports Orthop. 1 https://doi.org/10.15226/2374-6904/1/3/00115.

Vinkler, M., Bryjová, A., Albrecht, T., Bryja, J., 2009. Identification of the first Toll-like receptor gene in passerine birds: TLR4 orthologue in zebra finch (*Taeniopygia guttata*). Tissue Antigens 74, 32–41. https://doi.org/10.1111/j.1399-0039.2009.01273.x.

Vinkler, M., Bainová, H., Albrecht, T., 2010. Functional analysis of the skin-swelling response to phytohaemagglutinin. Funct. Ecol. 24, 1081–1086.

Vinkler, M., Schnitzer, J., Munclinger, P., Albrecht, T., 2012. Phytohaemagglutinin skin-swelling test in scarlet rosefinch males: low-quality birds respond more strongly. Anim. Behav. 83, 17–23.

Vinkler, M., Leon, A.E., Kirkpatrick, L., Dalloul, R.A., Hawley, D.M., 2018. Differing house finch cytokine expression responses to original and evolved isolates of mycoplasma gallisepticum. Front. Immunol. 9, 13. https://doi.org/10.3389/fimmu.2018.00013.

Vinkler, M., Adelman, J.S., Ardia, D.R., 2022. Chapter 20 - evolutionary and ecological immunology. In: Kaspers, B., Schat, K.A., Göbel, T.W., Vervelde, L. (Eds.), Avian Immunology, third ed. Academic Press, Boston, pp. 519–557. https://doi.org/10.1016/B978-0-12-818708-1.00008-7.

n.d. Vinkler, M., Fiddaman, S.R., Těšický, M., O'Connor, E.A., Savage, A.E., Lenz, T.L., Smith, A.L., Kaufman, J., Bolnick, D.I., Davies, C.S., Dedić, N., Flies, A.S., Gomez Samblás, M.M., Henschen, A.E., Novák, K., Palomar, G., Raven, N., Samaké, K., Slade, J., Kuttiyarthu Veetil, N., Voukali, E., Höglund, J., Richardson, D.S, Westerdahl, H., 2023. Understanding the evolution of immune genes in jawed vertebrates J. Evol. Biol. 36 (6), 847–873 https://doi.org/10.1111/jeb.14181.

Vo, T.T.M., Nguyen, T.V., Amoroso, G., Ventura, T., Elizur, A., 2021. Deploying new generation sequencing for the study of flesh color depletion in Atlantic Salmon (Salmo salar). BMC Genom. 22, 545. https://doi.org/10.1186/s12864-021-07884-9.

Wang, Z., Gerstein, M., Snyder, M., 2009. RNA-Seq: a revolutionary tool for transcriptomics. Nat. Rev. Genet. 10, 57–63. https://doi.org/10.1038/nrg2484.

Warren, W.C., Clayton, D.F., Ellegren, H., Arnold, A.P., Hillier, L.W., Künstner, A., Searle, S., White, S., Vilella, A.J., Fairley, S., Heger, A., Kong, L., Ponting, C.P., Jarvis, E.D., Mello, C.V., Minx, P., Lovell, P., Velho, T.A.F., Ferris, M., Balakrishnan, C.N., Sinha, S., Blatti, C., London, S.E., Li, Y., Lin, Y.-C., George, J., Sweedler, J., Southey, B., Gunaratne, P., Watson, M., Nam, K., Backström, N., Smeds, L., Nabholz, B., Itoh, Y., Whitney, O., Pfenning, A.R., Howard, J., Völker, M., Skinner, B.M., Griffin, D.K., Ye, L., McLaren, W.M., Flicek, P., Quesada, V., Velasco, G., Lopez-Otin, C., Puente, X.S., Olender, T., Lancet, D., Smit, A.F.A., Hubley, R., Konkel, M.K., Walker, J.A., Batzer, M.A., Gu, W., Pollock, D.D., Chen, L., Cheng, Z., Eichler, E.E., Stapley, J., Slate, J., Ekblom, R., Birkhead, T., Burke, T., Burt, D., Scharff, C., Adam, I., Richard, H., Sultan, M., Soldatov, A., Lehrach, H.,

Edwards, S.V., Yang, S.-P., Li, X., Graves, T., Fulton, L., Nelson, J., Chinwalla, A., Hou, S., Mardis, E.R., Wilson, R.K., 2010. The genome of a songbird. Nature 464, 757–762. https://doi.org/10.1038/nature08819.

Wegmann, M., Voegeli, B., Richner, H., 2015. Parasites suppress immune-enhancing effect of methionine in nestling great tits. Oecologia 177, 213–221. https://doi.org/10.1007/s00442-014-3138-9.

Wu, R., Kang, R., Tang, D., 2022. Mitochondrial ACOD1/IRG1 in Infection and Sterile Inflammation. J. Intensive Med. 2, 78–88. https://doi.org/10.1016/j.jointm.2022.01.001.

Yoshino, Y., Roy, B., Kumar, N., Shahid Mukhtar, M., Dwivedi, Y., 2021. Molecular pathology associated with altered synaptic transcriptome in the dorsolateral prefrontal cortex of depressed subjects. Transl. Psychiatry 11, 73. https://doi.org/10.1038/s41398-020-01159-9.

Zeng, J., Wang, Y., Luo, Z., Chang, L.-C., Yoo, J.S., Yan, H., Choi, Y., Xie, X., Deverman, B.E., Gradinaru, V., Gupton, S.L., Zlokovic, B.V., Zhao, Z., Jung, J.U., 2019. TRIM9-Mediated resolution of neuroinflammation confers neuroprotection upon ischemic stroke in mice. Cell Rep. 27, 549–560.e6. https://doi.org/10.1016/j.celrep.2018.12.055.

Zerega, B., Camardella, L., Cermelli, S., Sala, R., Cancedda, R., Descalzi Cancedda, F., 2001. Avidin expression during chick chondrocyte and myoblast development in vitro and in vivo: regulation of cell proliferation. J. Cell Sci. 114, 1473–1482.

Zheng, X., Levine, D., Shen, J., Gogarten, S.M., Laurie, C., Weir, B.S., 2012. A high-performance computing toolset for relatedness and principal component analysis of SNP data. Bioinformatics 28, 3326–3328. https://doi.org/10.1093/bioinformatics/bts606.

Zheng, D., Liwinski, T., Elinav, E., 2020. Interaction between microbiota and immunity in health and disease. Cell Res. 30, 492–506. https://doi.org/10.1038/s41422-020-0332-7.

PAPER V

Kuttiyarthu Veetil, Nithya, Amberleigh E. Henschen, Dana M. Hawley, **Balraj Melepat**, Rami A. Dalloul, Vladimír Beneš, James S. Adelman, and Michal Vinkler. "Varying conjunctival immune response adaptations of house finch populations to a rapidly evolving bacterial pathogen." Frontiers in Immunology 15 (2024): 1250818.

frontiers | Frontiers in Immunology

TYPE Original Research
PUBLISHED 02 February 2024
DOI 10.3389/fimmu.2024.1250818

OPEN ACCESS

EDITED BY
Ana Teles,
Max Planck Institute for Evolutionary Biology, Germany

REVIEWED BY
Magdalena Migalska,
Jagiellonian University, Poland
Molly Staley,
Loyola University Chicago, United States

*CORRESPONDENCE
Michal Vinkler
michal.vinkler@natur.cuni.cz

†These authors have contributed equally to this work

RECEIVED 30 June 2023
ACCEPTED 11 January 2024
PUBLISHED 02 February 2024

CITATION
Kuttiyarthu Veetil N, Henschen AE, Hawley DM, Melepat B, Dalloul RA, Beneš V, Adelman JS and Vinkler M (2024) Varying conjunctival immune response adaptations of house finch populations to a rapidly evolving bacterial pathogen.
Front. Immunol. 15:1250818.
doi: 10.3389/fimmu.2024.1250818

Varying conjunctival immune response adaptations of house finch populations to a rapidly evolving bacterial pathogen

Nithya Kuttiyarthu Veetil[1], Amberleigh E. Henschen[2], Dana M. Hawley[3], Balraj Melepat[1], Rami A. Dalloul[4], Vladimír Beneš[5], James S. Adelman[2†] and Michal Vinkler[1†*]

[1]Department of Zoology, Charles University, Faculty of Science, Prague, Czechia, [2]Department of Biological Sciences, The University of Memphis, Memphis, TN, United States, [3]Department of Biological Sciences, Virginia Tech, Blacksburg, VA, United States, [4]Department of Poultry Science, The University of Georgia, Athens, GA, United States, [5]European Molecular Biology Laboratory (EMBL), Genomics Core Facility, Heidelberg, Germany

Pathogen adaptations during host-pathogen co-evolution can cause the host balance between immunity and immunopathology to rapidly shift. However, little is known in natural disease systems about the immunological pathways optimised through the trade-off between immunity and self-damage. The evolutionary interaction between the conjunctival bacterial infection *Mycoplasma gallisepticum* (MG) and its avian host, the house finch (*Haemorhous mexicanus*), can provide insights into such adaptations in immune regulation. Here we use experimental infections to reveal immune variation in conjunctival tissue for house finches captured from four distinct populations differing in the length of their co-evolutionary histories with MG and their disease tolerance (defined as disease severity per pathogen load) in controlled infection studies. To differentiate contributions of host versus pathogen evolution, we compared house finch responses to one of two MG isolates: the original VA1994 isolate and a more evolutionarily derived one, VA2013. To identify differential gene expression involved in initiation of the immune response to MG, we performed 3'-end transcriptomic sequencing (QuantSeq) of samples from the infection site, conjunctiva, collected 3-days post-infection. In response to MG, we observed an increase in general pro-inflammatory signalling, as well as T-cell activation and IL17 pathway differentiation, associated with a decrease in the IL12/IL23 pathway signalling. The immune response was stronger in response to the evolutionarily derived MG isolate compared to the original one, consistent with known increases in MG virulence over time. The host populations differed namely in pre-activation immune gene expression, suggesting population-specific adaptations. Compared to other populations, finches from Virginia, which have the longest co-evolutionary history with MG, showed significantly higher expression of anti-inflammatory genes and Th1 mediators. This may explain the evolution of disease tolerance to MG infection in VA birds. We also show a potential modulating role

of BCL10, a positive B- and T-cell regulator activating the NFKB signalling. Our results illuminate potential mechanisms of house finch adaptation to MG-induced immunopathology, contributing to understanding of the host evolutionary responses to pathogen-driven shifts in immunity-immunopathology trade-offs.

KEYWORDS

adaptations diversifying populations, emerging disease, coevolution, parasite, host-pathogen interaction, inflammatory immune response, resistance, tolerance to infection

Introduction

Host-parasite co-evolution belongs among the most dynamic evolutionary phenomena (1). Novel adaptations rapidly shift pathogen virulence [i.e. pathogen damage to host fitness (2)] as well as host immune defence capacities. Given the frequent emergence of novel zoonotic infections transmitted to humans from wildlife, there is urgent need for improved understanding of the natural variation in both patterns and mechanisms of host-pathogen evolution (3, 4). Despite common expectation that long-term coevolution between hosts and their pathogens favours decrease in the pathogen virulence (1), present evidence suggests variation in these evolutionary patterns, with long-term increase in virulence observed in certain contexts (5). In response, hosts can rapidly adjust their resistance, i.e. evolve capacity to decrease pathogen replication, consistent with the arms-race model (1). Such adaptations have emerged, for example, in amphibians (6) and bats (7) challenged by fungal pathogens, or rabbits facing myxoma virus epidemics (8). However, if pathology caused by the excessive immune defence is too costly (9), the immunity-immunopathology trade-off can favour the evolution of tolerance to the infection instead of, or in addition to, resistance (10–12). Unlike resistance, tolerance mitigates the host's fitness loss through a reduction of tissue damage caused by infection or improved repair of this damage, without necessarily reducing pathogen replication. In contrast to resistance, evolution of tolerance to infection typically does not promote the arms race accelerating further increase in pathogen virulence (13, 14). However, if the increase in host's tolerance decreases immunopathology that favours pathogen transmission, pathogen can respond by evolving higher virulence (15, 16). This can further select on optimisation of the immune response, setting equilibrium between host immunity and immunopathology (9). Although recent research in different species of wild vertebrates (17–19) indicated that infection tolerance can be a common strategy to reduce the fitness costs in hosts facing novel pathogens, we still mostly lack evidence on the immunological mechanisms responsible for the shifts between resistance to tolerance in natural host-pathogen systems.

One of the few relevant vertebrate models for this investigation where we have evidence for tolerogenic adaptation (20) can be found in the recent evolutionary interaction between the bacterium *Mycoplasma gallisepticum* (MG) and its novel host, the house finch (*Haemorhous mexicanus*) (21). MG is a horizontally transmitted pathogen that shows high antigenic variation (22). Previously known to be a respiratory pathogen of domestic poultry (23), in 1994 MG was first detected in wild house finches in Virginia (eastern USA), causing mild to severe conjunctivitis (24). Within three years, the infection spread across eastern North American populations of the host and, after a few-year's lag, in the early 2000s the disease was detected in western North American house finch populations (25). Mycoplasmal conjunctivitis disease decreases survival of finches (26) in the wild, often causing severe decline (up to 60%) in affected house finch populations (27). However, the epizootic did not reach some isolated house finch populations, such as those introduced to the Hawaiian Islands which still remain naïve to MG. Further, because of the way that MG spread west across the northern part of the United States and then down the western coast, MG has only recently (or in some cases, never) been documented in host populations in areas of the southwest United States such as Arizona (28).

The house finch-MG model system is unique in avian evolutionary ecology given the precisely mapped spatiotemporal epizootic data and the wealth of pathogen isolates collected throughout time from various wild house finch populations that are presently available for infection experiments (29). This experimental research has shown that MG virulence has increased over time, with the evolutionarily original MG isolates (e.g. the isolate VA1994) causing milder disease than the more recent, evolutionarily derived isolates (e.g. the isolates NC2006 or VA2013) (30, 31). At the same time, there is inter-individual variability among hosts in their responses to the pathogen (32) and the host populations appear to have adapted to the MG selective pressure (33). We have recently shown that house finch populations with a longer co-evolutionary history with MG show more tolerance to the infection than the populations in recent or no contact with the pathogen (20), with tolerance quantified as milder

disease severity (i.e., conjunctivitis) at a given pathogen load. This is probably linked to regulation of the inflammatory response, which is less pronounced in the Harderian glands of house finch populations in longer contact with the pathogen, compared with populations with little or no contact with MG (20, 33).

Bacteria of the genus *Mycoplasma* are extracellular and intracellular parasites known in vertebrates to trigger excessive proinflammatory signalling (e.g. mediated by *IL1B* or *IL6*), while down-regulating regulatory signals with anti-inflammatory effects (e.g. *IL10*) (34). In humans, clinical manifestations of acute mycoplasmosis result from immunopathologic inflammation generated by the host, rather than by the direct pathogen-mediated tissue damage (35). Excessive inflammation may contribute to MG's ability to evade the host effector antibody response by disrupting regulation of the inflammation, improving pathogen transmission efficiency (36). In house finches, MG infection affects mainly the sites belonging to conjunctiva-associated lymphoid tissue, including conjunctiva and Harderian gland (37). Since its emergence in finches, MG appears to have evolved to trigger stronger pro-inflammatory cytokine levels in the host periocular lymphoid tissues, which is positively correlated with increased bacterial loads (37), disease severity (5), and pathogen spreadability (36). This promotes in the host an evolutionary trade-off between selection on stronger immunity to clear the pathogen infection, consistent with resistance, and constraint emerging from immunopathology, selecting on down-regulation of inflammation achieved through tolerance.

Transcriptomic analysis is an important approach to identify possible shifts in immune regulation of host-pathogen interactions. Previous studies using transcriptomics in house finches focused on gene expression changes in spleen, a secondary lymphoid tissue not topologically linked with the MG infection site where the primary direct contact between the host and the pathogen occurs (38, 39). Our previous RNA-seq transcriptomic research in the Harderian gland (20), a periocular secondary lymphoid tissue, has shown that 3 days post inoculation (DPI) with MG, house finches from more tolerant populations (those with a longer history of MG endemism) also showed reduced up-regulation of immune gene expression, notably among inflammation-regulating chemokines (20). Here we adopted the 3'-end transcriptomic QuantSeq approach to more closely explore the variation in immune regulation underlying the observed differences between the house finch populations in their tolerance to MG. Unlike the previously studied Harderian gland, conjunctiva is a lymphoid tissue directly exposed to the MG pathogen and thus the first tissue to be immunologically affected by the infection. Our objective was to describe the conjunctival immune response involved in directing the subsequent pathway regulation towards resistance or tolerance to MG. We used samples from the same birds for which Harderian gland tissues were analysed in Henschen et al. (20). MG-naïve house finch juveniles that were captured in one of four wild populations (Virginia = VA, Iowa = IA, Arizona = AZ and Hawaii = HI) were exposed to one of two MG isolates (original VA1994 or evolved VA2013) under controlled captive conditions. At the time of experimentation, the VA population had experienced the longest coevolution with MG (>20 years), the IA population only a slightly shorter co-evolution with MG than VA (~20 years (24);, while in AZ the MG epidemics are still relatively recent (0-5 years, with no detections in the population sampled (28);, and the HI population is likely entirely naïve to MG due to its geographic isolation (20). Differences between house finch populations in their co-evolutionary time with MG allowed us to track the variation in the immune responses associated with adaptation to the pathogen. The immune responses were assessed 3 DPI in order to describe the initial phase of the infection, during which innate immune regulation is being established at the infection site (37). Using differential gene expression (DGE) analysis, we first identified the immune pathways involved in response to MG and their differences between the four host populations (model 1). In our analysis, we focused namely on the variation in pro-inflammatory pathways that could promote resistance to MG and regulatory mechanisms that could increase tolerance to MG, indicating house finch adaptations to the pathogen. Second, we described differences between the four host populations in control individuals, where variation in baseline immune regulation can be identified (model 2). Third, we characterised differences in conjunctival immune responses associated with MG strain virulence (model 3).

Materials and methods

Experimental design and animals

Details of the experiment are provided in (20), so here we recapitulate it only briefly. Hatch-year house finches (identified as first-year based on plumage characteristics) were captured using mist nets and feeder traps (40) between June and September 2018 in Blacksburg, Virginia (VA), Ames, Iowa (IA), Tempe, Arizona (AZ) and Oahu, Hawaii (HI) (details provided in Supplementary Table S1, Electronic Supplementary Material 1, ESM1 and map displaying the details of sample collection is shown in Supplementary Figure 1, Supplementary Figure S1 in ESM2). Any finches that showed clinical signs of MG infection during capture were immediately released. Following capture, each bird received a uniquely numbered aluminium leg band, and an electronic balance was used to determine its mass. To eliminate ectoparasites, the birds were all dusted with 5% sevin powder. The trapped birds were brought to the Iowa State University animal facility. After arrival, all birds were subjected to an acclimation and quarantine period (minimum of 40 days), which included treatment with prophylactic medications to prevent naturally occurring infections. A serological assay was run on blood collected approximately two weeks post-capture to ensure that all birds used in experiments were seronegative for MG infection (20).

Birds were kept individually in medium flight cages (76 cm x 46 cm x 46 cm) for the duration of the experiment and were provided *ad libitum* access to water and food. The diet consisted of a 20:80 mixture of black oil sunflower seeds and pellets (Roudybush Maintenance Nibles; Roudybush, Inc., Woodland, CA). Temperatures (~22°C) and light-dark cycles (12h:12h) were kept constant.

The infection experiment was performed in October 2018 on a sample of 60 individuals representing the four different house finch

populations (VA, IA, AZ, HI). For each population, 5 individuals served as controls (C) treated with Frey's media with 15% swine serum alone, 5 were treatment individuals inoculated with the original MG isolate VA1994, and 5 were inoculated with the evolved MG isolate VA2013 (in both treatments the MG dose was 7.5×10^6 colour changing units, CCU/mL) following the same methodology as in (5, 41). Three days post-infection (3 DPI), the birds were euthanised by rapid decapitation and a panel of nine tissues were collected. All tissues were submerged into RNA later protectant within 15 minutes of euthanasia and immediately refrigerated at 4°C. The cooled periocular conjunctiva-associated lymphoid tissue (conjunctiva and nictitating membrane) samples were transported within 48 hours to Charles University, Czech Republic, where they were kept frozen to -80°C until further processing.

RNA extraction and sequencing

Our conjunctival samples contained both the conjunctiva-associated lymphoid tissue (CALT) and skin of the eye lid. For ensuring the proper RNA extraction of the lymphoid tissue, we used the following protocol. All conjunctival samples from the 60 birds were homogenized using PCR-clean beaded tubes (OMNI International, USA - Serial Number: 2150600) using the MagNa Lyser (Roche, Basel, Switzerland). The skin tissues present in the samples were separated during the centrifugation step and discarded, while the homogenised lymphoid tissue was used for the total RNA extraction with the High Pure RNA Tissue Kit (Roche, Basel, Switzerland). We used Nanodrop (NanoDrop ND-1000) and Agilent 2100 Bioanalyzer with nano chip (Agilent Technologies, California, USA) to calculate the RNA yield (in all cases >20 ng/ul) and integrity (in all cases RIN values >7) (details provided in Supplementary Table S2, ESM1).

To perform sufficiently deep transcriptomic sequencing in a representative sample of individuals with different treatments across four populations, we adopted the 3'-end transcriptomic QuantSeq approach, which is more cost-efficient in larger population samples than the classical RNA-seq ((42–44); Kuttiyarthu Veetil et al. in prep.). The library preparation and sequencing were performed at the European Molecular Biology Laboratory (EMBL), Heidelberg, Germany. All the samples were first barcoded with Illumina TruSeq adapters (45). The QuantSeq libraries were prepared using Lexogen QuantSeq 3'-polyadenylated RNA Library Prep Kit FWD (Illumina). The sequencing was carried out using the Illumina NextSeq 500 platform. QuantSeq is based on a protocol devoid of mRNAs fragmentation before reverse transcription (46), but the read fragment sequencing targets are generated close to the polyadenylated 3′ end. This method uses total RNA as an input and there is no prior poly(A) enrichment or rRNA depletion. QuantSeq generates only one read fragment per transcript, and the number of reads mapped to a given gene is, therefore, proportional to its expression (42). Eight samples failed during library preparation and were excluded from the sequencing. The rest of the 52 indexed samples were pooled together and single-end 80 bp reads were generated. Thus, the final analysis is based on the sequence data representing conjunctival samples from 52 birds (details on the birds provided in Supplementary Table S3, ESM1).

Transcriptomes

On average, we obtained ~10 million reads per sample, comparable to zebra finch 3'-end transcriptomic sequencing. The bioinformatic analysis was carried out using BAQCOM pipeline (https://github.com/hanielcedraz/BAQCOM). The samples were aligned to the zebra finch genome downloaded from Ensembl (47) (bTaeGut1_v1.p-GCA_003957565.1). The tools included Trimmomatic (version 0.39) (48) for the adapter trimming, STAR software (49) for the aligning with the reference and feature Counts from the Subread package (50) for assigning of the sequences and gene level quantification. The alignment percentage of the conjunctiva samples to the reference genome ranged between 52.42% to 80.62% (Supplementary Table S4, ESM1). Next, the DGE analysis was performed using the limma (Linear Models for Microarray Data) package (51) in R (version- version 4.1.1) (52). In this analysis, we considered the source population, sex, and MG treatment as fixed factors, testing them together with their interactions at the significance level of padj value ≤ 0.05 and a minimum log2fold change value ≥1. After the differential gene expression analysis, each gene in each transcriptome was annotated. Ensembl BioMart (47) was used to assign gene functional annotations (geneontology, GO), which were then manually supplemented with Uniprot annotations. In cases where gene names were not directly available, an orthologue search was performed (Ensembl and NCBI Blast) for human annotations and gene names were selected if the closest hit showed at least 60% sequence identity. We used ShinyGO (version-0.77) (53) for generating the figures for pathway analysis and using Venn (https://bioinformatics.psb.ugent.be/webtools/Venn/) to create the venn diagrams. The transcriptomic sequenced data were submitted to the NCBI Sequence Read Archive. As an alternative, guided by our research question, literature search (54) and previous results (33), we selected the following target cytokine and receptor genes potentially involved in regulation of the house finch immune interaction with MG: *IL1B, IL10, IL6, CXCL8, IL22, TNFSF15, TLR4, TLR3, TLR2, ACOD1, CSF1R, CCL4, IL18*, and *TLR7* (selected based on literature search and 3' end annotation availability; Supplementary Table S11, ESM1).

Statistical analysis

To identify potential transcriptomic groupings of our four populations, we first performed two Between group analyses (BGA) using made4 package in R (55). In the first analysis, we used the individual population identities as a grouping factor, while for the second analysis we adopted the distinction between eastern populations (VA and IA), which share a long co-evolutionary history with MG, and western (AZ and HI) populations which share a short (0-5 year) co-evolutionary history with MG, as applied in our previous research (20). BGA targets the between-group

variability by executing a principal component analysis (PCA) on group means.

Next, we adopted three different methodological strategies to reveal the transcriptomic variation between the house finch populations and the two MG isolates using limma package from R. Limma employs moderated t-statistics to assess differences in expression of individual genes across the transcriptome. It allows to design multiple-factor matrices (e.g., different time points, experimental conditions, batch effects) and covariates, from which it calculates the differential gene expression by accounting for all the variables. Limma generates a full list of genes with associated p-values and false discovery rate (FDR) for each gene, indicating the result reliability (51).

First, to reveal population-specific variation in immune responses to MG among the four house finch populations, in the whole dataset we tested the following linear model, considering population of origin, sex, MG treatment and the interaction between population and MG treatment as explanatory variables (model 1):

$$(\sim \text{Population} + \text{Sex} + \text{MG\_treatment} + \text{Population}:\text{MG\_treatment} + \text{MG\_treatment}:\text{Sex})$$

The target-gene analysis was performed only using the whole dataset. To normalize the target gene expression data, we first divided the total number of reference-aligned reads by the total number of reads in the sample (Cn). To scale the data, we then multiplied each of the normalized read counts by 10 million (approx. 10 million was the average number of reads per sample in our dataset). Given large number of zero expression levels detected, we could not make relative quantification of the expression and, therefore, the variation in gene expression is shown as a logarithm of the scaled-normalized read counts, with uniform scaling across all genes. These gene expression levels were visualised using heatmap: pheatmap package in R.

Since the results of model 1 indicated limited Population : MG_treatment interactions, but revealed main effects of the populations, to understand the pre-existing variation in gene expression among those populations we then run a second linear model, where in the control individuals alone we tested the parameters of population, sex and their interaction (model 2):

$$(\sim \text{Population} + \text{Sex} + \text{Population}:\text{Sex})$$

Third, to reveal the differences in immunity activation caused by the two MG isolates used (the original VA1994 vs. evolved VA2013), we finally separately analysed the DGE in the VA2013 treatments compared to the controls, and in the VA1994 treatments compared to the controls, later contrasting the two sets of results (model 3):

$$(\sim \text{Population} + \text{MG\_treatment} + \text{Population}:\text{MG\_treatment})$$

Results

First, to identify general transcriptomic similarities between birds from different populations, we performed the between-group analyses (BGA) comparing individual populations and their western and eastern sets. These did not reveal any clear grouping of the individuals based on their transcriptomic profiles (P>0.05; Supplementary Figures S2, S3, ESM2). To investigate variation among house finch populations in their responsiveness to MG infection, we first performed a general analysis on the whole dataset (model 1). In total we identified 1228 DEGs (Figure 1; Table 1; heatmap is provided in Supplementary Figure S4, ESM2). Among

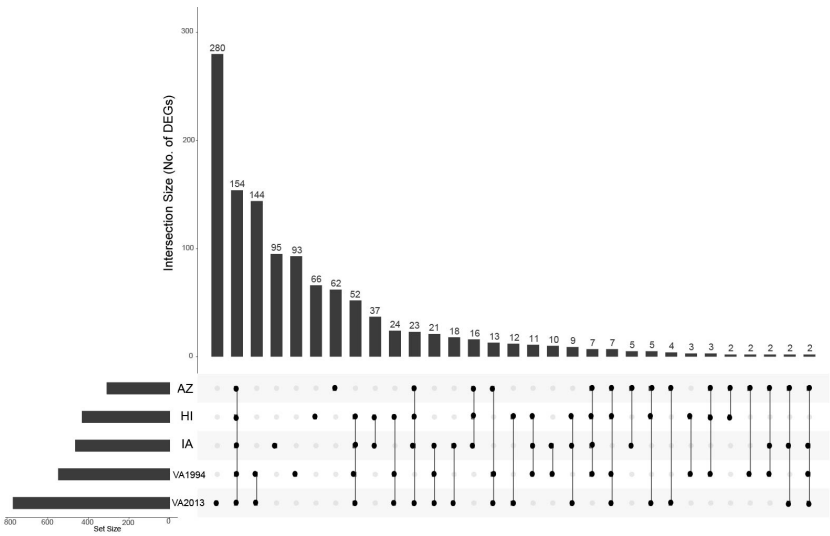

FIGURE 1
UpSet plot depicting the common differentially expressed genes in conjunctival tissue across the investigated house finch populations and the *Mycoplasma gallisepticum* (MG) treatments. The house finch populations namely, Arizona (AZ), Iowa (IA) and Hawaii (HI) are compared with the Virginia (VA) population, the MG treatments (VA1994 and VA2013) are compared with the controls. The gene set size is represented by the bar height, and the population-treatment interaction by the lines connecting the main category dots.

TABLE 1 Results of the general differential gene expression (DGE) analysis for conjunctival tissue collected 3 days post inoculation with *Mycoplasma gallisepticum* (MG) treatment (model 1).

Factors	Total DEG	Total Up	Total Down	Immune DEG	Immune Up	Immune Down
AZ	309	141	168	17	15	2
HI	431	151	280	29	24	5
IA	464	131	333	18	15	3
VA1994	548	310	238	76	71	5
VA2013	772	444	328	91	81	10
AZ : VA1994	5	0	5	0	0	0
AZ : VA2013	1	0	1	0	0	0
HI : VA1994	6	2	4	2	0	2
HI : VA2013	2	0	2	1	0	1
IA : VA1994	1	0	1	1	0	1
IA : VA2013	0	0	0	0	0	0
SEX	23	15	8	0	0	0
VA1994:SEX	0	0	0	0	0	0
VA2013:SEX	0	0	0	0	0	0

The table shows the total numbers of differentially expressed genes (Total DEG) and the total numbers of differentially expressed immune genes (Immune DEG) across different comparisons as well as numbers of up-regulated (Up) and down-regulated (Down) genes for the two infection treatments (VA1994 and VA2013) compared to controls and the populations Arizona (AZ), Hawaii (HI) and Iowa (IA) when compared to the Virginia (VA) population, including interactions.

the 23 genes which were differentially expressed between sexes, none showed any interaction with the MG treatment, and none were involved in immunity, indicating no sex-specific variation in immune responses to MG in the conjunctival gene expression. Therefore, sex effects were not further considered in our analysis.

Regardless of the MG treatment status, compared to the VA population, most DEGs were observed in the IA population (464), indicating baseline differences between these two populations in conjunctival gene expression. Though high number of DEGs were detected between both the MG treatments and controls (548 for VA1994 and 772 for VA2013), there was little interaction between MG treatment and house finch population origin (Table 1). To indicate the overlaps between the populations and MG treatments, we provide the UpSet plot in Figure 1. Among the 154 genes on the overlap of all groups, the majority of the genes were lacking any annotations (representing novel transcripts) and there were no genes annotated with any immune function.

While we identified in total 900 DEGs related to MG infection (across all population, combining VA1994 and VA2013, with the main effects and interactions), only 793 were annotated (Supplementary Table S5, ESM1), and among those we identified 113 DEGs involved in immunity (Supplementary Table S6, ESM1). There were 158 annotated DEGs down-regulated in their expression during MG infection. For example, *CHRNB2*, *ATP2B1*, *SCN2A*, *RYR2*, *NKAIN1* and *CACNA1C* are important for the ion transport [GO:0006811], synaptic signalling [GO:0032225] and response to muscle activity [GO:0014850] (Supplementary Figure S5, ESM2). Only 11 out of the 158 down-regulated genes showed clear links to immunity, including *IL12B* and *RAG1* that are involved in Th1/Th17 immune response activation [GO:0032735, GO:0032740], positive regulation of T cell differentiation [GO:0045582], pre-B cell allelic exclusion [GO:0002331] and adaptive immune response [GO:0002250]. Among the 457 annotated DEGs up-regulated during MG infection, we were able to identify 91 genes with immune function. In the MG-treated individuals, we observed increased expression of, e.g. *IL17RA* and *IL17RE* involved in inflammatory response [GO:0050729], regulation through IL17-mediated signalling pathway [GO:0097400], *CXCL12* involved in defence response [GO:0006952], *TLR1B* activating toll-like receptor TLR6:TLR2 signaling pathway [GO:0038124], a leukocyte marker *PTPRC* (*CD45*) regulating T cell proliferation [GO:0042102], *ACOD1* involved in positive regulation of antimicrobial humoral response [GO:0002760] and negative regulation of the inflammatory responses (56), and *CD74* involved in antigen processing and presentation [GO:0019882]. The main pathways in which the genes were up-regulated during MG infection are shown in Figure 2. Interestingly, while not statistically significant, *IL22* gene that plays a critical role in modulating tissue responses during inflammation [GO:0005125, GO:0006954], was found to be close to significance with increased expression in the birds treated with the VA2013 isolate (padj cut-off value = 0.07).

There were few genes for which we detected significant interactions between population and MG treatment (Supplementary Table S7, ESM1). Out of these, only 3 genes were involved in immune regulation. *BCL10* (positive regulation of interleukin-6 production [GO:0032755]; positive regulation of interleukin-8 production [GO:0032757], positive regulation of NFKB transcription factor activity [GO:0051092]; having roles in both innate immune response [GO:0045087] and adaptive immune

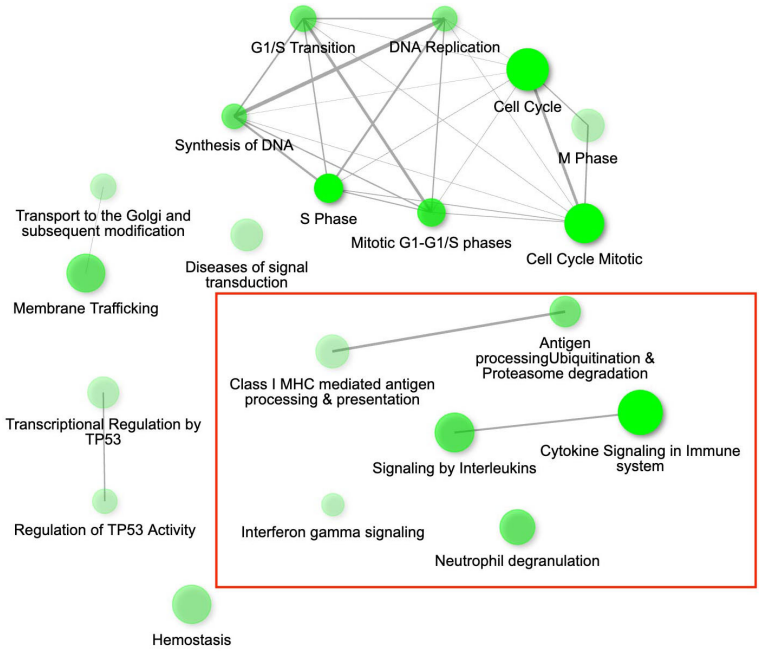

FIGURE 2
The gene interaction network for the differentially expressed genes (DEGs) up-regulated in conjunctival tissue 3 days post inoculation (DPI) with *Mycoplasma gallisepticum* (infected vs. non-infected birds across all house finch populations), showing the most significant pathways in the GO category Biological process. Immune genes grouped in the pathways of our interest are highlighted with red rectangles. Node colour intensity indicates significance of gene enrichment, node size indicates number of significant DEGs.

response [GO:0002250]) was significantly differentially expressed in interaction between both HI and IA population and treatment with the MG isolate VA1994. During MG infection, *BCL10* was down-regulated in these populations. *CNN2* (actomyosin structure organization [GO:0031032]) and *TRIM13* (innate immune response [GO:0045087]; positive regulation of cell death [GO:0010942]) were detected differentially expressed in interaction between HI population and VA1994.

In the same analysis, a large number of DEGs were revealed between different house finch populations, regardless of the MG infection. In AZ birds, out of the 309 DEGs identified (Supplementary Table S8, ESM1) we were able to annotate 106 genes with expression higher and 35 genes with expression lower than in the VA population. There were 17 genes with immune-related functions, out of which 15 genes showed higher expression in AZ than in VA, including e.g., *BCL10*, *IL17D* involved in positive regulation of interleukin-8 production [GO:0032757] and *CASP6* involved in activation of innate immune response [GO:0002218]. The main immune gene with lower expression in AZ versus VA birds was *NR1H4* involved in negative regulation of IL1 [GO:0032692] production and inflammatory response [GO:0050728]. For HI birds, we found 431 DEGs, out of which 130 annotated genes had higher and 81 genes lower expression than in the VA population (Supplementary Table S9, ESM1). There were 28 genes linked with immune functions, again most of them (23 genes) having higher expression in HI than in the VA population. Like in AZ, these genes included *BCL10* and *CASP6*, but also *MAST2* involved in negative regulation of IL12 production [GO:0032655]. The immune genes with lower expression in HI relative to VA were *NR1H4*, *RAG1* and *KPNA6* involved in positive regulation of cytokine production involved in inflammatory response [GO:1900017]. In the IA population we found as many as 464 DEGs compared to the VA population (Supplementary Table S10, ESM1), among which 114 annotated genes showed higher expression and 80 genes lower expression than in the VA population. Among the 17 genes annotated with immune function, 15 (including again *BCL10* and *CASP6*, and *TRIM13*) had higher expression and two genes (*RAG1* and *NR1H4*) lower expression in IA than in VA. Thus, our results indicate that there is important variation between the house finch populations in immune gene expression in conjunctival tissue that is independent of the actual MG treatment (no significant effect of the interaction between the MG treatment and population).

As an alternative approach, we also checked for the relative DGE changes in selected key immune genes with regulatory roles in immunity (target-gene analysis; Supplementary Table S11, ESM1) between the control and treatment groups of birds from different populations. Our results (statistics provided in Supplementary Table S12, ESM1) find that *IL1B, IL6*, *IL10*, *IL12B*, *IL17D*, *IL18*, *IL22*, *CXCL8*, *CCL4*, *ACOD1*, *TLR1*, *TLR4* and *TLR7* show clear distinction between the controls and the MG treatment groups (Figure 3), and at the same time *CCL4*, *TLR1*, *TLR4*, *TLR7* show also significant variation in expression between the populations. In *TLR1*, we even detected significant interaction between the MG treatment and population (AZ, HI) indicating differences in DGE between the populations in response to MG infection.

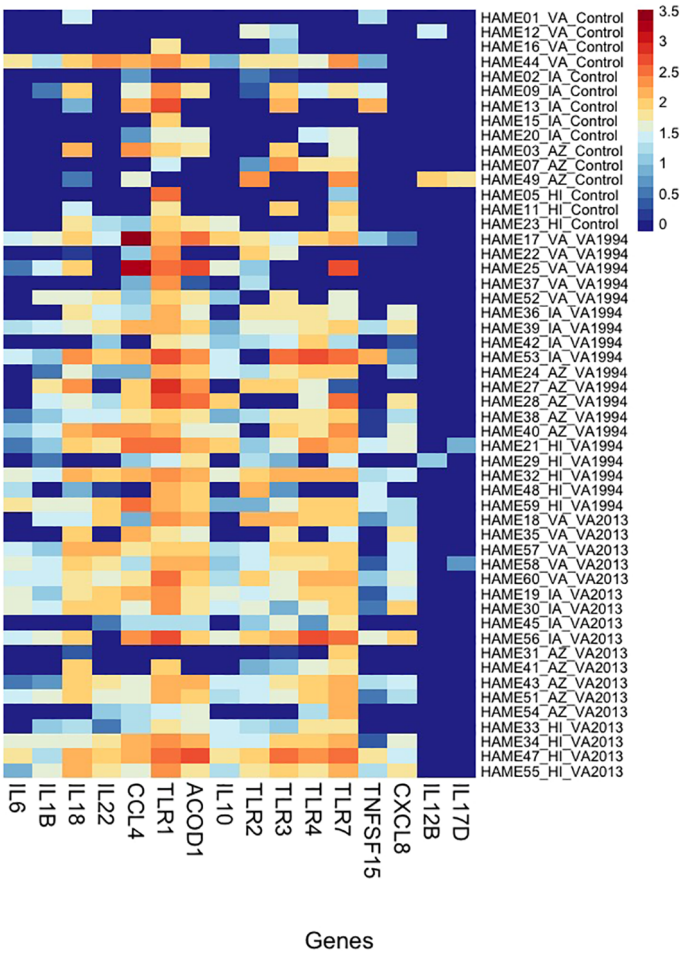

FIGURE 3
Heatmap showing variation in gene expression in selected inflammation-regulating genes (cytokines and receptors) in conjunctiva across house finches from four different populations belonging to two types of *Mycoplasma gallisepticum* (MG)-infected treatments (VA1994 and VA2013) and controls. Y-axis provides the information on individual birds (including population name and treatment group); X-axis shows the gene names; colour indicates the gene expression levels shown as a logarithm of the scaled-normalized read count varying from low expression (dark blue) to high expression (red). Please note that the scaling is not relative and, therefore, the colour pattern is common to all genes (highly as well as lowly expressed).

Immune genes differentially expressed between populations in the unstimulated controls

Since the differences between the house finch populations in expression of immune genes were largely independent of MG infection status, indicating potential population-specific adaptations to MG, we also checked for differences in immune regulation in the unstimulated control individuals across populations (model 2). Our analysis showed 748 DEGs in the control individuals, with 71 genes (out of the 498 genes with defined annotations) being involved in immunity (Table 2).

The lists of genes with lower expression in AZ, IA and HI populations compared to the VA population (Supplementary Table S13, ESM1) were mostly consistent (Supplementary Figure S6, ESM2), indicating generally increased expression of the genes in

TABLE 2 Results of the general differential gene expression (DGE) analysis in conjunctival tissue of control individuals (model 2).

Factors	Total DEG	Total Up	Total Down	Immune DEG	Immune Up	Immune Down
AZ	342	152	190	40	18	22
HI	270	55	215	31	8	23
IA	281	63	218	39	11	28

The table shows the total numbers of differentially expressed genes (Total DEG) and the total numbers of differentially expressed immune genes (Immune DEG) across the Arizona (AZ), Iowa (IA) and Hawaii (HI) and Virginia (VA) populations. Up = up-regulated (increased expression) in the tested population compared to VA, Down = down-regulated (decreased expression) in the tested population compared to the VA population.

the VA birds: out of the 31 DEGs with immune function, 19 were shared between AZ, IA and HI birds. Notably, these included *LIF* (having role in regulation of immune response [GO:0050776] and anti-inflammatory properties; (57)], *IL12B* and *IL7* [positive regulation of T cell differentiation [GO:0045582] and cytokine-mediated signaling pathway [GO:0001961]). Among the 184 genes (Supplementary Table S14, ESM1) that were consistently expressed at higher levels in other populations compared to VA, 35 genes (Supplementary Table S15, ESM1) were shared between the AZ, HI and IA, indicating decreased expression in the VA population. There were 25 DEGs annotated with immune function which had higher expression across these three populations when compared to VA birds. Out of them, however, only 4 genes were shared: *BCL10*, *GGT5* (role in inflammatory response [GO:0006954]), *RABGEF1* (negative regulation of inflammatory response [GO:0050728]) and *SYNCRIP* (cellular response to interferon-gamma [GO:0071346]) (Figure 4).

The main uniquely up-regulated immune genes (18 genes) in the AZ population included *IL17D, IL17C* (inflammatory response [GO:0006954]), *IRF6* (immune system process [GO:0002376]), *TLR15* (toll-like receptor signaling pathway [GO:0002224]) and *TLR1B* genes (up-regulated and down-regulated pathways are shown in Supplementary Figures S7, S8, ESM2). In contrast to AZ, the HI and IA populations (up-regulated and down-regulated pathways for IA and HI birds, respectively, are shown in Supplementary Figures S9–S12, ESM2) showed almost identical sets of DEGs in the control birds: out of a total of 40 DEGs with immune function revealed in these populations, 28 genes were shared between these two populations, including *TRIM13, PPARD* (negative regulation of inflammatory response [GO:0050728]) and *BCAR1* (antigen receptor-mediated signaling pathway [GO:0050851]) that were different from the AZ population. These genes are involved in immune pathways involved in cytokine production by mast cells and B cells.

Immune genes differentially expressed between individuals inoculated with different MG isolates

Our third analysis (model 3) showed only 160 DEGs for the MG VA1994 isolate, but 1229 DEGs for the VA2013 isolate (Table 3). Considering only the genes with annotations related to immune function, there were 54 genes differentially expressed during the infection with VA1994 and 230 genes during the infection with VA2013. In birds infected with VA1994, all the differentially expressed immune genes showed higher expression when compared to control birds. In birds infected with VA2013, there were 191 genes with higher expression and 39 genes with lower expression when compared to the controls (full list of the genes is provided in Supplementary Tables S16, S17, ESM1).

Since the DEGs common to infections with both isolates are consistent with those already discussed in the first analysis (model 1), here we focus only on the differences between the isolates. We found 20 specific genes differentially expressed on 3 DPI after inoculation with the VA1994 isolate, out of which only two genes were related with any defined immune functions: *NFATC3* and *PTAFR*, both involved in inflammation [GO:0006954] (Figure 5). For VA1994, there were no genes showing any significant interaction with the populations. The up-regulated and down-regulated gene interaction network for MG isolate VA1994 is shown in Figures S13, S14, ESM2.

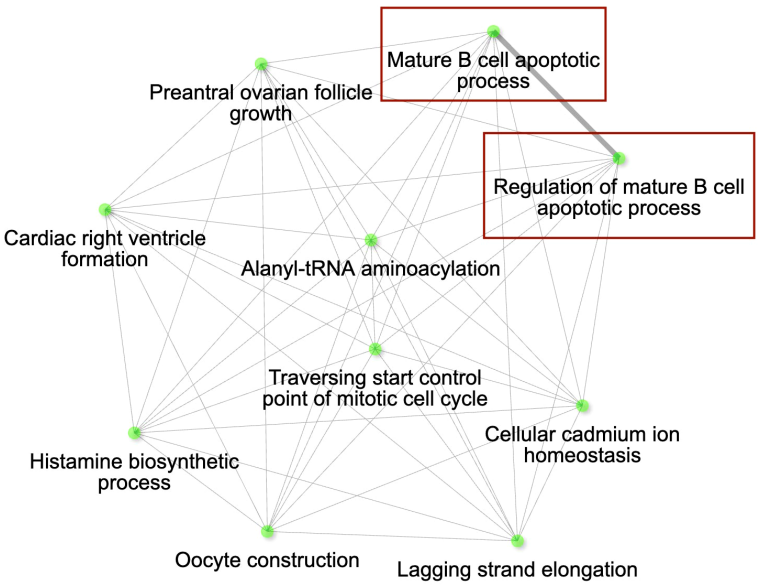

FIGURE 4
The gene interaction network for the differentially expressed genes (DEGs) with higher expression in conjunctiva of control birds in Iowa (IA), Arizona (AZ) and Hawaii (HI) compared to Virginia (VA). The most significant pathways in the GO category Biological process are shown. Immune genes grouped in the pathways of our interest are highlighted with red rectangles. Node colour intensity indicates significance of gene enrichment, node size indicates number of significant DEGs.

TABLE 3 Results of the differential gene expression (DGE) analysis in conjunctival tissue collected 3 days post inoculation with VA1994 and VA2013 isolates of *Mycoplasma gallisepticum* (MG) analysed separately (model 3).

Factors	Total DEG	Total Up	Total Down	Immune DEG	Immune Up	Immune Down
VA1994	160	148	12	22	22	0
AZ	6	6	0	0	0	0
HI	2	2	0	0	0	0
IA	14	11	3	0	1	0
VA1994:AZ	0	0	0	0	0	0
VA1994:HI	0	0	0	0	0	0
VA1994:IA	0	0	0	0	0	0
VA2013	1229	785	444	178	139	39
AZ	34	26	8	3	3	0
HI	45	28	17	3	2	1
IA	47	37	10	2	2	0
VA2013:AZ	2	0	2	0	0	0
VA2013:HI	2	1	1	0	0	0
VA2013:IA	1	1	0	0	0	0

The table shows the total numbers of differentially expressed genes (Total DEG) and the total numbers of differentially expressed immune genes (Immune DEG) for the MG isolates (Va1994 and VA2013), populations (AZ, Arizona; HI, Hawaii; IA, Iowa; VA, Virginia) and their interactions. Up = up-regulated compared to controls/increased expression in the tested population compared to VA, Down = down-regulated compared to controls/decreased expression in the tested population compared to the VA population.

Among the 1089 genes differentially expressed after inoculation with the MG isolate VA2013, there were 139 DEGs involved in immune function that were up-regulated, including *IL1B* (cytokine-mediated signaling pathway [GO:0019221]), *IL10* (negative regulation of cytokine activity [GO:0060302]), *IL18* (natural killer cell activation [GO:0030101)], *IL22* (inflammatory response [GO:0006954]), *TLR4* (activation of innate immune response [GO:0002218]), and *TLR7* (positive regulation of interferon-beta production [GO:0032728]) (see the pathways shown in Figure 6), and 39 immune DEGs that were down-regulated, including *ILRUN* (negative regulation of defense response to virus [GO:0050687]), *NTS* (positive regulation of NFKB transcription factor activity [GO:0051092]), *ROMO1* (defense response to Gram-negative bacterium [GO:0050829]), *AKAP1* (antiviral innate immune response [GO:0140374]), involved in the innate immune response, antimicrobial humoral immune response mediated by antimicrobial peptides, defense response to bacterium and antiviral innate immune response (Supplementary Figure S15).

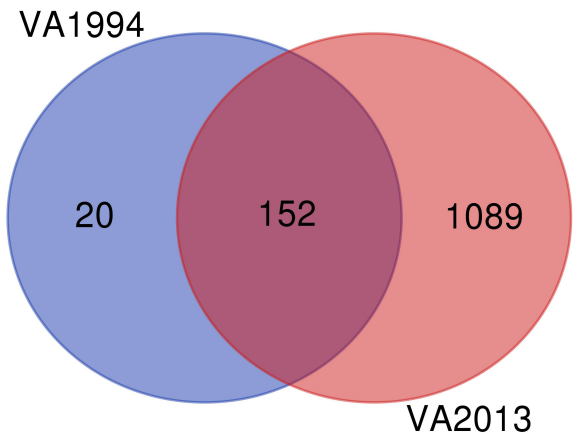

FIGURE 5
Venn diagram showing the number of differentially expressed genes (DEGs) during infection with the original *Mycoplasma gallisepticum* (MG) isolate VA1994 and the evolved isolate VA2013.

Two genes were significantly differentially expressed in VA2013 in interaction with the HI population: *CNN2* had lower expression, involved in wound healing [GO:0042060] and *YWHAZ* higher expression than in VA, having role in signal transduction [GO:0007165]. There was one gene with significant interaction between the IA population and VA2013 treatment, which is a long non-coding RNA with unknown function. For the AZ population, there were two genes with significant interaction to the VA2013 treatment, again both with unknown functions.

Differentially expressed genes commonly identified across the analyses

Finally, we searched for the genes that were identified as differentially expressed in all the three comparisons, i.e., the 1) DEGs during MG infection, 2) different pre-activation levels of expression between the populations unrelated to the MG infection, and 3) variation in expression based on the MG isolate used for the infection.

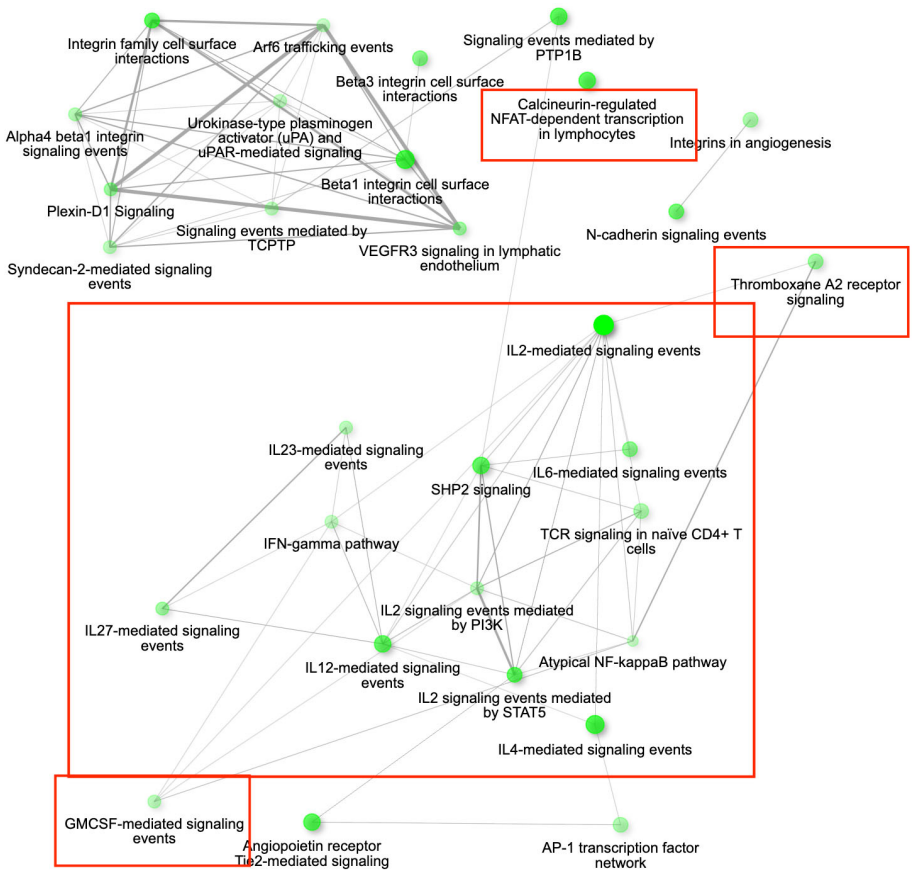

FIGURE 6
The gene interaction network for all the up-regulated differentially expressed genes (DEGs) in conjunctiva 3 days post inoculation (DPI) with *Mycoplasma gallisepticum* in birds infected with VA1994 versus VA2013. The network is showing the most significant pathways in the GO category Biological process across all the house finch populations analysed. Immune genes grouped in the pathways of our interest are highlighted in red rectangles. Node colour intensity indicates significance of gene enrichment, node size indicates number of significant DEGs.

We identified 8 common genes (Figure 7): *BCL10* integrating innate immune response [GO:0045087] and adaptive immune response regulation [GO:0002250], *USPL1* acting in cajal body organization [GO:0030576] and cell proliferation [GO:0008283], *VPS4B* acting in autophagy [GO:0016236] and cholesterol transport [GO:0030301], *RNF114* responsible for cell differentiation [GO:0030154] and protein polyubiquitination [GO:0000209], *AFMID* involved in tryptophan metabolisation to kynurenine, *ELMOD1* positively regulating the GTPase activity [GO:0019441], *CAPRIN1* responsible for negative regulation of translation [GO:0017148] and positive regulation of dendrite morphogenesis [GO:0050775] and *WDR5B* affecting histone H3-K4 methylation [GO:0051568]. Out of these genes, only BCL10 has any clear role in immunity. However, seven immune genes were also common DEGs between the first and second analysis, i.e. involved in the response to MG and also differentially pre-activated in different populations: *IL12B* regulating cellular response to IFNG [GO:0071346] and T-helper cells differentiation [GO:0042093], *PPARD* and *NR1H4* which are negative regulators of inflammatory responses [GO:0050728], including cellular responses to lipopolysaccharide [GO:0071222], *RAG1* that is key to immunoglobulin receptor recombination conditioning adaptive immune response during T-cell B-cell differentiation [GO:0002250], *RAC2* positively affecting neutrophil chemotaxis [GO:0090023] and T-cell proliferation [GO:0042129], *TRIM13* involved in positive regulation of NFKB signaling [GO:0043123] during innate immune responses, and *NCAPH2* involved in T-cell differentiation in the thymus [GO:0033077]. Finally, three immune genes showed as DEGs common to the second and third analyses, i.e. differentially pre-activated in different house finch populations and also involved in differential immune response to the two different MG isolates: *CDH17* involved in B-cell differentiation [GO:0002314], ACTG1 affecting cellular response to IFNG [GO:0071346] and *ROMO1* inducing production of reactive oxygen species (ROS) [GO:0034614], which is important in antimicrobial immune responses to bacteria.

Discussion

Using QuantSeq 3'-end RNA transcriptomic sequencing, in this study we characterised gene expression changes in a house finch

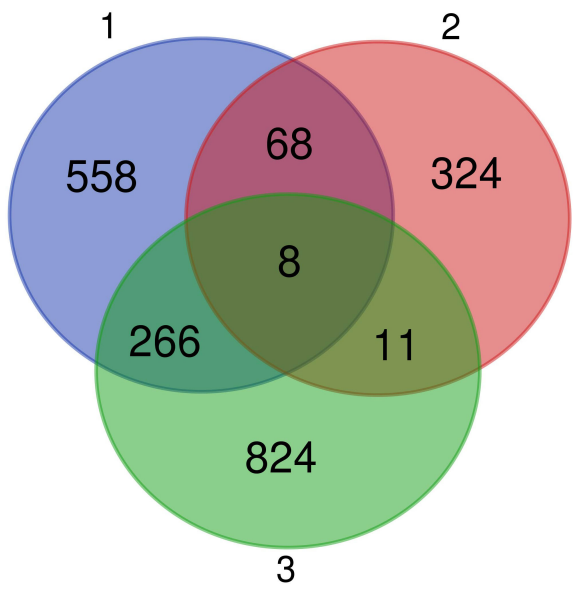

FIGURE 7
Venn diagram showing the genes in common between all the three comparative analyses performed. We found eight genes differentially expressed in conjunctiva during *Mycoplasma gallisepticum* (MG) infection (model 1), with pre-activation levels that differed among the four populations (model 2), and that differed in expression in response to the different MG isolates used for the inoculation (model 3).

periocular lymphoid tissue, the conjunctiva, during the initial phase of infection (day 3 post inoculation) with a naturally occurring pathogen, MG. We focused on DPI 3 as a period of innate immune regulation that later guides the subsequent phases of the response either towards immunopathology-linked resistance or towards tolerance. Our focus was on the DEGs involved in the immune response and showing variation between the house finch populations differing in their co-evolutionary history with MG, as this variation may indicate adaptations of the host to MG, including in response to the increasing pathogen virulence documented previously (5). We show significant variation in expression of many inflammatory genes, especially those relevant for regulation of the Th1/Th17 pathways. In response to MG, gene expression is up-regulated at the infection site in pathogen-recognition receptors (e.g. *TLR1B*), signalling molecules and their receptors (such as *CXCL12* and *IL17R*), adaptive cell-surface receptors (*CD74*) and various other immunomodulators (e.g. *ACOD1*). Several genes important for immune response regulation varied between individuals representing house finch populations differing in their co-evolutionary history with MG (e.g., *IL12B*, *IL17*, *CASP6*, *NR1H4* or *IRF6*). Most interestingly, our data suggest that in VA, the population with the longest co-evolutionary history with MG, the birds decrease the baseline *BCL10* gene expression compared to other populations (irrespective of MG infection in model 1, and only in controls in model 2). *BCL10* also showed significant interactions between house finch populations and the MG treatment (model 1). In our analyses, *BCL10* was revealed as up-regulated during MG infection caused by the evolved VA2013 isolate (model 3). This gene has important roles in NFKB signalling and activation of both innate and adaptive immune responses, so down-regulation of its expression in the VA population may adaptively increase tolerance to infection by minimizing damaging inflammation.

Previous transcriptomic research of the house finch-MG interaction suggested that the immediate adaptation of the host to MG favoured increases in host resistance. Bonneaud et al. (39) found that house finches from populations naïve to MG experience reduced splenic immune responsiveness to MG, while the populations with a 12-year history of MG exposure (at the time of that study) have up-regulated expression of genes associated with acquired immunity in the spleen 14 days post inoculation. While this immune response can be eventually protective, allowing recovery, important costs are likely associated with such immune response. Initial results of Adelman et al. (33) indicated that in populations with longer co-evolutionary history with MG, tolerance to the infection (defined as minimizing disease severity at a given pathogen load) can contribute to improving host health. Recently, this pattern was confirmed by Henschen et al. (20), who demonstrated tolerance to MG in the eastern house finch populations with >20-year coevolutionary history with the pathogen. This study revealed that in the Harderian glands of the same birds as used in this study, up-regulated expression of some cytokines and cytokine receptors (*CXCL8*, *CXCL14*, *CCL20*, *CSF3R*) was present only in the less-tolerant populations that have not yet or only recently experienced epidemics with MG (AZ, HI). In contrast to Henschen et al. (20), our transcriptomic results in conjunctiva do not indicate clear similarities in gene expression patterns between birds from the eastern populations that share a long co-evolutionary history with MG (VA and IA), when compared to western populations (AZ and HI). This suggests that each population might have evolved a slightly different mode of regulation of the immune response to MG at the conjunctival infection site.

Our results indicate that the immune response triggered by MG 3DPI in conjunctiva represents Th17-directed inflammation. From the total 109 genes differentially expressed, the majority of immune genes (58) were up-regulated, including e.g. *TLR1B* receptor activating inflammation, IL17 receptor genes *IL17RA* and *IL17RE*, chemokine *CXCL12*, but also *ACOD1*, a negative regulator of the inflammatory response. These immune genes have significant and interspecifically conserved roles in immune activation and regulation (59–64). Similar to our results, previous transcriptomic research in chickens has also shown increases in expression of *TLR1B*, *CXCL12* and *ACOD1* after infection with MG (65–67). Some genes, such as *CD74* expressed on antigen-presenting cells (68) as a receptor for macrophage migration inhibitory factor (MIF) (69) inducing inflammation (70), showed patterns of expression contrasting with previous research in the house finch-MG system. While our data show up-regulation, Bonneaud et al. (38) reported down-regulation of *CD74* during infection. This contrast could result from the difference in tissue used, the time of tissue collection post-infection, or differences in host population coevolutionary time with MG when the studies were performed: the population

with noted resistance in Bonneaud et al. (38) had ~12 years of co-evolution with MG versus 20-25 years of MG coevolution for the IA and VA populations used in this study. Increased CD74 expression during MG infection could improve activation of antigen-presenting cells (68), and through interaction with MIF (70), could also promote regenerative pathways in the tissue preventing the host damage. Overall, this could contribute to the observed host tolerance to MG in certain house finch populations. We found that only 11 immune genes were down-regulated in conjunctival tissue in response to MG, including *IL12B*, an essential mediator of the Th1 immune response. This is consistent with observations by Bonneaud et al. (39), suggesting that MG may be manipulating house finch gene expression during the acute immune response in order to allow efficient infection establishment. MG was revealed to cause immune suppression in the initial infection stages in chickens, suppressing expression of key cytokines involved in inflammation, including IL8, IL12 and CCL20 (71). Thus, our data support this hypothesis, indicating that MG may be down-regulating specific host immune pathways rather than overall immune activation.

Contrary to our expectations and to results from Harderian gland transcriptomes in the same birds (20), our general analysis of the conjunctival transcriptomes (model 1) suggested only limited interactions between MG infection status and population of origin. This result indicates tissue-specific differences in the immune regulation, but also that variation in the responses between populations may depend only on few key modifiers of the immune regulation rather than extensive transcriptome alterations. The most promising immune-controlling gene revealed in our results is *BCL10*, a positive regulator of cytokine expression involved in modulation of adaptive immune responses. In mammals, BCL10 has a vital role in channelling adaptive and innate immune signals downstream to CARMA/caspase-recruitment domain (CARD) scaffold proteins (72). BCL10 oligomerization via the CARD facilitates NFKB activation (73–75). Previous research in mice showed that BCL10 is a positive regulator of lymphocyte proliferation inducing antigen receptor signalling in B and T cells in response to NFKB activation (76). Impairment in BCL10 function negatively affects the development of memory B, $CD4^+$ and $CD8^+$ T cells (77). The immunomodulatory effects of *BCL10* are further documented by the up-regulation of its expression during experimental bacterial infections in cattle (78) and poultry (79). However, it has to be noted that there are also additional non-immune functions of *BCL10* described in other cells, including its involvement in neuronal regulation (80). Based on our data the precise role of BCL10 in the conjunctival tissue and causality of the changes in its expression cannot be inferred.

Although we did not find strong evidence for population differences in response to infection treatment, our results showed high number of immune genes that vary in their conjunctival expression between the house finch populations, independently of MG infection. These include key Th17 pathway regulators, such as the cytokine *IL17D* that is known to induce expression of other pro-inflammatory cytokines, including IL6 and CXCL8. This may suggest population-specific adaptations in conjunctival gene expression, potentially contributing to optimisation of the immune interaction with MG at the infection site. IL17 has a vital role in the initiation of chemotaxis and the functioning of Th17 cells (81, 82) and commonly shows up-regulation in birds immunized with various intracellular pathogens (83). Conjunctiva is colonised by innate lymphoid cells (ILCs), NK cells, γδT cells (84), αβT cells (85) and memory T cells (86), out of which the γδT cells were identified as the predominant source of IL17 during inflammation (87). In our study, *IL17D* was generally highly expressed in the AZ population, which, together with increased *BCL10*, *CASP6* and decreased *NR1H4* [a negative regulator of IL1B production; (88)] compared to the VA birds suggests disposition of the birds to resistance-oriented response through Th17 pathway pre-activation. Although the activity of *NR1H4* in conjunctiva is presently not entirely clear, its function at the site may be relevant, as in the gut this receptor negatively controls expression of a number of genes that activate inflammatory responses (58, 89, 90). In contrast to other populations, longer co-evolutionary history with MG may have selected the VA population to increase *NR1H4* and decrease *BCL10* expression, which is in agreement with the tolerance evolution described in house finches by Henschen et al. (20). This view is partially supported also by our target-gene analysis focusing on selected key immune genes with regulatory roles in immunity. All populations up-regulated *IL1B, IL6, IL10, IL18, IL22, CXCL8, CCL4, TLR1, ACOD1, TLR4*, and *TLR7* when infected with evolved MG (VA2013), which would propagate inflammation and facilitate pathogen transmission through pathological mycoplasmal conjunctivitis (15, 36). However, the AZ birds, compared to VA birds, showed a particularly high increase in expression of *TLR1* and *TLR4*, probably intensifying the resistance-oriented inflammatory response to MG. Our result thus shows similarity to the findings of Adelman et al. (33) in which house finches from populations with a longer coevolutionary history with MG (VA) showed lower inflammatory signalling and increased tolerance to infection than birds from populations with recent contact history (AZ) with MG. Further research is, however, needed to confirm the putative tolerogenic adaptations in the VA population.

Bonneaud et al. (39) proposed that the variation between house finch populations in resistance to MG likely results from some adaptations changing the initial innate immune regulation directing the subsequent adaptive immune response. This idea is consistent with the evidence from laboratory rodents showing that the initial innate immune regulation defines the efficiency of the clearance of mycoplasmal infections (91). Given the results we obtained from our general analysis (model 1), we tested this hypothesis using a subset of the data representing only the control individuals from the four house finch populations (model 2). From the high number of genes differentially expressed in the controls between the populations, 71 genes had clear roles in immunity. Consistent with our previous result, the control birds from the AZ population showed higher baseline expression of *IL17D, IL17C, IRF6, TLR15* and *TLR1B* genes putatively strengthening the overall Th17 responses, while the VA population showed stronger expression of *IL7*, *IL12B* and *LIF*, suggesting possible pre-activated Th1 immune pathway coupled with anti-inflammatory signalling, which was again linked with decreased *BCL10*

expression. We assume that immunological regulation of tolerance to infection must involve balanced changes of both pro- and anti-inflammatory pathways to prevent infection-caused mortality. *IL12B*, a subunit of IL12, primarily stimulates natural killer (NK) cells and induces the differentiation of naive $CD4^+$ T lymphocytes into T helper 1 (Th1) effectors (92). If the IL12B subunit is dimerized with the IL23A subunit, then functional IL23 is produced (93), which is necessary for Th17 development and function (94). Alternatively, *IL12B* can also mediate anti-inflammatory regulation increasing expression of other regulatory cytokines such as IL10 (95), with IL7 supporting the host defence by regulating immune cell growth and homeostasis (96). Thus, increased baseline expression of *IL12B* might have multiple functional roles in protecting the health of the VA birds during the onset of MG infection. Birds from the HI and IA populations showed similar up-regulation of immune-related pathways activated by mast cells and B cells (*TRIM13* and *PPARD*) when compared with the VA birds but also with AZ birds. Taken altogether, the pattern of immune gene expression in the VA birds was different from all the other three remaining house finch populations, putatively resulting, at least in part, from long-lasting adaptation to MG through a combination of resistance and tolerance (20).

We also examined pathogen contributions to differential conjunctival gene expression across populations (model 3). Consistent with previous research (5, 20, 37) we found that the evolved (VA2013) isolate triggers much stronger conjunctival immune responses than the original (VA1994) one, here indicated by the number of DEGs when compared to controls. In contrast to VA1994, the evolved isolate VA2013 activated pathways involving differential expression of both pro-inflammatory and anti-inflammatory genes, including key signal mediators such as *IL1B*, *IL10*, *IL18*, *IL22* and *CXCL8*. Especially negative regulators of inflammation, such as IL10, can play important roles in fine-tuning immunomodulation, since their down-regulation can improve pathogen clearance, but also increase tissue damage (97–100), optimising the immunity-immunopathology balance in the defence (9). Previous research in rodents performed both *in vivo* and *in vitro* shows that *Mycoplasma pneumoniae* antigens induce potent immune reactions through enhancement of the Th17 response, but regulatory T cell (Treg) activation linked with *IL10* expression simultaneously suppress *IL17A* expression (101). In contrast, *IL18* is a potent pro-inflammatory cytokine regulating both innate and acquired immune responses (102). Studies in chicken show that MG infection increased mRNA levels of *IL18* between 3 and 7 DPI, similar to our results (103). Also IL22 is a key mediator of inflammation that is produced immediately after stimulation to initiate an immune response, mediating also mucous production, wound healing, and tissue regeneration (104). Comparable to our results, *IL22* gene has been reported as up-regulated during *Mycoplasma ovipneumoniae* infection in sheep (105).

Overall, comparison of the results from all three analyses performed identifies *BCL10* as a potentially important immune gene that changes its conjunctival expression during the MG infection, varies in its expression between individuals from different house finch populations, and also varies in expression depending on the MG isolate infecting the birds. Furthermore, other genes involved in the response to MG (model 1 or model 3) and at the same time also differentially pre-activated in distinct host populations (model 2) may be of high importance for house finch adaptation to MG. Our results elucidated both positive and negative regulators of inflammation and Th1 immunity, including *IL12B* and possibly also *PPARD* and *NR1H4*. Roles of other genes repeatedly revealed in our analyses are less clear, but they may contribute to altered leukocyte differentiation, infiltration into the tissue or cell activation (*RAG1, RAC2, TRIM13, NCAPH2, CDH17, ACTG1* and *ROMO1*). Thus, all these 11 genes potentially provide adaptations to the selective pressures posed by MG varying between the house finch populations.

Our transcriptomic results obtained in conjunctiva apparently differ from the results obtained earlier by Henschen et al. (20) from the same experiment but for a different tissue, the Harderian gland. Most importantly, the pattern of variation between the house finch populations revealed for the two tissues in response to MG is different. While we assume that biologically significant differences in immune regulation between the tissues are responsible for the differences in gene expression patterns observed, we are, unfortunately, presently unable to explain them, because for the two studies different transcriptomic methods were adopted, RNA-seq and QuantSeq, respectively. The RNA-seq approach can be biased by more enriched DEGs for longer transcripts than for the shorter ones (106). Previous research has reported that RNA-seq identifies in general more DEGs, but QuantSeq can detect more of the shorter transcripts (46) that often act in immunity (107). Thus, future research is needed to validate the results and reveal if the difference in the transcriptomic results obtained for the two house finch tissues reflect true biological difference between the tissues, variation in the transcriptomic approaches adopted, or both.

Conclusion

Our results illuminate potential immunological pathways underlying increased tolerance to MG in birds from the VA population compared to the other house finch populations. Notably, they suggest the importance of evolving balance between the Th1 and Th17 pathway activation during the initial conjunctival response of the house finches to the MG infection. The populations in no or only recent contact with MG may have increased tendency for up-regulation of the *IL17*-linked pathway (observed in AZ), while the populations with long-established co-evolutionary history with MG (VA), could promote *IL12* signalling to increase Th1 and/or anti-inflammatory (possibly B-cell driven) immune responses. Further research should focus on understanding of specific roles of various cell types in the immune responses to MG in birds from populations differing in their co-evolutionary history with MG. Furthermore, our results also document that infection with a more recent MG isolate (VA2013) triggers in conjunctiva stronger expression of immune genes than infection with the original

isolate (VA1994). Since also non-immune pathways may be affected by this regulation [e.g. pathways regulating the extent of the sickness behaviour which might influence MG transmission in the finches; (36, 108)], further research should also investigate the expression changes in genes with other functions expressed in non-lymphoid tissues.

Data availability statement

The data presented in the study are deposited in the NCBI BioProject repository, accession number PRJNA981079.

Ethics statement

The animal study was approved by Institutional Animal Care and Use Committees (IACUC) at Iowa State University (ISU) and Virginia Tech, and the ISU Institutional Biosafety Committee. The study was conducted in accordance with the local legislation and institutional requirements.

Author contributions

Conceptualization: NKV, AEH, RAD, DMH, JSA, MV. Data Curation: NKV, AEH, RAD, DMH, JSA. Formal Analysis: NKV, BM. Funding Acquisition: NKV, BM, RAD, DMH, JSA, MV. Investigation: NKV, AEH, BM, RAD, DMH, JSA, MV. Methodology: NKV, AEH, BM, VB, RAD, DMH, JSA, MV. Project Administration: NKV, BM, AEH, DMH, JSA, MV. Resources: MV, RAD, DMH, JSA. Software: n/a. Supervision: AEH, RAD, DMH, JSA, MV. Validation: NKV, AEH, RAD, DMH, JSA, MV. Visualization: NKV. Writing – Original Draft Preparation: NKV, MV. Writing – Review and Editing: NKV, AEH, BM, RAD, VB, DMH, JSA, MV. All authors contributed to the article and approved the submitted version.

Funding

The author(s) declare financial support was received for theresearch, authorship, and/or publication of this article. The birds were trapped and the experiment was performed within the framework of the project No. 1755197 (Iowa State University), NSF 1950307 (University of Memphis) and No. 1754872 (Virginia Tech) (title 'Collaborative Research: Immune mechanisms and epidemiological consequences of tolerance in a naturally occurring host-pathogen system') supported by the U.S. National Science Foundation. This study was supported by the Grant Schemes at Charles University (grant nos. GAUK 646119 and START/SCI/113 with reg. no. CZ.02.2.69/0.0/0.0/19_073/0016935) and by the Ministry of Education, Youth and Sports of the Czech Republic (INTER-ACTION grant no. LUAUS24184. Computational resources and data storage were provided by the Czech Education and Scientific NETwork (CESNET; project e-INFRA CZ LM2018140 supported by the Ministry of Education, Youth and Sports of the Czech Republic). The study was further supported by the Institutional Research Support No. 260684/2023.

Acknowledgments

We would like to thank all the research assistants that helped with the field work (especially Marissa Langager and Allison Rowley) and the subsequent laboratory analysis. We are also grateful to P. Hutton and K. McGraw (Arizona State University), and S. Goldstein, P. Howard, and J. Omick (Hawaii USDA) for their help with logistics in the field.

Conflict of interest

The authors declare that the research was conducted in the absence of any commercial or financial relationships that could be construed as a potential conflict of interest.

Publisher's note

Supplementary material

The Supplementary Material for this article can be found online at: https://www.frontiersin.org/articles/10.3389/fimmu.2024.1250818/full#supplementary-material

References

1. Woolhouse ME, Webster JP, Domingo E, Charlesworth B, Levin BR. Biological and biomedical implications of the co-evolution of pathogens and their hosts. *Nat Genet* (2002) 32:569–77. doi: 10.1038/ng1202-569

2. Read AF. The evolution of virulence. *Trends Microbiol* (1994) 2:73–6. doi: 10.1016/0966-842X(94)90537-1

3. Bloom DE, Black S, Rappuoli R. Emerging infectious diseases: A proactive approach. *Proc Natl Acad Sci* (2017) 114:4055–9. doi: 10.1073/pnas.1701410114

4. Cunningham AA, Daszak P, Wood JL. One Health, emerging infectious diseases and wildlife: two decades of progress? *Philos Trans R Soc B Biol Sci* (2017) 372:20160167. doi: 10.1098/rstb.2016.0167

5. Hawley DM, Osnas EE, Dobson AP, Hochachka WM, Ley DH, Dhondt AA. Parallel patterns of increased virulence in a recently emerged wildlife pathogen. *PloS Biol* (2013) 11:e1001570. doi: 10.1371/journal.pbio.1001570

6. Voyles J, Woodhams DC, Saenz V, Byrne AQ, Perez R, Rios-Sotelo G, et al. Shifts in disease dynamics in a tropical amphibian assemblage are not due to pathogen attenuation. *Science* (2018) 359:1517–9. doi: 10.1126/science.aao4806

7. Langwig KE, Hoyt JR, Parise KL, Frick WF, Foster JT, Kilpatrick AM. Resistance in persisting bat populations after white-nose syndrome invasion. *Philos Trans R Soc B Biol Sci* (2017) 372:20160044. doi: 10.1098/rstb.2016.0044

8. Alves JM, Carneiro M, Cheng JY, Lemos de Matos A, Rahman MM, Loog L, et al. Parallel adaptation of rabbit populations to myxoma virus. *Science* (2019) 363:1319–26. doi: 10.1126/science.aau7285

9. Graham AL, Allen JE, Read AF. Evolutionary causes and consequences of immunopathology. *Annu Rev Ecol Evol Syst* (2005) 36:373–97. doi: 10.1146/annurev.ecolsys.36.102003.152622

10. Seal S, Dharmarajan G, Khan I. Evolution of pathogen tolerance and emerging infections: A missing experimental paradigm. *Elife* (2021) 10:e68874. doi: 10.7554/eLife.68874

11. Boots M, Bowers RG. Three mechanisms of host resistance to microparasites—avoidance, recovery and tolerance—show different evolutionary dynamics. *J Theor Biol* (1999) 201:13–23. doi: 10.1006/jtbi.1999.1009

12. Råberg L, Sim D, Read AF. Disentangling genetic variation for resistance and tolerance to infectious diseases in animals. *Science* (2007) 318:812–4. doi: 10.1126/science.1148526

13. Miller MR, White A, Boots M. The evolution of parasites in response to tolerance in their hosts: the good, the bad, and apparent commensalism. *Evolution* (2006) 60:945–56. doi: 10.1111/j.0014-3820.2006.tb01173.x

14. Little TJ, Shuker DM, Colegrave N, Day T, Graham AL. The coevolution of virulence: tolerance in perspective. *PloS Pathog* (2010) 6:e1001006. doi: 10.1371/journal.ppat.1001006

15. Henschen AE, Adelman JS. What does tolerance mean for animal disease dynamics when pathology enhances transmission? *Integr Comp Biol* (2019) 59:1220–30. doi: 10.1093/icb/icz065

16. Ruden RM, Adelman JS. Disease tolerance alters host competence in a wild songbird. *Biol Lett* (2021) 17:20210362. doi: 10.1098/rsbl.2021.0362

17. Savage AE, Zamudio KR. Adaptive tolerance to a pathogenic fungus drives major histocompatibility complex evolution in natural amphibian populations. *Proc R Soc B Biol Sci* (2016) 283:20153115. doi: 10.1098/rspb.2015.3115

18. Atkinson CT, Saili KS, Utzurrum RB, Jarvi SI. Experimental evidence for evolved tolerance to avian malaria in a wild population of low elevation Hawai 'i 'Amakihi (Hemignathus virens). *EcoHealth* (2013) 10:366–75. doi: 10.1007/s10393-013-0899-2

19. Weber JN, Steinel NC, Peng F, Shim KC, Lohman BK, Fuess LE, et al. Evolutionary gain and loss of a pathological immune response to parasitism. *Science* (2022) 377:1206–11. doi: 10.1126/science.abo3411

20. Henschen AE, Vinkler M, Langager MM, Rowley AA, Dalloul RA, Hawley DM, et al. Rapid adaptation to a novel pathogen through disease tolerance in a wild songbird. *PloS Pathog* (2023) 19:e1011408. doi: 10.1371/journal.ppat.1011408

21. Vinkler M, Fiddaman SR, Těšický M, O'Connor EA, Savage AE, Lenz TL, et al. Understanding the evolution of immune genes in jawed vertebrates. *J Evol Biol* (2023) 36:847–73. doi: 10.1111/jeb.14181

22. Ley DH. *Mycoplasma gallisepticum* infection. In: Saif YM, editor. *Diseases of poultry* (12th ed). Ames, IA, USA: Blackwell Publishing (2008) pp. 807-834.

23. Ferguson-Noel N, Armour NK, Noormohammadi AH, El-Gazzar M, Bradbury JM. Mycoplasmosis. *Dis Poult* (2020), 907–65. doi: 10.1002/9781119371199.ch21

24. Ley DH, Berkhoff JE, McLaren JM. Mycoplasma gallisepticum Isolated from House Finches (*Carpodacus mexicanus*) with Conjunctivitis. *Avian Dis* (1996) 40:480. doi: 10.2307/1592250

25. Dhondt AA, Altizer S, Cooch EG, Davis AK, Dobson A, Driscoll MJL, et al. Dynamics of a novel pathogen in an avian host: Mycoplasmal conjunctivitis in house finches. *Acta Trop* (2005) 94:77–93. doi: 10.1016/j.actatropica.2005.01.009

26. Faustino CR, Jennelle CS, Connolly V, Davis AK, Swarthout EC, Dhondt AA, et al. Mycoplasma gallisepticum infection dynamics in a house finch population: seasonal variation in survival, encounter and transmission rate. *J Anim Ecol* (2004) 73:651–69. doi: 10.1111/j.0021-8790.2004.00840.x

27. Hochachka WM, Dhondt AA. Density-dependent decline of host abundance resulting from a new infectious disease. *Proc Natl Acad Sci* (2000) 97:5303–6. doi: 10.1073/pnas.080551197

28. Staley M, Bonneaud C, McGraw KJ, Vleck CM, Hill GE. Detection of Mycoplasma gallisepticum in house finches (Haemorhous mexicanus) from Arizona. *Avian Dis* (2018) 62:14–7. doi: 10.1637/11610-021317-Reg.1

29. Ley DH, Hawley DM, Geary SJ, Dhondt AA. House Finch (*Haemorhous mexicanus*) Conjunctivitis, and *Mycoplasma* spp. Isolated from North American Wild Birds, 1994–2015. *J Wildl Dis* (2016) 52:669–73. doi: 10.7589/2015-09-244

30. Grodio JL, Hawley DM, Osnas EE, Ley DH, Dhondt KV, Dhondt AA, et al. Pathogenicity and immunogenicity of three *Mycoplasma gallisepticum* isolates in house finches (*Carpodacus mexicanus*). *Vet Microbiol* (2012) 155:53–61. doi: 10.1016/j.vetmic.2011.08.003

31. Hawley DM, Dhondt KV, Dobson AP, Grodio JL, Hochachka WM, Ley DH, et al. Common garden experiment reveals pathogen isolate but no host genetic diversity effect on the dynamics of an emerging wildlife disease: Host genetic diversity and disease resistance. *J Evol Biol* (2010) 23:1680–8. doi: 10.1111/j.1420-9101.2010.02035.x

32. Hill GE, Farmer KL. Carotenoid-based plumage coloration predicts resistance to a novel parasite in the house finch. *Naturwissenschaften* (2005) 92:30–4. doi: 10.1007/s00114-004-0582-0

33. Adelman JS, Kirkpatrick L, Grodio JL, Hawley DM. House Finch Populations Differ in Early Inflammatory Signaling and Pathogen Tolerance at the Peak of *Mycoplasma gallisepticum* Infection. *Am Nat* (2013) 181:674–89. doi: 10.1086/670024

34. Razin S, Yogev D, Naot Y. Molecular biology and pathogenicity of mycoplasmas. *Microbiol Mol Biol Rev* (1998) 62:63. doi: 10.1128/MMBR.62.4.1094-1156.1998

35. Atkinson TP, Waites KB. Mycoplasma pneumoniae infections in childhood. *Pediatr Infect Dis J* (2014) 33:92–4. doi: 10.1097/INF.0000000000000171

36. Hawley DM, Thomason CA, Aberle MA, Brown R, Adelman JS. High virulence is associated with pathogen spreadability in a songbird–bacterial system. *R Soc Open Sci* (2023) 10:220975. doi: 10.1098/rsos.220975

37. Vinkler M, Leon AE, Kirkpatrick L, Dalloul RA, Hawley DM. Differing house finch cytokine expression responses to original and evolved isolates of *Mycoplasma gallisepticum*. *Front Immunol* (2018) 9:13. doi: 10.3389/fimmu.2018.00013

38. Bonneaud C, Balenger SL, Russell AF, Zhang J, Hill GE, Edwards SV. Rapid evolution of disease resistance is accompanied by functional changes in gene expression in a wild bird. *Proc Natl Acad Sci* (2011) 108:7866–71. doi: 10.1073/pnas.1018580108

39. Bonneaud C, Balenger SL, Zhang J, Edwards SV, Hill GE. Innate immunity and the evolution of resistance to an emerging infectious disease in a wild bird. *Mol Ecol* (2012) 21:2628–39. doi: 10.1111/j.1365-294X.2012.05551.x

40. Pyle P. Molt limits in North American passerines. *North Am Bird Bander* (1997) 22:49–89.

41. Fleming-Davies AE, Williams PD, Dhondt AA, Dobson AP, Hochachka WM, Leon AE, et al. Incomplete host immunity favors the evolution of virulence in an emergent pathogen. *Science* (2018) 359:1030–3. doi: 10.1126/science.aao2140

42. Corley SM, Troy NM, Bosco A, Wilkins MR. QuantSeq. 3′ Sequencing combined with Salmon provides a fast, reliable approach for high throughput RNA expression analysis. *Sci Rep* (2019) 9:18895. doi: 10.1038/s41598-019-55434-x

43. Jarvis S, Birsa N, Secrier M, Fratta P, Plagnol V. A comparison of low read depth quantSeq 3′ Sequencing to total RNA-seq in FUS mutant mice. *Front Genet* (2020) 11:562445. doi: 10.3389/fgene.2020.562445

44. Moll P, Ante M, Seitz A, Reda T. QuantSeq 3′ mRNA sequencing for RNA quantification. *Nat Methods* (2014) 11:i–iii. doi: 10.1038/nmeth.f.376

45. Zhong S, Joung J-G, Zheng Y, Chen Y, Liu B, Shao Y, et al. High-throughput illumina strand-specific RNA sequencing library preparation. *Cold Spring Harb Protoc* (2011) pdb–prot5652. doi: 10.1093/nar/gkaa942

46. Ma F, Fuqua BK, Hasin Y, Yukhtman C, Vulpe CD, Lusis AJ, et al. A comparison between whole transcript and 3' RNA sequencing methods using Kapa and Lexogen library preparation methods. *BMC Genomics* (2019) 20:9. doi: 10.1186/s12864-018-5393-3

47. Howe KL, Achuthan P, Allen J, Allen J, Alvarez-Jarreta J, Amode MR, et al. Ensembl 2021. *Nucleic Acids Res* (2021) 49:D884–91. doi: 10.1093/nar/gkaa942

48. Bolger AM, Lohse M, Usadel B. Trimmomatic: a flexible trimmer for Illumina sequence data. *Bioinformatics* (2014) 30:2114–20. doi: 10.1093/bioinformatics/btt656

49. Dobin A, Davis CA, Schlesinger F, Drenkow J, Zaleski C, Jha S, et al. STAR: ultrafast universal RNA-seq aligner. *Bioinformatics* (2013) 29:15–21. doi: 10.1093/nar/gkv007

50. Liao Y, Smyth GK, Shi W. featureCounts: an efficient general purpose program for assigning sequence reads to genomic features. *Bioinformatics* (2014) 30:923–30. doi: 10.1093/bioinformatics/btt656

51. Ritchie ME, Phipson B, Wu D, Hu Y, Law CW, Shi W, et al. limma powers differential expression analyses for RNA-sequencing and microarray studies. *Nucleic Acids Res* (2015) 43:e47–7. doi: 10.1093/nar/gkv007

52. Team RC. *R: A language and environment for statistical computing*. R Foundation for Statistical Computing (2020).

53. Ge SX, Jung D, Yao R. ShinyGO: a graphical gene-set enrichment tool for animals and plants. *Bioinformatics* (2020) 36:2628–9. doi: 10.1093/bioinformatics/btz931

54. Kaspers B, Schat KA, Göbel T, Vervelde L. *Avian immunology*. London, UK: Academic Press (2021).

55. Culhane AC, Perriere G, Considine EC, Cotter TG, Higgins DG. Between-group analysis of microarray data. *Bioinformatics* (2002) 18:1600–8. doi: 10.1073/pnas.0509592103

56. Wu R, Kang R, Tang D. Mitochondrial ACOD1/IRG1 in infection and sterile inflammation. *J Intensive Med* (2022) 2(2):78–88. doi: 10.1016/j.jointm.2022.01.001

57. Guo D, Dong W, Cong Y, Liu Y, Liang Y, Ye Z, et al. LIF aggravates pulpitis by promoting inflammatory response in macrophages. *Inflammation* (2024) 47:307–22. doi: 10.1007/s10753-023-01910-6

58. Inagaki T, Moschetta A, Lee Y-K, Peng L, Zhao G, Downes M, et al. Regulation of antibacterial defense in the small intestine by the nuclear bile acid receptor. *Proc Natl Acad Sci* (2006) 103:3920–5. doi: 10.3389/fimmu.2019.01172

59. Guyon A. CXCL12 chemokine and its receptors as major players in the interactions between immune and nervous systems. *Front Cell Neurosci* (2014) 8:65. doi: 10.2147/OTT.S237162

60. Wu R, Chen F, Wang N, Tang D, Kang R. ACOD1 in immunometabolism and disease. *Cell Mol Immunol* (2020) 17:822–33. doi: 10.1038/s41423-020-0489-5

61. Lee Y, Clinton J, Yao C, Chang SH. Interleukin-17D promotes pathogenicity during infection by suppressing CD8 T cell activity. *Front Immunol* (2019) 10:1172. doi: 10.1128/IAI.01356-12

62. Zhu C, Chen X, Guan G, Zou C, Guo Q, Cheng P, et al. IFI30 is a novel immune-related target with predicting value of prognosis and treatment response in glioblastoma. *OncoTargets Ther* (2020) 13:1129. doi: 10.3389/fimmu.2020.628804

63. Chen Y, Zhao H, Feng Y, Ye Q, Hu J, Guo Y, et al. Pan-cancer analysis of the associations of TGFBI expression with prognosis and immune characteristics. *Front Mol Biosci* (2021) 8:745649. doi: 10.3389/fmolb.2021.745649

64. de Almeida LA, Macedo GC, Marinho FA, Gomes MT, Corsetti PP, Silva AM, et al. Toll-like receptor 6 plays an important role in host innate resistance to Brucella abortus infection in mice. *Infect Immun* (2013) 81:1654–62. doi: 10.1016/j.dci.2016.01.008

65. Kulappu Arachchige SN, Young ND, Kanci Condello A, Omotainse OS, Noormohammadi AH, Wawegama NK, et al. Transcriptomic analysis of long-term protective immunity induced by vaccination with *Mycoplasma gallisepticum* strain ts-304. *Front Immunol* (2021) 11:628804. doi: 10.1016/S0167-4889(01)00166-5

66. Beaudet J, Tulman E, Pflaum K, Liao X, Kutish G, Szczepanek S, et al. Transcriptional profiling of the chicken tracheal response to virulent Mycoplasma gallisepticum strain Rlow. *Infect Immun* (2017) 85:e00343–17. doi: 10.1016/j.celrep.2022.111572

67. Tian W, Zhao C, Hu Q, Sun J, Peng X. Roles of Toll-like receptors 2 and 6 in the inflammatory response to *Mycoplasma gallisepticum* infection in DF-1 cells and in chicken embryos. *Dev Comp Immunol* (2016) 59:39–47. doi: 10.1016/j.dci.2016.01.008

68. Stumptner-Cuvelette P, Benaroch P. Multiple roles of the invariant chain in MHC class II function. *Biochim Biophys Acta BBA - Mol Cell Res* (2002) 1542:1–13. doi: 10.1016/S0167-4889(01)00166-5

69. David K, Friedlander G, Pellegrino B, Radomir L, Lewinsky H, Leng L, et al. CD74 as a regulator of transcription in normal B cells. *Cell Rep* (2022) 41:111572. doi: 10.1016/j.celrep.2022.111572

70. Fukuda Y, Bustos MA, Cho S-N, Roszik J, Ryu S, Lopez VM, et al. Interplay between soluble CD74 and macrophage-migration inhibitory factor drives tumor growth and influences patient survival in melanoma. *Cell Death Dis* (2022) 13:117. doi: 10.1016/S0092-8674(00)80957-5

71. Mohammed J, Frasca S, Cecchini K, Rood D, Nyaoke AC, Geary SJ, et al. Chemokine and cytokine gene expression profiles in chickens inoculated with Mycoplasma gallisepticum strains Rlow or GT5. *Vaccine* (2007) 25:8611–21. doi: 10.1074/jbc.274.29.20127

72. Gehring T, Seeholzer T, Krappmann D. BCL10 – bridging CARDs to immune activation. *Front Immunol* (2018) 9:1539. doi: 10.3389/fimmu.2018.01539

73. Willis TG, Jadayel DM, Du M-Q, Peng H, Perry AR, Abdul-Rauf M, et al. Bcl10 is involved in t (1; 14)(p22; q32) of MALT B cell lymphoma and mutated in multiple tumor types. *Cell* (1999) 96:35–45. doi: 10.1016/s0092-8674(00)80957-5

74. Costanzo A, Guiet C, Vito P. c-E10 is a caspase-recruiting domain-containing protein that interacts with components of death receptors signaling pathway and activates nuclear factor-κB. *J Biol Chem* (1999) 274:20127–32. doi: 10.3389/fimmu.2021.786572

75. Koseki T, Inohara N, Chen S, Carrio R, Merino J, Hottiger MO, et al. CIPER, a novel NF κB-activating protein containing a caspase recruitment domain with homology to herpesvirus-2 protein E10. *J Biol Chem* (1999) 274:9955–61. doi: 10.1152/physiolgenomics.00098.2006

76. Ruland J, Duncan GS, Elia A, del Barco Barrantes I, Nguyen L, Plyte S, et al. Bcl10 is a positive regulator of antigen receptor–induced activation of NF-κ B and neural tube closure. *Cell* (2001) 104:33–42. doi: 10.1016/S0092-8674(01)00189-1

77. Garcia-Solis B, Van Den Rym A, Pérez-Caraballo JJ, Al–Ayoubi A, Alazami AM, Lorenzo L, et al. Clinical and immunological features of human BCL10 deficiency. *Front Immunol* (2021) 4732. doi: 10.1073/pnas.0608388103

78. Murphy JT, Sommer S, Kabara EA, Verman N, Kuelbs MA, Saama P, et al. Gene expression profiling of monocyte-derived macrophages following infection with *Mycobacterium avium* subspecies *avium* and *Mycobacterium avium* subspecies *paratuberculosis*. *Physiol Genomics* (2006) 28:67–75. doi: 10.1111/j.1600-065X.2008.00699.x

79. Wang Y, Miao X, Li H, Su P, Lin L, Liu L, et al. The correlated expression of immune and energy metabolism related genes in the response to *Salmonella enterica* serovar Enteritidis inoculation in chicken. *BMC Vet Res* (2020) 16:1–9. doi: 10.1016/j.jdermsci.2011.11.007

80. Klemm S, Zimmermann S, Peschel C, Mak TW, Ruland J. Bcl10 and Malt1 control lysophosphatidic acid-induced NF-κB activation and cytokine production. *Proc Natl Acad Sci* (2007) 104:134–8. doi: 10.1016/j.meegid.2013.12.004

81. Iwakura Y, Nakae S, Saijo S, Ishigame H. The roles of IL-17A in inflammatory immune responses and host defense against pathogens. *Immunol Rev* (2008) 226:57–79. doi: 10.1038/s41385-022-00551-6

82. Mabuchi T, Chang TW, Quinter S, Hwang ST. Chemokine receptors in the pathogenesis and therapy of psoriasis. *J Dermatol Sci* (2012) 65:4–11. doi: 10.1007/BF02539415

83. Luo C, Qu H, Ma J, Wang J, Hu X, Li N, et al. A genome-wide association study identifies major loci affecting the immune response against infectious bronchitis virus in chicken. *Infect Genet Evol* (2014) 21:351–8. doi: 10.1016/j.meegid.2013.12.004

84. de Paiva CS, Leger AJS, Caspi RR. Mucosal immunology of the ocular surface. *Mucosal Immunol* (2022) 15:1143–57. doi: 10.1167/iovs.63.12.13

85. Bialasiewicz AA, Schaudig U, Ma J-X, Vieth S, Richard G. α/β-and γ/δ-T cell-receptor-positive lymphocytes in healthy and inflamed human conjunctiva. *Graefes Arch Clin Exp Ophthalmol* (1996) 234:467–71. doi: 10.1136/gut.2010.233304

86. Arnous R, Arshad S, Sandgren K, Cunningham AL, Carnt N, White A. Tissue resident memory T cells inhabit the deep human conjunctiva. *Sci Rep* (2022) 12:6077. doi: 10.4049/jimmunol.0803978

87. Li L, Li Y, Zhu X, Wu B, Tang Z, Wen H, et al. Conjunctiva resident γδ T cells expressed high level of IL-17A and promoted the severity of dry eye. *Invest Ophthalmol Vis Sci* (2022) 63:13–3. doi: 10.2741/A845

88. Gaudet P, Livstone MS, Lewis SE, Thomas PD. Phylogenetic-based propagation of functional annotations within the Gene Ontology consortium. *Brief Bioinform* (2011) 12:449–62. doi: 10.12688/f1000research.7010.1

89. Wildenberg ME, van den Brink GR. FXR activation inhibits inflammation and preserves the intestinal barrier in IBD. *Gut* (2011) 60:432–3. doi: 10.1016/S1074-7613(00)00070-4

90. Vavassori P, Mencarelli A, Renga B, Distrutti E, Fiorucci S. The bile acid receptor FXR is a modulator of intestinal innate immunity. *J Immunol* (2009) 183:6251–61. doi: 10.1038/nm.3895

91. Hickman-Davis JM. Role of innate immunity in respiratory mycoplasma infection. *Front Biosci-Landmark* (2002) 7:1347–55. doi: 10.4049/jimmunol.173.3.1779

92. Ma X, Yan W, Zheng H, Du Q, Zhang L, Ban Y, et al. Regulation of IL-10 and IL-12 production and function in macrophages and dendritic cells. *F1000Research* (2015) 4:1465. doi: 10.12688/f1000research.7010.1

93. Oppmann B, Lesley R, Blom B, Timans JC, Xu Y, Hunte B, et al. Novel p19 protein engages IL-12p40 to form a cytokine, IL-23, with biological activities similar as well as distinct from IL-12. *Immunity* (2000) 13:715–25. doi: 10.1128/IAI.67.9.4435-4442.1999

94. Teng MW, Bowman EP, McElwee JJ, Smyth MJ, Casanova J-L, Cooper AM, et al. IL-12 and IL-23 cytokines: from discovery to targeted therapies for immune-mediated inflammatory diseases. *Nat Med* (2015) 21:719–29. doi: 10.1002/eji.200636012

95. Wassink L, Vieira PL, Smits HH, Kingsbury GA, Coyle AJ, Kapsenberg ML, et al. ICOS expression by activated human th cells is enhanced by IL-12 and IL-23: increased ICOS expression enhances the effector function of both th1 and th2 cells. *J Immunol* (2004) 173:1779–86. doi: 10.4049/jimmunol.173.3.1779

96. Chen D, Tang T-X, Deng H, Yang X-P, Tang Z-H. Interleukin-7 biology and its effects on immune cells: mediator of generation, differentiation, survival, and homeostasis. *Front Immunol* (2021) 12:747324. doi: 10.3389/fimmu.2021.747324

97. Li C, Corraliza I, Langhorne J. A defect in interleukin-10 leads to enhanced malarial disease in Plasmodium chabaudi chabaudi infection in mice. *Infect Immun* (1999) 67:4435–42. doi: 10.1186/1471-2180-14-156

98. Siewe L, Bollati–Fogolin M, Wickenhauser C, Krieg T, Müller W, Roers A. Interleukin-10 derived from macrophages and/or neutrophils regulates the inflammatory response to LPS but not the response to CpG DNA. *Eur J Immunol* (2006) 36:3248–55. doi: 10.3389/fimmu.2022.919973

99. Sun J, Madan R, Karp CL, Braciale TJ. Effector T cells control lung inflammation during acute influenza virus infection by producing IL-10. *Nat Med* (2009) 15:277–84. doi: 10.1186/s13567-020-00777-x

100. Ejrnaes M, Filippi CM, Martinic MM, Ling EM, Togher LM, Crotty S, et al. Resolution of a chronic viral infection after interleukin-10 receptor blockade. *J Exp Med* (2006) 203:2461–72. doi: 10.3389/fimmu.2020.02148

101. Kurata S, Osaki T, Yonezawa H, Arae K, Taguchi H, Kamiya S. Role of IL-17A and IL-10 in the antigen induced inflammation model by Mycoplasma pneumoniae. *BMC Microbiol* (2014) 14:1–11. doi: 10.1371/journal.pone.0278853

102. Ihim SA, Abubakar SD, Zian Z, Sasaki T, Saffarioun M, Maleknia S, et al. Interleukin-18 cytokine in immunity, inflammation, and autoimmunity: Biological role in induction, regulation, and treatment. *Front Immunol* (2022) 4470. doi: 10.1038/nrg2484

103. Chen C, Li J, Zhang W, Shah SWA, Ishfaq M. Mycoplasma gallisepticum triggers immune damage in the chicken thymus by activating the TLR-2/MyD88/NF-κB signaling pathway and NLRP3 inflammasome. *Vet Res* (2020) 51(1):52. doi: 10.1186/s13567-020-00777-x

104. Arshad T, Mansur F, Palek R, Manzoor S, Liska V. A double edged sword role of interleukin-22 in wound healing and tissue regeneration. *Front Immunol* (2020) 11:2148. doi: 10.1098/rsbl.2010.0020

105. Gupta SK, Parlane N, Bridgeman B, Lynch AT, Dangerfield EM, Timmer MS, et al. The trehalose glycolipid C18Brar promotes antibody and T-cell immune responses to *Mannheimia haemolytica* and *Mycoplasma ovipneumoniae* whole cell antigens in sheep. *PloS One* (2023) 18:e0278853. doi: 10.1371/journal.pone.0278853

106. Wang Z, Gerstein M, Snyder M. RNA-Seq: a revolutionary tool for transcriptomics. *Nat Rev Genet* (2009) 10:57–63. doi: 10.1038/nrg2484

107. Vo TTM, Nguyen TV, Amoroso G, Ventura T, Elizur A. Deploying new generation sequencing for the study of flesh color depletion in Atlantic Salmon (*Salmo salar*). *BMC Genomics* (2021) 22:545. doi: 10.1186/s12864-021-07884-9

108. Bouwman KM, Hawley DM. Sickness behaviour acting as an evolutionary trap? Male house finches preferentially feed near diseased conspecifics. *Biol Lett* (2010) 6:462–5. doi: 10.1093/bib/bbr042

PAPER VI

Balraj Melepat, Amberleigh E. Henschen, Nithya Kuttiyarthu Veetil, Dana M. Hawley, Rami A. Dalloul, James S. Adelman and Michal Vinkler "Cytokine regulation of the house finch population-specific immune responses to an evolving pathogen, *Mycoplasma gallisepticum*". (Manuscript draft).

Title: **Cytokine regulation of the house finch population-specific immune responses to an evolving pathogen, *Mycoplasma gallisepticum***

Authors: Balraj Melepat[1], Amberleigh E. Henschen[2], Nithya Kuttiyarthu Veetil[1], Dana M. Hawley[3], Rami A. Dalloul[4], James S. Adelman[2#] and Michal Vinkler[1#*]

Addresses:

1) Charles University, Faculty of Science, Department of Zoology, Viničná 7, 128 43 Prague, Czech Republic, EU
2) The University of Memphis, Department of Biological Sciences, 3720 Alumni Ave, Memphis, TN 38152, USA
3) Virginia Tech, Department of Biological Sciences, Blacksburg, VA 24061, USA
4) The University of Georgia, Department of Poultry Science, Athens, GA 30602, USA

# These authors contributed equally

* Author for correspondence: Michal Vinkler, e-mail: michal.vinkler@natur.cuni.cz, tel.: +420221951845

Correspondence address: Michal Vinkler, Charles University, Department of Zoology, Viničná 7, 128 43 Prague, Czech Republic, EU

Abstract

During co-evolution, pathogen adaptations can rapidly alter the balance between immunity and immunopathology in hosts, selecting for reciprocal adaptations. Our previous transcriptomic research of the host-pathogen interaction between house finch (*Haemorhous mexicanus*) and its conjunctival bacterial infection *Mycoplasma gallisepticum* (MG) suggested that house finch populations differing in the length of co-evolutionary history with MG differ in the patterns of immune gene expression, indicating population-specific adaptations. In the experiment conducted under controlled conditions, birds from the populations with the longest co-evolutionary history with MG exhibited the highest tolerance to the infection (defined as disease severity per pathogen load). Here we expanded this research with a targeted RT-qPCR approach aimed at elucidating the molecular shifts in the evolution of immune regulation. We compared the gene expression patterns in key inflammatory cytokines (*IL1B* and *IL10*) with those of *BCL10*, an NFKB signaling modulator. Across four different house finch populations (Virginia, Iowa, Arizona, Hawaii), we found significant differences in the expression of *IL1B*, *IL10* and *BCL10*, dependent also on the MG isolate (original VA1994 or evolved VA2013) used for the treatment. Our results evidence that during the initial phase of immune response to MG, *IL1B* mRNA expression is up-regulated in birds from the Iowa population compared to others, while this cytokine is down-regulated in the Virginia population (both for the VA1994 and VA2013 treatment). Also, *IL10* levels are lower in Virginian birds. This indicates a decrease in activation of the inflammatory response in the Virginia population that has the longest co-evolutionary history with MG. The pattern was different for *BCL10*, where decreased levels of gene expression were consistently observed in the birds from the Iowa population. This suggests that the birds from Iowa evolved a different mechanism of tolerance to MG, activating a relatively strong cytokine response which is, however, subsequently quenched by the *BCL10* down-regulation. Our findings offer a clearer understanding of the distinct immunological pathways being differentially optimized during the evolution of tolerance to the pathogen in different host populations.

Keywords:

Adaptations diversifying populations, emerging disease, coevolution, parasite, host-pathogen interaction, inflammatory immune response, resistance, tolerance to infection

Introduction

The virulence of a pathogen is determined by the extent of damage it inflicts on the host (Casadevall and Pirofski, 1999). This virulence can either increase or decrease as a result of the co-evolutionary arms race between the host and the pathogen. Hosts employ various strategies against pathogens, such as creating barriers to infection, rapidly clearing infections, and reducing the spread of pathogens (Roy and Kirchner, 2000), while the pathogen develops countermeasures to subvert the host's defense. Such reciprocal selection involving cycles of adaptations and counter-adaptations is perpetual, with the host immune system playing a critical role in shaping the actual outcomes. One of the most ancient and also most efficient mechanisms of host immunity providing pathogen clearance is inflammation (Ashley et al., 2012; Danilova, 2006). However, inflammation acts as a double-edged sword, since the benefit of the pathogen clearance can be diminished by the harm caused by the associated self-damage and destruction of the host's tissues (Ashley et al., 2012). Therefore, evolutionary adaptations may optimize the regulatory balance in inflammation intensity. This regulation of the inflammatory response is achieved through distributed cell-to-cell communication mediated on distance through signal molecules called cytokines (Zhang and An, 2007). By their effects on the inflammatory response, the cytokines can be described as either pro- (e.g. IL1B, IL6) or anti-inflammatory (e.g. IL10). The levels of expression of the individual cytokines thus reflect the intensity of inflammation (Dinarello, 2000). The proteins involved in downstream signaling of immune regulation, such as BCL10 or NFkB also play a pivotal role in modulating immune responses by influencing cytokine production (Wang et al., 2007; Yang et al., 2021; Zhang et al., 2022). In addition to this, there are several intrinsic and extrinsic factors affect the quality and quantity of the inflammatory response reflecting the evolutionary history of the host-pathogen interactions (Adelman et al., 2013b; Horns and Hood, 2012; Okin and Medzhitov, 2012). It has been suggested that in principle the evolutionary arms race between the host and pathogen can lead the host to either of two possible response strategies: (i) evolution of resistance to the pathogen, defined as the host's improved ability to decrease the pathogen loads or (ii) evolution of tolerance to the infection, defined as host's ability to limit the damage caused by the pathogen burden (Habtewold et al., 2017; Medzhitov et al., 2012; Råberg et al., 2007). Unlike resistance that can accelerate the arms race and promote immunopathology in the host (Graham et al., 2005), the evolution of tolerance detaches the pathogen loads from the host's fitness and hence allows relaxation of the arms race evolution (Råberg et al., 2007). However, how frequent the evolution of tolerance to infection is in animals remains unknown as much as the precise adaptations in immune regulation allowing this evolutionary response to the pathogen infection. Thus, revealing specific evolutionary trajectories of immune adaptations in natural host-pathogen systems is essential to improve our understanding of the mechanisms shaping defense against diseases.

Only a limited number of well-established naturally occurring co-evolutionary systems that can provide insights into host immune adaptations to pathogens are available in vertebrates (Vinkler et al., 2018). Notable and well-documented examples include the European rabbit with the Myxoma virus (Alves et al., 2019; Kerr and Best, 1998), the co-evolution of the host-pathogen interaction led to the bats and fungus causing white-nose syndrome (Langwig et al., 2017), the lowland leopard frog with the chytrid fungus (Berger et al., 1998), and the common frog with the rana virus (Price et al., 2014). In birds, a well-studied system is formed by a wild passerine host the house finch (*Haemorhous mexicanus*) and its bacterial pathogen *Mycoplasma gallisepticum* (Adelman et al., 2013b; Bonneaud et al., 2011; Dhondt et al., 1998; Grodio et al., 2012; Hawley et al., 2005).

86 MG is a widespread pathogen of poultry, responsible for respiratory diseases of great economic significance
87 (Ley, 2008). In the 1990s the pathogen switched its host and the first cases of the infection in house finches
88 were reported in 1994 (Dhondt et al., 1998). In finches, MG causes acute conjunctivitis, which can
89 significantly decrease the visual capacities of the birds and affect their survival (Hawley et al., 2005). This
90 infection caused massive mortality that was responsible for a 60% local population decrease (Hochachka
91 and Dhondt, 2000). This host-pathogen system has been now tracked and investigated for over 25 years,
92 providing interesting data on the disease phenotype (Hotchkiss et al., 2005; Lindström et al., 2005) and
93 transmission routes (Dhondt et al., 2007), dynamics of the epidemic (Altizer et al., 2004; Dhondt et al.,
94 2005) or changes in the pathogen virulence (Adelman et al., 2013a; Grodio et al., 2012; Hawley et al., 2013).
95 An important part of the research focused also on the host, analyzing its phenotypic traits affecting
96 probability of recovery (Hill and Farmer, 2005; Nolan et al., 1998) or key immunological features of the
97 host response to the pathogen, including MG-specific antibody production (Grodio et al., 2009), leukocyte
98 frequencies in blood during the infection (Davis et al., 2004), or bacterial killing capacity of plasma (Fratto
99 et al., 2014). Importantly, recent research also described transcriptomic changes in the house finch
100 secondary lymphoid tissues (the spleen; (Bonneaud et al., 2012, 2011), and at the infection site (conjunctiva
101 and Harderian gland) (Henschen et al., 2023) and (Kuttiyarthu Veetil et al., 2024b). The local and systemic
102 immune response to MG is regulated by cytokine profile changes that have been described in blood and
103 tissues (Adelman et al., 2013b; Vinkler et al., 2018).

104 The house finch-MG coevolution has an interesting spatial-temporal dynamic. The initial cases of
105 mycoplasmosis were reported in the house finches in 1994 in the states of Maryland (MA) and Virginia
106 (VA), situated on the eastern coast of North America (Dhondt et al., 1998). In a few years, the disease
107 subsequently disseminated throughout the entire eastern United States, including Iowa (IA) or Alabama
108 (AL). Only about a decade later MG reached the western states (Washington, WA) possibly further
109 spreading towards Arizona (AZ), where the evidence of infection is not presently available. This epidemic
110 missed the geographically isolated house finch populations, such as the population introduced by humans
111 to Hawaii islands (HI) (Bonneaud et al., 2011; Henschen et al., 2023; Vinkler et al., 2018). Interestingly,
112 given the reciprocal selection between the host and the pathogen, over the thirty years of the investigation,
113 both the house finch host (Henschen et al., 2023) and the MG pathogen (Tulman et al., 2012) evolved. The
114 patterns of adaptations can be presently investigated by comparing the virulence of MG isolates obtained at
115 different locations in distinct time points and patterns of the immune response measured in different host
116 populations (Adelman et al., 2013b; Bale et al., 2020; Hawley et al., 2023; Vinkler et al., 2018). Testing
117 these interactions in wild-reared birds originating from different populations, but kept in a single animal
118 facility, previous transcriptomic research by (Henschen et al., 2023) and (Kuttiyarthu Veetil et al., 2024b)
119 revealed evolutionary adaptation towards tolerance of the MG infection in the house finch populations with
120 longest co-evolutionary history with the pathogen, compared to the populations naïve to MG or only recently
121 affected by the pathogen. Presently, however, the precise immune regulatory pathways responsible for the
122 tolerogenic response in the long-adapted populations remain unknown.

123 Here we focused on the association between expression of an immune integrative regulatory protein *BCL10*
124 and pro-inflammatory (*IL1B*) and anti-inflammatory (*IL10*) cytokine markers. *BCL10* is involved regulation
125 of the NF-kappaB signaling that plays a paramount role in the inflammatory immune response, as well as
126 in the regulation of survival and differentiation of many immune cell types (Blonska et al., 2007; Wang et
127 al., 2007; Zhang et al., 2022). In our previous transcriptomic study of the conjunctiva tissue (Kuttiyarthu
128 Veetil et al., 2024b), this gene has been revealed as differentially expressed during MG infection and also
129 differing in its pre-activation levels between the house finch populations. This makes it a promising
130 candidate for the essential role in the house finch adaptation to MG. Adopting highly sensitive RT-qPCR,
131 we develop this work through in-depth analysis of the target-gene expression within the conjunctiva tissue,

132 a secondary lymphoid that is in direct contact with MG during the infection. We examined the gene
133 expression pattern in birds originating from four different house finch populations (VA, IA, AZ and HI),
134 each characterized by a distinct evolutionary history with mycoplasmosis. The experimental birds were
135 infected with MG isolates obtained in Virginia at two different time points (VA1994) and VA2013). We
136 predicted that the *BCL10* gene expression affects the *IL1B*/*IL10* expression levels, underlying variation in
137 tolerance among the house finch populations.

138 Materials and Methods

139 *Experimental design and animals*

140 A detailed explanation of the experimental procedure is provided in our previous two experiments,
141 (Henschen et al., 2023; Kuttiyarthu Veetil et al., 2024b) so here we recapitulate it only briefly. Sixty young
142 and healthy house finches were trapped by using the mist nets and feeder traps (Pyle, 1997) between June
143 and September 2018 in Virginia, VA (Blacksburg), Iowa, IA (Ames), Arizona, AZ (Tempe) and Hawaii,
144 HI (Oahu) (15 individuals per population; details not shown). Once the birds were captured, they received
145 a uniquely numbered aluminium leg band, and their mass was determined by using an electronic balance.
146 Later the birds were dusted with 5% Sevin powder to eliminate ectoparasites and they were brought to the
147 Iowa State University animal facility. A minimum of 40 days of quarantine period was provided to all birds,
148 during which they were treated with prophylactic medications to prevent naturally occurring infections.
149 During the experiment, all birds were kept single in medium-sized flight cages (76 cm x 46 cm x 46 cm)
150 and were granted *ad libitum* access to food and water. The diet consisted of black oil sunflower seeds and
151 pellets mixed in an 80:20 ratio (Roudybush Maintenance NiblesTM; Roudybush, Inc., Woodland, CA). The
152 light-dark cycles (12h:12h) and temperatures (~22°C) were kept constant. All the animal captures and
153 experimental activities were approved by the Institutional Animal Care and Use Committees (IACUC) at
154 Iowa State University (ISU) and the ISU Institutional Biosafety Committee with appropriate permissions
155 provided by state and federal agencies (see (Henschen et al., 2023)).

156 In October 2018 the 60 individuals representing the four different house finch populations (VA, IA, AZ,
157 HI) were divided into 3 experimental groups: for each population, 5 individuals served as controls (C)
158 treated with Frey's media with 15% swine serum alone, 5 were treatment individuals inoculated with the
159 original MG isolate VA1994, and 5 were treatment individuals inoculated with the evolved MG isolate
160 VA2013. Three days post-infection (3 DPI) two observers blind to the birds' population origin and treatment,
161 did the eye scoring in all birds on a scale from 0 (no conjunctivitis) to 3 (strong pathology) at 0.5 intervals
162 (Hawley et al., 2011; Sydenstricker et al., 2006). The total eye score is calculated by combining the eye
163 score from both eyes. After eye score reading the birds were euthanised by rapid decapitation and
164 immediately a panel of 9 tissues was collected. These included the periocular conjunctiva-associated
165 lymphatic tissue samples (conjunctiva, nictitating membrane, and the adjacent skin). All tissue samples were
166 submerged in RNA protectant within 15 minutes after euthanisation and refrigerated. The cooled
167 conjunctival samples were then transported within 48 hours to Charles University, Prague, Czech Republic,
168 where they were stored frozen at -80°C until further processing.

169 *Quantitative reverse transcription polymerase chain reaction (RT-qPCR)*

170 As mentioned in our previous studies (Divín et al., 2022; Kuttiyarthu Veetil et al., 2024a) using PCR clean
171 beaded tubes (OMNI International, Kennesaw GA USA - cat. no.: 2150600) we have homogenized the
172 conjunctival tissue samples using the MagNa Lyser (Roche, Basel, Switzerland). The total RNA was

extracted using a High Pure RNA Tissue Kit.-We used Nanodrop (NanoDrop ND-1000) and Agilent 2100 Bioanalyzer with nano chip (Agilent Technologies, California, USA) to calculate the RNA yield and check for RNA integrity.

The RT-qPCR and cDNA synthesis were performed as previously described (Divín et al., 2022). For the *ILIB* and *IL10* genes, the RT-qPCR primers, probe and synthetic DNA standards were adopted (Vinkler et al., 2018). For the *BCL10* gene, the RT-qPCR primers were designed using Geneious software (http://www.geneious.com) based on a conserved avian interspecific alignment constructed from sequences downloaded from Ensemble, targeting the coding region. This gene was PCR amplified and Sanger-sequenced using cDNA from the house finch conjunctival tissue samples. The *BCL10* partial coding DNA sequences (CDS) were submitted to GenBank under the following accession numbers: OR529380-OR529393. These sequences were then used to check for any intraspecific sequence variability that could affect the RT-qPCR and the primers and probe were designed in the conserved regions, which were also covered by the designed synthetic DNA standard. The efficiency of each primer pair was calculated by constructing a calibration curve with a synthetic DNA standard (gBlocks; IDT, Coralville, IA, USA) using a dilution series of 10^8 to 10^2 copies / µl (Vinkler et al., 2018).

The total RNA extracted from the samples was diluted in molecular grade water enriched with carrier tRNA (Qiagen, cat. no. 1068337), in a 1:5 ratio for the target genes and 1:500 for the housekeeping gene which was used as the reference gene. The standards and the RNA samples were amplified using the Luna Universal Probe One-Step RT-PCR Kit (E3006, BioLabs Inc, Ipswich, MA, USA), with a final concentration of 0.6 mM and 0.2 mM for the primers and probe respectively. The cDNA synthesis and RT-qPCR quantification were conducted using a Light Cycler Instrument (Roche Diagnostics, Rotkreuz, Switzerland). All reactions were performed along with a set of template-free negative controls and freshly prepared synthetic DNA standard positive controls on each plate. The Cq (quantification cycle) values were calculated by the second derivative maximum method, and the efficiency E and Cq data were calculated using the inbuild LightCycler480 software v.1.5.1. The gene expression quantification was calculated either as standard gene expression quantity (Qst) (Vinkler et al., 2018) which allows for the comparison of gene expression between the treatments and controls or as the relative gene expression ratio (R) (Pfaffl, 2001), which specifies the measures of gene expression fold change between the treatments normalized by the controls.

We implemented the 3'- end transcriptomics QuantSeq method. The sequencing and library preparation was done at the European Molecular Biology Laboratory (EMBL), Heidelberg, Germany. The sequencing was conducted on the Illumina NextSeq 500 platform. The bioinformatics analysis was performed using the BAQCOM pipeline (https://github.com/hanielcedraz/BAQCOM). The transcriptomic data on the relative expression of the individual genes were extracted from the BioSample project Accession No. PRJNA981079.

Statistical analysis

The statistical analysis was done using the R version 4.1.0 and R-studio software version v.2021.09.0 (R Core Team, 2021; RStudio Team, 2021) The data normality distribution was checked using the Shapiro-Wilk test. Due to their non-Gaussian distribution, the Qst values were normalized using decadic logarithms (logQst). The effects of experimental treatment on gene expression changes were checked using the linear models (LMs) in the 'lme4' package, where we used the target gene expression (continuous: R or logQst) as the response variable. The correlation between the transcriptomics and RT-qPCR data was checked using

Pearson's product-moment correlation tests. The full model consists of treatment and population and the interaction between treatment and population as explanatory variables. The minimum adequate model (here defined as models with all terms significant at $p \leq 0.05$) was achieved by backward elimination of non-significant terms from the full models. The backward elimination steps were confirmed by changes in deviance between the models with an accompanying change in degrees of freedom using the Akaike information criterion for identification of the exclusion terms and ANOVA, with F-statistics for testing the significance. The post-hoc test for multiple mean comparisons among different populations and treatment groups is done using the TukeyHSD test. The variation in gene expression between the populations and treatment groups was plotted as boxplots using the ggplot2 package. The correlation matrix was visualised using the corrplot package.

Results

Correlations between the transcriptomic and RT-qPCR gene expression data

First, we tested correlations between the normalized gene expression data from the RT-qPCR (Qst) and transcriptomics obtained for the *IL1B*, *IL10* and *BCL10* genes across the whole dataset (Table1, Figure1). Our results demonstrated a highly significant correlation between the RT-qPCR expression data of *IL1B* gene with the QuantSeq data of *IL1B* gene expression ($r = 0.556$, $p \ll 0.001$, Table1, Figure1). For the *IL10* gene also the correlation between the RT-qPCR and QuantSeq data was highly significant ($r = 0.526$, $p \ll 0.001$, Table1, Figure1). The *IL10* gene RT-qPCRRT-qPCR expression data also showed a highly significant correlation with the RT-qPCR data of the *IL1B* gene ($r = 0.569$, $p \ll 0.001$, Table, Figure1). For the *BCL10* gene expression, there was no significant correlation demonstrated between the RT-qPCR data and the QuantSeq data ($r = 0.116$, $p = 0.413$, Table 1, Figure 1). Yet, the *BCL10* RT-qPCR gene expression data displayed a significant correlation with the RT-qPCR data of *IL1B* gene expression ($r = 0.294$, $p = 0.034$, Table 1, Figure 1).

Figure 1. **Correlations between gene expression levels revealed by RT-qPCR and QuantSeq in house finch conjunctiva 3 days after inoculation with MG.** In the elliptical correlation plot, the circular shapes indicate no correlation, narrow ellipses indicate a strong correlation, tilted to the right indicates a positive correlation and tilted to the left indicates a negative correlation; the blue color represents a positive correlation, red color represents negative correlation, the intensity of color indicates the strength of the correlation.

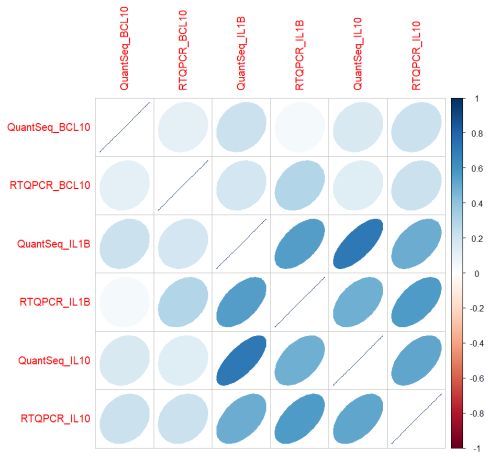

Table 1. **Correlations between gene expression levels with core values and P values revealed by RT-qPCR and QuantSeq in house finch conjunctiva 3 days after inoculation with MG**. Above the diagonal P values are given and below the diagonal core (r) values are given.

	QuantSeq_BCL10	RT-qPCR BCL10	QuantSeq_IL1B	RT-qPCR_IL1B	QuantSeq_IL10	RT-qPCR _IL10	
QuantSeq_BCL10	**1.000**	0.413	0.128	0.755	0.247	0.119	
RT-qPCR BCL10	0.116	**1.000**	0.189	0.034	0.325	0.130	**P-Values**
QuantSeq_IL1B	0.214	0.185	**1.000**	<<0.001	<<0.001	<<0.001	
RT-qPCR IL1B	0.044	0.294	0.556	**1.000**	<<0.001	<<0.001	
QuantSeq_IL10	0.163	0.139	0.719	0.480	**1.000**	<<0.001	
RT-qPCR _IL10	0.219	0.213	0.492	0.569	0.526	**1.000**	
Core-Values							

Cytokines and *BCL10* gene expression

Table 2. The minimum adequate model with degree of freedom, F-value and P-value for Cytokines and *BCL10* gene expression

	MAM /Variables	DF	F	P
MAM1	IL1B_Expression ~ Treatment + Population	4/35	23.291	<<0.001
	Treatment	1/35	4.222	0.047
	Population	3/35	29.648	<<0.001
MAM2	IL10_Expression ~ Population	3/36	15.550	<<0.001
MAM3	BCL10_Expression ~ Treatment + Population	4/35	15.429	<<0.001
	Treatment	4/35	8.703	0.006
	Population	3/35	17.671	<<0.001

The R expression values of the *IL1B* gene were compared across the 4 different populations (VA, IA, AZ, HI) and two treatment groups (VA1994 and VA2013). We found a statistically significant difference in the expression of *IL1B* among house finch populations (MAM1, Population: $p << 0.001$; Table 2, Figure 2) and between the treatment groups (MAM1, Treatment: $p = 0.047$; Table 1, Figure 2). Our analysis did not reveal any significant interaction between treatment and population groups. Further post-hoc analysis showed a significant difference in *IL1B* gene expression between birds from the VA population (treated with either the VA1994 or the VA2013 isolate) and the IA population (again, treated either with the VA1994 or the VA2013; TukeyHSD: in all cases $p <<0.001$; Table 3, Figure 2), consistent with strong up-regulation of *IL1B* in IA. The VA individuals treated with the VA1994 isolate exhibited down-regulation of *IL1B* expression compared to birds from the HI population treated with both the VA1994 isolate (TukeyHSD: $p = 0.005$) and VA2013 isolate (TukeyHSD: $p = 0.016$), and also compared with birds from the AZ population treated with the VA2013 isolate (TukeyHSD: $p = 0.019$; Table 3, Figure 2). At the same time, the IA

population treated with VA2013 isolate showed a significant up-regulation of the *IL1B* expression compared to the AZ birds treated with both VA1994 (TukeyHSD: p <<0.001), and VA2013 isolate (TukeyHSD: p = 0.004), and also with the HI birds treated with both VA1994 (TukeyHSD: p = 0.015), and VA2013 (TukeyHSD: p = 0.005; Table 3, Figure 2) isolates. (This pattern was to a lesser extent consistent also for the birds from the IA population inoculated with the VA1994 isolate (TukeyHSD: AZ_VA2013 p = 0.082; AZ_VA1994 p = 0.001; HI_VA2013 p= 0.091; Table 3, Figure 2). The results for Qst values are consistent with the results based on R (data not shown).

Table 3. Tukey multiple comparisons of means with p-adjusted values for *IL1B* gene expression in the conjunctiva in the four house finch populations treated with the two different MG treatments. A total of 60 birds, 15 birds from each population (5 control, 5 VA1994 treatment, 5 VA2013 treatment). Difference = Difference between the means, Lower bound = Lower bound of a confidence interval, Upper bound = Upper bound of a confidence interval. Padj= Adjusted P value.

Population_Treatement	Difference	Lower Bound	Upper Bound	Padj-value
AZ_VA94-AZ_VA13	-0.940	-2.638	0.757	0.628
HI_VA13-AZ_VA13	0.026	-1.672	1.723	1.000
HI_VA94-AZ_VA13	0.253	-1.444	1.951	1.000
IA_VA13-AZ_VA13	2.214	0.517	3.912	0.004
IA_VA94-AZ_VA13	1.583	-0.115	3.280	0.082
VA_VA13-AZ_VA13	-1.101	-2.798	0.597	0.436
VA_VA94-AZ_VA13	-1.911	-3.608	-0.213	0.019
HI_VA13-AZ_VA94	0.966	-0.732	2.663	0.597
HI_VA94-AZ_VA94	1.193	-0.504	2.891	0.337
IA_VA13-AZ_VA94	3.154	1.457	4.852	<<0.001
IA_VA94-AZ_VA94	2.523	0.825	4.220	0.001
VA_VA13-AZ_VA94	-0.161	-1.858	1.537	1.000
VA_VA94-AZ_VA94	-0.971	-2.668	0.727	0.591
HI_VA94-HI_VA13	0.227	-1.470	1.925	1.000
IA_VA13-HI_VA13	2.188	0.491	3.886	0.005
IA_VA94-HI_VA13	1.557	-0.141	3.255	0.091
VA_VA13-HI_VA13	-1.126	-2.824	0.571	0.407
VA_VA94-HI_VA13	-1.936	-3.634	-0.239	0.016
IA_VA13-HI_VA94	1.961	0.263	3.659	0.015
IA_VA94-HI_VA94	1.330	-0.368	3.027	0.217
VA_VA13-HI_VA94	-1.354	-3.051	0.344	0.199
VA_VA94-HI_VA94	-2.164	-3.861	-0.466	0.005
IA_VA94-IA_VA13	-0.631	-2.329	1.066	0.925
VA_VA13-IA_VA13	-3.315	-5.012	-1.617	<<0.001
VA_VA94-IA_VA13	-4.125	-5.822	-2.427	<<0.001
VA_VA13-IA_VA94	-2.683	-4.381	-0.986	<<0.001
VA_VA94-IA_VA94	-3.493	-5.191	-1.796	<<0.001
VA_VA94-VA_VA13	-0.810	-2.508	0.887	0.777

Figure 2. **Variation in relative expression changes of *IL1B* in the conjunctiva in the four house finch populations treated with the two different MG treatments.** At the y-axis, the *IL1B* mRNA expression is shown in R values indicating relative fold change in treatments compared to controls. At the x-axis, the four house finch populations are shown: VA = Virginia, IA = Iowa, AZ = Arizona, HI = Hawaii. The two MG treatments are differentiated in color: VA1994 = orange, VA2013 = red.

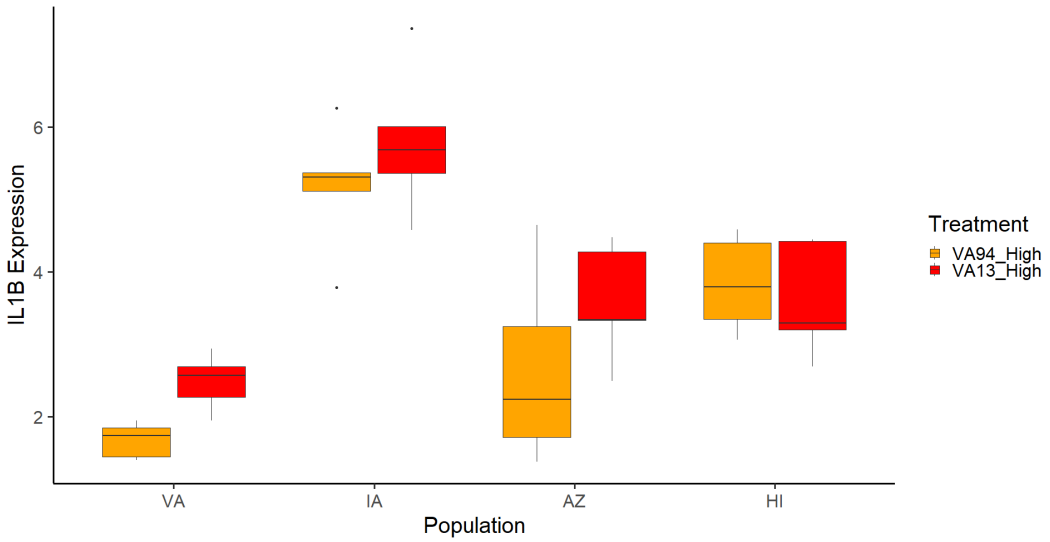

The R expression values of the *IL10* gene were compared across the 4 different populations (VA, IA, AZ, HI) and two treatment groups (VA1994 and VA2013). The *IL10* gene expression showed significant differences among the different house finch populations ($p << 0.001$, Population, MAM2, Table 2, Figure 3) but not among the different treatment groups. However, the gene expression pattern did not exhibit any significant interaction between the population and treatment groups. However, among the VA1994 isolate-treated birds, the VA population showed a significant down-regulation in the *IL10* gene expression compared to the IA population ($p = 0.014$, TukeyHSD) and AZ population ($p << 0.001$, TukeyHSD) and marginally non-significant down-regulation in *IL10* expression with respect to the HI population of house finches ($p = 0.068$, TukeyHSD, Table 4, Figure 3). The AZ population treated with 2013 isolate of the mycoplasma also demonstrated a significant up-regulation in the *IL10* gene expression compared to the VA population treated with both VA2013 ($p = 0.018$, TukeyHSD), and VA1994 ($p = 0.001$, TukeyHSD, Table 4, Figure 3), isolates of mycoplasma. Also, the AZ population treated with VA1994 showed an up-regulation in the *IL10* gene expression compared to the VA population treated with the VA2013 isolate of mycoplasma ($p = 0.002$, TukeyHSD, Table 4, Figure 3). The Iowa population treated with the VA2013 isolate also displayed a significant up-regulation in the *IL10* gene expression compared to the VA population of birds treated with the VA1994 isolate ($p = 0.017$, TukeyHSD, Table 4, Figure 3). The results for Qst values are consistent with the results based on R (data not shown).

Table 4. Tukey multiple comparisons of means with p values for *IL10* gene expression in the conjunctiva in the four house finch populations treated with the two different MG treatments. A total of 60 birds, 15 birds from each population (5 control, 5 VA1994 treatment, 5 VA2013 treatment). Difference = Difference between the means, Lower bound = Lower bound of a confidence interval, Upper bound = Upper bound of a confidence interval. Padj= Adjusted P value.

331

Population_Treatement	Difference	Lower Bound	Upper Bound	Padj-value
AZ_VA94-AZ_VA13	0.485	-1.483	2.452	0.992
HI_VA13-AZ_VA13	-1.014	-2.982	0.953	0.706
HI_VA94-AZ_VA13	-0.912	-2.879	1.056	0.801
IA_VA13-AZ_VA13	-0.569	-2.536	1.399	0.980
IA_VA94-AZ_VA13	-0.516	-2.483	1.452	0.988
VA_VA13-AZ_VA13	-2.219	-4.186	-0.251	0.018
VA_VA94-AZ_VA13	-2.795	-4.763	-0.828	0.001
HI_VA13-AZ_VA94	-1.499	-3.467	0.468	0.245
HI_VA94-AZ_VA94	-1.397	-3.364	0.571	0.325
IA_VA13-AZ_VA94	-1.054	-3.021	0.914	0.666
IA_VA94-AZ_VA94	-1.001	-2.968	0.967	0.719
VA_VA13-AZ_VA94	-2.703	-4.671	-0.736	0.002
VA_VA94-AZ_VA94	-3.280	-5.248	-1.313	<<0.001
HI_VA94-HI_VA13	0.102	-1.865	2.070	1.000
IA_VA13-HI_VA13	0.446	-1.522	2.413	0.995
IA_VA94-HI_VA13	0.498	-1.469	2.466	0.991
VA_VA13-HI_VA13	-1.204	-3.172	0.763	0.508
VA_VA94-HI_VA13	-1.781	-3.749	0.186	0.099
IA_VA13-HI_VA94	0.343	-1.624	2.311	0.999
IA_VA94-HI_VA94	0.396	-1.572	2.364	0.998
VA_VA13-HI_VA94	-1.307	-3.274	0.661	0.406
VA_VA94-HI_VA94	-1.883	-3.851	0.084	0.069
IA_VA94-IA_VA13	0.053	-1.915	2.020	1.000
VA_VA13-IA_VA13	-1.650	-3.617	0.318	0.154
VA_VA94-IA_VA13	-2.227	-4.194	-0.259	0.018
VA_VA13-IA_VA94	-1.703	-3.670	0.265	0.130
VA_VA94-IA_VA94	-2.279	-4.247	-0.312	0.014
VA_VA94-VA_VA13	-0.577	-2.544	1.391	0.978

332

333 **Figure 4. Variation in relative expression changes of *IL10* in the conjunctiva in the four house finch**
334 **populations treated with the two different MG treatments.** At the y-axis, the *IL10* mRNA expression is
335 shown in R values indicating relative fold change in treatments compared to controls. At the x-axis, the four
336 house finch populations are shown: VA = Virginia, IA = Iowa, AZ = Arizona, HI = Hawaii. The two MG
337 treatments are differentiated in color: VA1994 = orange, VA2013 = red.

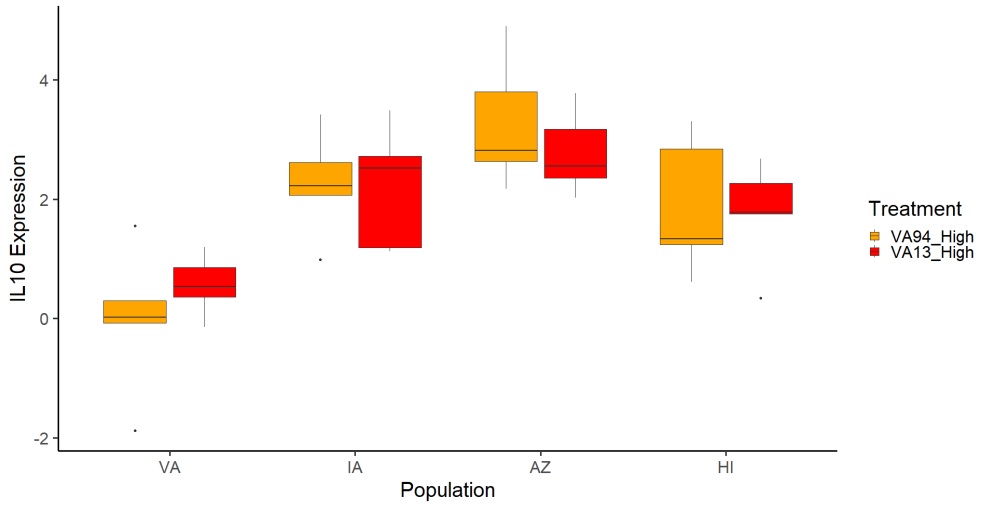

The R expression values of the *BCL10* gene were compared across the 4 different populations (VA, IA, AZ, HI) and two treatment groups (VA1994 and VA2013). The *BCL10* gene also showed a significant difference in the expression, among the various house finch populations ($p << 0.001$, MAM3, Table 2, Figure 4) and between the two treatment groups ($p = 0.006$, MAM3, Table 1, Figure 4). However, the interaction between treatments and populations did not display any significant difference in the *BCL10* expression. However, we found significant down-regulation of the *BCL10* expression in the IA population of birds treated with the VA2013 isolate in comparison with the VA ($p = 0.001$, TukeyHSD), AZ ($p << 0001$, TukeyHSD), and HI ($p = 0.001$, TukeyHSD, Table 5, Figure 4) populations from the same treatment group. The IA population of birds treated with the VA2013 isolate of mycoplasma also showed significant down-regulation in the *BCL10* gene expression compared to the VA1994 isolates of the AZ population ($p = 0.004$, TukeyHSD, Table 5, Figure 4). The VA1994 treated IA population showed a significant down-regulation of the *BCL10* gene, compared to the VA population treated with VA2013 isolate ($p = 0.001$, TukeyHSD), and the AZ population treated with both VA1994 ($p = 0.004$, TukeyHSD) and VA2013 ($p << 0001$, TukeyHSD, Table 5, Figure 4) isolates. There is a marginally non-significant up-regulation of the *BCL10* gene expression found in the AZ birds treated with VA2013 isolate compared to the HI population of birds treated with VA1994 isolate of mycoplasma ($p = 0.072$, TukeyHSD, Table 5, Figure 4). The results for Qst values are consistent with the results based on R (data not shown).

Table 5. Tukey multiple comparisons of means with p values for *BCL10* gene expression in the conjunctiva in the four house finch populations treated with the two different MG treatments. A total of 60 birds, 15 birds from each population (5 control, 5 VA1994 treatment, 5 VA2013 treatment). Difference = Difference between the means, Lower bound = Lower bound of a confidence interval, Upper bound = Upper bound of a confidence interval. Padj= Adjusted P value.

Population_Treatement	Difference	Lower Bound	Upper Bound	Padj-value
AZ_VA94-AZ_VA13	-0.579	-2.008	0.849	0.887
HI_VA13-AZ_VA13	-0.373	-1.801	1.056	0.989
HI_VA94-AZ_VA13	-1.358	-2.787	0.070	0.072
IA_VA13-AZ_VA13	-2.446	-3.875	-1.018	<< 0.001
IA_VA94-AZ_VA13	-2.463	-3.892	-1.035	<< 0.001
VA_VA13-AZ_VA13	-0.331	-1.760	1.097	0.994

VA_VA94-AZ_VA13	-1.368	-2.796	0.061	0.069
HI_VA13-AZ_VA94	0.206	-1.222	1.635	1.000
HI_VA94-AZ_VA94	-0.779	-2.207	0.650	0.646
IA_VA13-AZ_VA94	-1.867	-3.295	-0.438	0.004
IA_VA94-AZ_VA94	-1.884	-3.312	-0.455	0.004
VA_VA13-AZ_VA94	0.248	-1.180	1.677	0.999
VA_VA94-AZ_VA94	-0.788	-2.217	0.640	0.633
HI_VA94-HI_VA13	-0.985	-2.414	0.443	0.360
IA_VA13-HI_VA13	-2.073	-3.502	-0.645	0.001
IA_VA94-HI_VA13	-2.090	-3.519	-0.662	0.001
VA_VA13-HI_VA13	0.042	-1.387	1.470	1.000
VA_VA94-HI_VA13	-0.995	-2.423	0.434	0.348
IA_VA13-HI_VA94	-1.088	-2.517	0.340	0.245
IA_VA94-HI_VA94	-1.105	-2.534	0.323	0.229
VA_VA13-HI_VA94	1.027	-0.402	2.455	0.310
VA_VA94-HI_VA94	-0.010	-1.438	1.419	1.000
IA_VA94-IA_VA13	-0.017	-1.445	1.412	1.000
VA_VA13-IA_VA13	2.115	0.687	3.544	0.001
VA_VA94-IA_VA13	1.079	-0.350	2.507	0.255
VA_VA13-IA_VA94	2.132	0.704	3.561	0.001
VA_VA94-IA_VA94	1.096	-0.333	2.524	0.238
VA_VA94-VA_VA13	-1.036	-2.465	0.392	0.299

Figure 4. **Variation in relative expression changes of *BCL10* in the conjunctiva in the four house finch populations treated with the two different MG treatments.** At the y-axis, the *BCL10* mRNA expression is shown in R values indicating relative fold change in treatments compared to controls. At the x-axis, the four house finch populations are shown: VA = Virginia, IA = Iowa, AZ = Arizona, HI = Hawaii. The two MG treatments are differentiated in color: VA1994 = orange, VA2013 = red.

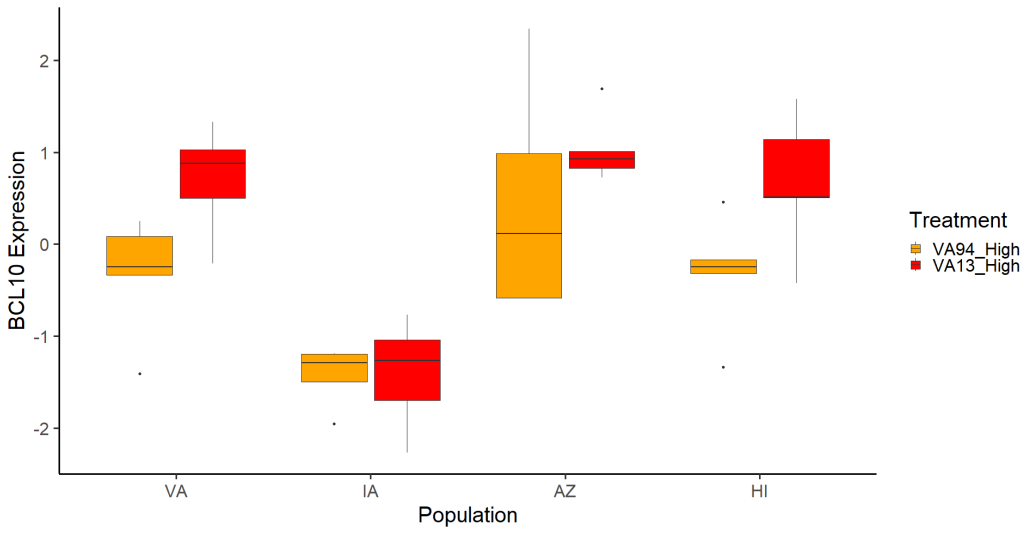

386 # Discussion

387 For the past three decades, a novel infection of mycoplasma evolved to cause severe conjunctivitis in the
388 house finch. Here we used RT-qPCR analysis to reveal the evolving nature of the molecular regulation of
389 the host immune system. Developing our previous transcriptomic research showing that birds from the
390 populations with the longest co-evolutionary history with MG exhibit the highest tolerance to MG, we
391 compared the expression patterns of two cytokines (*IL1B* and *IL10*) and a signal integrator, *BCL10* in
392 conjunctiva on the 3rd-day post inoculation. We revealed highly significant correlations between the RT-
393 qPCR and QuantSeq expression data for the key cytokine genes (*IL1B* and *IL10*). The expression of the
394 signal modulator *BCL10* was linked to *IL1B* gene expression. Across the four different house finch
395 populations (VA, IA, AZ, HI), we found statistically significant differences in the expression of *IL1B*, *IL10*
396 and *BCL10*, dependent on the MG isolate (original VA1994 or evolved VA2013) used for the treatment.
397 Post-hoc analysis indicated significant up-regulation in *IL1B* mRNA expression in the birds from the IA
398 population, especially strong when compared to the VA population which showed down-regulation
399 compared to all other populations (both for the VA1994 and VA2013 treatment). Also, for *IL10* the birds
400 from the VA population showed decreased levels of gene expression compared to other populations. This
401 indicates a decrease in activation of the inflammatory response in the VA population that has experienced
402 the longest co-evolutionary history with MG. The pattern was different for *BCL10*, where decreased levels
403 of gene expression were consistently observed in the birds from the IA population. Given their relatively
404 high *IL1B* levels, this suggests that the IA birds activated a relatively strong cytokine response to MG, but
405 the inflammation was subsequently decreased downstream by the *BCL10* down-regulation. This suggests
406 distinct molecular mechanisms involved in the evolution of tolerance in different house finch populations.

407 In our prior research, we explored the differential gene expression in conjunctiva during an immune
408 response to MG between birds originating from distinct house finch populations using 3'-end transcriptomic
409 sequencing (QuantSeq) (Kuttiyarthu Veetil et al., 2024b). We showed that MG triggers strong pro-
410 inflammatory signaling that can affect T-cell activation, and IL17 pathway differentiation, along with
411 decreasing the IL12/IL23 pathway signaling. The VA house finches that have the longest co-evolutionary
412 history with MG, activate higher expression of anti-inflammatory genes and Th1 mediators than birds from
413 other populations, which may explain their relative tolerance to MG. Here we used the same conjunctiva
414 samples from the experiment in which we collected the tissue during the initial phase of the infection, three
415 days post-inoculation and supplemented the transcriptomics with RT-qPCR focusing on selected immune-
416 related genes which were found differentially expressed in the QuantSeq results or which are key to reveal
417 the immune regulatory mechanism.

418 First, the comparison of the QuantSeq and RT-qPCR data supported high consistency in the expression
419 patterns of the pro-inflammatory cytokine *IL1B* and anti-inflammatory cytokine *IL10*. *IL1B* and *IL10* RT-
420 qPCR levels were also correlated. This is in agreement with the previous findings by (Vinkler et al., 2018),
421 showing correlations between different inflammation-related cytokines in the house finches infected with
422 MG. Although we did not find any significant correlation between the QuantSeq and RT-qPCR gene
423 expression levels of *BCL10*, our analysis evidenced a weak, but significant positive correlation between
424 *BCL10* expression and expression of *IL1B* determined using RT-qPCR. This supports the idea that *BCL10*
425 is in the house finch up-regulated during the MG infection in the same way as other inflammatory genes,
426 but the interaction is weak and affected by variability between the individuals. Analyzing the RT-qPCR
427 patterns of the gene expression in response to MG, we revealed important differences among the four
428 different house finch populations. However, the gene expression patterns obtained for the two MG isolates
429 (the original VA1994 isolate and the evolutionarily derived VA2013) used to describe the effects of
430 pathogen evolution were surprisingly similar. Previous research has shown that MG evolves by increasing
431 its virulence (Hawley et al., 2013), causing more pathology, but also triggering stronger immune responses

(Vinkler et al., 2018). This has been observed on the transcriptomic level also in our experiment, where the evolved MG isolate elicited a stronger immune response compared to the original isolate (Henschen et al., 2023; Kuttiyarthu Veetil et al., 2024b). This result is consistent with the RT-qPCR data because the *IL1B* and *BCL10* levels were generally higher after inoculation with the VA2013 isolate than during the response to the VA1994 isolate. Yet, the pattern of inter-populational differences was in the house finches mostly consistent between the two MG treatments, which is supported by the lack of any significant interaction between the population and the treatment.

During the initial response to MG, birds from the VA population triggered significantly weaker expression of *IL1B* than individuals from the other populations. This can be indicative of a weaker pro-inflammatory response that is consistent with tolerogenic adaptation to MG in this population with a long co-evolutionary history with MG. To our surprise individuals originating from the IA population, which has a co-evolutionary history with MG only a few years shorter, showed stronger *IL1B* expression during the immune response to MG, when compared to the HI and AZ birds. Given the known tolerance to MG in the IA population (Henschen et al. 2023), this is an unexpected result, because high *IL1B* expression typically indicates activation of a strong inflammation (Vinkler et al., 2018) that can cause severe tissue damage harming the host (Ashley et al., 2012). However, a previous study mentioned that the pathogen load and immune-related gene expressions are not directly related in house finch populations (Bonneaud et al., 2011). Additionally, our prior research has demonstrated that inflammatory responses can vary across different tissues in house finches and avian species more broadly (Kuttiyarthu Veetil et al., 2024b, 2024a). Notably, the AZ population with short or no evolutionary history with the MG and the entirely naïve HI population showed comparable levels of *IL1B* gene expression.

Similar to *IL1B*, also the anti-inflammatory cytokine *IL10* had the lowest expression in the VA population, in particular when the birds were treated with the original MG isolate VA1994. This result is consistent with several previous studies in the house finch populations with slight changes (Adelman et al., 2013b; Bonneaud et al., 2011; Vinkler et al., 2018). Adelman et al (2013b) (Adelman et al., 2013b) found that after the first 24 hours of MG infection, the house finches from Alabama that also have a relatively long co-evolutionary history with MG experienced lower fever, and activated lower levels of the pro-inflammatory signaling through IL1B, but higher anti-inflammatory signaling through IL10 compared to the Arizona population lacking the experience with the MG pathogen. Compared to this study, in our VA population, the anti-inflammatory signaling mediated by *IL10* was not increased. The lowered *IL10* expression can be either a reciprocated effect of the reduced *IL1B* expression as previously described in mice and human cell line studies (De Waal Malefyt et al., 1991; Sun et al., 2019) or it can be part of the tolerance adaptation in the VA population.

The house finches from the AZ and HI populations with little or no co-evolutionary history with MG (Henschen et al., 2023), displayed a similar expression of *IL10* as IA, which may be part of the general regulation of the *IL1B* pro-inflammatory pathway. Although the expression of these two cytokines is antagonistic in nature (Sun et al., 2019), the *IL10* feedback probably helps to regulate over-responsive inflammation.

Finally, our previous research (Kuttiyarthu Veetil et al., 2024b) identified the possible immunomodulating role of *BCL10* in the emergence of tolerance to MG. BCL10 is a positive regulator of B- and T-cells that activates NFKB signaling (Blonska et al., 2007; Xue et al., 2003). In primary mouse embryonic fibroblasts, the *BCL10* expression positively stimulates the proinflammatory interleukins (Jiang et al., 2016). The BCL10 also plays a crucial role in the development and suppressive function of regulatory T cells (Yang et al., 2021). Compared to birds from VA and the other populations, IA birds showed a decrease in the *BCL10* mRNA expression during the MG infection. Contrasting the *BCL10* and *IL1B* patterns, our results suggest

that the birds from IA evolved a different mechanism of tolerance to MG than the VA birds. While in VA the population adaptively decreased the very expression of the pro-inflammatory signals, the IA population still activates a relatively strong pro-inflammatory cytokine response upon the MG infection. However, this response is subsequently quenched by the *BCL10* down-regulation, weakening the overall inflammatory immune response that harms to host health.

Conclusion

To conclude, our study contributes to the understanding of the diverse evolutionary paths of molecular immune adaptations in the hosts. In the house finch, our results suggest distinct parallel adaptations providing the host tolerance to MG. Both adaptive patterns of the inflammatory gene expression emerged in the house finch populations with a long co-evolutionary history with the pathogen. In VA the birds manage to down-regulate the proinflammatory signaling mediated by *IL1B* while in IA they up-regulate *IL1B*, down-regulating also the signal integrator *BCL10*. Both these population-specific adaptations appear to contribute to the tolerance to MG (mild pathology despite high pathogen loads). Our findings offer clearer insight into the house finch adaptations against the MG-induced immunopathology and contribute to the general understanding of host evolutionary responses to pathogen virulence increase.

Acknowledgement

We would like to thank all the research assistants who helped with the fieldwork (especially Marissa Langager and Allison Rowley) and the subsequent laboratory analysis. We are also grateful to P. Hutton and K. McGraw (Arizona State University), and S. Goldstein, P. Howard, and J. Omick (Hawaii USDA) for their help with logistics in the field. The birds were trapped, and the experiment was performed within the framework of project No. 1755197 (Iowa State University), NSF 1950307 (University of Memphis) and No. 1754872 (Virginia Tech) (title 'Collaborative Research: Immune mechanisms and epidemiological consequences of tolerance in a naturally occurring host-pathogen system') supported by the U.S. National Science Foundation. This study was supported by the Grant Schemes at Charles University (grant nos. GAUK 646119 and START/SCI/113 with reg. no. CZ.02.2.69/0.0/0.0/19_073/0016935) and by the Ministry of Education, Youth and Sports of the Czech Republic (INTER-ACTION grant no. LUAUS24184. The study was further supported by Institutional Research Support No. 260684/2023.

Author contributions

Conceptualization: BM, AEH, RAD, DMH, JSA, MV

Data Curation: BM, AEH, DMH, JSA

Formal Analysis: BM, NKV

Funding Acquisition: MV, BM, NKV, RAD, DMH, JSA

Investigation: BM, NKV, AEH, RAD, DMH, JSA, MV

Methodology: BM, AEH, VB, RAD, DMH, JSA, MV

Project Administration: BM, AEH, DMH, JSA, MV

Resources: MV, RAD, DMH, JSA

Software: n/a

Supervision: AEH, RAD, DMH, JSA, MV

Validation: BM, AEH, RAD, DMH, JSA, MV

Visualization: BM

Writing – Original Draft Preparation: BM, MV

Writing – Review and Editing: BM, NKV, AEH, RAD, VB, DMH, JSA, MV

Ethics statement

All animal work was approved by the Institutional Animal Care and Use Committees (IACUC) at Iowa State University (ISU) and Virginia Tech, and the ISU Institutional Biosafety Committee with appropriate permissions provided by state and federal agencies.

Reference

Adelman, J.S., Carter, A.W., Hopkins, W.A., Hawley, D.M., 2013a. Deposition of pathogenic *Mycoplasma gallisepticum* onto bird feeders: host pathology is more important than temperature-driven increases in food intake. Biol. Lett. 9, 20130594. https://doi.org/10.1098/rsbl.2013.0594

Adelman, J.S., Kirkpatrick, L., Grodio, J.L., Hawley, D.M., 2013b. House Finch Populations Differ in Early Inflammatory Signaling and Pathogen Tolerance at the Peak of *Mycoplasma gallisepticum* Infection. The American Naturalist 181, 674–689. https://doi.org/10.1086/670024

Altizer, S., Hochachka, W.M., Dhondt, A.A., 2004. Seasonal dynamics of mycoplasmal conjunctivitis in eastern North American house finches. Journal of Animal Ecology 73, 309–322. https://doi.org/10.1111/j.0021-8790.2004.00807.x

Alves, J.M., Carneiro, M., Cheng, J.Y., Lemos De Matos, A., Rahman, M.M., Loog, L., Campos, P.F., Wales, N., Eriksson, A., Manica, A., Strive, T., Graham, S.C., Afonso, S., Bell, D.J., Belmont, L., Day, J.P., Fuller, S.J., Marchandeau, S., Palmer, W.J., Queney, G., Surridge, A.K., Vieira, F.G., McFadden, G., Nielsen, R., Gilbert, M.T.P., Esteves, P.J., Ferrand, N., Jiggins, F.M., 2019. Parallel adaptation of rabbit populations to myxoma virus. Science 363, 1319–1326. https://doi.org/10.1126/science.aau7285

Ashley, N.T., Weil, Z.M., Nelson, R.J., 2012. Inflammation: Mechanisms, Costs, and Natural Variation. Annu. Rev. Ecol. Evol. Syst. 43, 385–406. https://doi.org/10.1146/annurev-ecolsys-040212-092530

Bale, N.M., Leon, A.E., Hawley, D.M., 2020. Differential house finch leukocyte profiles during experimental infection with *Mycoplasma gallisepticum* isolates of varying virulence. Avian Pathology 49, 342–354. https://doi.org/10.1080/03079457.2020.1753652

Berger, L., Speare, R., Daszak, P., Green, D.E., Cunningham, A.A., Goggin, C.L., Slocombe, R., Ragan, M.A., Hyatt, A.D., McDonald, K.R., Hines, H.B., Lips, K.R., Marantelli, G., Parkes, H., 1998. Chytridiomycosis causes amphibian mortality associated with population declines in the rain forests of Australia and Central America. Proc. Natl. Acad. Sci. U.S.A. 95, 9031–9036. https://doi.org/10.1073/pnas.95.15.9031

554 Blonska, M., Pappu, B.P., Matsumoto, R., Li, H., Su, B., Wang, D., Lin, X., 2007. The CARMA1-Bcl10
555 Signaling Complex Selectively Regulates JNK2 Kinase in the T Cell Receptor-Signaling Pathway.
556 Immunity 26, 55–66. https://doi.org/10.1016/j.immuni.2006.11.008
557 Bonneaud, C., Balenger, S.L., Russell, A.F., Zhang, J., Hill, G.E., Edwards, S.V., 2011. Rapid evolution of
558 disease resistance is accompanied by functional changes in gene expression in a wild bird. Proc.
559 Natl. Acad. Sci. U.S.A. 108, 7866–7871. https://doi.org/10.1073/pnas.1018580108
560 Bonneaud, C., Balenger, S.L., Zhang, J., Edwards, S.V., Hill, G.E., 2012. Innate immunity and the evolution
561 of resistance to an emerging infectious disease in a wild bird. Molecular Ecology 21, 2628–2639.
562 https://doi.org/10.1111/j.1365-294X.2012.05551.x
563 Casadevall, A., Pirofski, L., 1999. Host-Pathogen Interactions: Redefining the Basic Concepts of Virulence
564 and Pathogenicity. Infect Immun 67, 3703–3713. https://doi.org/10.1128/IAI.67.8.3703-
565 3713.1999
566 Danilova, N., 2006. The evolution of immune mechanisms. J. Exp. Zool. 306B, 496–520.
567 https://doi.org/10.1002/jez.b.21102
568 Davis, A.K., Cook, K.C., Altizer, S., 2004. Leukocyte Profiles in Wild House Finches with and without
569 Mycoplasmal Conjunctivitis, a Recently Emerged Bacterial Disease. EcoHealth 1, 362–373.
570 https://doi.org/10.1007/s10393-004-0134-2
571 De Waal Malefyt, R., Abrams, J., Bennett, B., Figdor, C.G., De Vries, J.E., 1991. Interleukin 10(IL-10)
572 inhibits cytokine synthesis by human monocytes: an autoregulatory role of IL-10 produced by
573 monocytes. The Journal of experimental medicine 174, 1209–1220.
574 https://doi.org/10.1084/jem.174.5.1209
575 Dhondt, A.A., Altizer, S., Cooch, E.G., Davis, A.K., Dobson, A., Driscoll, M.J.L., Hartup, B.K., Hawley, D.M.,
576 Hochachka, W.M., Hosseini, P.R., Jennelle, C.S., Kollias, G.V., Ley, D.H., Swarthout, E.C.H.,
577 Sydenstricker, K.V., 2005. Dynamics of a novel pathogen in an avian host: Mycoplasmal
578 conjunctivitis in house finches. Acta Tropica 94, 77–93.
579 https://doi.org/10.1016/j.actatropica.2005.01.009
580 Dhondt, A.A., Dhondt, K.V., Hawley, D.M., Jennelle, C.S., 2007. Experimental evidence for transmission of
581 *Mycoplasma gallisepticum* in house finches by fomites. Avian Pathology 36, 205–208.
582 https://doi.org/10.1080/03079450701286277
583 Dhondt, A.A., Tessaglia, D.L., Slothower, R.L., 1998. Epidemic mycoplasmal conjunctivitis in house finches
584 from eastern North America. J Wildl Dis 34, 265–280. https://doi.org/10.7589/0090-3558-
585 34.2.265
586 Dinarello, C.A., 2000. Proinflammatory Cytokines. Chest 118, 503–508.
587 https://doi.org/10.1378/chest.118.2.503
588 Divín, D., Goméz Samblas, M., Kuttiyarthu Veetil, N., Voukali, E., Świderská, Z., Krajzingrová, T., Těšický,
589 M., Beneš, V., Elleder, D., Bartoš, O., Vinkler, M., 2022. Cannabinoid receptor 2 evolutionary
590 gene loss makes parrots more susceptible to neuroinflammation. Proc. R. Soc. B. 289, 20221941.
591 https://doi.org/10.1098/rspb.2022.1941
592 Fratto, M., Ezenwa, V.O., Davis, A.K., 2014. Infection with *Mycoplasma gallisepticum* Buffers the Effects
593 of Acute Stress on Innate Immunity in House Finches. Physiological and Biochemical Zoology 87,
594 257–264. https://doi.org/10.1086/674320
595 Graham, A.L., Allen, J.E., Read, A.F., 2005. Evolutionary Causes and Consequences of Immunopathology.
596 Annu. Rev. Ecol. Evol. Syst. 36, 373–397.
597 https://doi.org/10.1146/annurev.ecolsys.36.102003.152622
598 Grodio, J.L., Buckles, E.L., Schat, K.A., 2009. Production of house finch (Carpodacus mexicanus) IgA
599 specific anti-sera and its application in immunohistochemistry and in ELISA for detection of
600 Mycoplasma gallisepticum-specific IgA. Veterinary Immunology and Immunopathology 132, 288–
601 294. https://doi.org/10.1016/j.vetimm.2009.06.006

602 Grodio, J.L., Hawley, D.M., Osnas, E.E., Ley, D.H., Dhondt, K.V., Dhondt, A.A., Schat, K.A., 2012.
603 Pathogenicity and immunogenicity of three Mycoplasma gallisepticum isolates in house finches
604 (Carpodacus mexicanus). Veterinary Microbiology 155, 53–61.
605 https://doi.org/10.1016/j.vetmic.2011.08.003
606 Habtewold, T., Groom, Z., Christophides, G.K., 2017. Immune resistance and tolerance strategies in
607 malaria vector and non-vector mosquitoes. Parasites Vectors 10, 186.
608 https://doi.org/10.1186/s13071-017-2109-5
609 Hawley, D.M., Grodio, J., Frasca, S., Kirkpatrick, L., Ley, D.H., 2011. Experimental infection of domestic
610 canaries (*Serinus canaria domestica*) with *Mycoplasma gallisepticum* : a new model system for a
611 wildlife disease. Avian Pathology 40, 321–327. https://doi.org/10.1080/03079457.2011.571660
612 Hawley, D.M., Hanley, D., Dhondt, A.A., Lovette, I.J., 2005. Molecular evidence for a founder effect in
613 invasive house finch (Carpodacus mexicanus) populations experiencing an emergent disease
614 epidemic: FOUNDER EFFECT IN INTRODUCED HOUSE FINCHES. Molecular Ecology 15, 263–275.
615 https://doi.org/10.1111/j.1365-294X.2005.02767.x
616 Hawley, D.M., Osnas, E.E., Dobson, A.P., Hochachka, W.M., Ley, D.H., Dhondt, A.A., 2013. Parallel
617 Patterns of Increased Virulence in a Recently Emerged Wildlife Pathogen. PLoS Biol 11,
618 e1001570. https://doi.org/10.1371/journal.pbio.1001570
619 Hawley, D.M., Thomason, C.A., Aberle, M.A., Brown, R., Adelman, J.S., 2023. High virulence is associated
620 with pathogen spreadability in a songbird–bacterial system. R. Soc. open sci. 10, 220975.
621 https://doi.org/10.1098/rsos.220975
622 Henschen, A.E., Vinkler, M., Langager, M.M., Rowley, A.A., Dalloul, R.A., Hawley, D.M., Adelman, J.S.,
623 2023. Rapid adaptation to a novel pathogen through disease tolerance in a wild songbird. PLoS
624 Pathog 19, e1011408. https://doi.org/10.1371/journal.ppat.1011408
625 Hill, G.E., Farmer, K.L., 2005. Carotenoid-based plumage coloration predicts resistance to a novel parasite
626 in the house finch. Naturwissenschaften 92, 30–34. https://doi.org/10.1007/s00114-004-0582-0
627 Hochachka, W.M., Dhondt, A.A., 2000. Density-dependent decline of host abundance resulting from a
628 new infectious disease. Proc. Natl. Acad. Sci. U.S.A. 97, 5303–5306.
629 https://doi.org/10.1073/pnas.080551197
630 Horns, F., Hood, M.E., 2012. The evolution of disease resistance and tolerance in spatially structured
631 populations: Evolution of Disease Resistance and Tolerance in Space. Ecology and Evolution 2,
632 1705–1711. https://doi.org/10.1002/ece3.290
633 Hotchkiss, E., Davis, A., Cherry, J., Altizer, S., 2005. Mycoplasmal Conjunctivitis and the Behavior of Wild
634 House Finches (Carpodacus mexicanus) at Bird Feeders. Bird Behavior 17, 1–8.
635 Jiang, C., Zhou, Z., Quan, Y., Zhang, S., Wang, T., Zhao, X., Morrison, C., Heise, M.T., He, W., Miller, M.S.,
636 Lin, X., 2016. CARMA3 Is a Host Factor Regulating the Balance of Inflammatory and Antiviral
637 Responses against Viral Infection. Cell Reports 14, 2389–2401.
638 https://doi.org/10.1016/j.celrep.2016.02.031
639 Kerr, P.J., Best, S.M., 1998. Myxoma virus in rabbits: -EN- -FR- -ES-. Rev. Sci. Tech. OIE 17, 256–268.
640 https://doi.org/10.20506/rst.17.1.1081
641 Kuttiyarthu Veetil, N., Cedraz De Oliveira, H., Gomez-Samblas, M., Divín, D., Melepat, B., Voukali, E.,
642 Świderská, Z., Krajzingrová, T., Těšický, M., Jung, F., Beneš, V., Madsen, O., Vinkler, M., 2024a.
643 Peripheral inflammation-induced changes in songbird brain gene expression: 3' mRNA
644 transcriptomic approach. Developmental & Comparative Immunology 151, 105106.
645 https://doi.org/10.1016/j.dci.2023.105106
646 Kuttiyarthu Veetil, N., Henschen, A.E., Hawley, D.M., Melepat, B., Dalloul, R.A., Beneš, V., Adelman, J.S.,
647 Vinkler, M., 2024b. Varying conjunctival immune response adaptations of house finch
648 populations to a rapidly evolving bacterial pathogen. Front. Immunol. 15, 1250818.
649 https://doi.org/10.3389/fimmu.2024.1250818

650 Langwig, K.E., Hoyt, J.R., Parise, K.L., Frick, W.F., Foster, J.T., Kilpatrick, A.M., 2017. Resistance in
651 persisting bat populations after white-nose syndrome invasion. Phil. Trans. R. Soc. B 372,
652 20160044. https://doi.org/10.1098/rstb.2016.0044
653 Ley, D.H., 2008. Mycoplasma gallisepticum Infection, in: Diseases of Poultry. Blackwell publ, Ames (Iowa),
654 pp. 807–834.
655 Lindström, K.M., Hawley, D.M., Davis, A.K., Wikelski, M., 2005. Stress responses and disease in three
656 wintering house finch (Carpodacus mexicanus) populations along a latitudinal gradient. General
657 and Comparative Endocrinology 143, 231–239. https://doi.org/10.1016/j.ygcen.2005.04.005
658 Medzhitov, R., Schneider, D.S., Soares, M.P., 2012. Disease Tolerance as a Defense Strategy. Science 335,
659 936–941. https://doi.org/10.1126/science.1214935
660 Nolan, P.M., Hill, G.E., Stoehr, A.M., 1998. Sex, size, and plumage redness predict house finch survival in
661 an epidemic. Proc. R. Soc. Lond. B 265, 961–965. https://doi.org/10.1098/rspb.1998.0384
662 Okin, D., Medzhitov, R., 2012. Evolution of Inflammatory Diseases. Current Biology 22, R733–R740.
663 https://doi.org/10.1016/j.cub.2012.07.029
664 Pfaffl, M.W., 2001. A new mathematical model for relative quantification in real-time RT-PCR. Nucleic
665 Acids Research 29, 45e–445. https://doi.org/10.1093/nar/29.9.e45
666 Price, S.J., Garner, T.W.J., Nichols, R.A., Balloux, F., Ayres, C., Mora-Cabello de Alba, A., Bosch, J., 2014.
667 Collapse of Amphibian Communities Due to an Introduced Ranavirus. Current Biology 24, 2586–
668 2591. https://doi.org/10.1016/j.cub.2014.09.028
669 Pyle, P., 1997. Molt limits in North American passerines. North American Bird Bander 22, 49–89.
670 R Core Team, 2021. R: A Language and Environment for Statistical Computing.
671 Råberg, L., Sim, D., Read, A.F., 2007. Disentangling Genetic Variation for Resistance and Tolerance to
672 Infectious Diseases in Animals. Science 318, 812–814. https://doi.org/10.1126/science.1148526
673 Roy, B.A., Kirchner, J.W., 2000. Evolutionary Dynamics of Pathogen Resistance and Tolerance. Evolution
674 54, 51–63.
675 RStudio Team, 2021. RStudio: Integrated Development Environment for R.
676 Sun, Y., Ma, J., Li, D., Li, P., Zhou, X., Li, Y., He, Z., Qin, L., Liang, L., Luo, X., 2019. Interleukin-10 inhibits
677 interleukin-1β production and inflammasome activation of microglia in epileptic seizures. J
678 Neuroinflammation 16, 66. https://doi.org/10.1186/s12974-019-1452-1
679 Sydenstricker, K.V., Dhondt, A.A., Hawley, D.M., Jennelle, C.S., Kollias, H.W., Kollias, G.V., 2006.
680 Characterization of Experimental Mycoplasma gallisepticum Infection in Captive House Finch
681 Flocks. Avian Diseases 50, 39–44. https://doi.org/10.1637/7403-062805R.1
682 Tulman, E.R., Liao, X., Szczepanek, S.M., Ley, D.H., Kutish, G.F., Geary, S.J., 2012. Extensive variation in
683 surface lipoprotein gene content and genomic changes associated with virulence during
684 evolution of a novel North American house finch epizootic strain of Mycoplasma gallisepticum.
685 Microbiology 158, 2073–2088. https://doi.org/10.1099/mic.0.058560-0
686 Vinkler, M., Leon, A.E., Kirkpatrick, L., Dalloul, R.A., Hawley, D.M., 2018. Differing House Finch Cytokine
687 Expression Responses to Original and Evolved Isolates of Mycoplasma gallisepticum. Front.
688 Immunol. 9, 13. https://doi.org/10.3389/fimmu.2018.00013
689 Wang, D., You, Y., Lin, P.-C., Xue, L., Morris, S.W., Zeng, H., Wen, R., Lin, X., 2007. Bcl10 plays a critical
690 role in NF-κB activation induced by G protein-coupled receptors. Proc. Natl. Acad. Sci. U.S.A. 104,
691 145–150. https://doi.org/10.1073/pnas.0601894104
692 Xue, L., Morris, S.W., Orihuela, C., Tuomanen, E., Cui, X., Wen, R., Wang, D., 2003. Defective
693 development and function of Bcl10-deficient follicular, marginal zone and B1 B cells. Nat
694 Immunol 4, 857–865. https://doi.org/10.1038/ni963
695 Yang, D., Zhao, X., Lin, X., 2021. Bcl10 is required for the development and suppressive function of
696 Foxp3+ regulatory T cells. Cell Mol Immunol 18, 206–218. https://doi.org/10.1038/s41423-019-
697 0297-y

698 Zhang, J.-M., An, J., 2007. Cytokines, Inflammation, and Pain. International Anesthesiology Clinics 45, 27–
699 37. https://doi.org/10.1097/AIA.0b013e318034194e
700 Zhang, T., Sun, J., Wang, Liyan, Yao, H., Guo, Z., Wu, W., Li, Y., Wang, Lingling, Song, L., 2022. BCL10
701 regulates the production of proinflammatory cytokines by activating MAPK–NF–κB/Rel signaling
702 pathway in oysters. Fish & Shellfish Immunology 120, 369–376.
703 https://doi.org/10.1016/j.fsi.2021.12.009
704